The effects of altered membrane fatty acid composition on the toxic interactions of heavy metals with Saccharomyces Cerevisiae

Niall G Howlett (1998)

THE EFFECTS OF ALTERED MEMBRANE FATTY ACID COMPOSITION ON THE TOXIC INTERACTIONS OF HEAVY METALS WITH *SACCHAROMYCES CEREVISIAE*

Niall G. Howlett

A thesis submitted in partial fulfilment of the requirements of Oxford Brookes University for the degree of Doctor of Philosophy

January 1998

Abstract

The effects of altered membrane fatty acid composition on the toxic interactions of heavy metals with *Saccharomyces cerevisiae* were examined. *Saccharomyces cerevisiae* was enriched with the polyunsaturated fatty acids (PUFAs) linoleate (18:2) and linolenate (18:3) by growth in 18:2- or 18:3-supplemented medium. Incorporation of the exogenous PUFAs resulted in them comprising greater than 65% and 40% of the total fatty acids in whole-cell and plasma membrane lipids, and nuclear membrane lipids, respectively. Incorporation of the exogenous PUFAs had no discernible adverse effects on cell division. However, inhibition of cell division in the presence of $Cd(NO_3)_2$ was accentuated by growth in the presence of the di-unsaturated fatty acid linoleate. Furthermore, susceptibility to both Cd^{2+}- and Cu^{2+}-induced plasma membrane permeabilisation and whole cell toxicity was markedly accentuated in PUFA-enriched cells, and increased with the degree of fatty acid unsaturation. The increased sensitivity of PUFA-enriched cells to membrane permeabilisation and whole-cell toxicity was correlated with increased levels of lipid peroxidation in these cells. Cu^{2+}- and Cd^{2+}-induced lipid peroxidation was rapid and associated with a decline in plasma membrane lipid order, detected by fluorescence depolarization measurements. Levels of the lipid peroxidation products thiobarbituric acid-reactive substances (TBARS) and conjugated dienes were markedly higher in PUFA-enriched cells, compared with unsupplemented cells, following exposure to cadmium or copper. Thus, lipid peroxidation was demonstrated as a major means of heavy metal toxicity in a microorganism for the first time. In addition, the effects of PUFA-enrichment on the interactions of heavy metals with cellular nucleic acids were examined. Exposure of PUFA-enriched cells to the redox-active metals chromium and copper resulted in the uncoupling of DNA synthesis from cell division, leading to sequential S phases. For example, DNA levels of up to 8C were evident in 18:3-enriched cells after only 4.5 h exposure to 100 μM $Cu(NO_3)_2$. Using flow cytometry, the heterogeneity in susceptibility to copper toxicity of exponential phase *S. cerevisiae* was also examined. Susceptibility towards copper toxicity was demonstrated to be cell cycle stage-dependent, whereby G_2/M phase cells were found to be the most susceptible towards copper toxicity. Staining with the oxidant-sensitive probe 2',7'-dichlorodihydrofluorescein diacetate (H_2DCFDA) revealed that the greater copper sensitivity of G_2/M phase cells correlated with elevated endogenous levels of reactive oxygen species in these cells.

Abstracts, presentations and publications

Howlett, N. G. and Avery, S. V. (1995). Relationship between the surface properties of microorganisms and heavy metal uptake and toxicity. Society for General Microbiology 132nd Meeting, University of Aberdeen, Scotland, *Abstracts* p. 102.

Howlett, N. G. (1995). Influence of membrane lipid composition on cadmium toxicity towards *Saccharomyces cerevisiae* (oral presentation). Joint winner of Ph.D. student symposium, Oxford Brookes University, U.K..

Howlett, N. G. and Avery, S. V. (1996). Membrane properties determining cadmium-induced plasma-membrane permeabilisation in *Saccharomyces cerevisiae.* Society for General Microbiology 135th Meeting, University of Essex, U.K., *Abstracts* p. 53.

Avery, S. V., Howlett, N. G., and Radice, S. (1996). Copper toxicity towards *Saccharomyces cerevisiae*: Dependence on plasma membrane fatty acid composition. *Applied and Environmental Microbiology* **62**, 3960-3966.

Howlett, N. G. and Avery, S. V. (1997). Induction of lipid peroxidation during heavy metal stress in *Saccharomyces cerevisiae* and influence of cellular fatty acid composition. American Society for Microbiology 97th General Meeting, Miami Beach, FLA, U.S.A., *Program* p. 23. Recipient of ASM sustaining member student travel grant award.

Howlett, N. G. and Avery, S. V. (1997). Induction of lipid peroxidation during heavy metal stress in *Saccharomyces cerevisiae* and influence of plasma membrane fatty acid unsaturation. *Applied and Environmental Microbiology* **63**, 2971-2976.

Howlett, N. G. and Avery, S. V. (1997). Relationship between cadmium sensitivity and degree of plasma membrane fatty acid unsaturation in *Saccharomyces cerevisiae*. *Applied Microbial Biotechnology* **48**, 539-545.

Howlett, N. G. (1997). Relationship between the surface properties of microorganisms and heavy metal uptake and toxicity (seminar). Emory University, Atlanta, GA, U.S.A..

Howlett, N. G. (1997). Relationship between the surface properties of microorganisms and heavy metal uptake and toxicity (seminar). Harvard School of Public Health, Boston, MA, U.S.A..

Howlett, N. G., Houghton, J. E., Smith, A. M., and Avery, S. V. (1998). Rationalizing the phenotypic variability (in copper sensitivity) of genetically-homogeneous *Saccharomyces cerevisiae* using flow cytometry. American Society for Microbiology 98th General Meeting, Atlanta, GA, U.S.A., *Abstracts* p. 543.

Howlett, N. G., Malkapuram, S., Barata, A. C., and Avery, S. V. (1998). Heavy metal-induced disruption of the temporal order of DNA replication and mitosis in polyunsaturated fatty acid enriched-*Saccharomyces cerevisiae*. In preparation.

Acknowledgements

I would like to express my immense gratitude to my supervisor Dr. Simon V. Avery, and both past and present members of the Avery laboratory, in particular, Michael J. Hoptroff, Stefania Radice, Kimberly S. Babb, Kevin J. Blackwell, and Shareeka L. Smith. I also wish to thank Profs. P. C. Tai and S. A. Crow Jr. for enabling me to continue my PhD research at Georgia State University, Atlanta. In addition, I would like to thank all those in Kell Hall, Atlanta, and the Tonge Building, Oxford for helpful discussion, times well spent, and for often fanning the embers. Last, but not least, I would like to thank my family for their generosity and continued encouragement.

Table of Contents

List of Figures

List of Tables

Abbreviations

A	
ade	adenine sulphate
AP	Alkaline phosphatase
ATPase	Adenosine triphosphatase
B	
BSA	Bovine serum albumin
C	
can	L-Canavaline
CDK	Cyclin-dependent kinase
ConA-FITC	Concanavalin A-fluorescein isothiocyanate
D	
DAPI	4',6-Diamidine-2'-phenylindole dihydrochloride
dATP	2'-Deoxyadenosine-5'-triphosphate
DCF	2',7'-Dichlorofluorescein
dCTP	2'-Deoxycytidine-5'-triphosphate
dGTP	2'-Deoxyguanosine-5'-triphosphate
DMSO	Dimethyl sulphoxide
DNA	Deoxyribonucleic acid
DNase I	Deoxyribonuclease I
dNTP	Deoxynucleoside triphosphate

DTT	1,4-Dithiothreitol
dTTP	2'-Deoxythymidine-5'-triphosphate
E	
EDTA	Ethylenediamine tetraacetic acid
EDTA-Na_2	Ethylenediamine tetraacetic acid disodium salt
EPA	Environmental protection agency
F	
FACS	Fluorescence-activated cell sorting
FAMES	Fatty acid methyl esters
FDA	Fluorescein diacetate
FITC	Fluorescein isothiocyanate
FSC	Forward-angle light scatter
G	
GFP	Green fluorescent protein
H	
H_2DCFDA	2',7'-dichlorodihydrofluorescein diacetate
HEPES	4-(2-Hydroxyethyl)-1-piperazineethanesulphonic acid
his	L-Histidine
L	
LB	Luria-Bertani base
leu	L-Leucine

M

MDA	Malondialdehyde
Mes	4-Morpholineethanesulphonic acid
MOPS	4-Morpholinepropanesulphonic acid

O

OGYE	Oxytetracycline glucose yeast extract base

P

PBS	Phosphate-buffered saline
PCR	Polymerase chain reaction
PE	Phycoerythrin
PI	Propidium iodide
PMSF	Phenyl-methyl-sulphonyl fluoride
PUFA	Polyunsaturated fatty acid

R

RNase A	Ribonuclease A
ROS	Reactive oxygen species

S

SDS-PAGE	Sodium dodecyl sulphate-polyacrylamide gel electrophoresis
SSC	Side-angle light scatter

T

TAE	Tris-acetate-EDTA
TBA	Thiobarbituric acid

TBARS	Thiobarbituric acid-reactive substances
TBS	Tris-buffered saline
TCA	Trichloroacetic acid
TEMED	N,N,N'N'-Tetramethylethylenediamine
TMA-DPH	Trimethylammonium diphenylhexatriene
TMP	1,1,3,3,-Tetramethoxypropane
Tris	Tris(hydroxymethyl)-amino-methane
Tris.Cl	Tris(hydroxymethyl)-amino-methane hydrochloride
TRITC	Tetramethylrhodamine isothiocyanate
Trp	L-Tryptophan
U	
ura	L-Uracil
Y	
YEPD	Yeast extract peptone dextrose base
YNB	yeast nitrogen broth

CHAPTER 1

Literature review

The continuing flux of heavy metals in the biosphere is an ever present concern. A wide variety of activities result in the release of heavy metals into the environment. However, release of metals from anthropogenic sources generally exceeds that emanating from natural sources. Indeed, on the EPA's list of most commonly discharged priority pollutants, five out of sixteen pollutants are heavy metals (Novotny, 1995).

Examples of natural sources of metal fluxes include emissions from hydrothermal vents, volcanic eruptions and biogenic processes (Nisbet and Fowler, 1995; Novotny, 1995). For example, it is estimated that between 500,000 and 5 million tonnes of heavy metals are released by the Broken Spur hydrothermal vent field in the North Atlantic each year (Nisbet and Fowler, 1995). Furthermore, metallic minerals are abundant elements of the earth's crust. Natural sources of cadmium, chromium and copper include zinc carbonate and sulphide ores, chromite and chromium oxide, and copper sulphide and chalcopyrite, respectively (Novotny, 1995).

The principal anthropogenic point sources of heavy metals include industrial activities such as the smelting and refining of metal ores, and the production and fabrication of metallic commercial products (Novotny, 1995; Nriagu, 1991). Diffuse enrichment of aquatic ecosystems with heavy metals is a consequence of municipal and industrial effluents, urban runoff, e.g. combustion of lead gasoline and deterioration of lead pipes, mine effluents, sewage discharges and atmospheric fallout, often resulting in severe localised pollution (Nriagu, 1991). The enrichment of soils with heavy metals arises primarily from both industrial and household refuse, industrial solid wastes, sewage, organic wastes, coal and wood ashes, fertilisers and pesticides, as well as atmospheric fallout (Novotny, 1995; Nriagu, 1991).

Thriving biological communities exist around natural metal-rich deposits, e.g. chemolithotrophic bacterial mats on polymetal sulphide-enriched surfaces of mid-ocean ridges (Nisbet and Fowler, 1995). Iron, manganese and sulphur are essential for planktonic photosynthesis, while copper, zinc, and mercury act as essential co-factors for microbial metalloproteins (Nisbet and Fowler, 1995). However, ecosystem over-enrichment, caused by the anthropogenic mobilisation of toxic metals, disrupts the stable, biogeochemical equilibrium of trace elements. Unlike organic xenobiotic compounds, toxic metallic compounds are not subject to natural degradation. While acute ecosystem stress has been demonstrated at the local scale, the chronic effects associated with regional and global metal over-enrichment have yet to be fully discerned. The continuing mobilisation of toxic metals, organometallic compounds and radionuclides has thus resulted in considerable research attention on interactions between these compounds and biota (Gadd, 1993; Vernet, 1992; Hughes and Poole, 1989).

Metal-microbe interactions have been the focus of major research attention for several reasons. Microorganisms generally occupy the lowest trophic levels in food chains that may ultimately lead to humans. Concern has arisen because of the ubiquity of microorganisms, and their high capacities for accumulation of heavy metals, organometallic compounds, and radionuclides. Consequently, these toxic compounds may have multiple exposure pathways to humans via food, water and air. For example, ^{137}Cs may be transferred through food chains originating from microorganisms and eventually leading to humans. Certain food chains have been identified as routes of high ^{137}Cs transfer, e.g. Lichen-caribou-man food chain (Avery, 1995*a*). Heavy metal toxicity

towards humans generally involves neurotoxicity, hepatotoxicity and nephrotoxicity. For example, prolonged environmental exposure to cadmium can result in nephritis, severe kidney failure, and skeletal disease (Elinder, 1992). Furthermore, compounds of cadmium (II), chromium (VI), and nickel (II) are known human carcinogens (Dally and Hartwig, 1997; Wetterhahn and Dudek, 1996; Xu *et al.*, 1996).

Microorganisms also play crucial roles in the biogeochemical cycling of many essential elements, e.g. carbon (C), nitrogen (N), phosphorous (P), and sulphur (S), thus ensuring their stable environmental equilibrium. However, microbial activity is severely diminished in the presence of elevated levels of heavy metals, organometallic compounds, and radionuclides. For example, exposure of soil microbial populations to elevated levels of Cd, Ni, Pb, and Zn results in significant decreases in CO_2 evolution, and specific inhibition of cyanobacterial nitrogen fixation (Trevors *et al.*, 1986). Thus, enrichment of terrestrial and aquatic ecosystems with heavy metals could adversely affect the biogeochemical cycling of C, N, P and S, essential trace elements, and organic matter decomposition processes (Nriagu, 1991).

Furthermore, as a consequence of the high heavy metal uptake-capacities of microorganisms, metal-microbe interactions have also been the subject of considerable biotechnological research attention in the last two decades, due to the potential use of microorganisms for the bioremediation of toxic industrial effluents (Avery, 1995*a*; Macaskie, 1991). Microorganisms generally accumulate metals in two distinct and well characterised phases; a metabolism-independent phase involving adsorption to the cell wall and a metabolism-dependent phase of intracellular transport across the plasma membrane (Gadd, 1993). Metabolism-independent metal accumulation is facilitated by

the presence of numerous metal-coordinating ligands such as sulphydryl, carboxyl and hydroxyl groups on the cell surface, and in membrane proteins (Shumate II and Strandberg, 1985). Microbial extracellular products, e.g. phytochelatins, siderophores, and exopolysaccharides, also have the capacity to sequester and complex metals. Metabolism-dependent intracellular transport of metals in microorganisms is generally mediated by membrane-bound proteins. For example, iron transport into the yeast *S. cerevisiae* is mediated by the *FET3*, *FTR1* and *FET4* plasma membrane-bound transporters (Stearman *et al.*, 1996), while a high affinity copper transporter is encoded by *CTR1* (Dancis *et al.*, 1994). Current methodologies for the detoxification of metal/radionuclide-containing industrial effluents include ion-exchange techniques, e.g. natural and synthetic zeolites, and elevated pH-metal precipitation (Avery, 1995*b*). However, metal-removal efficiencies of zeolites can be reduced significantly as a result of competition by ions of similar charge and ionic radii, while elevated pH metal-precipitation is ineffective for certain metal species, e.g. Cs^+ (Avery, 1995*b*; Macaskie, 1991; Harjula and Lehto, 1986). The use of microbial biomass for the removal of toxic heavy metals, organometallic compounds and radionuclides from industrial effluents may represent an effective and cheap alternative to existing methodologies (Avery, 1995*b*). Currently, microbial mats consisting predominantly of sulphate-reducing bacteria of the *Thiobacillus* genus, and cyanobacteria offer the greatest potential for the decontamination of heavy metal-enriched sediments and effluents (Bender *et al.*, 1994; Fude *et al.*, 1994).

Transition metals are chemically defined as those with *d* electrons and incompletely filled *d* orbitals. The Groups of the *d* block contain only three elements that

correspond to the filling of the 3*d*, 4*d* and 5*d* shells, respectively.. Each transition Group typically divides into two parts; the lightest element and the pair of heavy elements. The chemistry of the heavy elements is very similar due to the lanthanide contraction (Mackay and Mackay, 1991). Ligand field theory is particularly confined to *d*-element chemistry as transition metal ions are small. The M^{2+} and M^{3+} ions are centres of high charge density and can be strongly coordinated to lone pair donors (Mackay and Mackay, 1991). The toxic effects of heavy metals can thus be attributed partly to the multiplicity of coordination complexes and clusters that they can form (Butler and Harrod, 1989). Microbial cells provide a ligand-rich environment in which heavy metals can exert their deleterious effects through a variety of mechanisms. For example, cadmium reacts with polythiol groups on cellular macromolecules, and both cobalt and cadmium can substitute for zinc in Zn-containing enzymes, e.g. carboxypeptidases (Price and Morel, 1990). While the redox-active metal copper is an essential cellular redox component; copper is required for catalysis by enzymes such as Cu, Zn superoxide dismutase, lysyl oxidase, cytochrome c oxidase, and dopamine β hydroxylase (Knight *et al.*, 1996), at elevated concentrations copper is extremely cytotoxic. Among other mechanisms of toxicity, copper indiscriminately binds to thiolate moieties and interacts with enzyme active sites (Cervantes and Gutierrez-Corona, 1994). Moreover, the interaction of both cadmium and copper, along with other transition metals, with cellular and organellar membranes can result in the rapid loss of membrane stability and impairment of membrane function (Fodor *et al.*, 1995; Ohsumi *et al.*, 1988). Cadmium- and copper-induced plasma-membrane permeabilisation with associated cellular K^+ efflux has been extensively reported in the yeast *Saccharomyces cerevisiae*, and is considered a major mechanism of

toxicity in this organism (Ohsumi *et al.*, 1988; De Rome and Gadd, 1987; Kessels *et al.*, 1985; Gadd and Mowll, 1983). However, the underlying mechanism of heavy metal-induced membrane permeabilisation has yet to be clearly discerned.

One general cause for loss of membrane integrity in biological systems, in response to a variety of stimuli, can arise through reactive oxygen species (ROS)-mediated damage (Halliwell and Gutteridge, 1989). Redox-active metals, such as copper, are known to be capable of inducing ROS-generation through redox-cycling activity. Furthermore, nonredox-active metals, such as cadmium, may indirectly induce the accumulation of ROS through depletion of ROS-scavenging molecules such as glutathione and protein-bound sulfhydryl groups (Figueiredo-Pereira *et al.*, 1998; Li *et al.*, 1997; Hassoun and Stohs, 1996; Stohs and Bagchi, 1995).

Free radicals, which includes the vast majority of reactive oxygen species, are chemically defined as highly unstable molecules that have an unpaired electron(s) in an outer orbital (Davies, 1995; Dix and Aikens, 1993). Free radicals are stabilised through abstraction of electrons from donor molecules, with the concomitant destabilisation of the donor molecule. In biological systems ROS are generated endogenously via normal metabolic processes. Primarily, ROS are generated during electron transport events such as mitochondrial respiration, or the respiratory burst of neutrophils, monocytes, and macrophages (James *et al.*, 1998; Pongracz and Lord, 1998; Akaike *et al.*, 1996). ROS are also generated during steroidogenesis and the β-oxidation of high-molecular weight fatty acids (Rapoport *et al.*, 1998; Davidge *et al.*, 1995). In addition to ROS generation during normal metabolism, exposure to numerous exogenous chemical agents such as the

monofunctional alkylating agent methyl methanesulfonate (MMS), methyl viologen (paraquat), mitomycin C, menadione, phenylhydrazine, and cumene hydroperoxide, as well as heavy metals, may result in the generation of ROS (Flattery O'Brien and Dawes, 1998; Brennan *et al.*, 1994; Hama-Inaba *et al.*, 1994).

The major ROS that occur in biological systems include superoxide anion ($O_2^{\cdot-}$) (a mono-radical), hydroxyl radical ($OH^{\cdot}$), hydrogen peroxide (H_2O_2), and dioxygen (O_2) (a bi-radical; two unpaired electrons in the π^* orbital). The non-enzymatic, univalent, reduction of molecular oxygen results in the generation of several highly reactive intermediates (1) (Davies, 1995).

$$\begin{array}{ccccccccc} & e^- & & e^- & & e^- & & e^- & \\ & \searrow & & \searrow & & \searrow & & \searrow & \\ O_2 & \rightarrow & O_2^{\cdot-} & \rightarrow & H_2O_2 & \rightarrow & HO^{\cdot} & \rightarrow & H_2O \\ & & \nearrow & & \searrow & & \nearrow & & \\ & & 2H^+ & & OH^- & & H^+ & & \end{array} \qquad (1)$$

In mitochondria, superoxide anion can be generated at complex I (NADH-Ubiquinone) or at complex II (cytochrome c) of the electron transport chain. Furthermore, iron-sulphur clusters within the respiratory chain mediate the generation of superoxide anions (Keyer and Imlay, 1996). Superoxide anion can also be generated through auto-oxidation via interactions with cellular reductants, such as ascorbate, glutathione and NADH (Park *et al.*, 1998; Minasi and Willsky, 1991). In addition, phagocytic cells, such as monocytes, neutrophils, and macrophages, utilise an NADPH oxidase enzymatic system to generate superoxide anion as part of their defence against pathogenic microorganisms (James *et al.*, 1998; Pongracz and Lord, 1998). While the superoxide anion itself is not highly

reactive, it can give rise to highly reactive ROSs. For example, protonation of the superoxide anion generates the highly active oxidising agent, the perhydroxyl radical ($HO_2^{\cdot}$) (Valentine *et al.*, 1998; Dix *et al.*, 1996). Hydrogen peroxide is generated through the β-oxidation of high molecular weight fatty acids, and upon superoxide anion dismutation (Van der Leij *et al.*, 1992; Seaman *et al.*, 1982). Despite being a ROS, hydrogen peroxide is not a free radical as it has no unpaired electrons. However, hydrogen peroxide efficiently crosses biological membranes and leads to the generation of the highly reactive hydroxyl radical. Hydrogen peroxide undergoes both a slow, spontaneous decomposition, and a more rapid, metal-dependent decomposition, via the Fenton reaction (2), to yield the hydroxyl radical.

$$Fe^{2+} + H_2O_2 + H^+ \rightarrow Fe^{3+} + HO^{\cdot} + H_2O \qquad (2)$$

Significantly, many redox-active transition metals, including Cu^+, Ni^{2+} and Ti^{3+}, facilitate the generation of the hydroxyl radical, via Fenton-type reactions. Furthermore, the reduction of Cu^{2+} and Fe^{3+} by the superoxide anion, via the Haber-Weiss reaction (3), results in the regeneration of the reduced metal form which can subsequently undergo another Fenton reaction.

$$Fe^{3+} + O_2^{\cdot-} \rightarrow Fe^{2+} + O_2 \qquad (3)$$

Thus, while transition metals play essential roles as cellular enzymatic redox components, excess levels of transition metals in biological systems promote the formation of several highly reactive oxygen species.

Reactive oxygen species, primarily $O_2^{\cdot-}$, $HO^{\cdot}$, $HO_2^{\cdot}$, H_2O_2, and O_2 are capable of eliciting cellular damage through interactions with DNA, protein and lipids. The

interactions of ROS with DNA results in the formation of a wide variety of DNA lesions, including strand breaks, base loss or damage, and fragmentation of the deoxyribose moiety (Demple and Harrison, 1994; Ramotar *et al.*, 1991). Indeed, DNA double-strand breaks may lead to genome rearrangements, such as deletions, duplications, and translocations, which have been implicated in carcinogenesis (Brennan and Schiestl, 1998; Manivasakam and Schiestl, 1998; Brennan *et al.*, 1994). The hydroxyl radical has been implicated as a key ROS responsible for eliciting DNA damage, generating several base lesions in double-stranded DNA, including thymine glycol, 8-oxoguanine and formamido-pyrimidine among other base oxidation products (Demple and Harrison, 1994). Hydrogen peroxide-mediated cell toxicity results predominantly from the generation of hydroxyl radical via the Fenton reaction (2) (Flattery O'Brien and Dawes, 1998; Brennan *et al.*, 1994). The DNA damage elicited by ionizing radiation, the antitumour antibiotic bleomycin, and peroxides is mediated via the formation of ROS, with the subsequent generation of apurinic/apyrimidinic (AP) sites and single-strand breaks with 3'-deoxyribose fragments (Teoule, 1986). Exposure to the oxidative mutagens methyl viologen (paraquat), mitomycin C, phenylhydrazine, and cumene hydroperoxide also induces a variety of DNA lesions, both directly (N7-methylguanine, O6-methylguanine, 3-methyladenine), and as a result of lesion processing (abasic sites, nicks, gaps, double-strand breaks). Oxidative mutagens also increase the frequency of both intrachromosomal and interchromosomal recombination (Brennan *et al.*, 1994). A role for the hydroxyl radical in H_2O_2-induced gross chromosomal rearrangements has been implicated by the ability of the free radical scavenger dimethyl sulphoxide (DMSO)

to significantly inhibit the induction of both intrachromosomal and interchromosomal recombination by H_2O_2 (Brennan *et al.*, 1994).

ROS-mediated protein damage occurs via oxidation of the amino acids histidine, lysine, arginine, tyrosine, phenylalanine, tryptophan, proline, methionine and cysteine, and through the formation of protein-crosslinks (Iwai *et al.*, 1998; Luikenhuis *et al.*, 1998; Moskovitz *et al.*, 1997). Oxidative damage to proteins leads to increased proteolytic susceptibility; oxidation of amino acids to carbonyl derivatives signals proteins for proteasome degradation (Iwai *et al.*, 1998; Jungmann *et al.*, 1993*a*). For example, oxidation of arginine, lysine, proline, and threonine residues of the iron-dependent degradation domain of iron regulatory protein 2 (IRP2), to their corresponding carbonyl derivatives, results in ubiquitination and subsequent proteasomal degradation (Iwai *et al.*, 1998). While oxidation of amino acids is primarily mediated by the hydroxyl radical, the superoxide anion also exhibits considerable protein reactivity; $O_2^{\cdot-}$ reacts with proteins that contain transition metal-prosthetic groups, such as haem moieties or iron-sulphur clusters (Keyer and Imlay, 1996; Prasad *et al.*, 1989).

In addition to causing severe DNA and protein damage, ROS can also induce membrane lipid damage via lipid peroxidation. The cumulative effects of lipid peroxidation have been implicated in several pathological conditions including atherosclerosis, haemolytic anaemias and ischaemia reperfusion injuries (Davies, 1995; Steinbrecher *et al.*, 1990). ROS-induced lipid peroxidation proceeds via the abstraction of hydrogen atoms from methylene groups separating unsaturated fatty acid double bonds (Glende and Recknagel, 1994; Dix and Aikens, 1993). The ROS $O_2^{\cdot-}$, in equilibrium with $HO_2^{\cdot}$ (perhydroxyl radical), $HO_2^{\cdot}$ alone, $HO^{\cdot}$, O, and H_2O_2 in the presence of $O_2^{\cdot-}$, and

trace quantities of transition metals, are capable of initial H atom abstraction from methylene groups separating unsaturated fatty acid double bonds, thus initiating the lipid peroxidative chain reaction (Dix and Aikens, 1993). Initiation of the lipid peroxidative chain results in the generation of carbon centered radicals (L$^{\cdot}$), with the concomitant formation of conjugated dienes. Propagation of the lipid peroxidative chain proceeds via radical coupling, whereby L$^{\cdot}$ reacts with O_2 resulting in the formation of lipid peroxyl radicals (LOO$^{\cdot}$). Lipid peroxyl radicals can then abstract further bis-allylic H atoms from adjacent unsaturated fatty acids in a reaction classified as an atom transfer reaction (Porter *et al.*, 1995; Dix and Aikens, 1993). Propagation is cycled through rounds of LOO$^{\cdot}$ abstraction of bis-allylic H atoms in the presence of O_2 to generate new LOO$^{\cdot}$, which ultimately results in the conversion of lipids to lipid hydroperoxides (LOOH) (Dix and Aikens, 1993). LOOHs are subsequently degraded to a variety of compounds including alkanals, alkenals, hydroxyalkenals, ketones, aldehydes and alkanes (Coudray *et al.*, 1995). Termination of lipid peroxidative chains occurs via the Russel mechanism, whereby two LOO$^{\cdot}$s react to form a nonradical product, or where one LOO$^{\cdot}$ reacts with another terminating radical, or free radical inhibitor, to generate self-quenching, nonpropagating radical species (Dix and Aikens, 1993).

The generation of lipid hydroperoxides within the hydropohobic core of membranes results in several deleterious biophysical effects. Principally, oxidized lipids alter the packing behaviour of membrane phospholipids. The accumulation of polar residues within the membrane induces a repulsive effect between adjacent oxidised fatty acyl chains, increasing their spatial separation (Van Ginkel and Sevanian, 1994). The destabilisation of hydrophobic membrane bilayers, through the incorporation of polar

hydroperoxide groups and short-chain oxidation products into membrane phospholipids, results in deterioration of membrane integrity, with the subsequent loss of membrane function (Van Ginkel and Sevanian, 1994; Mehlhorn, 1986).

Biological systems have evolved numerous antioxidant activities to sense, protect, and repair ROS-mediated damage to cellular constituents. The molecular defences against ROS in the model organism *Saccharomyces cerevisiae* have been well characterised (Santoro and Thiele, 1997; Moradas-Ferreira *et al.*, 1996; Jamieson 1995). Yeast antioxidant activities include enzymatic systems, non-enzymatic systems comprising low molecular weight antioxidants, heavy metal-chelators, and damage repair systems (Santoro and Thiele, 1997; Moradas-Ferreira *et al.*, 1996; Jamieson, 1995). Furthermore, *S. cerevisiae* possesses distinct protective oxidative stress responses to both hydrogen peroxide, and superoxide-generating compounds such as menadione (Jamieson, 1992).

The yeast enzymatic oxidative stress defence system consists primarily of cytosolic copper/zinc-containing superoxide dismutase (*SOD1*), mitochondrial manganese-containing superoxide dismutase (*SOD2*), peroxisomal catalase A (*CTA1*), cytosolic catalase T (*CTT1*), mitochondrial cytochrome-c peroxidase (*CCP1*), and thiol-specific antioxidant (*TSA*) (Santoro and Thiele, 1997; Moradas-Ferreira *et al.*, 1996; Jamieson, 1995). Superoxide dismutases (SODs) catalyse the disproportionation of the superoxide anion to hydrogen peroxide and dioxygen (Chang *et al.*, 1991; Gralla and Valentine, 1991). Exposure of yeast to the superoxide anion-generating compounds menadione and paraquat has been reported to result in increased *SOD1* and *SOD2* mRNA

transcript levels (Galiazzo and Labbe-Rois, 1993). Furthermore, mutations in either *SOD1* or *SOD2* results in elevated sensitivity to oxygen and free-radical generating compounds. In addition, *sod1Δ* mutants exhibit a variety of abnormal phenotypes, including auxotrophies for the amino acids lysine, cysteine and methionine (Liu and Culotta, 1994; Gralla and Valentine, 1991). However, the oxygen sensitivity, and lysine and methionine auxotrophies of *sod1Δ sod2Δ* double mutants can be suppressed by mutations in either the *BSD1*or *BSD2* genes (Liu and Culotta, 1994). Significantly, both the *BSD1* and *BSD2* genes encode proteins involved in metal ion-homeostasis. The *BSD1* gene is identical to the *PMR1* gene, which encodes a golgi-located P-type ATPase homologue (Rudolph *et al.*, 1989). It has been proposed that *BSD1/PMR1* functions in maintaining low cytosolic levels of calcium and manganese. Thus, it is thought that *pmr1* mutants suppress oxygen toxicity in *sod1* mutants as a result of the hyper-accumulation of manganese ions (Lapinskas *et al.*, 1995). The *BSD2* encoded transmembrane protein is thought to play a role in the intracellular transport and sequestration of copper and cadmium, into cellular compartments such as the vacuole and golgi apparatus (Liu and Culotta, 1994). In addition to suppressing oxygen toxicity in *sod1* mutants, *bsd2* mutants display increased resistance to, and accumulation of, both cadmium and copper. Both manganese and copper have known SOD mimetic activities. Therefore it is thought that alterations in intracellular levels of both copper and manganese may generate bioavailable metal complexes which can serve as SOD mimetics. The interactions of *SOD1, SOD2, BSD1, BSD2* and *PMR1* further highlight the important biological relationship between metal ion homeostasis and oxidative stress in *S. cerevisiae.*

Peroxisomal catalase A, cytosolic catalase T, and glutathione peroxidase catalyse the dismutation of hydrogen peroxide to water and molecular oxygen (Lapinskas *et al.*, 1993; Cohen *et al.*, 1985). Peroxisomal catalase A (*CTA1*) serves primarily to remove hydrogen peroxide formed from the β-oxidation of high-molecular weight fatty acids. While the exact function of cytosolic catalase T (*CTT1*) is as yet unknown, *CTT1* is important for survival under conditions of severe osmotic stress (Schüller *et al.*, 1994). Under conditions of osmotic stress HOG (high osmolarity glycerol response)-dependent *CTT1* transcription is mediated via the stress response element (STRE) (Schüller *et al.*, 1994). Post-translational modification of an STRE-binding transcription factor, mediated by the MAP kinase products of the *HOG1* and *PBS2* genes, most likely facilitates increased *CTT1* mRNA transcription (Schüller *et al.*, 1994). Expression of both *CTT1* and *CTA1* is induced by oxygen via positive control by heme (Hortner *et al.*, 1982). Regulation of *CTT1* and *CTA1* gene expression by heme is mediated by the transcriptional activator Hap1p (Ruis and Hamilton, 1992). *CTT1* transcription is also induced by Cu^{2+} via the *MAC1* transcription factor (Jungmann *et al.*, 1993*b*; Lapinskas *et al.*, 1993; Thiele, 1992). Acatalasaemic double mutants (*ctt1Δ cta1Δ*) have similar growth rates, and comparable susceptibility to hydrogen peroxide in the exponential growth phase, to wild-type cells under non-oxidative stress conditions. However, stationary phase acatalasaemic mutants are much more sensitive to hydrogen peroxide than wild-type cells, indicating that catalase plays an important role in the yeast hydrogen peroxide-adaptive stress response (Izawa *et al.*, 1996).

The product of the *TSA* gene, thiol-specific antioxidant, is a cytosolic enzyme that protects cellular components against oxidation systems in which a thiol functions as a

reducing equivalent, e.g. di-thiothreitol (DTT)/Fe^{3+}/O_2 (Kim *et al.*, 1988). It is thought that Tsap protects cells from oxidative damage by catalysing the removal of thiyl radicals (Yim *et al.*, 1994). Exposure to 100% O_2 or Fe^{3+} results in an increase of Tsap levels. Futhermore, *tsa* mutants grow more slowly under aerobic conditions, and in the presence of peroxides and paraquat, indicating that Tsap has an important physiological antioxidant role (Yim *et al.*, 1994; Chae *et al.*, 1993).

The yeast non-enzymatic defence system consists primarily of metallothionein (*CUP1*), glutathione (*GSH1*) and thioredoxin (*TRX1* and *TRX2*). Metallothioneins are highly conserved, small cysteine-rich metal binding proteins that are essential for the detoxification of metals. The yeast *CUP1* metallothionein gene is transcriptionally activated by copper, superoxide anion-generating chemicals, particularly menadione, and by growth on non-fermentable carbon sources (Liu and Thiele, 1996). Over-expression of *CUP1* can suppress the cysteine and methionine auxotrophies of *sod1Δ* mutants, and can also restore the growth of *sod1Δsod2Δ* double mutants on non-fermentable carbon sources (Tamai *et al.*, 1993). Copper activates *CUP1* via the copper metalloregulatory transcription factor *ACE1*. However, induction of *CUP1* by menadione requires the yeast heat shock transcription factor (Hsf1p) which acts at the *CUP1* promoter heat shock element (Liu and Thiele, 1996). *CUP1* transcriptional activation is not observed in the presence of hydrogen peroxide, suggesting that *CUP1* transcriptional activation is not a consequence of ROS exposure in general.

The tripeptide γ-L-glutamyl-L-cystinylglycine (glutathione) is one of the major and most abundant antioxidant molecules of *S. cerevisiae*. Glutathione possesses a redox-active sulphydryl group which reacts with oxidants to produce oxidised glutathione

(GSSG) (Stephen and Jamieson, 1996). The *GSH1* gene product γ-glutamylcysteine synthetase catalyses the first and rate-limiting step in the biosynthesis of glutathione. *GSH1* is more strongly induced by the superoxide anion generating compounds menadione and plumbagin than by hydrogen peroxide (Stephen and Jamieson, 1996). *GSH1* transcription is controlled by the transcription factor encoded by the *YAP1* gene (Stephen *et al.*, 1995). The *YAP1* and *YAP2* gene products are leucine zipper-containing transcription factors similar to the c-Jun mammalian transcriptional activators. The expression of numerous oxidative stress response genes in *S. cerevisiae*, including *GSH1*, *GLR1* (glutathione reductase), *TRX2* (thioredoxin), *TPS2* (trehalose-6-phosphate phosphatase), and *YCF1* (Mg-ATP-dependent transporter of glutathione-conjugated moieties) has been shown to be Yap1p-dependent. High level expression of Yap1p and Yap2p confers resistance to alkylating agents, cycloheximide, iron chelators and zinc (Stephen *et al.*, 1995; Hussain and Lenard, 1991). While menadione-mediated induction of *GSH1* is only slightly reduced in *yap1Δ* mutants, *yap1Δ* and *yap2Δ* mutants are considerably more sensitive to hydrogen peroxide, indicating that *YAP1* and *YAP2* are critical for the hydrogen peroxide-adaptive stress response.

Thioredoxin is a dithiol, sulphydryl-rich protein (two redox-active cysteines in its active site) with antioxidant activity. *Saccharomyces cerevisiae* contains two genes encoding thioredoxins, *TRX1* and *TRX2* (Gan, 1991). The precise molecular antioxidant mechanism of thioredoxin is unknown, however *TRX2* is induced by hydrogen peroxide but not by menadione. In addition, *trx1Δtrx2Δ* mutants cannot grow in the absence of methionine or cysteine, and contain elevated levels of GSSG (Muller, 1991; Muller 1996). As stated previously, *TRX2* is transcriptionally activated by the Yap1p

transcription factor (Kuge and Jones, 1994). Deletion of both *TRX1* and *TRX2* is a non-lethal event in *S. cerevisiae*, however *trx2Δ* mutants are hypersensitive to hydrogen peroxide and the alkyl hydroperoxide, *t*BOOH, indicating a role for *TRX2* in hydrogen peroxide dismutation (Kuge and Jones, 1994).

Direct repair of ROS-induced AP sites and 3'-damage in yeast is mediated primarily by the class II AP endonuclease/3'-diesterase, encoded by the *APN1* gene. Yeast strains containing mutations in the *APN1* gene display an elevated spontaneous mutation rate (Ramotar *et al.*, 1991). In addition, DNA repair enzymes encoded by genes belonging to the *RAD52* epistasis group repair double-strand breaks by homologous recombination (Guzder *et al.*, 1994; Klein, 1988). Re-reduction of oxidised protein sulphydryl groups is thought to be mediated by enzymes such as disulphide reductase, glutaredoxin (*GRX1* and *GRX2)* (Luikenhuis *et al.*, 1998), and methionine sulphoxide reductase (*MSRA*) (Moskovitz *et al.*, 1997). Both *GRX1* and *GRX2* have been found to contain putative STREs, and their expression is increased in response to hydrogen peroxide, menadione, heat and osmotic shock (Luikenhuis *et al.*, 1998). In addition, oxidatively modified soluble proteins in *S. cerevisiae* are recognised by ubiquitin-conjugating enzymes, encoded by *UBC1*, *UBC4*, *UBC5* and *UBC7*, and are thus tagged for degradation by the proteasome (Jungmann *et al.*, 1993*a*). Phospholipase enzymes are responsible for the hydrolysis of lipid hydroperoxides within lipid bilayers, while lipid hydroperoxides that have been released into the cytosol are thought to be cleaved by glutathione peroxidase (Tran *et al.*, 1993). Indeed, a membrane-bound glutathione peroxidase from the yeast *Hansenula mrakii* has been purified, and displayed high

substrate specificity for the lipid peroxidation by-products oleic acid hydroperoxide and phosphatidylcholine hydroperoxide *in vitro* (Tran *et al.*, 1993).

The lipid composition of the plasma membrane of *S. cerevisiae* is complex and tightly regulated. The major lipid classes of the yeast plasma membrane are glycerophospholipids, sphingolipids, and sterols. Glycerophospholipids consist of two fatty acyl chains ester-linked to glycerol-3-phosphate; various substituents such as choline [in phosphatidylcholine (PC)], ethanolamine (in PE), serine (in PS), myoinositol (in PI), and glycerol [in phosphatidylglycerol (PG)], can be linked to the phosphoryl group. The phospholipid component of the inner leaflet of the *S. cerevisiae* plasma membrane is enriched in phosphatidylethanolamine (PE), phosphatidylinositol (PI) and phosphatidylserine (PS). Diphosphatidyl glycerol or cardiolipin, the dimeric form of PG, is also present in yeast cells. Sphingolipids have a ceramide backbone which is composed of a long-chain base phytosphingosine that is N-acylated with a hydroxy C_{26} fatty acid. *Saccharomyces cerevisiae* contains only three major sphingolipids: inositol phosphate ceramide, mannosyl-inositolphosphate-ceramide, and mannosyl-diinositolphosphate-ceramide (Van der Rest *et al.*, 1995). Sterols are compact rigid hydrophobic molecules with a polar hydroxyl group. In contrast to higher eukaryotes, in which cholesterol is the most abundant sterol, the yeast plasma membrane contains mainly ergosterol and minor amounts of zymosterol (Paltauf *et al.*, 1992; Zinser *et al.*, 1991; Rattray *et al.*, 1975). Between 70-80% of the fatty acids in membrane phospholipids of *S. cerevisiae* consist of the monounsaturates palmitoleic acid (16:1) and oleic acid (18:1). Δ7-*cis*-Heptenoic acid (14:1) is also present (particularly in PS and

PE), but in much smaller quantities (Wagner and Paltauf, 1994). The remaining fatty acids are saturated and consist of palmitic acid (16:0) and lesser amounts of stearic acid (18:0) and myristic acid (14:0). Yeast Δ-9 fatty acid desaturase (encoded by the *OLE1* gene) catalyses the formation of the initial double bond between the 9th and 10th carbons of both palmitoyl (16:0) and stearoyl (18:0) coenzyme A (CoA) substrates to form 16:1 and 18:1. *Saccharomyces cerevisiae* however does not have the ability to synthesise polyunsaturated fatty acids (PUFAs) (Van der Westhuizen *et al.*, 1994; Wagner and Paltauf, 1994).

Whereas the molecular basis of both constitutive and inducible elements of the yeast antioxidant and heavy metal defence systems have been well characterised (Li *et al.*, 1997; Stephen and Jamieson, 1996; Liu and Culotta, 1994; Chang *et al.*, 1991), no studies have sought to investigate membrane compositional modifications in response to oxidative stress, or how membrane composition influences susceptibility to heavy metal toxicity. This is surprising in view of the large variability in microbial membrane composition which exists. In order to maintain a relatively constant membrane environment, and thus maintain correct membrane functionality, microorganisms rapidly alter their lipid metabolism and membrane composition during changes in external physico-chemical parameters, e.g. ethanol concentration, temperature, pressure and salinity (Schulthess and Hauser, 1995; Alexandre *et al.*, 1994; Hosono, 1992; Hazel and Williams, 1990; Suutari *et al.*, 1990). Genetically determined intrinsic inter-species differences in microbial membrane lipid composition are also widespread (Van der Westhuizen *et al.*, 1994; Vestal and White, 1989). The biochemical effects of altered yeast plasma membrane phospholipid composition have been investigated. For example,

increased affinity constants for amino acid transport have been observed for yeast choline and ethanolamine auxotrophs, with plasma membranes enriched with PC or PE, respectively (Triveldi *et al.*, 1982). PI-enrichment of the yeast plasma membrane has also been associated with enhanced H^+-ATPase activity (Triveldi *et al.*, 1987). Also, the effects of specific enrichment of the plasma membrane of *S. cerevisiae* with exogenously-supplied PUFAs and sterols on growth dynamics, and amino acid and pyrimidine transport have been described (Parks *et al.*, 1995; Bossie and Martin, 1989; Keenan *et al.*, 1982; Watson and Rose, 1980). Hoptroff *et al.* (1997) recently demonstrated an elevated rate of Cs^+-accumulation in *S. cerevisiae* exogenously enriched with the di-unsaturated fatty acid linoleate. Thus, maintenance of membrane homeoviscosity appears to be critical for the regulation of plasma membrane protein activity. In addition, the effects of modification of membrane fatty acid composition on the heat shock and H_2O_2-stress responses have also been examined (Polla *et al.*, 1997; Carratu *et al.*, 1996; Steels *et al.*, 1994). Incorporation of an exogenous PUFA into membrane phospholipids of anaerobically grown *S. cerevisiae* resulted in decreased intrinsic and induced thermotolerance, and an increase in sensitivity towards H_2O_2 (Steels *et al.*, 1994). Furthermore, incorporation of a saturated fatty acid into membrane phospholipids of a temperature-sensitive *H. capsulatum* strain (up-regulated *OLE1* promoter) resulted in an increase in heat shock protein (hsp82 and hsp70) mRNA transcription at 37 °C (Carratu *et al.*, 1996). Here, it was postulated that a primary membrane-associated heat shock sensor (which initiates the signal cascade leading to phosphorylation of heat shock factor (HSF)) is regulated in part through active modification of membrane lipid composition. However, while Polla *et al.* (1997) also

demonstrated the increased H_2O_2-sensitivity of PUFA-enriched human premonocytic cells, no discernible differences in HSP synthesis were observed following heat shock.

Microorganisms, particularly yeast and fungi, are highly amenable to manipulation of membrane lipid composition, and thus serve as ideal experimental organisms for modelling membrane lipid-dependent functions in higher organisms. Enrichment of the yeast plasma membrane with PUFAs has no effect on growth rate, thus circumventing the major problem associated with blunt-tools such as temperature-dependent manipulations of membrane lipid composition (Guerzoni *et al.*, 1993). PUFA-enrichment in *S. cerevisiae* is known to result in sharp repression of *OLE1* transcription, resulting in decreased synthesis of 16:1 and 18:1 (Bossie and Martin, 1989).

Incorporation of long chain PUFAs into membrane phospholipids alters the packing behaviour of phospholipid moieties, and ultimately leads to a decline in membrane stability (Vossen *et al.*, 1995; De Vos *et al.*, 1993). However, to date no reports have examined how heavy metal-induced membrane permeabilisation is related to initial membrane phospholipid composition. Furthermore, the susceptibility of membrane phosholipids to ROS-induced lipid peroxidation is known to increase with the degree of phospholipid fatty acyl chain unsaturation (Van Ginkel and Sevanian, 1994). The latter point is of particular relevance to the present studies as heavy metals can promote the generation of ROS through redox-cycling activity via the Fenton (2) and Haber-Weiss (3) reactions, and by depletion of free radical scavengers (Figueiredo-Pereira *et al.*, 1998; Li *et al.*, 1997; Hassoun and Stohs, 1996; Stohs and Bagchi, 1995). However, the relationship between membrane fatty acid composition, ROS-mediated

cellular damage, and heavy metal toxicity towards microorganisms has yet to be elucidated.

Thus, the objectives of this research were to examine the effects of altered membrane fatty acid composition on the toxic interactions of heavy metals with the model organism *Saccharomyces cerevisiae.*

CHAPTER 2

Investigation of the Relationship Between Cadmium Toxicity and Degree of Plasma Membrane Fatty Acid Unsaturation in *Saccharomyces cerevisiae*

2.1. Introduction

The toxicity of cadmium, along with several other heavy metals, towards microorganisms has attracted considerable research attention in recent years as a result of the continuing anthropogenic mobilisation of heavy metals in the environment. The principal anthropogenic point sources of cadmium in the environment include the electroplating, galvanising, zinc and lead mining, and smelting industries. In addition, nickel-cadmium alkaline batteries are extensively used throughout the aircraft industry and in numerous portable devices, e.g. cellular phones. Cadmium is a potent toxin to living cells, for which limited biological function has been defined to date (Price and Morel, 1990). Cadmium is a nephrotoxin and potential carcinogen, with a long biological half-life in humans (Dally and Hartwig, 1997; Brennan and Schiestl, 1996).

Cadmium, along with Zn and Hg, is a d-block element that forms M^{2+} ions of high charge density which can be strongly coordinated to lone pair donors. As a consequence, the toxic effects of these transition metal ions can be attributed partly to the multiplicity of coordination complexes and clusters that they can form (Mackay and Mackay, 1991; Butler and Harrod, 1989). Most heavy metal ions have a strong affinity for ligands such as phosphates, purines, pteridines, porphyrins, and cysteinyl and histidyl side chains of proteins, which are all abundant in microbial cells. Thus, microbial cells provide an environment in which heavy metals can exert deleterious effects through a variety of mechanisms (Gadd, 1993). Cadmium reacts with polythiol groups on cellular macromolecules, particularly protein sulphydryl groups, and can substitute for zinc in Zn-

containing enzymes, e.g. carboxypeptidases (Li *et al.*, 1997; Price and Morel, 1990). In addition, cadmium resistance in yeast can be mediated by ubiquitin-dependent proteolysis (Jungmann *et al.*, 1993*a*), suggesting that cadmium exerts its toxic effects in part through the formation of abnormal proteins. Furthermore, as stated previously, cadmium, along with other transition metals, causes perturbations in the integrity of certain structural components, e.g. cellular and organellar membranes (Aβmann *et al.*, 1996; Kessels *et al.*, 1985). Plasma-membrane permeabilisation with associated cellular K^+ efflux has been reported in a variety of microorganisms following cadmium exposure, and is considered a major mechanism of cadmium toxicity in the yeast *Saccharomyces cerevisiae* (Aβmann *et al.*, 1996; Kessels *et al.*, 1985; Gadd and Mowll, 1983).

Recent studies with higher organisms have indicated that susceptibility to heavy metal toxicity may be partly dependent on the lipid composition and physical properties of cellular membranes (Vossen *et al.*, 1995; De Vos *et al.*, 1993). These observations are of considerable pertinence to metal-microbe interactions as many microorganisms exhibit large fatty acid compositional changes during environmental acclimation (Hazel and Williams, 1990). Intrinsic inter-species differences in microbial fatty acid profiles are also widespread (Van der Westhuizen *et al.*, 1994; Vestal and White, 1989). Many membrane-dependent functions are sensitive to such alterations (Avery *et al.*, 1995*a*; Hazel and Williams, 1990; Murata, 1989). However, there is currently a notable lack of information relating to how this variation might influence microbial susceptibility to plasma membrane-targeting toxic agents.

Recently, a link between plasma membrane composition and metal sensitivity was reported in yeast. It was found that copper-induced plasma membrane disruption in *S.*

cerevisiae was markedly accelerated in cells enriched with the di-unsaturated fatty acid linoleate (18:2) (Avery *et al.*, 1996). Because polyunsaturated fatty acids are particularly susceptible to free radical attack, these results were also consistent with a role of oxidative stress in copper-toxicity towards yeast, as has been indicated for higher organisms (Stohs and Bagchi, 1995; Shinar *et al.*, 1989). A role of free radicals has been further supported by studies in other laboratories which have demonstrated copper hyper-sensitivity in *S. cerevisiae* strains which carry mutations in genes encoding components of the oxidative stress response (Culotta *et al.*, 1995; Tamai *et al.*, 1993; Greco *et al.*, 1990). Brennan and Schiestl (1996) have recently demonstrated the elevated Cd^{2+}-sensitivity of *sod1Δ sod2Δ* and *gsh1Δ S. cerevisiae* strains. In addition, Cd^{2+}-induced toxicity and recombination were inhibited in the presence of the free radical scavenger *N*-acetyl cysteine (Brennan and Schiestl, 1996). In the present study we address the question of whether the nonredox-active nature of cadmium (unlike copper) therefore precludes a role of plasma membrane lipid composition in determining its toxicity to *S. cerevisiae.*

Interestingly, cadmium toxicity was also found to be highly dependent on plasma membrane composition and showed increases with the degree of fatty acid unsaturation; maximal Cd^{2+} sensitivity was evident in cells enriched with the tri-unsaturated fatty acid, linolenate. The dependence of yeast sensitivity to metals on plasma membrane composition appears to be more widespread than originally anticipated.

2.2. Materials and Methods

2.2.1. Organism and culture conditions. *S. cerevisiae* NCYC 1383 (*MATα, his3-Δ1, leu2-3, leu2-112, ura3-52, trp1-289*) was routinely maintained on solid YEPD medium, comprising 2% (w/v) neutralised bacteriological peptone, 1% (w/v) yeast extract (Oxoid, U.K.), 2% (w/v) glucose, and 1.6% (w/v) agar (no. 3, technical, Oxoid, U.K.), and solid YNB selective medium comprising 0.67% (w/v) yeast nitrogen base without amino acids, 1.6% (w/v) technical agar, 60 μg ml^{-1} leucine, 40 μg ml^{-1} tryptophan, and 20 μg ml^{-1} histidine and uracil. For experimental purposes, *S. cerevisiae* was grown in 100 ml of YEPD broth, of the same composition as solid YEPD, but lacking agar and supplemented with 1% (w/v) of the non-ionic surfactant tergitol (NP-40, Sigma, U.K.), in 250 ml Erlenmeyer flasks (tergitol supplementation, to help solubilise fatty acids, was found to have no discernible effect on the fatty acid composition of *S. cerevisiae*). Experimental flasks were inoculated to OD_{550}~0.1 from 48 h starter cultures, and incubated at 25 °C with orbital shaking at 120 rev. min^{-1}. Where indicated, linoleate or linolenate (Sigma, U.K.) (final concentrations, 1 mM) were added from filter-sterilised 20 mM stock solutions, solubilised with 5% (w/v) tergitol. When specified, $Cd(NO_3)_2$ was aseptically added from a stock solution, previously sterilised by autoclaving. Cell numbers were determined using a modified Fuchs-Rosenthal haemocytometer slide after appropriate dilution with distilled deionised water: more than 400 cells were counted in each sample.

2.2.2. **Preparation of cell homogenates.** Cells were harvested by centrifugation at 1,500 *g* for 5 min and washed twice with distilled deionised water at 4 °C to restrict further lipid metabolism. Cells were disrupted by vigorous shaking with 0.5 mm-diameter glass beads (Sigma, U.K.) for 15 min at 4 °C using a Mickle homogeniser (Mickle Laboratories, Guildford, U.K.). The beads were removed by vacuum filtration through a glass-sintered filter and washed with distilled deionised water.

2.2.3. **Plasma membrane isolation.** It was found that the method used for isolation of plasma membranes from unsupplemented and linoleate-supplemented cells did not yield membranes of sufficient purity from linolenate-enriched cells [possibly for the reasons suggested by Alterthum and Rose (1973)], thus, two methods for preparation of plasma membranes were used. Unsupplemented and linoleate-enriched plasma membranes were purified from whole-cell homogenates by differential and density-gradient centrifugation, using a modified method of Serrano (1988). Late-exponential/early-stationary phase cells were harvested by centrifugation at 1,500 *g* for 5 min and washed twice with distilled deionised water at 4 °C. The pellet was resuspended in 5 mM Tris.Cl (pH 7.5), 700 mM sorbitol to give $O.D._{800} \sim 6.0$. The suspension was then mixed with ¼ volume of 300 units ml^{-1} lyticase (Sigma, U.K.), prepared in the above buffer, and DTT was added to a final concentration of 6.5 mM. The suspension was then incubated for 1-2 h at 30 °C, with occasional shaking to aid cell wall digestion. Spheroplast formation was followed by examining for birefringence using phase-contrast microscopy (Rose and Veazey, 1992). Approximately 80-90% spheroplast yield was usually observed after 2 h incubation. Spheroplasts were harvested by centrifugation at 3,000 *g* for 10 min and

washed twice with lyticase-free buffer. The spheroplast pellet was finally resuspended in 10-15 ml of 15 mM Mes-Tris (pH 6.5), 500 mM sorbitol, 100 mM glucose, and incubated at 30 °C for 10 min to activate the plasma membrane H^+-ATPase. Osmotic lysis was achieved by dilution with two volumes of 25 mM Mes-Tris (pH 6.5), 5 mM EDTA, 0.2% (w/v) BSA, 0.2% (w/v) casein hydrolysate, 1 mM DTT and 1 mM PMSF, at 4 °C. All subsequent steps were carried out at 4 °C. To aid spheroplast homogenisation the suspension was subjected to gentle mechanical disruption with five slow strokes of a hand-held homogeniser (BDH, U.K., 0.15-0.25 mm clearance). The suspension was centrifuged at 700 *g* for 10 min to remove cell-wall debris. The resulting supernatant was then centrifuged at 35,000 *g* for 15 min, yielding a total-membrane pellet. The pellet was resuspended in 20% (v/v) glycerol, 10 mM PMSF. The resuspended total-membrane fraction was applied to a discontinuous sucrose gradient comprising 2 parts 43% (w/w) sucrose and 1 part 53% (w/w) sucrose. After centrifugation for 6 h at 120,000 *g* in a Beckman SW40Ti swinging bucket rotor, the plasma membrane-enriched fraction was collected at the 43/53 interface with a Pasteur pipette (narrow tip). The plasma membrane-enriched fraction was diluted with 4 volumes of distilled deionised water and centrifuged at 80,000 *g* for 20 min. After centrifugation, the final pellet was resuspended in 20% (v/v) glycerol, 10 mM PMSF, flash frozen in liquid nitrogen and stored at -70 °C until used.

Isolation of linolenate-enriched plasma membranes was achieved using a method of two-phase partitioning, adapted from Menendez *et al.* (1995). Purification of the total-membrane pellet was as described above. The total-membrane pellet was resuspended in buffer (5 mM KH_2PO_4 (pH 7.8), 330 mM sucrose, 1 mM DTT) to give a total weight of

4.0 g. The resuspended total-membrane fraction (4.0 g) was then added to a 12.0 g dextran/polyethylene glycol polymer mixture, to generate a 16.0 g two-phase system of final composition 5.7% (w/w) dextran T500 (Pharmacia Biotech, U.K.), 5.7% (w/w) polyethylene glycol 3350 (Sigma, U.K.), 5 mM KH_2PO_4 (pH 7.8), 330 mM sucrose, 1 mM EDTA, 1 mM DTT. The two-phase system was mixed thoroughly, transferred to a 25 ml separating funnel and allowed to settle for 2 h at 4 °C, until a sharp interface separating the two phases was clearly observable. The upper phase was removed using a Pasteur pipette (wide tip). The remaining lower phase, with interface, was then diluted with nine volumes of 15 mM Mes-Tris (pH 6.5), 330 mM sucrose, 1 mM DTT, and centrifuged at 60,000 *g* for 30 min. After centrifugation, pellets were resuspended in fresh buffer, divided into 100 µl aliquots, flash frozen in liquid nitrogen and stored at -70 °C until used.

2.2.4. **Enzyme assays.** The purity of plasma membranes and whole-cell homogenates in fractions obtained after sucrose density-gradient centrifugation or phase-partitioning were determined by assaying for vanadate-sensitive (plasma membrane) and azide-sensitive (mitochondrial membrane) ATPase activities, using the methods described by Widell and Larsson (1990). Optimal detergent activation of plasma membrane ATPase, after sucrose density-gradient centrifugation, was achieved according to the method of Serrano (1988). Protein determination was by the method of Bradford (1976), using BSA (Sigma, U.K.) as a standard.

2.2.5. **Lipid extraction and fatty acid analysis.** Lipids were extracted from whole-cell homogenates or membrane fractions using the method of Bligh and Dyer (1959) as modified by Griffiths and Harwood (1991), with the following modifications. Lipids from whole-cell homogenates or membrane fractions were extracted in to a methanol/chloroform/water (2:1:0.8) monophasic solvent mixture. Chloroform and distilled deionised water were added, resulting in the formation of a biphasic solvent mixture. After centrifugation at 1,000 *g* for 5 min the upper (aqueous) phase was removed and the lower (organic) phase, containing the lipids, was transferred to a clean glass tube. The chloroform was evaporated under N_2, and for fatty acid analysis methyl esters were generated by acid-catalysed esterification [2.5% (v/v) H_2SO_4 in dry methanol] at 70 °C for 2 h. Methyl esters were extracted with redistilled petroleum spirit (b.p. 60-80 °C) and subsequently analysed by gas-liquid chromatography. Pentadecanoate was used as an internal standard. Separations were routinely achieved using 10% SP-2330 on 100/120 Chromosorb-WAW (Supelco, Saffron Waldon, Essex, U.K.) packed into a stainless steel column [1.8 m x 0.3 mm (outer diameter)]. Fatty acids were identified by comparison with authentic standards.

2.2.6. **Potassium efflux.** Cells from the late-exponential/early-stationary phase were harvested by centrifugation at 1,500 *g* for 5 min and washed twice with distilled deionised water. Washed cells were suspended to a density of approximately 5×10^7 ml^{-1} in 40 ml of 20 mM Mes buffer (pH 6.0), and the suspension agitated by magnetic stirring. After 2 min, glucose was added to a final concentration of 1% (w/v). After a further 10 min equilibration, $Cd(NO_3)_2$ was added to the desired concentration. Extracellular K^+ was

measured continuously using an EE-K K^+-selective electrode (EDT Instruments, Dover, U.K.) coupled to a Jenway 3045 ion-analyser. Cd^{2+}-induced K^+ efflux measurements were corrected for small non-cadmium-induced changes in extracellular K^+ [which never exceeded 0.1 nmol K^+ $(10^6$ cells$)^{-1}$ over the time courses examined] that occurred in control suspensions in the absence of $Cd(NO_3)_2$.

2.2.7. **Cell viability.** Cell viability was determined as the ability to produce colony-forming units. At specified intervals after the addition of $Cd(NO_3)_2$ to cell suspensions (see above), aliquots were removed and, after appropriate dilution with sterile, distilled deionised water, plated on yeast-selective OGYE agar (Lab M, U.K.), containing 0.1% (w/v) oxytetracycline (Sigma, U.K.). Colonies were enumerated after 4 d incubation at 25 °C. Colony counts did not change with prolonged incubation up to 20 d.

2.2.8. **Cadmium uptake.** Late exponential/early stationary phase cells were harvested by centrifugation at 1,500 *g* for 5 min and washed twice with 20 mM Mes (pH 6.0). The final pellet was resuspended in 150 ml of the buffer to give an approximate cell density of 5×10^7 ml^{-1}. 50 ml-portions of this suspension were incubated with shaking at 120 rev. min^{-1} in 100 ml Erlenmeyer flasks at room temperature. After 10 min, glucose was added to a final concentration of 1% (w/v). After a further 10 min equilibration, $Cd(NO_3)_2$ was added. At specified intervals (up to 2 h), samples were removed, harvested by centrifugation at 1,500 *g* for 5 min and washed twice with distilled deionised water at 4 °C. Final cell pellets were digested by addition of 0.5 ml of 6 M HNO_3 and immersion of tubes in a water bath at 100 °C for 2 h. Cell debris was removed by centrifugation and,

after appropriate dilution with deionised water, the cadmium concentrations of the supernatants determined using a Baird alpha-2 atomic absorption spectrophotometer, with reference to appropriate standard solutions.

2.3. Results

2.3.1. **Influence of linoleate-supplementation on growth of *S. cerevisiae* NCYC 1383 in the absence and presence of $Cd(NO_3)_2$.** Linoleate (1 mM) supplementation was found to have no discernible effect on the growth of *S. cerevisiae* in YEPD medium. Cell doubling times during the exponential phase were approximately 2.5 h, and final cell yields after 24 h approximately 1.5×10^8 ml^{-1}, in both unsupplemented and linoleate (18:2)-supplemented media (Fig. 2.1). Growth in the presence of 80 μM $Cd(NO_3)_2$ was associated with extended lag phases, longer doubling times and reduced final cell yields. However, these effects were considerably more marked for 18:2-supplemented cultures. For example, cell yields after 24 h growth in the presence of $Cd(NO_3)_2$ were approximately 4×10^7 ml^{-1} and 1.8×10^7 ml^{-1} in unsupplemented and 18:2-supplemented cultures, respectively; these represented respective 74% and 88% decreases compared to the cell yield of cultures incubated without $Cd(NO_3)_2$ (Fig. 2.1).

2.3.2. **Fatty acid composition of *S. cerevisiae* NCYC 1383 during growth in unsupplemented, linoleate- and linolenate-supplemented media.** In order to confirm that growth of *S. cerevisiae* in polyunsaturated fatty acid (PUFA)-supplemented medium resulted in incorporation of exogenous fatty acids into total cellular lipids, lipid extracts from cells grown in unsupplemented and PUFA-supplemented media were analysed. *Saccharomyces cerevisiae* readily incorporated exogenous PUFAs from its growth medium (Fig. 2.2; Table 2.1).

Fig. 2.1. Influence of linoleate-supplementation on growth of *Saccharomyces cerevisiae* NCYC 1383 in the absence and presence of cadmium. *S. cerevisiae* from a 48 h starter culture was inoculated to A_{550} ~ 0.1 in unsupplemented (○,●) and linoleate-supplemented (□,■) medium. Cell numbers were determined during growth in the absence (○,□) and presence (●,■) of 80 μM $Cd(NO_3)_2$. Points represent means from three replicate counts (more than 400 cells total); Standard error of the mean (SEM) values are smaller than the dimensions of the symbols.

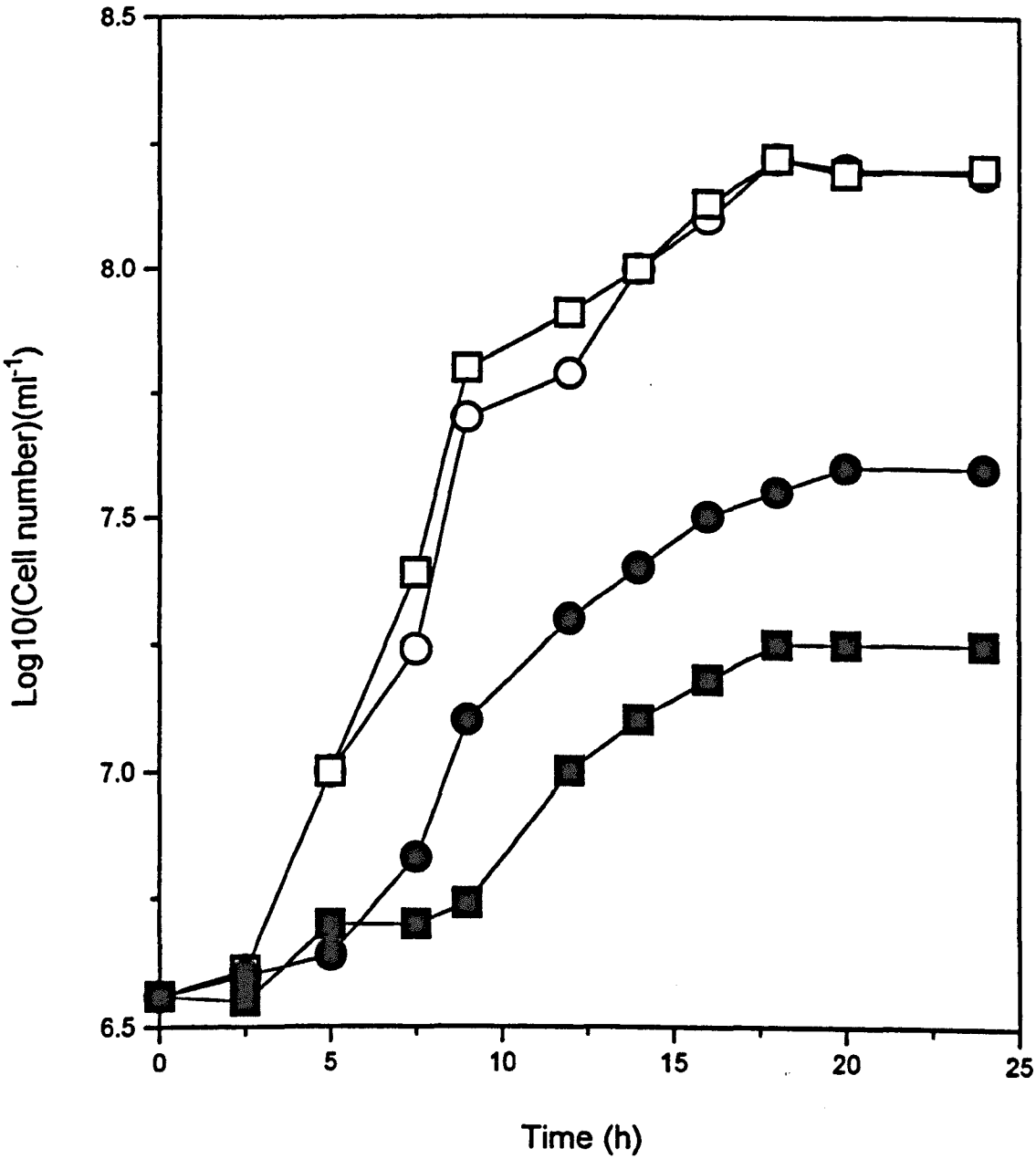
8.5
8.0
7.5
7.0
6.5
0
5
10
15
20
25
Log10(Cell number)(ml-1)
Time (h)

Fig. 2.2. Gas-chromatograph trace of the fatty acid profiles of *S. cerevisiae* NCYC 1383 previously grown in unsupplemented (a) and linoleate-supplemented (b) medium.

a.

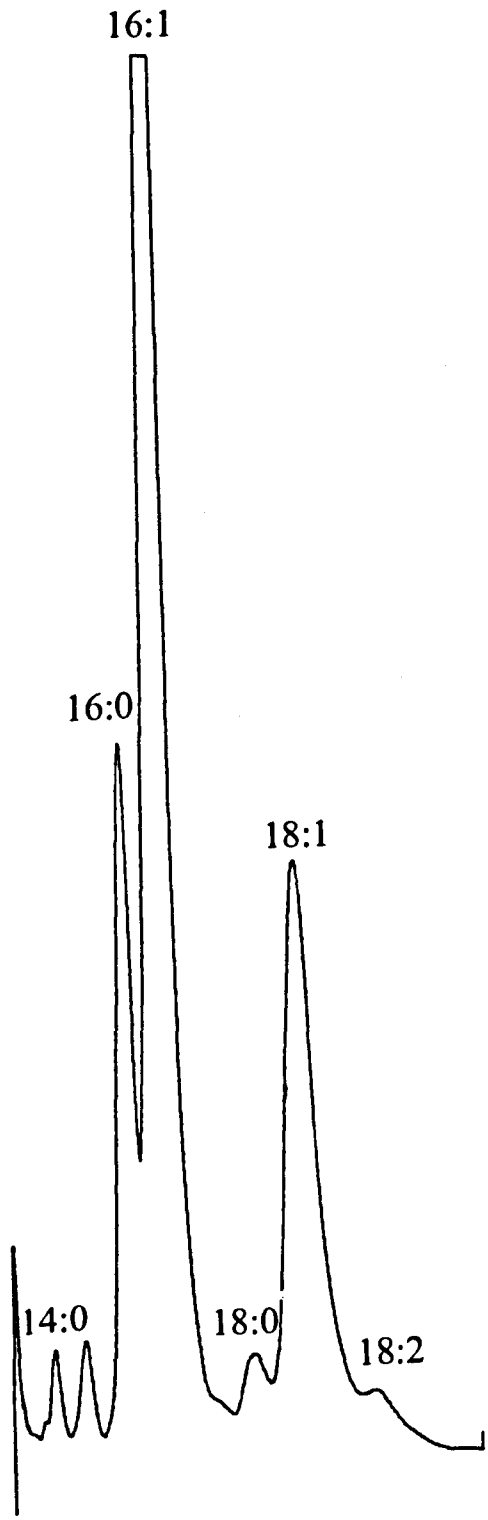

b.

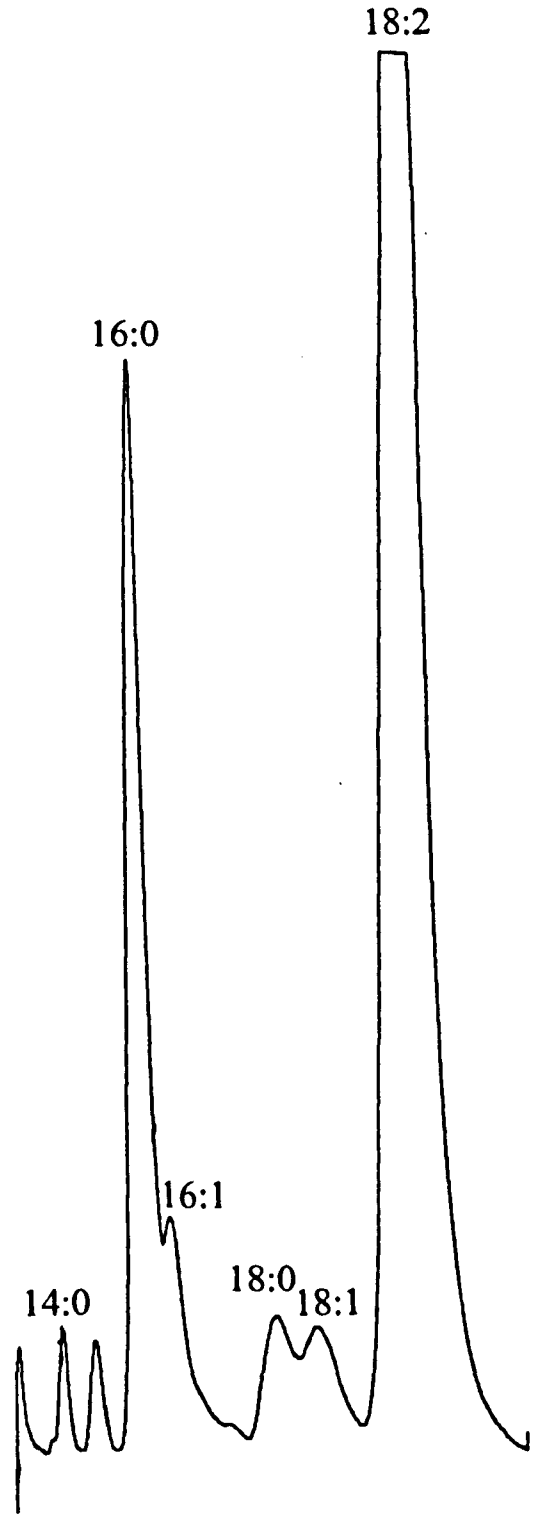

In agreement with other reports (Bossie and Martin, 1989; Stukey *et al.*, 1989), analysis of cell lipid extracts from *S. cerevisiae* grown in unsupplemented medium revealed only trace quantities of 18:2, while 18:3 was not detected. However, cells grown in the presence of 18:2 or 18:3 readily incorporated high levels of these fatty acids. For example, after 16 h growth (late-exponential/early-stationary phase), when incorporation of exogenous fatty acids was at a maximum, 18:2 constituted approximately 68% (Fig. 2.2) and 18:3 approximately 69% of total fatty acids in cells from 18:2- and 18:3-supplemented cultures, respectively (Table 2.1). Increases in PUFA content, as a proportion of total cellular fatty acids, during growth in supplemented media were contemporaneous with decreases in the monounsaturated fatty acids palmitoleate (16:1) and oleate (18:1); the fatty acid composition at 0 h (not shown) was similar to that of cells in unsupplemented medium at 16 h. The unsaturation index (average number of double bonds per fatty acid) was found to increase during exponential growth, and was maximal during the late-exponential/early-stationary phase (Fig. 2.3; Table 2.1). At any time, values for cellular unsaturation index decreased in the order 18:3-supplemented > 18:2-supplemented > unsupplemented (Fig. 2.3; Table 2.1).

The fatty acid composition of *S. cerevisiae* grown in the presence of 80 μM $Cd(NO_3)_2$ showed differences to that of cells grown without $Cd(NO_3)_2$ (Table 2.2). Between 0 and 16 h, cells growing in the presence of Cd^{2+} generally displayed a lower content of PUFAs, as a proportion of total cellular fatty acids, than cells growing in the absence of Cd^{2+} after corresponding periods of growth. This was most evident as lower proportions of 18:2 and 18:3 during early growth in 18:2- and 18:3-supplemented

Table 2.1. Changes in cellular fatty acid composition during growth of *S. cerevisiae* NCYC 1383 in unsupplemented, linoleate- and linolenate-supplemented media

Medium	Fatty acid	Age of culture (h)					
		4	8	12	16	20	24
Unsupple-	16:0	29.1±0.3	25.5±1.6	24.1±0.3	20.2±0.7	17.1±0.1	17.0±0.3
mented	16:1	38.2±0.2	46.0±6.6	51.7±0.2	55.7±1.4	57.4±0.1	54.4±1.1
	18:0	15.9±0.1	10.7±3.9	4.6±0.1	4.2±0.9	3.1±0.1	4.1±0.1
	18:1	16.8±0.7	17.8±1.2	19.5±0.2	19.9±0.3	22.4±0.1	24.5± tr.
	18:2	tr.	tr.	tr.	tr.	tr.	tr.
	U.I.	*0.55*	*0.64*	*0.71*	*0.76*	*0.80*	*0.79*
18:2-sup-	16:0	21.9±0.1	20.5±0.9	20.6±0.1	19.6±0.3	20.1±0.2	19.7±0.7
plemented	16:1	22.9±3.1	9.8±0.3	7.4±0.1	5.7±1.0	6.3± tr.	7.7±1.1
	18:0	9.4±0.7	6.0± tr.	5.0±0.1	4.6± tr.	4.6± tr.	5.5±0.2
	18:1	10.7±0.3	5.0± tr.	3.2±0.1	2.4± tr.	2.8±0.1	3.4±0.3
	18:2	35.1±2.8	58.7±0.5	63.8±1.2	67.7±0.8	66.2±0.3	63.7±0.5
	U.I.	*1.04*	*1.32*	*1.38*	*1.44*	*1.42*	*1.38*
18:3-sup-	16:0	23.9±0.3	20.4±1.0	19.6±0.4	18.8± tr.	20.6±0.4	18.5± tr.
plemented	16:1	27.0±1.2	10.3±1.8	6.9±0.5	5.2±0.2	6.2±0.4	7.7±0.6
	18:0	9.8±0.4	6.4±0.3	5.0±0.1	4.9± tr.	5.5±0.2	5.2± tr.
	18:1	15.1±0.8	5.0±0.7	3.1±0.2	2.4± tr.	3.3±0.2	4.1±0.2
	18:2	tr.	tr.	tr.	tr.	tr.	tr.
	18:3	24.2±0.9	57.9±4.9	65.4±1.8	68.7±1.0	64.4±1.6	64.5±0.2
	U.I.	*1.15*	*1.89*	*2.06*	*2.14*	*2.03*	*2.05*

Fatty acids are abbreviated with the first figure representing the number of carbon atoms in the fatty acyl chain and the second representing the number of double bonds. U.I. refers to the unsaturation index (average number of double bonds per fatty acid). Values for percentage fatty acid composition are means from two replicate determinations ± SD. (tr. < 0.1).

Table 2.2. Changes in cellular fatty acid composition during growth of *S. cerevisiae* NCYC 1383 in unsupplemented, linoleate- and linolenate-supplemented media in the presence of 80 μM $Cd(NO_3)_2$

Medium	Fatty acid	Age of culture (h)					
		4	8	12	16	20	24
Unsupple-	16:0	34.7±1.0	39.9±2.1	37.3±1.1	18.1±0.7	17.8±0.3	17.2±0.3
mented	16:1	34.1± tr.	35.8±0.7	36.8±1.1	49.6±1.0	49.5±1.3	49.7±0.6
	18:0	11.4±1.1	7.2±1.4	8.9±0.3	5.8±0.3	6.1±0.2	5.9±0.2
	18:1	19.8±0.2	17.1±1.4	17.0±0.3	26.5±0.6	26.6±0.8	27.3±0.7
	U.I	*0.54*	*0.53*	*0.54*	*0.76*	*0.76*	*0.77*
18:2-sup-	16:0	32.2±5.0	28.1±0.2	23.2±0.3	22.2±0.8	16.3±2.0	9.5±1.0
plemented	16:1	20.0± tr.	19.8±3.6	13.4±0.5	12.4±0.3	9.1±0.7	6.6±0.7
	18:0	8.8±1.0	6.2±0.3	4.0±0.1	3.1±0.2	3.2±0.2	2.2±0.4
	18:1	11.5±0.7	8.8±0.7	4.1±0.3	3.5±0.2	3.2±0.2	2.1±0.8
	18:2	27.5±3.0	37.1±4.8	55.3±0.6	58.8± tr.	68.2±2.7	79.6±3.2
	U.I.	*0.87*	*1.03*	*1.28*	*1.34*	*1.49*	*1.68*
18:3-sup-	16:0	28.1±0.4	23.6±2.5	21.6±0.1	21.6±3.6	15.2±0.2	6.9±0.4
plemented	16:1	20.3±1.5	14.4±1.3	12.7±1.1	12.6±1.8	9.7±0.1	5.3±1.1
	18:0	8.7±1.1	5.8±0.3	4.9±0.2	5.3±0.7	4.5±0.1	2.8±0.3
	18:1	10.2±0.3	8.3±1.7	7.0±1.9	5.3±1.3	4.6± tr.	3.4±0.5
	18:2	5.3±1.2	3.4±1.6	3.0±0.9	3.0±0.1	1.9±0.2	2.3±1.4
	18:3	27.4±1.4	44.5±7.9	50.8±4.3	52.2±0.3	64.1±0.1	79.3±2.3
	U.I.	*1.23*	*1.63*	*1.78*	*1.81*	*2.10*	*2.51*

Footnotes as for Table 2.1.

media (although 18:2 comprised between 2% and 5% of fatty acids in 18:3-supplemented Cd^{2+}-exposed cells), and a lower proportion of 16:1 in cells grown in unsupplemented medium. However, whereas no further incorporation of exogenous fatty acids was evident during stationary phase in the absence of Cd^{2+} (Table 2.1), 18:2 and 18:3 incorporation continued up to 24 h in Cd^{2+}-exposed fatty acid-supplemented cultures (Table 2.2). After 24 h growth, unsaturation indices of the latter cultures were approximately 22% higher than those of corresponding cultures grown in the absence of Cd^{2+} (Fig. 2.3). Despite these differences, the results presented in Figure 2.3 and Table 2.2 confirm that cultures grown in the presence of Cd^{2+} still incorporate exogenous fatty acids to an extent that can markedly alter their overall degree of fatty acid unsaturation. Thus, the cultures that were most inhibited by Cd^{2+} in Fig. 2.1 were those that had the higher fatty acid unsaturation index (Fig. 2.3; Table 2.2).

2.3.3. **Fatty acid composition of plasma membrane-enriched fractions.** The incorporation of exogenous linoleate and linolenate was maximal after 16 h growth (Fig. 2.3; Table 2.1), when cultures were in the late-exponential/early-stationary phase. Hence, cells from 16 h cultures were used for all subsequent short-term experiments. However, as this study was primarily concerned with cadmium toxicity exerted at the plasma membrane, it was initially necessary to confirm incorporation of exogenous 18:2 and 18:3 into plasma membrane lipids. In order to assess purity of isolated plasma membrane fractions (see Section 2.2.4), vanadate-sensitive ATPase (plasma membrane marker) and azide-sensitive ATPase (mitochondrial membrane marker) activities were assayed. Plasma membrane-enriched fractions from cells grown in unsupplemented and

Fig. 2.3. Fatty acid unsaturation of *S. cerevisiae* NCYC 1383 during growth in unsupplemented and PUFA-supplemented medium, in the absence and presence of cadmium. Cells from a 48 h starter culture (lacking fatty acid supplements) were inoculated in to fresh medium to a concentration of 2×10^6 cell ml^{-1}. Unsaturation indices were determined during growth at 25 °C in unsupplemented (○,●), linoleate- (□,■) or linolenate- (Δ,▲) supplemented medium in the absence (○,□,Δ) or presence (●,■,▲) of 80 μM $Cd(NO_3)_2$. Because of the large differences in unsaturation index values, the data for unsupplemented and linoleate-supplemented cells (a), and linolenate-supplemented cells (b), are presented separately.

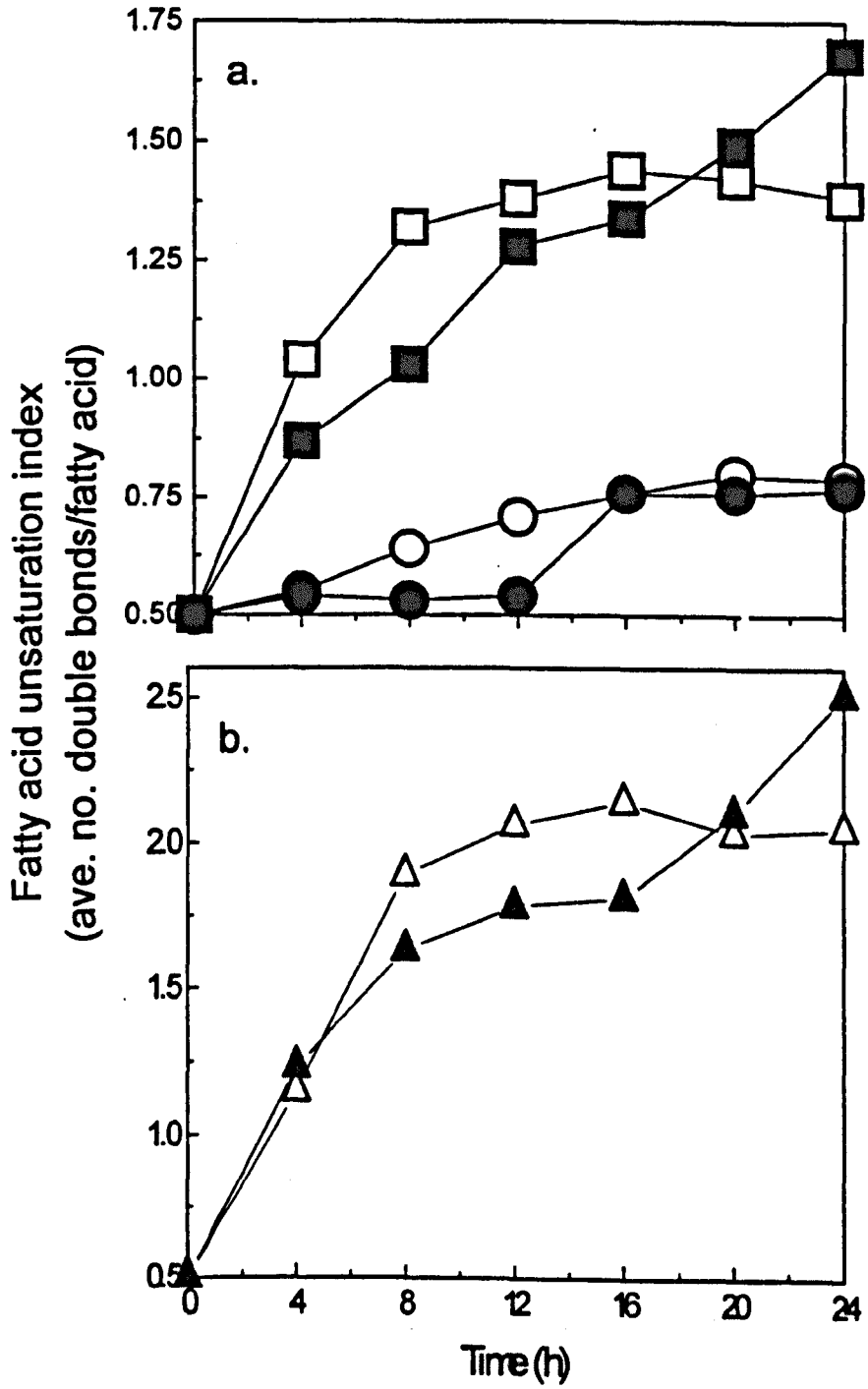
a.
b.
Fatty acid unsaturation index
(ave. no. double bonds/fatty acid)
Time (h)
1.75
1.50
1.25
1.00
0.75
0.5
25
20
1.5
1.0
0.5
0
4
8
12
16
20
24

18:2-supplemented media displayed vanadate-sensitive ATPase activities 15-fold and 26-fold greater than those of respective whole-cell homogenates (Table 2.3). In contrast, azide-sensitive activities were higher in the homogenates. The lower phase of the aqueous two-phase polymer system, used for purification of plasma membranes from 18:3-supplemented cells, displayed vanadate-sensitive ATPase activity approximately 7-fold greater than that of the upper phase and 16-fold greater than that of the homogenate. However, whereas azide-sensitive activity was highest in the upper phase, enrichment of the mitochondrial ATPase was evident in both upper and lower phases when compared to homogenate activity, suggesting some contamination of the 18:3-enriched plasma membrane fraction. Repeated partitioning resulted in no further improvement in plasma membrane purity. However, in view of the greater relative enrichment of the vanadate-sensitive ATPase (16-fold compared to 8-fold for azide-sensitive activity), and, most importantly, that all plasma membrane fractions displayed high vanadate-sensitive activities, similar to those of plasma membranes isolated by other workers (Serrano, 1988; Schmidt *et al.*, 1983), it was considered that the fractions obtained were of sufficient purity for lipid analysis.

The fatty acid compositions of plasma membrane-enriched fractions from cells grown for 16 h in unsupplemented, 18:2- and 18:3-supplemented media (Table 2.4) were very similar to those of their corresponding whole-cell homogenates (Table 2.1). The proportions of 18:2 and 18:3 in plasma membrane fractions from supplemented cells were approximately 5% higher and 5% lower, respectively, than those of whole cells. In unsupplemented cells, the relative proportion of 16:1 was slightly lower in plasma membranes than in whole-cell homogenates. In spite of these minor differences, fatty

Table 2.3. Purification of plasma membranes from *S. cerevisiae* NCYC 1383 grown for 16 h in unsupplemented, linoleate- and linolenate-supplemented media

Fraction	Specific ATPase activity [μmol (mg protein)$^{-1}$ min^{-1}] Vanadate-sensitive	Azide-sensitive
Unsupplemented		
Homogenate	0.055	0.146
Plasma membrane	0.799	0.053
18:2-supplemented		
Homogenate	0.026	0.076
Plasma membrane	0.679	0.042
18:3-supplemented		
Homogenate	0.066	0.086
Upper phase	0.145	0.721
Lower phase	1.078	0.704

The results shown are typical values from one of at least three experiments.

Table 2.4. Fatty acid composition of plasma membrane-enriched fractions from *S. cerevisiae* NCYC 1383 grown for 16 h in unsupplemented, linoleate- and linolenate-supplemented media

Fatty acid	Medium		
	Unsupplemented	18:2-supplemented	18:3-supplemented
16:0	23.4±1.1	19.2±0.5	20.4±1.0
16:1	50.7±0.8	4.1±0.4	5.0±0.3
18:0	5.3±0.9	3.7±0.3	5.4±0.3
18:1	20.6±1.1	2.0±0.1	3.9±0.6
18:2	tr.	71.0±1.3	tr.
18:3	n.d.	n.d.	65.3±1.7
U.I.	*0.71*	*1.48*	*2.05*

Values for percentage fatty acid composition are means from two separate experiments ± SD. (n.d. = not detectable; tr. < 0.1).

acid unsaturation indices calculated for plasma membrane-enriched fractions were similar to those of whole cells and again decreased in the order 18:3-supplemented > 18:2-supplemented > unsupplemented (Table 2.4).

2.3.4. **Cd^{2+}-induced K^+ efflux from unsupplemented and PUFA-supplemented *S. cerevisiae* NCYC 1383.** Cadmium can cause perturbations in the structural integrity of microbial organellar and cellular membranes (Aβmann *et al.*, 1996; Gadd and Mowll, 1983). Here, release of intracellular K^+ was used as a means of assessing cadmium-induced impairment of plasma membrane integrity. Following $Cd(NO_3)_2$ addition, K^+ efflux from *S. cerevisiae* previously grown in PUFA-supplemented media was markedly higher than that from cells grown in unsupplemented medium (Fig. 2.4). Rates of K^+ release were maximal between 5 and 10 min after Cd^{2+} addition. After 12 min exposure to 50 μM $Cd(NO_3)_2$, amounts of K^+ released from 18:2- and 18:3-enriched cells were approximately equal at 1.5 nmol $(10^6 \text{ cells})^{-1}$, while that from cells grown in unsupplemented medium was only 0.6 nmol $(10^6 \text{ cells})^{-1}$ (Fig. 2.4a). At 100 μM Cd^{2+}, K^+ efflux was greater, indicating more rapid plasma membrane permeabilisation at this higher Cd^{2+} concentration (Fig. 2.4b). However, relative rates of K^+ release showed a similar pattern to those at 50 μM Cd^{2+}, although a difference between 18:2- and 18:3-supplemented cells also became apparent. Thus, amounts of K^+ released after 12 min exposure to 100 μM Cd^{2+} were approximately 1.9, 5.0 and 5.9 nmol $(10^6 \text{ cells})^{-1}$ from cells grown in unsupplemented, 18:2- and 18:3-supplemented media, respectively. The results indicate that the susceptibility of *S. cerevisiae* to Cd^{2+}-induced plasma membrane-disruption increases with the degree of plasma membrane fatty acid unsaturation.

Fig. 2.4. Cadmium-induced potassium efflux in unsupplemented and PUFA-supplemented *S. cerevisiae* NCYC 1383. Cells were grown for 16 h in unsupplemented (○), linoleate- (●) and linolenate- (□) supplemented medium, harvested, washed and resuspended in 20 mM Mes (pH 6.0). After addition of glucose (1% w/v), Cd^{2+} was added to a final concentration of (a) 50 μM and (b) 100 μM. Values for K^+ release are means from three replicate determinations ± SEM where these values exceed the dimensions of the symbols.

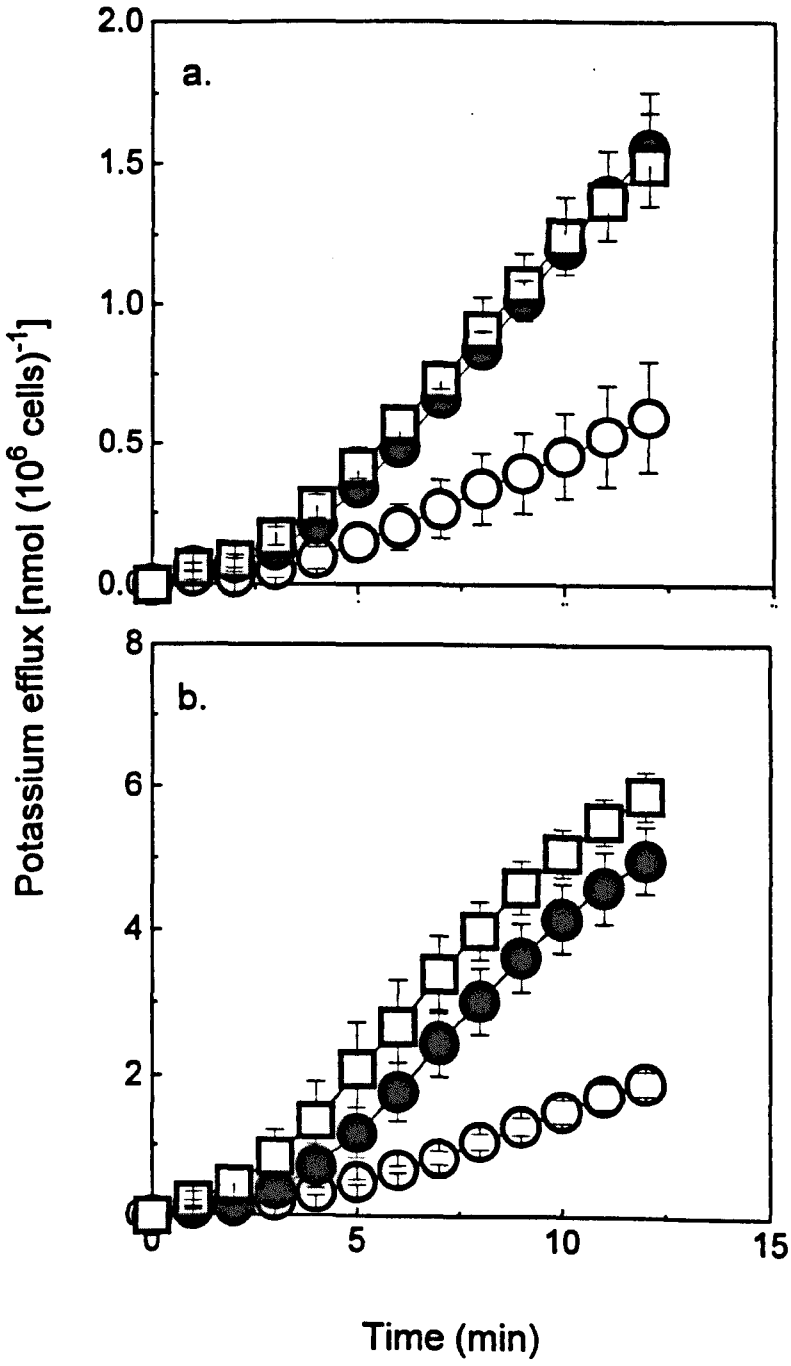
a.
b.
2.0
1.5
1.0
0.5
0.0
8
6
4
2
0
5
10
15
Potassium efflux [nmol (10^6 cells)$^{-1}$]
Time (min)

2.3.5. Effect of cadmium on the viability of unsupplemented and PUFA-supplemented *S. cerevisiae* NCYC 1383. In order to determine whether increases in the susceptibility of cells grown in unsaturated fatty acid-supplemented media to Cd^{2+}-induced K^+ efflux were reflected in whole-cell toxicity measurements, changes in cell viability were determined after Cd^{2+} exposure (Fig. 2.5). Cd^{2+} exposure resulted in losses of cell viability that were particularly sharp during the first 1-2 h of incubation. Reductions in viability were greater in PUFA-supplemented cells than in unsupplemented cells. For example, after 1 h incubation in the presence of 50 μM $Cd(NO_3)_2$, only 51% and 37% of cells previously grown in 18:2- and 18:3-supplemented media, respectively, were still viable (capable of colony formation), whereas 87% viability was maintained in cells from unsupplemented medium (Fig. 2.5a). Between 2 and 5 h incubation in the presence of 50 μM Cd^{2+}, small increases in the percentage viability of unsupplemented and 18:2-supplemented cells were evident, possibly representing cell division among *S. cerevisiae* sub-populations of lower cadmium-sensitivity. Thus, after 5 h incubation, the percentage viability of unsupplemented cells was approximately seven-fold higher than that of 18:3-supplemented cells. Incubation in the presence of 100 μM $Cd(NO_3)_2$ had a more marked effect on cell viability, which in all cases was reduced to less than 20% within 2 h (Fig. 2.5b). Again, the decline in viability was most rapid in PUFA-supplemented cells. After 5 h, percentage viability was reduced to approximately zero in 18:2- and 18:3-supplemented *S. cerevisiae*, whereas 14% viability was maintained in unsupplemented cells. Similar results and trends to those described above were obtained using alternative methods for determining viability, e.g. dye (methylene violet) exclusion (results not shown).

Fig. 2.5. Effect of cadmium on the viability of unsupplemented and PUFA-supplemented *S. cerevisiae* NCYC 1383. Cells were grown for 16 h in unsupplemented (○), linoleate- (●) and linolenate- (□) supplemented medium, harvested, washed and resuspended in 20 mM Mes (pH 6.0). After addition of glucose (1% w/v), Cd^{2+} was added to a final concentration of (a) 50 μM and (b) 100 μM. Percentage viability was calculated by reference to colony counts from samples obtained just prior to Cd^{2+} addition. Values are means from three replicate determinations from single experimental flasks ± SEM. Results from one of at least three experiments are shown.

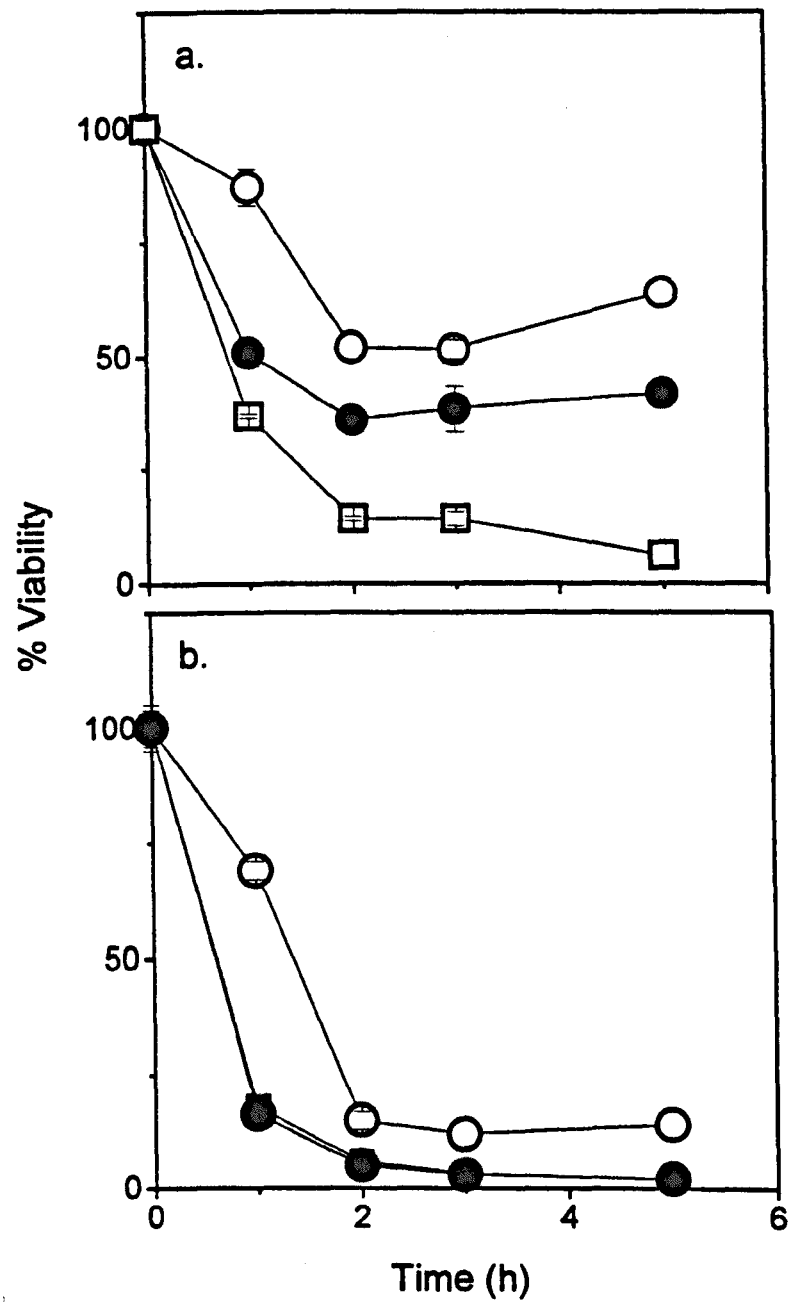
a.
b.
100
50
0
% Viability
0
2
4
6
Time (h)

2.3.6. Cd^{2+} uptake by unsupplemented and PUFA-supplemented *S. cerevisiae* NCYC 1383.

In order to determine whether differences in Cd^{2+}-induced K^+-efflux and whole-cell toxicity could be accounted for by differences in levels of cellular Cd^{2+} uptake, the latter was examined in cells previously grown in unsupplemented, 18:2- and 18:3-supplemented media (Fig. 2.6). Cd^{2+} uptake was characterised by an initial rapid phase (complete within 10 min), which probably represented metabolism-independent cell-surface adsorption, followed by a slower phase most likely corresponding to intracellular Cd^{2+} transport, or plasma membrane permeabilisation and inward Cd^{2+} diffusion (Gadd and Mowll, 1983). Cd^{2+} uptake during both phases was similar in the presence of 50 μM and 100 μM Cd^{2+}, and did not appear to be affected by the fatty acid composition of *S. cerevisiae*. Thus, after 4 h incubation, cellular Cd^{2+} levels were approximately 0.4 nmol $(10^6 \text{ cells})^{-1}$ in all cases (Fig. 2.6). Differences in Cd^{2+}-induced toxicity in cells grown in unsupplemented, 18:2- and 18:3-supplemented media were, therefore, not attributable to differences in cellular Cd^{2+} uptake.

Fig. 2.6. Cadmium uptake by unsupplemented and PUFA-supplemented *S. cerevisiae* NCYC 1383. Cells were grown for 16 h in unsupplemented (○), linoleate- (●) and linolenate- (□) supplemented medium, harvested, washed and resuspended in 20 mM Mes (pH 6.0). After addition of glucose (1% w/v), Cd^{2+} was added to a final concentration of (a) 50 μM and (b) 100 μM. Values for cellular Cd^{2+} are means from three replicate determinations ± SEM where these values exceed the dimensions of the symbols.

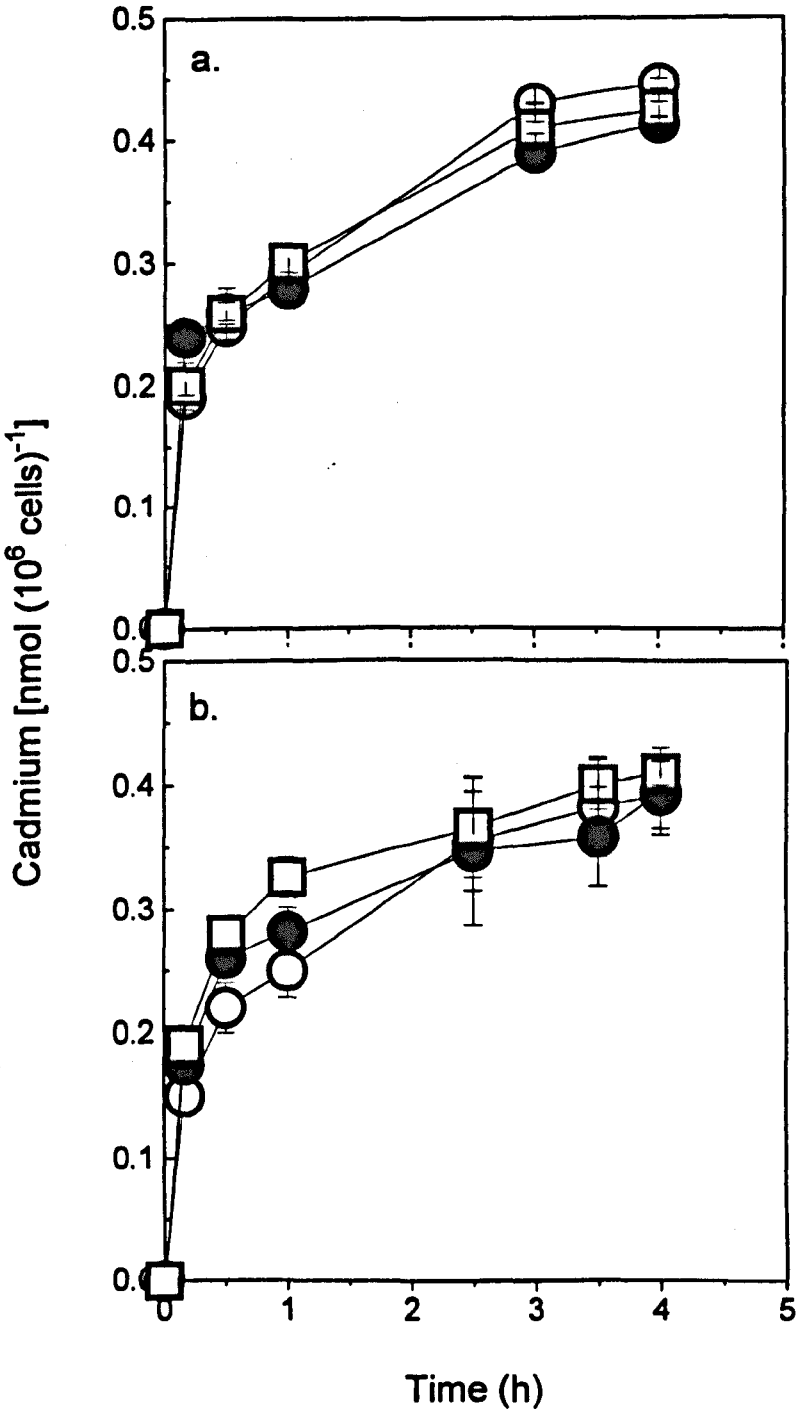
a.
b.
0.5
0.4
0.3
0.2
0.1
0.0
0
1
2
3
4
5
Cadmium [nmol (10^6 cells)$^{-1}$]
Time (h)

2.4. Discussion

Cadmium toxicity towards *S. cerevisiae* NCYC 1383 was accentuated when cells were enriched with the polyunsaturated fatty acids (PUFAs) linoleate and linolenate. *Saccharomyces cerevisiae* does not normally synthesise PUFAs but can readily incorporate exogenous unsaturated fatty acids into cellular lipids during growth, and this has no adverse effect on cell division (Van der Westhuizen *et al.*, 1994; Wagner and Paltauf, 1994; Bossie and Martin, 1989). The consequent advantages of such a model system for determining physiological effects directly related to altered fatty acid composition have been highlighted (Avery *et al.*, 1996; Maresca and Cossins, 1993). Conventional systems used to manipulate fatty acid composition, which include anaerobic culturing (Watson and Rose, 1980), low-temperature shift (Suutari *et al.*, 1990), or the use of cerulenin (specific inhibitor of sterol and fatty acid synthesis) (Awaya *et al.*, 1975), often adversely affect growth parameters and a range of physiological characteristics.

The very high incorporation of linoleate and linolenate observed here, which was maximal during the late-exponential/early-stationary growth phase at > 65% of total fatty acids, was similar in whole-cell homogenates and plasma membrane-enriched fractions. Therefore, the effects of cadmium on the plasma membrane integrity of cells enriched with different fatty acids could be correlated with their plasma membrane fatty acid compositions. Observed decreases in the relative proportions of monounsaturated fatty acids in linoleate- and linolenate-enriched cells were in keeping with a sharp repression

of Δ-9 fatty acid desaturase activity in PUFA-supplemented *S. cerevisiae*, as reported elsewhere (Bossie and Martin, 1989; Stukey *et al.*, 1989).

Exposure of *S. cerevisiae* to toxic concentrations of Cd^{2+} generally results in plasma membrane permeabilisation, which is readily detectable as a rapid non-stoichiometric loss of cellular K^+ (Gadd and Mowll, 1983; Norris and Kelly, 1977). Extensive K^+ efflux (such as the approximately 50% loss within 12 min at 100 μM Cd^{2+} reported here) is generally irreversible, although, in mixed populations, K^+ released by sensitive cells may subsequently be taken up by non-sensitive cells (Gadd and Mowll, 1983). In the present study, the slight lag (~2 min) in K^+ efflux may have represented the time taken for Cd^{2+} to traverse the plasma membrane; no membrane permeabilisation was evident in the absence of metabolism-dependent cadmium uptake (where glucose was not included in incubations) (results not shown). As described elsewhere (e.g. Avery *et al.*, 1996), reductions in yeast viability were correlated with the relative extent of plasma membrane permeabilisation; a one-to-one relationship between percentage viability and percentage K^+ retention was not evident, although such comparisons are complicated by all-or-none effects (Kuypers and Roomans, 1979). Cd^{2+} uptake did not vary with fatty acid composition. Thus, the elevated susceptibility of linoleate- and particularly linolenate-enriched cells to Cd^{2+} toxicity could not be related to altered Cd^{2+} transport activity [it is well documented that the activity of certain membrane transport proteins can be altered by changes in plasma membrane fatty acid composition (Hazel and Williams, 1990; Serrano, 1978). Indeed, increased V_{max} and K_m values for Cs^+ transport in linoleate-supplemented *S. cerevisiae* have recently been reported (Hoptroff *et al.*,

1997)]. Hence, this effect was, therefore, likely to be directly related to plasma membrane properties.

Under non-stressed conditions (e.g. in the absence of toxic metals) the introduction of unsaturated fatty acyl chains into plasma membrane lipid bilayers tends to result in reduced membrane order, or increased membrane 'fluidity' (De Vos *et al.*, 1993; Hazel and Williams, 1990). Large increases in membrane disorder can disrupt plasma membrane functions, including impermeability to the passive diffusion of ions such as K^+ and Na^+ (Hazel and Williams, 1990). Such effects alone could not account for the rapid Cd^{2+}-induced losses in cellular K^+ observed here, but they may be accentuated through oxidation of unsaturated fatty acids (Tyson and Frazier, 1994). Reactive oxygen species (e.g. superoxide anions and hydroxyl radicals), which may be generated during normal cellular respiratory metabolism, promote lipid peroxidation (Dix and Aikens, 1993). This can result in destabilisation of hydrophobic membrane bilayers by the need to accommodate polar hydroperoxide groups, with a subsequent deterioration of membrane integrity (Van Ginkel and Sevanian, 1994; Dix and Aikens, 1993), such as that indicated here. Studies with higher organisms have shown that certain metal species can actively promote the generation of reactive oxygen species in cells, leading to saturation of cellular protective mechanisms [e.g. glutathione, superoxide dismutases] at toxic concentrations (Stohs and Bagchi, 1995). Furthermore, recent evidence suggests that the toxicity of the redox-active metal copper towards *S. cerevisiae* may also linked to oxyradical generation (Avery *et al.*, 1996; Culotta *et al.*, 1995; Greco *et al.*, 1990).

Redox-cycling activity cannot account for effects induced by the non-redox-active metal cadmium in this study. However, metals without redox capacity may promote lipid

peroxidation by depleting glutathione and protein-bound sulphydryl groups (Figueiredo-Pereira *et al.*, 1998; Li *et al.*, 1997; Stohs and Bagchi, 1995), or by interacting with membranes to stimulate Fe^{3+}/Cu^{2+}-initiated lipid peroxidation indirectly (Verstraeten and Oteiza, 1995; Halliwell and Gutteridge, 1989) [it should be noted that enhancement of Cd^{2+} toxicity in the presence of the latter ions may not be evident in intact *S. cerevisiae* because of simultaneous alleviation of Cd^{2+}-induced perturbations of Fe metabolism (Lesuisse and Labbe, 1995)]. Indeed, the yeast cadmium factor, encoded by *YCF1*, specifically catalyzes the MgATP-energized uptake of bis(glutathionato)cadmium ($Cd{\cdot}GS_2$) by vacuolar membrane vesicles (Li *et al.*, 1997). The increasing susceptibility of lipids with increasing degrees of fatty acid unsaturation to such oxy-radical induced lipid peroxidation (Halliwell and Gutteridge, 1989) could thus account for the results from K^+-efflux and whole-cell toxicity experiments presented here. Variations in cellular levels of a single PUFA (linoleate) may also give corresponding variations in metal sensitivity (Avery *et al.*, 1996).

Oxidative degradation of unsaturated fatty acids was supported by the lower cellular fatty acid unsaturation indices evident during exponential growth in the presence of Cd^{2+}; depletion of unsaturated fatty acids is a useful marker of lipid peroxidation (De Vos *et al.*, 1993). That this effect could not simply be attributed to reduced incorporation of exogenous unsaturated fatty acids, was supported by the lower degree of fatty acid unsaturation in the presence of Cd^{2+} also evident in cells grown in the absence of a fatty acid supplement. The increased unsaturation index apparent at later stages of growth was probably a consequence of the elevated anti-oxidant status and stress-resistance of stationary phase yeast cells (Morodas-Ferreira *et al.*, 1996; Steels *et al.*, 1994).

Thus, cadmium toxicity towards *S. cerevisiae* was found to be markedly dependent on plasma membrane fatty acid composition. These findings are of pertinence to metal toxicity in the natural environment, where the fatty acid composition of microorganisms displays considerable heterogeneity (Pennanen *et al.*, 1996; White, 1993; Hazel and Williams, 1990). While several other determinants (constitutive and inducible) of microbial resistance to cadmium have already been described (Li *et al.*, 1997; Jungmann *et al.*, 1993*a*), this is the first report suggesting a possible passive role of cellular or plasma membrane fatty acid composition and further investigation of this relationship is warranted.

CHAPTER 3

Induction of Lipid Peroxidation during Heavy-Metal Stress in *Saccharomyces cerevisiae* and Influence of Plasma Membrane Fatty Acid Unsaturation

3.1. Introduction

In chapter 2 the relationship between plasma membrane fatty acid unsaturation and susceptibility towards the toxicity of the nonredox-active metal cadmium was investigated. *Saccharomyces cerevisiae* NCYC 1383 was demonstrated to readily incorporate high levels of the exogenously-supplied polyunsaturated fatty acids (PUFAs) linoleate (18:2) and linolenate (18:3) into whole-cell and plasma membrane lipids. In agreement with several reports, incorporation of exogenous PUFAs had no adverse effects on cell division (Bossie and Martin, 1989; Stukey *et al.*, 1989; Watson and Rose, 1980). However, PUFA-enriched *S. cerevisiae* were demonstrated to be markedly more susceptible towards Cd^{2+}-induced plasma membrane permeabilisation and whole-cell toxicity. Furthermore, Avery *et al.* (1996) had also demonstrated the elevated sensitivity of linoleate-enriched *S. cerevisiae* to plasma membrane permeabilisation and whole-cell toxicity upon exposure to the redox-active metal copper. While several reports have previously demonstrated heavy metal-induced perturbation of plasma membrane integrity, with associated cytosolic-solute leakage, e.g. K^+ efflux, in *S. cerevisiae* (Aβmann *et al.*, 1996; Ohsumi *et al.*, 1988; De Rome and Gadd, 1987; Kessels *et al.*, 1985), this was the first report indicating increased susceptibility with increasing degrees of plasma membrane fatty acid unsaturation.

The mechanism underlying the increased metal sensitivity of PUFA-enriched cells was not elucidated. However, one general cause for loss of membrane integrity in biological systems, in response to a variety of stimuli, can arise through oxy-radical

mediated lipid peroxidation (Halliwell and Gutteridge, 1989; Mehlhorn, 1986). The accumulation of lipid peroxidation products, such as lipid hydroperoxides, within the hydrophobic core of plasma membranes can result in disturbances in the arrangement of phospholipid moieties, an increase in the membrane phase transition temperature, and ultimate impairment of membrane function (manifested as K^+ loss) (Weckx and Clijsters, 1996; Van Ginkel and Sevanian, 1994). Indeed, the oxidative degradation of PUFAs was supported by the lower cellular fatty acid unsaturation indices evident during exponential growth in the presence of $Cd(NO_3)_2$ (Chapter 2). Depletion of PUFAs has been employed as a useful marker of lipid peroxidation (De Vos *et al.*, 1993). Several studies have indicated that the susceptibility of fatty acids to lipid peroxidation increases with the degree of fatty acyl chain unsaturation (Porter *et al.*, 1995; Vossen *et al.*, 1995; De Vos *et al.*, 1993), supporting a possible link with the results of Chapter 2.

As stated earlier, through redox-cycling, redox-active metals such as copper, are known to generate reactive oxygen species (ROS) such as the hydroxyl radical ($HO^{\cdot}$) and the superoxide anion/perhydroxyl radical ($O_2^{\cdot-}/HO_2^{\cdot}$), via Fenton and Haber-Weiss reactions (Dix and Aikens, 1993; Shinar *et al.*, 1989). In addition, nonredox-active metals such as cadmium have the capacity to indirectly promote oxidative stress through depletion of free radical scavengers such as glutathione and protein-bound sulphydryl groups, and by displacement of redox-active metals from enzyme active sites, thereby stimulating Fe^{3+}/Cu^{2+}-initiated lipid peroxidation (Figueiredo-Pereira *et al.*, 1998; Hassoun and Stohs, 1996; Verstraeten and Otieza, 1995; Halliwell and Gutteridge, 1989). The metal hyper-sensitivity of various mutants of *S. cerevisiae*, defective in components of the oxidative stress response, supports a role of oxygen free radicals in microbial metal

toxicity. For example, *SOD1* mutants deficient in copper/zinc superoxide dismutase activity are hypersensitive to copper (Greco *et al.*, 1990) [these observations may be complicated, however, by the involvement of *SOD1* in copper buffering (Culotta *et al.*, 1995)]. Furthermore, mutations in the *YAP1* and *YAP2* genes of *S. cerevisiae* (key transcriptional activators of oxidative stress response genes) confer hypersensitivity to cadmium (Wu *et al.*, 1993). An important role for lipid peroxidation in the toxicity of heavy metal ions towards higher organisms has also been implicated from several recent studies (Stohs and Bagchi, 1995; Kalyanaraman *et al.*, 1992). However, to date no reports have investigated the relationship between heavy metal toxicity, plasma membrane fatty acid unsaturation, and lipid peroxidation in microorganisms.

In the present study, heavy metal-induced lipid peroxidation is demonstrated in a microorganism for the first time. Furthermore the increased susceptibility of PUFA-enriched *S. cerevisiae* to cadmium- and copper-induced plasma membrane perturbation and toxicity is shown here to correlate with elevated levels of lipid peroxidation in these cells.

3.2. Materials and Methods

3.2.1. **Organism and culture conditions.** *Saccharomyces cerevisiae* S150-2B (*MAT***a**, *leu2-3, -112, ura3-52, trp1-289, his3-Δ1,* Gal^+) (kindly provided by D. J. Jamieson, Heriot Watt University, Edinburgh, U.K.) was selected for this study because of its well characterised responses to oxidative stress (Stephen and Jamieson, 1996; Stephen *et al.*, 1995; Jamieson, 1992). S150-2B was routinely maintained on solid YEPD and YNB medium as described previously for NCYC 1383 (see Section 2.2.1.). For experimental purposes, S150-2B was grown as previously described for NCYC 1383 (see Section 2.2.1.).

3.2.2. **Preparation of cell homogenates.** Whole-cell homogenates were prepared as described previously for *S. cerevisiae* NCYC 1383 (see Section 2.2.2.).

3.2.3. **Lipid extraction and fatty acid analysis.** Lipids were extracted from whole-cell homogenates as described previously (see Section 2.2.5.).

3.2.4. **Preparation of cell suspensions for metal toxicity experiments.** Cells from the late-exponential phase (13 h) were harvested by centrifugation at 1,500 *g* for 5 min and washed twice with distilled deionised water. Washed cells were suspended to a density of approximately 5×10^7 ml^{-1} in 40 ml of 10 mM Mes buffer (pH 5.5), 1% (w/v) glucose, and incubated at room temperature with orbital shaking at 120 rev. min^{-1}. After 10 min equilibration, $Cd(NO_3)_2$ or $Cu(NO_3)_2$ was added to the desired concentration.

3.2.5. **Cell viability.** Cell viability was once again determined as the ability to produce colony-forming units on OGYE medium, as described previously (see Section 2.2.7.).

3.2.6. **Potassium efflux.** At specified intervals after the addition of $Cd(NO_3)_2$ or $Cu(NO_3)_2$ to cell suspensions, 0.5 ml aliquots were removed, microcentrifuged for 3 min, and the supernatant then diluted with 4 volumes of distilled deionised water. Extracellular K^+ was measured using a Corning 410 flame photometer, with reference to appropriate standard KCl solutions.

3.2.7. **Evaluation of lipid peroxidation.** Lipid peroxidation was quantified by two methods: determination of thiobarbituric acid (TBA)-reactive substances (TBARS) and conjugated dienes. TBARS were determined using a method adapted from that described by Aust (1994). At specified intervals (up to 3 h), after the addition of $Cd(NO_3)_2$ or $Cu(NO_3)_2$, 0.5 ml samples of cell suspension were removed and added to 1 ml of TBA reagent [0.25 M HCl, 15% (w/v) trichloroacetic acid, 0.375% (w/v) TBA]. Addition of the reagent terminated lipid peroxidation and initiated the assay. Samples were heated for 15 min in a boiling water bath and, after cooling, centrifuged at 1,000 *g* for 5 min in order to remove any cell debris. Absorbances of samples were then measured at 535 nm, using a Shimadzu UV-120-02 spectrophotometer, against a reference solution comprising 1 ml TBA reagent with the sample replaced by an equal volume (0.5 ml) of distilled deionised water. The concentrations of TBARS in samples were calculated by reference to a standard curve prepared using 1,1,3,3,-tetramethoxypropane (TMP).

For the determination of conjugated dienes (Glende and Recknagel, 1994), 10 ml samples were removed from cell suspensions and lipid extracts prepared from whole-cell homogenates as described above. After evaporation of chloroform under nitrogen, dried lipids were resuspended in 3 ml cyclohexane. UV spectra of lipid solutions were recorded between 215 and 280 nm using a Perkin-Elmer lambda-7 UV/Visible spectrophotometer. Conjugated dienes absorb light between approximately 215 nm and 255 nm, with a peak at 233 nm (Corongiu *et al.*, 1994). Peak absorbances at 233 nm were normalized against absorbance values at 260 nm and relative conjugated diene content expressed as A_{233}/A_{260}.

3.2.8. **Fluorescence depolarization.** Plasma membrane lipid-order was determined by measuring steady-state fluorescence anisotropy in whole cells labeled with trimethylammonium diphenylhexatriene (TMA-DPH). The cationic probe TMA-DPH becomes primarily anchored at the plasma membrane of intact cells (Gille *et al.*, 1993; Block, 1991). TMA-DPH was added to *S. cerevisiae* cell suspensions (5×10^7 cells ml^{-1}, see above) from a 1 mM stock solution, prepared in concentrated dimethylformamide, to give a final concentration of 1 μM. After 30 min equilibration, when measurements had stabilised, $Cd(NO_3)_2$ was added to cell suspensions. Triplicate 3 ml samples of suspension were removed at intervals, transferred to 10-mm-pathlength quartz cuvettes, and analysed using a Perkin Elmer LS5 fluorescence spectrometer with polarization accessory. TMA-DPH was excited with vertically polarized light at 360 nm, and the vertical and horizontal vectors of emitted light measured at 450 nm. Membrane order

was expressed as the order parameter S, which reflects the orderliness of membrane phospholipids.

$$S = (r/r_o)^{0.5} \quad \text{(Gille } et\ al.\text{, 1993)}$$

where r_o is the theoretical limiting anisotropy (0.395 for TMA-DPH) in the absence of rotational motion, and r is the steady-state anisotropy measured in the membrane. The effects of Cd^{2+} on membrane order were determined by measuring S at intervals over 60 min. Light scatter, determined in the absence of TMA-DPH, was found to account for less than 5% of the total emitted light and therefore no corrections were employed (Avery *et al.*, 1995*a*).

3.3. Results

In the previous studies (Avery *et al.*, 1996; Chapter 2), it was demonstrated that *S. cerevisiae* NCYC 1383 readily incorporated exogenous PUFAs (linoleate and linolenate) from its growth medium to greater than 65% of total fatty acids. *Saccharomyces cerevisiae* S150-2B was selected for this study because of its well characterised responses to oxidative stress (Stephen and Jamieson, 1996; Stephen *et al.*, 1995; Jamieson, 1992). *Saccharomyces cerevisiae* S150-2B was also observed to incorporate exogenous PUFAs; levels of incorporation were very similar to those described previously (results not shown). Increases in PUFA content, as a proportion of total fatty acids, were contemporaneous with decreases in the monounsaturated fatty acids palmitoleate (16:1) and oleate (18:1). Cellular fatty acid unsaturation indices (average number of double bonds per fatty acid) decreased in the order 18:3-supplemented cells (2.28) > 18:2-supplemented cells (1.48) > unsupplemented cells (0.82). The fatty acid compositions of plasma membrane-enriched fractions from *S. cerevisiae* match their corresponding whole-cell homogenates very closely (Avery *et al.*, 1996; Chapter 2).

3.3.1. Effect of cadmium and copper on the viability of unsupplemented and PUFA-supplemented *S. cerevisiae* S150-2B.

Saccharomyces cerevisiae S150-2B previously grown in PUFA-supplemented media was markedly more susceptible to Cd^{2+} (Fig. 3.1) and Cu^{2+} (Table 3.1) toxicity than cells grown in unsupplemented medium. For example,

Fig. 3.1. Effect of cadmium exposure on the viability of unsupplemented and PUFA-supplemented *S. cerevisiae* S150-2B. Cells were grown for 13 h in unsupplemented (○), linoleate-supplemented (●), or linolenate-supplemented (□) medium and then harvested, washed, and resuspended in 10 mM Mes (pH 5.5), 1% w/v glucose. $Cd(NO_3)_2$ was added to a final concentration of 50 (a) or 200 (b) μM. Typical results from one of at least two experiments are shown. Points represent means of three replicate samples from single experimental flasks. Standard errors of the mean (SEM) are smaller than the dimensions of the symbols.

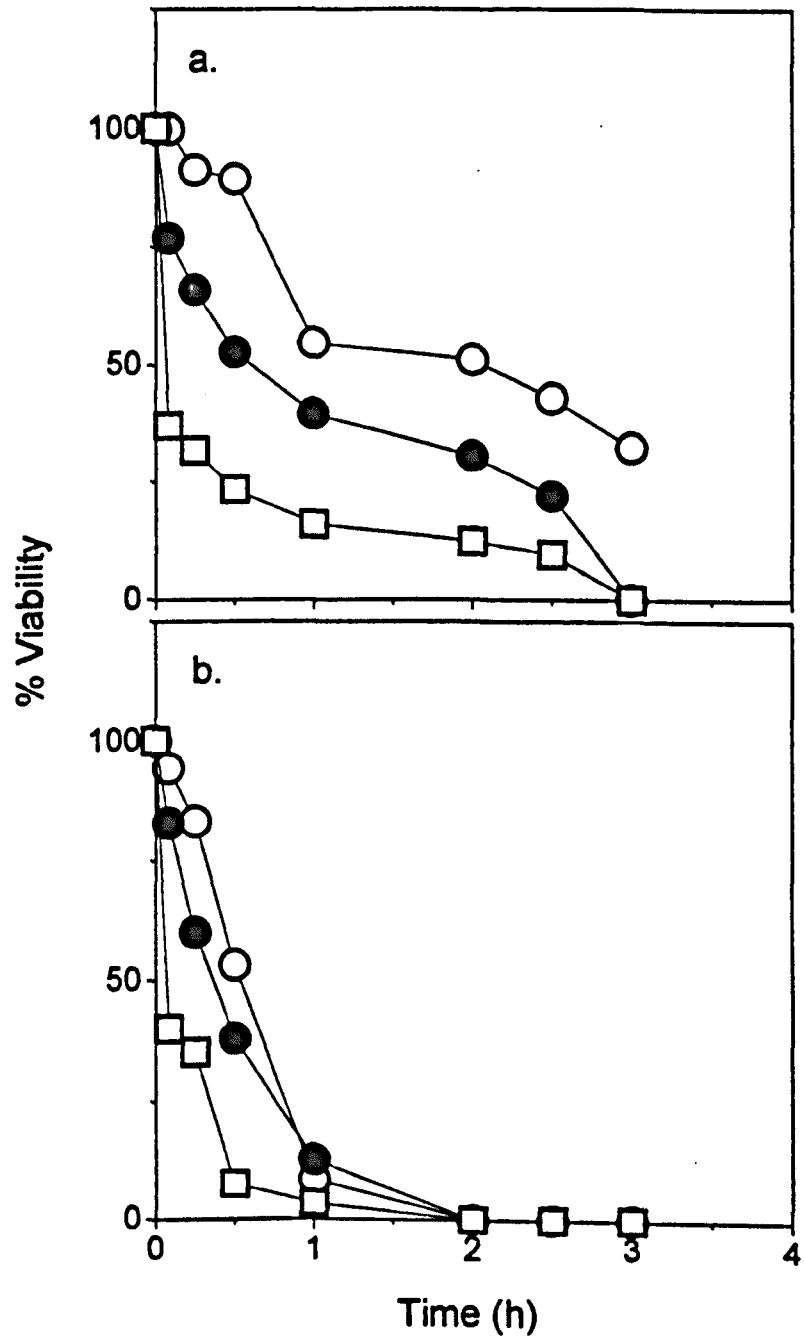
a.
b.
100
50
0
% Viability
0
1
2
3
4
Time (h)

Table 3.1. Effect of $Cu(NO_3)_2$ on viability of *S. cerevisiae* S150-2B cells previously grown in unsupplemented and PUFA-supplemented media

$[Cu(NO_3)_2]$	% Viability of the indicated cell type[a]		
(μM)	Unsupplemented	18:2-supplemented	18:3-supplemented
5[b]	88 ± 1	70 ± 5	63 ± 3
40[c]	11.0 ± 1.1	1.4 ± 1.6	0

[a] Values are means ± SEM derived from three replicate determinations

[b] Determined after 60 min

[c] Determined after 5 min

after 1 h incubation in the presence of 50 μM $Cd(NO_3)_2$, only 40% and 16% of cells previously grown in 18:2- and 18:3-supplemented media, respectively, were still viable (capable of colony formation) (Fig. 3.1a), whereas 55% viability was maintained in cells from unsupplemented medium. Similar trends were evident at 200 μM $Cd(NO_3)_2$, albeit over a shorter time-scale. No viable cells were detected after 2 h incubation in the presence of 200 μM Cd^{2+}. This was also the case after 5 min exposure of 18:3-supplemented cells to 40 μM $Cu(NO_3)_2$, although some capacity for colony formation was retained by Cu^{2+}-exposed unsupplemented and 18:2-supplemented cells (Table 3.1). Incubation for 60 min in the presence of 5 μM $Cu(NO_3)_2$ had far less marked effects on cell viability, although here again percentage viability decreased in the order unsupplemented cells > 18:2-supplemented cells > 18:3-supplemented cells.

3.3.2. **Cadmium- and copper-induced K^+ efflux from unsupplemented and PUFA-supplemented *S. cerevisiae* S150-2B.** Release of intracellular K^+ was used as an indicator of plasma membrane permeabilisation (Avery *et al.*, 1996; Chapter 2; Ohsumi *et al.*, 1988). Following heavy metal addition, K^+ efflux was initially very rapid, but slowed considerably after 15 min (Fig. 3.2). Metal-induced K^+ release from *S. cerevisiae* previously grown in PUFA-supplemented medium was markedly higher than that from cells grown in unsupplemented medium. For example, amounts of K^+ released from 18:2- and 18:3-enriched cells were approximately equal at 5.6 nmol $(10^6 \text{ cells})^{-1}$ after 15 min exposure to 50 μM $Cd(NO_3)_2$, whereas that from cells grown in unsupplemented medium was only 3.1 nmol $(10^6 \text{ cells})^{-1}$ (Fig. 3.2a). K^+ loss continued after 15 min, and amounts

Fig. 3.2. Cadmium-induced K^+ efflux in unsupplemented and PUFA-supplemented *S. cerevisiae* S150-2B cells. Cells were grown for 13 h in unsupplemented (○), linoleate-supplemented (●) and linolenate-supplemented (❐) medium and then harvested, washed, and resuspended in 10 mM Mes (pH 5.5), 1% w/v glucose. $Cd(NO_3)_2$ was added to a final concentration of 50 (a) or 200 (b) μM. Typical results from one of at least two experiments are shown. Values for K^+ release are means from three replicate determinations. SEM are smaller than the dimensions of the symbols.

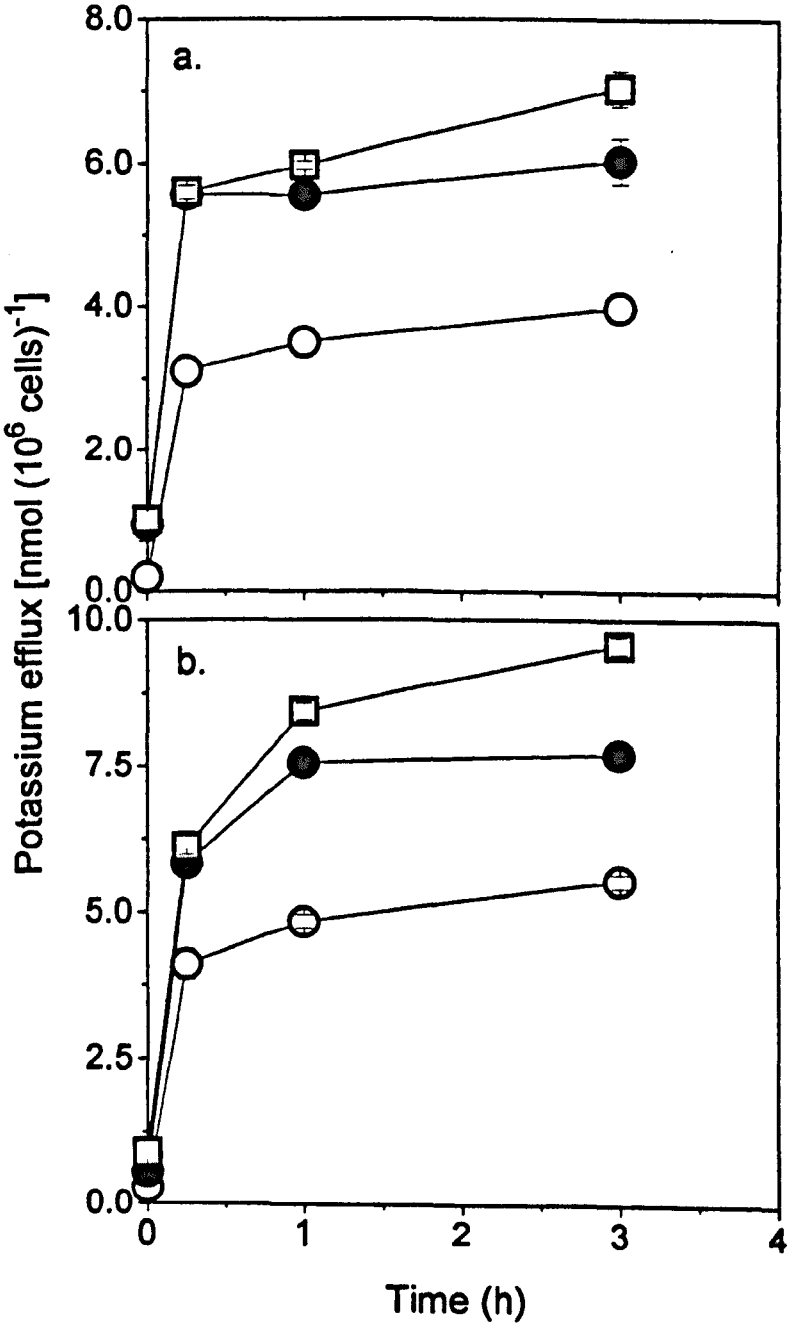
a.
b.
8.0
6.0
4.0
2.0
0.0
10.0
7.5
5.0
2.5
0.0
0
1
2
3
4
Time (h)
Potassium efflux [nmol (10^6 cells)$^{-1}$]

Table 3.2. Copper-induced K^+ release from *S. cerevisiae* S150-2B cells grown previously in unsupplemented and PUFA-supplemented media

$[Cu(NO_3)_2]$	Exposure time	K^+ release from the indicated cell type[a]		
(μM)	(min)	Unsupplemented	18:2-supplemented	18:3-supplemented
5	30	0.55 ± 0.04	1.18 ± 0.03	1.10 ± 0.0
	210	0.62 ± 0.03	1.14 ± 0.06	1.14 ± 0.10
40	30	3.4 ± 0.1	5.0 ± 0.1	5.7 ± 0.1
	210	4.1 ± 0.1	5.0 ± 0.1	6.1 ± 0.1

[a] Nanomoles of K^+ released per 10^6 cells. Values are means ± SEM derived from three replicate determinations

released from 18:3-supplemented cells after 3 h were approximately 17% higher than those from 18:2-supplemented cells. K^+ efflux was greater at 200 μM $Cd(NO_3)_2$ than at 50 μM $Cd(NO_3)_2$, and differences between 18:2- and 18:3-supplemented cells were more marked. Thus, amounts of K^+ released after 1 h exposure to 200 μM Cd^{2+} were approximately 4.8, 7.6 and 8.4 nmol $(10^6 \text{ cells})^{-1}$ from cells previously grown in unsupplemented, 18:2- and 18:3-supplemented media, respectively (Fig. 3.2b). Similar trends were apparent during copper exposure (Table 3.2). Amounts of K^+ released from 18:2- and 18:3-enriched cells incubated in the presence of 5 μM $Cu(NO_3)_2$ were similar, but approximately 100% and 84% higher after 30 min and 210 min, respectively, than those from unsupplemented cells under the same conditions. At 40 μM $Cu(NO_3)_2$, a greater relative permeabilisation of the plasma membrane of 18:3-supplemented cells compared to 18:2-supplemented cells also became apparent (Table 3.2).

3.3.3. **Cadmium- and copper-induced lipid peroxidation in unsupplemented and PUFA-supplemented *S. cerevisiae* S150-2B.** Lipid peroxidation was evaluated as thiobarbituric acid-reactive substances (TBARS) production and conjugated diene formation. Two different analytical methods were used to assess lipid-localised oxidative stress as no single method adequately measures the range of reactions possible (Coudray *et al.*, 1995). Furthermore, the TBA assay alone was not suitable for direct comparison of linolenate-enriched cells with the other cell types as malondialdehyde, to which the assay is particularly sensitive, is only formed upon the breakdown of linolenate, and not linoleate or monounsaturated fatty acids (Mihaljevic *et al.*, 1996; Aust, 1994).

Fig. 3.3. Cadmium-induced TBARS production in unsupplemented and linoleate-supplemented *S. cerevisiae* S150-2B. Cells were grown for 13 h in unsupplemented (○) and linoleate-supplemented (●) medium and then harvested, washed, and resuspended in 10 mM Mes (pH 5.5), 1% w/v glucose. $Cd(NO_3)_2$ was added to a final concentration of 50 (a) or 200 (b) μM. Typical results from one of at least two experiments are shown. Values for TBARS are means of three replicate determinations from single experimental flasks, ± SEM where these values exceed the dimensions of the symbols.

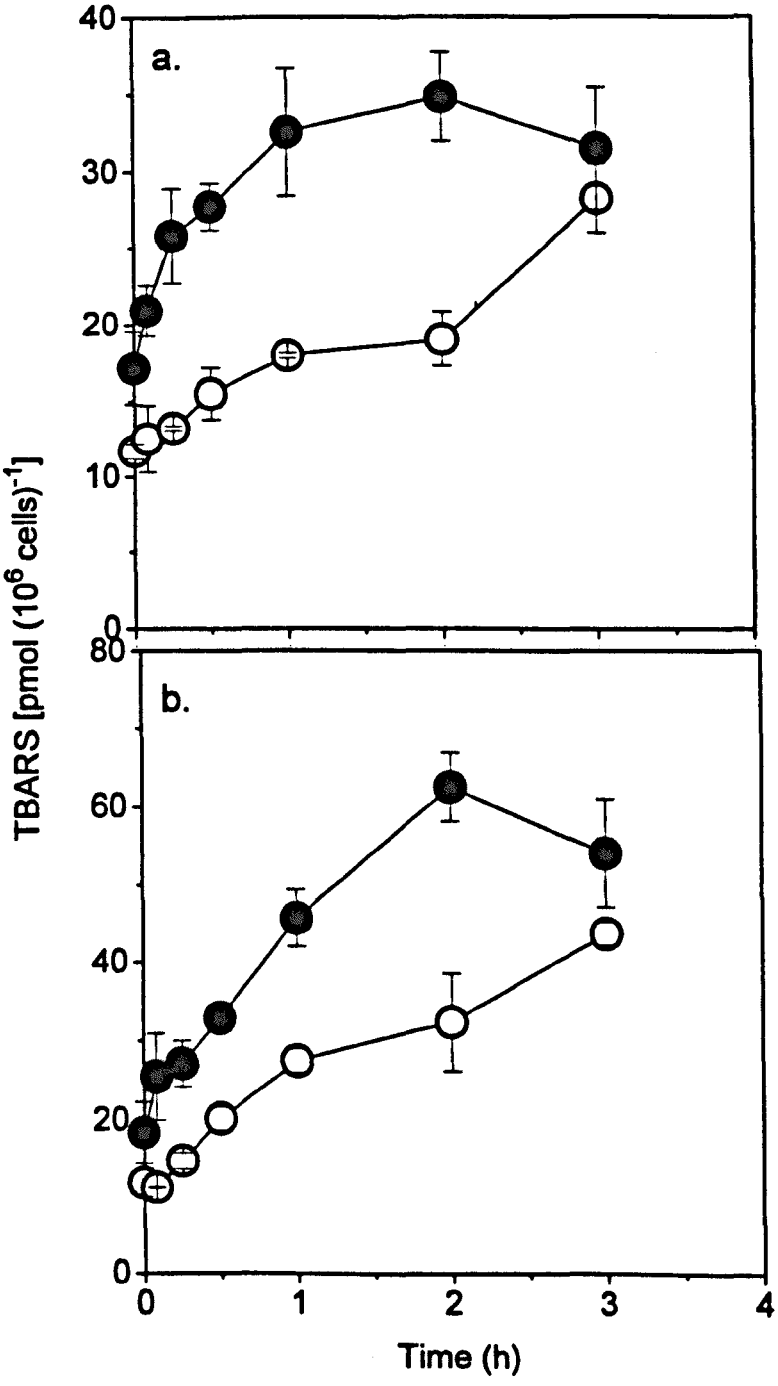
a.
b.
TBARS [pmol (10^6 cells)$^{-1}$]
Time (h)
0
10
20
30
40
0
20
40
60
80
0
1
2
3
4

Table 3.3. Copper-induced TBARS production in *S. cerevisiae* S150-2B cells grown previously in unsupplemented and linoleate-supplemented media

$[Cu(NO_3)_2]$	Exposure time	TBARS produced by the indicated cell type[a]	
(μM)	(min)	Unsupplemented	18:2-supplemented
5	0	5.7 ± 1.1	7.3 ± 0.9
	60	8.9 ± 1.8	12.4 ± 1.5
	180	14.3 ± 0.4	14.1 ± 3.1
40	0	5.4 ± 1.7	7.0 ± 0.4
	60	14.2 ± 0.2	17.5 ± 1.1
	180	17.2 ± 1.0	16.0 ± 0.7

[a] Picomoles of TBARS produced per 10^6 cells. Values are means ± SEM derived from three replicate determinations

Difficulties were encountered with the purification of plasma membranes from cells following metal exposure: these were related to altered membrane density and partitioning behaviour. Thus, the values for whole-cell lipid peroxidation (given) include contributions from organellar membranes. Because the plasma membrane is a primary target for metal toxicity (Aβmann *et al*, 1996; Verstraeten and Oteiza, 1995; Ohsumi *et al.*, 1988), and its fatty acid composition is similar to that of organellar membranes (Avery *et al.*, 1996), it can be inferred that lipid peroxidation per unit plasma membrane was at least equal to (probably greater than) that of organellar membranes.

Prior to the addition of metal, amounts of TBARS were generally approximately 25-55% larger in linoleate-enriched cells than in cells grown previously in unsupplemented medium (Fig. 3.3; Table 3.3). Marked increases in TBARS formation were evident following metal addition. Control experiments confirmed that no detectable rise in TBARS levels occurred during 3 h incubation in buffer in the absence of cadmium or copper (results not shown). Metal-induced increases were particularly large during the first minutes of metal exposure, although in certain cases TBARS formation continued up to 3 h (Fig. 3.3). The level of metal-induced TBARS production was considerably higher in *S. cerevisiae* previously grown in 18:2-supplemented medium than that in cells grown in unsupplemented medium (Fig. 3.3). For example, after 1 h exposure to 50 μM $Cd(NO_3)_2$, the level of TBARS in 18:2-enriched cells was approximately 33 pmol $(10^6$ cells$)^{-1}$, whereas that from cells grown in unsupplemented medium was only 18 pmol $(10^6$ cells$)^{-1}$ (Fig. 3.3a). The level of TBARS production was higher at 200 μM $Cd(NO_3)_2$ than at 50 μM $Cd(NO_3)_2$. Up to 2 h, levels of TBARS were between 1.6- and 2-fold greater in 18:2-supplemented cells than in unsupplemented cells at either $Cd(NO_3)_2$ concentration

(Fig. 3.3). A reduction in cellular TBARS levels between 2 and 3 h incubation with cadmium was evident only in 18:2-supplemented cells, whereas lipid peroxidation continued to rise in unsupplemented cells during this period. Thus, after 3 h, the levels of TBARS measured in 18:2-supplemented cells were only approximately 1.2-fold higher than those of unsupplemented cells (Fig. 3.3). Similar trends were observed for copper exposure, with which TBARS production was also associated. Again, lipid peroxidation increased with metal concentration and, after 1 h, levels of Cu-induced TBARS were between 20% and 40% higher in 18:2-enriched cells than in unsupplemented cells. However, between 1 h and 3 h, TBARS levels in 18:2-supplemented cells either increased only slightly (5 μM Cu^{2+}) or declined (40 μM Cu^{2+}). In contrast, those of unsupplemented cells continued to increase and, at 3 h, exceeded TBARS levels evident in 18:2-enriched cells (Table 3.3).

Lipid peroxidation was also evaluated by measuring conjugated dienes, which are early intermediates in the lipid peroxidative chain (Glende and Recknagel, 1994). Relative levels of conjugated dienes were determined after 1 h exposure to Cd and Cu and expressed as A_{233}/A_{260}. At 50 μM $Cd(NO_3)_2$, A_{233}/A_{260} values for cells grown previously in unsupplemented and 18:2- and 18:3-supplemented media were 1.03, 1.12 and 1.18, respectively, indicating increased Cd-induced conjugated diene formation in cells displaying elevated fatty acid unsaturation indices (Fig. 3.4a). A similar trend was evident at 200 μM $Cd(NO_3)_2$, although the A_{233}/A_{260} values were higher in all cases at this increased cadmium concentration. Conjugated diene levels also increased with the unsaturation index in copper-exposed cells. A_{233}/A_{260} values after 1 h at 5 μM $Cu(NO_3)_2$, for cells grown previously in unsupplemented, 18:2- and 18:3-supplemented media were

Fig. 3.4. Cadmium- and copper-induced conjugated-diene formation in unsupplemented and PUFA-supplemented *S. cerevisiae* S150-2B. Cells were grown for 13 h in unsupplemented, linoleate- or linolenate-supplemented medium and then harvested, washed, and resuspended in 10 mM Mes (pH 5.5), 1% w/v glucose. (a) Cd^{2+} was added to a final concentration of 50 (❒) or 200 (■) μM. (b) Cu^{2+} was added to a final concentration of 5 (❒) or 20 (■) μM. Values are means for three individual lipid extracts ± SEM.

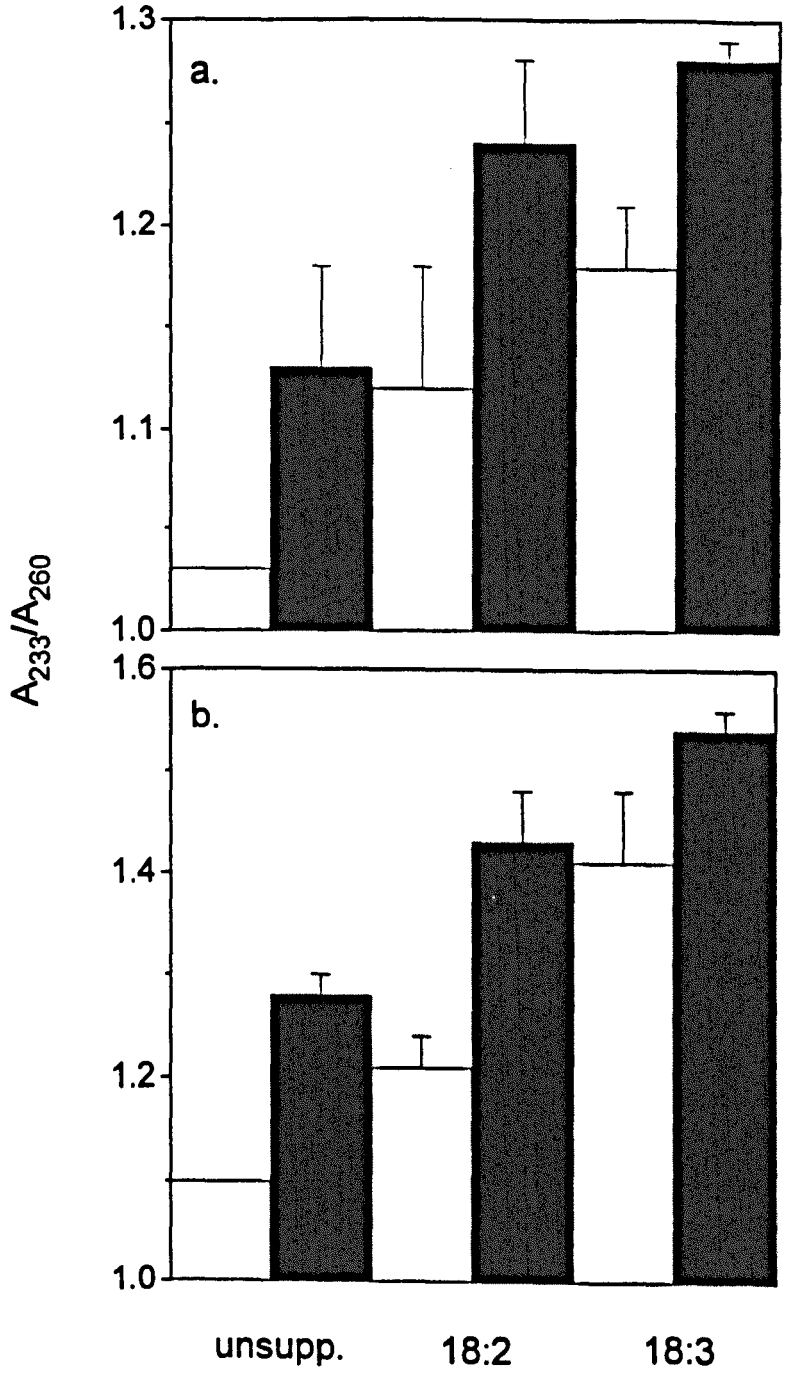
a.
b.
1.3
1.2
1.1
1.0
1.6
1.4
1.2
1.0
A_{233}/A_{260}
unsupp.
18:2
18:3

1.10, 1.21 and 1.41, respectively (Fig. 3.4b). Conjugated diene formation was greater at 20 μM than at 5 μM $Cu(NO_3)_2$, although again the A_{233}/A_{260} values were highest for cells that had previously been grown in the presence of linoleate, and particularly linolenate. Interestingly, despite the lower copper concentrations employed, and in contrast to the TBARS results, copper-exposed cells generally displayed higher conjugated diene levels than cadmium-exposed cells. The elevated levels of lipid peroxidation evident (from both sets of data) in PUFA-enriched *S. cerevisiae* were correlated with the increased susceptibility of these cells to Cd^{2+} and Cu^{2+}-induced plasma membrane permeabilisation and whole-cell toxicity.

3.3.4. **Effect of cadmium on plasma membrane order of unsupplemented and PUFA-supplemented *S. cerevisiae* S150-2B.** In order to assess metal-induced changes in plasma membrane physical properties, plasma membrane lipid order was monitored (by fluorescence depolarization with TMA-DPH-labelled cells) during the 50 min period following addition of 50 μM $Cd(NO_3)_2$ (Fig. 3.5). Prior to the addition of metal, S (membrane order parameter) values for cells previously grown in unsupplemented and 18:2- and 18:3-supplemented media were 0.74, 0.71 and 0.69, respectively, indicating decreased orderliness in plasma membranes enriched with PUFAs. After the addition of metal, decreases in plasma membrane order in all three types of cell were clearly evident, and these continued for at least 50 min. The Cd^{2+}-induced change in S was slightly greater for cells previously grown in unsupplemented medium than for 18:2- and 18:3-enriched cells. However, after 50 min of incubation in the presence of Cd^{2+}, values for S still decreased in the order unsupplemented cells > 18:2-supplemented cells > 18:3-

Fig. 3.5. Effect of cadmium on membrane order in unsupplemented and PUFA-supplemented *S. cerevisiae* S150-2B cells. Cells were grown for 13 h in unsupplemented (○), linoleate-supplemented (●), or linolenate-supplemented (□) medium and then harvested, washed, and resuspended in 10 mM Mes (pH 5.5), 1% w/v glucose. TMA-DPH was added to a final concentration of 1 μM, and 30 min later, Cd^{2+} was added to a final concentration of 50 μM. Typical results from one of at least two experiments are shown. Values for S are means for three replicate samples from single experimental flasks, ± SEM where these values exceed the dimensions of the symbols.

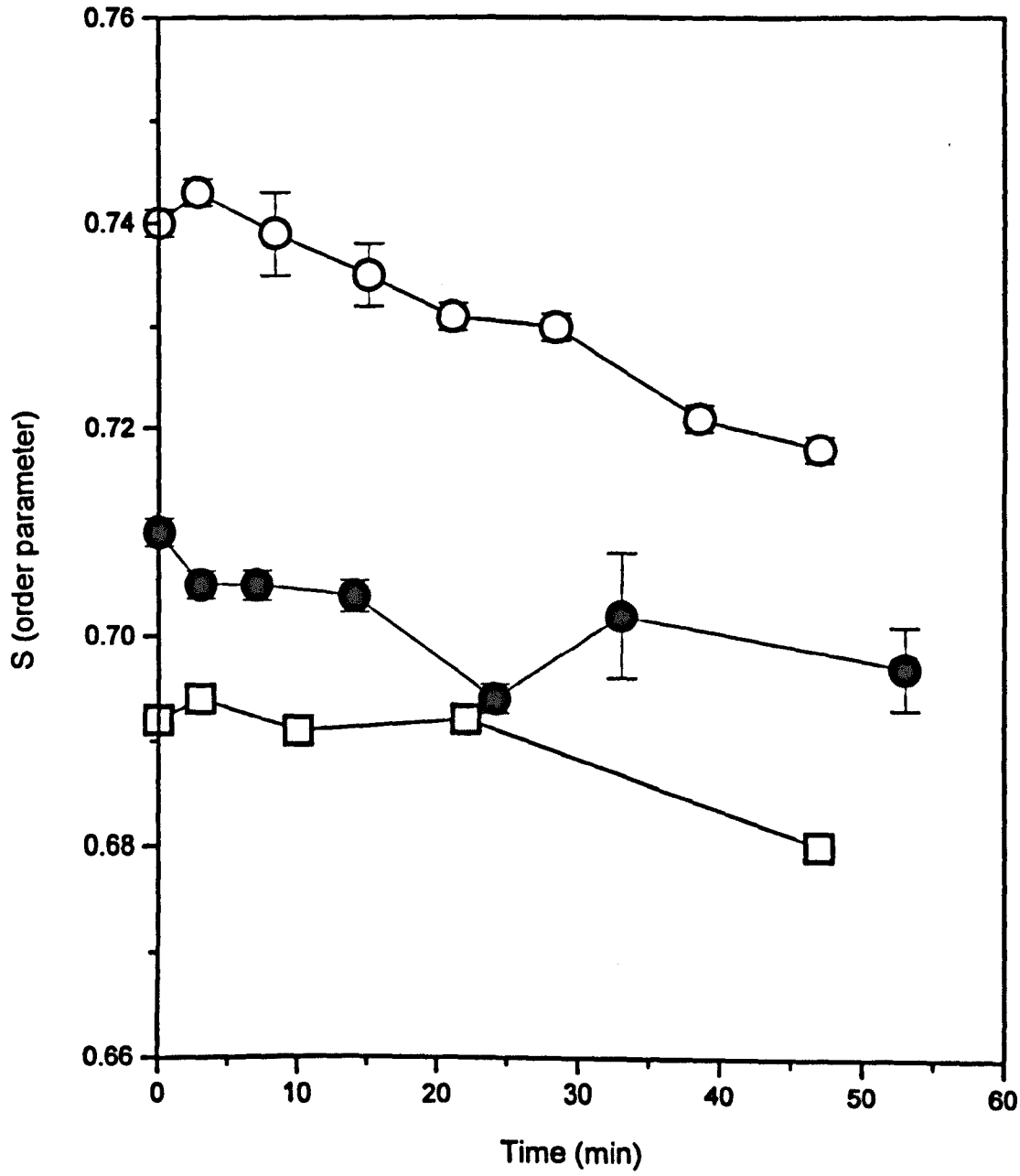
0.76
0.74
0.72
0.70
0.68
0.66
S (order parameter)
0
10
20
30
40
50
60
Time (min)

supplemented cells. The order parameter for plasma membranes of Cd^{2+}-exposed unsupplemented cells did not decrease below the values for PUFA-enriched cells determined prior to cadmium addition (Fig. 3.5).

3.4. Discussion

Metal-induced plasma membrane permeabilisation and whole-cell toxicity in *S. cerevisiae* S150-2B [a strain for which various components of the oxidative stress response have been well characterised (Stephen and Jamieson, 1996; Stephen *et al.*, 1995; Jamieson, 1992)] were initially confirmed to be greater in cells enriched with the PUFAs linoleate and linolenate. Similar effects of plasma membrane fatty acid composition on copper (Avery *et al.*, 1996) toxicity, albeit more marked, have also been observed in *S. cerevisiae* NCYC 1383. Hence, this effect is clearly not strain-specific. The results also suggest that the ability of *S. cerevisiae* to incorporate exogenous PUFAs with little effect on growth rate may be widespread; previous reports of this characteristic were restricted to *S. cerevisiae* NCYC 1383 (Avery *et al.*, 1996; Bossie and Martin, 1989; Chapter 2). The consequent experimental advantages of *S. cerevisiae* for modelling membrane-dependent effects have been highlighted elsewhere (Avery *et al.*, 1996).

As in previous reports (Avery *et al.*, 1996; Belde *et al.*, 1988; Chapter 2; Ohsumi *et al.*, 1988), extensive metal-induced potassium release was associated with a loss of viability of *S. cerevisiae*. Whereas a stoichiometric relationship between physiological metal uptake and potassium release can occur at non-toxic metal concentrations (Gadd and Mowll, 1983), our previous studies have confirmed nonstoichiometry at the toxic metal concentrations used here (Avery *et al.*, 1996; Chapter 2). Thus, potassium release can be attributed to plasma membrane permeabilisation and toxicity (Avery *et al.*, 1996; Chapter 2; Ohsumi *et al.*, 1988). As is usually the case among yeast and fungi (De Rome

and Gadd, 1987; Gadd and Mowll, 1983), copper was more toxic than cadmium for *S. cerevisiae*. However, copper exposure resulted in less K^+ release than that observed during cadmium exposure at the concentrations used. Thus, it can be inferred that effects other than membrane permeabilisation, e.g. direct interaction with nucleic acids or misincorporation into metallothioneins (Cervantes and Gutierrez-Corona, 1994), may make a more important contribution in copper toxicity than cadmium toxicity to loss of *S. cerevisiae* viability. An important role of copper-induced membrane effects was nevertheless implicated by the observed influence of membrane fatty acid composition.

A role of lipid-targeted oxy-radical attack in the toxicity of heavy metals towards higher organisms has been inferred from observations of elevated lipid peroxidation in metal-exposed organisms (Kalyanaraman *et al.*, 1992; Halliwell and Gutteridge, 1989). In this study, metal-induced lipid peroxidation in a microorganism was demonstrated for the first time.

The integration of different analytical methods for the measurement of lipid peroxidation was necessary (Coudray *et al.*, 1995). Results from conjugated-diene and TBARS analyses suggested contrasting pathways of cadmium- and copper-induced lipid peroxidation. Unlike TBARS, conjugated dienes are primary products in the lipid peroxidative chain, arising through oxy-radical mediated abstraction of hydrogen atoms from methylene groups separating PUFA double-bonds (Glende and Recknagel, 1994). Therefore, the higher relative levels of conjugated dienes in Cu-exposed cells suggest that initiation of lipid peroxidation occurs at a greater rate in the presence of copper than cadmium in *S. cerevisiae*; such a conclusion is consistent with the respective redox-activities and inactivities of these metals (Stohs and Bagchi, 1995). The mechanism of

lipid peroxidation initiation is unlikely to differ as the principal initiating species generated by both copper (direct catalysis of the Fenton reaction) and cadmium (indirect promotion of the Fenton reaction by glutathione depletion) is most likely the hydroxyl radical (Dix and Aikens, 1993). However, observed differences in initial TBARS levels, prior to metal addition, do suggest the possibility of additional initiation via pre-formed lipid hydroperoxides (Dix and Aikens, 1993).

While the TBARS assay detects products arising from the decomposition of lipid hydroperoxides, such as the decomposition products of oleate and linoleate hydroperoxides detected in this study, the assay is particularly sensitive to malondialdehyde (Aust, 1994). Malondialdehyde is formed only upon oxidation of PUFAs containing at least three methylene-separated double bonds (Mihaljevic *et al.*, 1996). Thus, while the results demonstrate elevated levels of lipid peroxidation in linoleate-enriched cells, compared to unsupplemented cells, the total cellular amounts of lipid hydroperoxides for all cell types are most likely underestimated.

The formation of high levels of TBARS can be precluded by glutathione peroxidase activity during normal cellular metabolism. Glutathione peroxidase converts lipid hydroperoxides to their corresponding hydroxy fatty acids (Tran *et al.*, 1993). However, glutathione is a principal cellular target or sequestration site of cadmium (Figueiredo-Pereira *et al.*, 1998; Li *et al.*, 1997; Lesuisse and Labbe, 1995). Thus, the higher relative levels of TBARS in Cd-exposed than in Cu-exposed cells may reflect glutathione depletion, and hence, a reduced capacity of the former to repair lipid peroxidation damage.

The convergence of TBARS levels in unsupplemented and linoleate-supplemented *S. cerevisiae*, after prolonged metal-exposure may reflect a greater induction of antioxidant activity in the latter cells; the oxidative stress response of *S. cerevisiae*, which includes the induction of glutathione, catalase, metallothionein, and glutathione peroxidase, increases with the extent of initial insult (Steels *et al.*, 1994; Jamieson, 1992).

Exposure to neither metal was associated with a decline in the degree of cellular fatty acid unsaturation within one hour (results not shown). However, longer term reductions in the proportion of unsaturated fatty acids were previously noted during growth of *S. cerevisiae* NCYC 1383 in cadmium-supplemented medium (Chapter 2). This supports the view that reduced polyunsaturated fatty acid content can be a late marker of lipid peroxidation (De Vos *et al.*, 1993).

The similarities between the short initiation time-scales (noting that TBARS are not immediate products of lipid peroxidation) and between the relative extents, of lipid peroxidation and K^+ release observed here, were consistent with the former process being associated with a deterioration of membrane integrity (Corongiu *et al.*, 1994; Van Ginkel and Sevanian, 1994). Loss of membrane impermeability during lipid peroxidation may arise through covalent bond formation between adjacent acyl radicals, resulting in increased membrane rigidity, or through the incorporation of short-chain and/or polar oxidation products, resulting in decreased membrane order (Van Ginkel and Sevanian, 1994; Dix and Aikens, 1993). The small cadmium-induced reductions in plasma membrane order reported here were indicative of a predominance of the latter type of effect, and in agreement with the reported effects of cadmium on *Schizosaccharomyces*

pombe plasma membranes (Aβmann *et al.*, 1996). Unlike K^+ efflux, the effect of Cd^{2+} on plasma membrane order was apparently no more pronounced in PUFA-enriched cells than in unsupplemented cells. Thus, a threshold value for membrane order, below which K^+ efflux occurred, was not discernible. It appears that values for the membrane order parameter (S) do not provide a clear linear index of the state of a membrane in relation to either its integrity or its content of lipid peroxidation products. Nevertheless, values for plasma membrane order determined after metal-exposure decreased in the same order (unsupplemented cells > linoleate-supplemented cells > linolenate-supplemented cells) as that predicted from metal toxicity and lipid peroxidation experiments. Note that this is also the order to be expected on the basis of differences in initial fatty acid composition, irrespective of the extent of lipid peroxidation (Avery *et al.*, 1996). In addition to the rapid gross effects on membrane permeability observed at the high metal concentrations used here, smaller changes in membrane physical properties at lower non-toxic metal concentrations might still elicit changes in cellular activity; the function of many membrane-bound enzymes is known to be sensitive to the enzymes' lipid environment (Hazel and Williams, 1990).

The accentuated levels of lipid peroxidation and heavy metal-toxicity in linoleate- and linolenate-enriched *S. cerevisiae* were consistent with the known susceptibility of polyunsaturated fatty acids to oxidation (Porter *et al.*, 1995; Dix and Aikens, 1993). The possibility that the results might also be partly attributable to differences in the physical properties of PUFA-enriched plasma membranes cannot be discounted (Verstraeten and Oteiza, 1995); in common with studies on higher organisms (Weckx and Clijsters, 1996; Vossen *et al.*, 1995), the fatty acid unsaturation index of *S. cerevisiae* (1.5-fold higher for

linolenate- than linoleate-enriched cells) was not linearly related to susceptibility to lipid peroxidation. Sensitivity may relate more closely to initial plasma membrane order.

The potentially major role of membrane lipid peroxidation in heavy metal toxicity towards yeast implicated from the present results suggests that changes in a number of highly-variable cellular properties, including antioxidant status (e.g. the induction of antioxidant defences during respiratory adaptation (Steels *et al.*, 1994; Jamieson *et al.*, 1994)) and membrane fatty acid composition (e.g. changes occurring during environmental acclimation (Hazel and Williams, 1990)), could seriously alter the cells' ability to cope with heavy metal stress. As well as being of relevance to the stress biochemistry of yeast, these findings may have significant implications for metal-microbe interactions in the natural environment.

CHAPTER 4

Factors determining the differential sensitivity to copper toxicity among heterogeneous populations of *Saccharomyces cerevisiae*

4.1. Introduction

In our previous chapters a major role of plasma membrane fatty acid composition on the susceptibility of *S. cerevisiae* towards the toxic effects of both the redox-active metal copper and the nonredox-active metal cadmium was demonstrated. *Saccharomyces cerevisiae* enriched with the exogenously-supplied polyunsaturated fatty acids (PUFAs) linoleate and linolenate were markedly more susceptible towards heavy metal-induced plasma membrane permeabilisation and whole-cell toxicity (Avery *et al.*, 1996; Chapters 2 and 3). While differences in the metal-sensitivities of unsupplemented and PUFA-supplemented *S. cerevisiae* were examined, the differential susceptibility to metal toxicity observed within heterogeneous yeast cell suspensions was not investigated. In this particular study the nature of the heterogeneity in susceptibility towards metal toxicity observed for exponential phase *S. cerevisiae* suspensions was examined. Thus, the relationship between cell cycle stage-repartition and susceptibility towards metal toxicity was investigated.

Cellular growth is considered as successive phases, characterised by specific biochemical processes and called, from one division to the next, the cell cycle. The yeast cell cycle consists of a DNA replicating phase, S phase, a mitotic phase, M phase, and G_1 and G_2 gap phases. Proper progression through the cell cycle of *S. cerevisiae* requires the periodical expression of regulatory proteins such as the CLN- and B-type cyclins (Cln1p-Cln3p and Clb1p-Clb6p), cyclin-dependent kinases, primarily Cdc28p (Lew *et al.*, 1997), and checkpoint proteins such as Rad9p, Mec1p, and Rad53p (Li and Cai, 1997; Paulovich

et al., 1997 ; Weinert *et al.*, 1994). Cdc28p levels do not fluctuate during the yeast cell cycle. However, the pattern of cyclin accumulation/degradation leads to overlapping waves of activity of distinct cyclin/Cdc28p complexes, which in turn regulate gene transcription during the cell cycle (Lew *et al.*, 1997).

Studies on cell cycle-specific gene expression are usually carried out using synchronous cultures, or on a relatively small number of cells, by time-lapse studies. Cell cycle-synchrony studies in yeast are performed using a variety of techniques, e.g. α-factor-induced G_1 phase arrest, hydroxyurea-induced G_1/S phase arrest, and nocodazole-induced G_2/M phase arrest (Heichman and Roberts, 1996), sucrose density gradients, or through the use of temperature-sensitive *cdc* mutants, e.g. temperature-sensitive *cdc7* (Siede *et al.*, 1994; Kitada *et al.*, 1992) and *cdc15* mutants (Cocker *et al.*, 1996). However, such methods tend to perturb the dynamic state of the cells (Avery *et al.*, 1995*b*; Lloyd, 1987). Flow cytometry can be used to circumvent cell synchronisation in many cases, and has become the method of choice for cell cycle analysis (Kalejta *et al.*, 1997; Avery *et al.*, 1995*b*; Jayat and Ratinaud, 1993; Lloyd, 1993). Indeed, Porro *et al.* (1995) have recently applied flow cytometry to track the dynamics of cell cycle progression of new-born *S. cerevisiae* using the cell wall- and protein-specific fluorescent dyes, conjugated ConA-FITC and TRITC, respectively. Typically, monoparametric analyses, using cellular DNA content alone, are used to determine the approximate cell cycle stage (Jayat and Ratinaud, 1993). However, by simultaneously monitoring cell volume (proportional to forward-angle light scatter (FSC)) and cellular DNA content, one can more accurately estimate cell repartition in the various cell cycle stages (Lopezamoros *et al.*, 1995; Jayat and Ratinaud, 1993). Therefore, by appropriate FSC-

histogram gate adjustment it is possible to analyse distinct cell cycle phase sub-populations (of differing cell volumes) within a heterogeneous population (Avery *et al.*, 1995*b*). Thus, flow cytometry permits distinction of a variety of types of sub-populations within heterogeneous microbial suspensions.

The phenotypic heterogeneity observed within microbial cultures is most likely a consequence of differential gene transcription, such as that regulated through cell cycle-dependent oscillations of cyclin/Cdc28p kinase activity (Lew *et al.*, 1997; Heichmann and Roberts, 1996). The green fluorescent protein (GFP) of the jellyfish *Aequorea victoria* has been extensively used for both localisation and gene expression studies in *S. cerevisiae*, including microtubule visualisation, tracking of the kinetics of spindle pole body formation, and determination of expression levels of *GAL1* and *URA3* (Anderson *et al.*, 1996; Niedanthal *et al.*, 1996). The longer wavelength peak (470 nm) of GFPs bimodal absorption spectrum allows excitation with an argon ion laser (488 nm excitation) used in fluorescence-activated cell sorting (FACS) systems (Cormack *et al.*, 1996; Ropp *et al.*, 1995). Construction of GFP-promoter fusion vectors, and subsequent transformation of yeast allows the expression of the gene of interest to be determined *in vivo* using GFP as a reporter fluorophore, by flow cytometry. Therefore, using flow cytometry it is possible to analyse distinct cell cycle phase sub-populations for GFP fluorescence, and thus monitor cell cycle-changes in gene expression.

In this present study the differential susceptibility to metal toxicity in exponential phase *S. cerevisiae* cultures was investigated. Specifically, flow cytometry was used to examine whether repartition in the various cell cycle stages was associated with differential metal sensitivity. Furthermore, in this context, cell cycle stage-dependent

phenotypic alterations in yeast heavy metal resistance determinants, such as altered fatty acid composition, and differential levels of expression of metal homeostasis and oxidative stress response genes were examined.

4.2. Materials and Methods

4.2.1. **Organisms and culture conditions.** Yeast strains used for cell cycle studies were *S. cerevisiae* NCYC 1383 (*MATα, his3-Δ1, leu2-3, 112, ura3-52, trp1-289*) and DY150 (*MAT***a**, *ura3-52, leu2-3, 112, trp1-1, ade2-1, his3-11, can1-100*) (kindly provided by A. M. Avery, Emory University, Atlanta, GA). Maintenance of yeast strains, and preparation of strains for experimental purposes was as previously described (see Section 2.2.1.).

4.2.2. **Preparation of cell homogenates.** Cells were harvested by centrifugation at 1,500 *g* for 5 min and washed twice with distilled deionised water at 4 °C. Cells were disrupted by shaking with 0.5 mm-diameter glass beads (Sigma, MO) using a Biospec Products Mini-Beadbeater™ (or Mini-Beadbeater –8™ for multiple samples) homogeniser for 4 x 30 s pulses. Samples were placed on ice between pulses.

4.2.3. **Lipid extraction and fatty acid analysis.** Lipids were extracted from whole-cell homogenates, and fatty acid methyl esters generated as described previously (see Section 2.2.5). In this study, FAMEs were separated using a Stabilwax-DA 30 m capillary column and analysed using a Perkin Elmer Autosystem gas chromatograph. Fatty acids were again identified by comparison with authentic standards.

4.2.4. **Preparation of cell suspensions for metal toxicity experiments.** Cells from the late-exponential phase (15 h) were harvested by centrifugation at 1,500 *g* for 5 min and washed twice with distilled deionised water. Washed cells were suspended to a density of approximately 5 x 10^7 ml^{-1} in 40 ml of 10 mM Mes buffer (pH 5.5), 1% (w/v) glucose, and incubated at room temperature with orbital shaking at 120 rev. min^{-1}. After 10 min equilibration, $Cu(NO_3)_2$ was added to the desired concentration.

4.2.5. **Cell viability.** For the flow cytometric assessment of viability, cells were stained with propidium iodide (PI) (Sigma, MO), and fluorescein diacetate (FDA) (Molecular Probes Inc., OR). PI is a phenanthridinium intercalator which is taken up by dead cells because of loss of membrane impermeability (Kalejta *et al.*, 1997; Lopezamoros *et al.*, 1995). Once bound to intracellular nucleic acids PI-fluorescence is enhanced 20- to 30-fold (Lopezamoros *et al.*, 1995). PI has an absorption maximum of 536 nm and an emission maximum of 617 nm (Haugland, 1996). FDA is taken up by live cells and converted to its fluorescent derivative fluorescein by non-specific intracellular esterases (Breeuwer, 1995). Fluorescein has an absorption maximum of 494 nm and emission maximum of 518 nm (Haugland, 1996).

Aliquots (1.5 ml) from control and Cu^{2+}-treated suspensions were taken at regular intervals, washed twice with 10 mM Mes buffer (pH 5.5), 1% (w/v) glucose, and resuspended in 1 ml phosphate-buffered saline (PBS) containing 10 μg ml^{-1} FDA and 25 μg ml^{-1} PI. Samples were incubated at 4 °C for 15 min prior to analysis. Stained cells were visualised by fluorescence microscopy using an Olympus BH2 fluorescence microscope and analysed by flow cytometry (see below).

4.2.6. **Measurement of *in vivo* molecular oxidation.** Direct evidence of *in vivo* intracellular molecular oxidation was assessed using the oxidant-sensitive probe 2',7'-dichlorodihydrofluorescein diacetate (H_2DCFDA) (Molecular Probes Inc., OR) (Davidson *et al.*, 1996; Haugland, 1996). Nonionic H_2DCFDA traverses cell membranes and is enzymatically hydrolysed to the non-fluorescent compound H_2DCF by non-specific intracellular esterases (LeBel *et al.*, 1992). H_2DCF reacts with intracellular reactive oxygen species, particularly hydrogen peroxide, and is oxidised to the highly fluorescent derivative 2',7'-dichlorofluorescein (DCF) (Davidson *et al.*, 1996). DCF has an absorption maximum of 510 nm and emission maximum of 532 nm (Haugland, 1996).

Aliquots (1.5 ml) were taken at regular time intervals, washed with 1 ml of 10 mM Mes buffer (pH 5.5), 1% (w/v) glucose, and resuspended in 1 ml PBS containing 10 µl of 5 mM H_2DCFDA. Samples were incubated for 15 min at room temperature, washed twice in ice-cold distilled deionised water and resuspended in 1 ml PBS. Samples were kept at 4 °C until flow cytometric analysis (see below).

4.2.7. **Cellular DNA staining.** Cellular DNA was stained with PI according to the method of Butler *et al.* (1991), with the following modifications. At specified intervals after the addition of $Cu(NO_3)_2$ to cell suspensions (see above), 1.5 ml aliquots were removed, washed with 1 ml of 10 mM Mes buffer (pH 5.5), 1% (w/v) glucose, and immediately fixed in 70% (v/v) ethanol for 30 min at 4 °C. Samples were washed once with 1 ml 50 mM sodium citrate and resuspended in 1 ml of the same solution containing 1 mg ml^{-1}

boiled RNase A and 20 μg ml^{-1} PI. Samples were then incubated at 37 °C for 3 h in the dark and stored at 4 °C until analysis.

4.2.8. **Flow cytometry.** All samples were analysed using a Becton Dickinson FACSCalibur™ instrument, equipped with a 15 mW, 488 nm argon ion laser. Prior to sample data acquisition FACSComp software was run. FACSComp software uses CaliBRITE unlabeled, fluorescein isothiocyanate (FITC)- and phycoerythrin (PE)-labeled beads to check both the instrument sensitivity and alignment, and the bead-positive signal and noise separation for forward-angle light scatter (FSC), side-angle light scatter (SSC) and fluorescence (FL1 and FL2). Fluorescein and 2',7'-dichlorofluorescein fluorescence were monitored in channel FL1 (lower absorption maximum), while PI fluorescence was monitored in channel FL2. Fluorescence compensation was routinely adjusted to minimise overlapping emission spectra. The detection threshold was set in the FSC channel at a level just below the lowest yeast cell signal ($threshold_{FSC}$ ~ 18). For sample data acquisition in non-sorting applications, cells were diluted in FACSFlow™ sheath fluid to a density of approximately 1 x 10^7 cells ml^{-1}. Samples were aspirated into a stream of 0.22 μm pre-filtered FACSFlow™ sheath fluid and passed across the argon ion laser. Samples were analysed on high flow rate (60 μl min^{-1}). Typically, 10,000 cells were analysed per sample. For sorting applications, 0.22 μm pre-filtered PBS was used as sheath fluid, and samples were sorted at low flow rate (12 μl min^{-1}). Gated populations were physically separated (sorted) into sterile 50 ml Falcon tubes, previously coated with 4% (w/v) bovine serum albumin (BSA) in PBS for 1 h at 4 °C, to minimise adhesion of cells to the tube surface. Sorted populations were immediately placed on ice,

then centrifuged at 1,500 *g* for 5 min at 4 °C and resuspended in 0.5 ml PBS for analysis. Data acquisition and analysis were performed using CELLQuest software integrated with a Macintosh Quadra 650 computer with Apple 7.1 operating system software.

4.2.9. **Bacterial genetic manipulations.** *E. coli* DH5α competent cells (GIBCOBRL, MD) were routinely transformed with plasmid DNA according to standard transformation protocol (Ausubel *et al.*, 1998), with the following modifications. Competent cells (50 µl) were transferred to pre-chilled microcentrifuge tubes and placed on ice. Plasmid DNA (< 1 µg) was gently mixed with the competent cells and incubated on ice for 30 min. The cells were heat-shocked at 42 °C for 45-90 sec. Cells were placed on ice for 2 min. Room temperature S.O.C. medium (900 µl), comprising 1.2% (w/v) tryptone, 2.4% (w/v) yeast extract, 0.4% (v/v) glycerol, 0.23% (w/v) KH_2PO_4, 1.25% (w/v) K_2HPO_4 (GIBCOBRL, MD), was added and the mixture incubated at 37 °C for 2 h with shaking at 225 rev. min^{-1}. Aliquots were spread-plated onto LB medium containing 50 µg ml^{-1} ampicillin (Sigma, MO) and incubated at 37 °C overnight. Transformation efficiencies were determined using pUC19 DNA (0.1 µg ml^{-1}) as control plasmid. Plasmids were isolated from bacterial strains using the standard alkaline lysis mini-prep procedure (Ausubel *et al.*, 1998). Restriction enzyme digestions were performed according to standard protocol (Ausubel *et al.*, 1998). DNA fragments were typically separated by agarose gel electrophoresis performed on 1% (w/v) agarose (GIBCOBRL, MD) mini-gels, using Pharmacia Biotech gel electrophoresis apparatus (GNA-100 or GNA-200) coupled to a Pharmacia Biotech electrophoresis power supply EPS-200. Agarose gels were run

for 45 min at 75 V and 60 mA. Hi-Lo™ DNA marker (Minnesota Molecular, MN) was used to track DNA bands.

PCR amplification was performed in 100 µl reaction volumes containing 1 x PCR reaction buffer (Boehringer Mannheim, IN), 1 µg ml^{-1} plasmid DNA or 10 µg ml^{-1} chromosomal DNA as template, 1 µM of each primer, 200 µM each of 2'-deoxythymidine-5'-triphosphate (dTTP), 2'-deoxyadenosine-5'-triphosphate (dATP), 2'-deoxyguanosine-5'-triphosphate (dGTP) and 2'-deoxycytidine-5'-triphosphate (dCTP), 100 U ml^{-1} of Taq DNA polymerase (Boehringer Mannheim, IN), and nuclease-free sterile, distilled deionised water. PCR was performed in a Perkin Elmer Cetus DNA thermal cycler. For all reactions, strand denaturation was carried out at 94 °C for 3 min, and was followed by five preliminary cycles of 94 °C for 60 s, 40 °C for 60 s and 72 °C for 90 s, and 25 cycles of 94 °C for 60 s, 45 °C for 60 s and 72 °C for 90 s. PCR products were purified using phenol/chloroform/isoamyl alcohol (25:24:1 v/v/v) and ethanol precipitated prior to gel electrophoresis and/or restriction enzyme analysis.

4.2.10. **Yeast genetic manipulations.** Yeast cells were transformed with plasmid DNA using the Frozen-EZ™ yeast transformation kit (Zymo Research Inc., CA).

Both plasmid and chromosomal DNA were isolated from yeast according to standard protocols (Ausubel *et al.*, 1998), with the following modifications. Cell pellets were resuspended in 400 µl breaking buffer (2% (v/v) triton X-100, 1% (w/v) SDS, 100 mM NaCl, 10 mM Tris.Cl (pH 8.0), 1 mM EDTA) and 400 µl phenol/chloroform/isoamyl alcohol (25:24:1 v/v/v). The cell suspension was transferred to a 2 ml screw-cap microcentrifuge vial filled one-half to two-thirds full with 0.5 mm diameter glass beads

(Biospec Products Inc., OK). Yeast cells were disrupted using a Biospec Products Mini-Beadbeater™ (or Mini-Beadbeater –8™ for multiple samples) homogeniser for 4 x 30 s pulses. Yeast suspensions were placed on ice between pulses. For yeast plasmid purification, the aqueous phase was extracted and 2 µl used to transform *E. coli* DH5α cells (see above). Chromosomal DNA was precipitated with 95% ethanol and washed once with 70% ethanol. The pellet was dried under vacuum and resuspended in 100 µl sterile, distilled deionised water.

4.2.11. **Plasmid construction.** The *CUP1*::*GFP* transcriptional promoter gene fusion plasmid, pYEX-GFP$_{CUP1}$ (kindly provided by A. M. Avery, Emory University, Atlanta, GA) had been constructed by ligation of the 0.72 kb green fluorescent protein (GFP) coding sequence of *Aequorea victoria* to the large *Eco*RI-*Xho*I fragment of pYEX 4T-1 (Clontech, CA), downstream of the Cu^{2+}-inducible *CUP1* promoter.

The *SOD1*::*GFP* gene fusion plasmid, pYEX-GFP$_{SOD1}$ was constructed by first amplifying a 0.6 kb *SOD1* promoter sequence, from –600 to +5 (relative to the ATG start codon). The 0.6 kb fragment was amplified from genomic DNA using the following oligonucleotide primers in a PCR reaction:

5'-GTGGGT**TCTAGA**ATACTACCAATGGTGC-3'

(*Xba*I)

5'-ACTGCGACTGC**GAATTC**CATTATAAATTAA-3'

(*Eco*RI)

The amplified fragment was then digested with *Xba*I and *Eco*RI, and ligated to the large *Xba*I-*Eco*RI fragment of pYEX-GFP$_{CUP1}$, according to the following ligation protocol.

Following digestion with *Xba*I and *Eco*RI, the *SOD1* promoter fragment was purified with phenol/chloroform/isoamyl alcohol (25:24:1 v/v/v) and ethanol precipitated. *Xba*I/*Eco*RI-digested pYEX-GFP$_{CUP1}$ was ethanol precipitated and calf intestinal-alkaline phosphatase- (Promega, WI) treated to prevent re-circularisation. Phosphatase-treated vector DNA was subsequently purified with phenol/chloroform/isoamyl alcohol (25:24:1 v/v/v) and ethanol precipitated prior to the ligation reaction. The ligation reaction was performed in a 10 µl reaction volume containing 1 x T4 DNA ligase buffer (Promega, WI), 300 U ml^{-1} T4 DNA ligase (Promega, WI), approximately 17 µg ml^{-1} vector DNA and 7 µg ml^{-1} insert DNA (1:5 molar ratio of vector:insert DNA ends) and nuclease-free sterile, distilled deionised water. The ligation reaction was performed at 16 °C overnight. *E. coli* DH5α competent cells were transformed with 5 µl of the ligation reaction mixture, as described above. Insertion of the 0.6 kb *SOD1* promoter fragment created a transcriptional fusion with the *GFP* gene.

4.3. Results

4.3.1. **Relationship between percentage maximum cell volume, cellular DNA content and cell cycle stage.** In order to establish a direct correlation between cell volume and cell cycle stage, the cellular DNA content of ten different fractions, distinguished by cell volume, of an exponential phase *S. cerevisiae* NCYC 1383 suspension was monitored using flow cytometry. *Saccharomyces cerevisiae* NCYC 1383 was selected for this study and subsequent toxicity experiments because of its well characterised interactions with heavy metals (Avery *et al.*, 1996; Chapter 2). Cell volume increases as cells progress through the cell cycle (Lord and Wheals, 1980). Forward-angle light scatter (FSC) histograms correspond to cell volume distributions in heterogeneous yeast cell suspensions (Lloyd, 1992). Cell volume is directly proportional to FSC signal. Hence, by simultaneously monitoring cellular FSC signal and PI fluorescence intensity (FL2) (PI fluorescence is proportional to cellular DNA content), it was hoped to be able to demonstrate a correlation between cell volume and cell cycle stage. An FSC histogram was plotted, which demonstrated the normal distribution of cell volume, and divided into ten regions (R2-R11), each representing 10% of the total population (10,000 cells region^{-1}) (Fig. 4.1). Individual FL2 histograms were subsequently plotted for each of the 10% regions (Fig. 4.2c-l). An FSC-SSC dot plot of the total heterogeneous yeast cell population is shown in Figure 4.2a. The cellular DNA content of the total population is displayed in Figure 4.2b. Two distinctly resolved peaks can be observed, which

Fig. 4.1. Forward-angle light scatter (FSC) histogram of *S. cerevisiae* NCYC 1383. The FSC histogram representing the total cell population has been gated into 10 x 10% regions (R2-R11). The FSC histogram contains data collected from at least 100,000 cells, and each region represents approximately 10,000 cells.

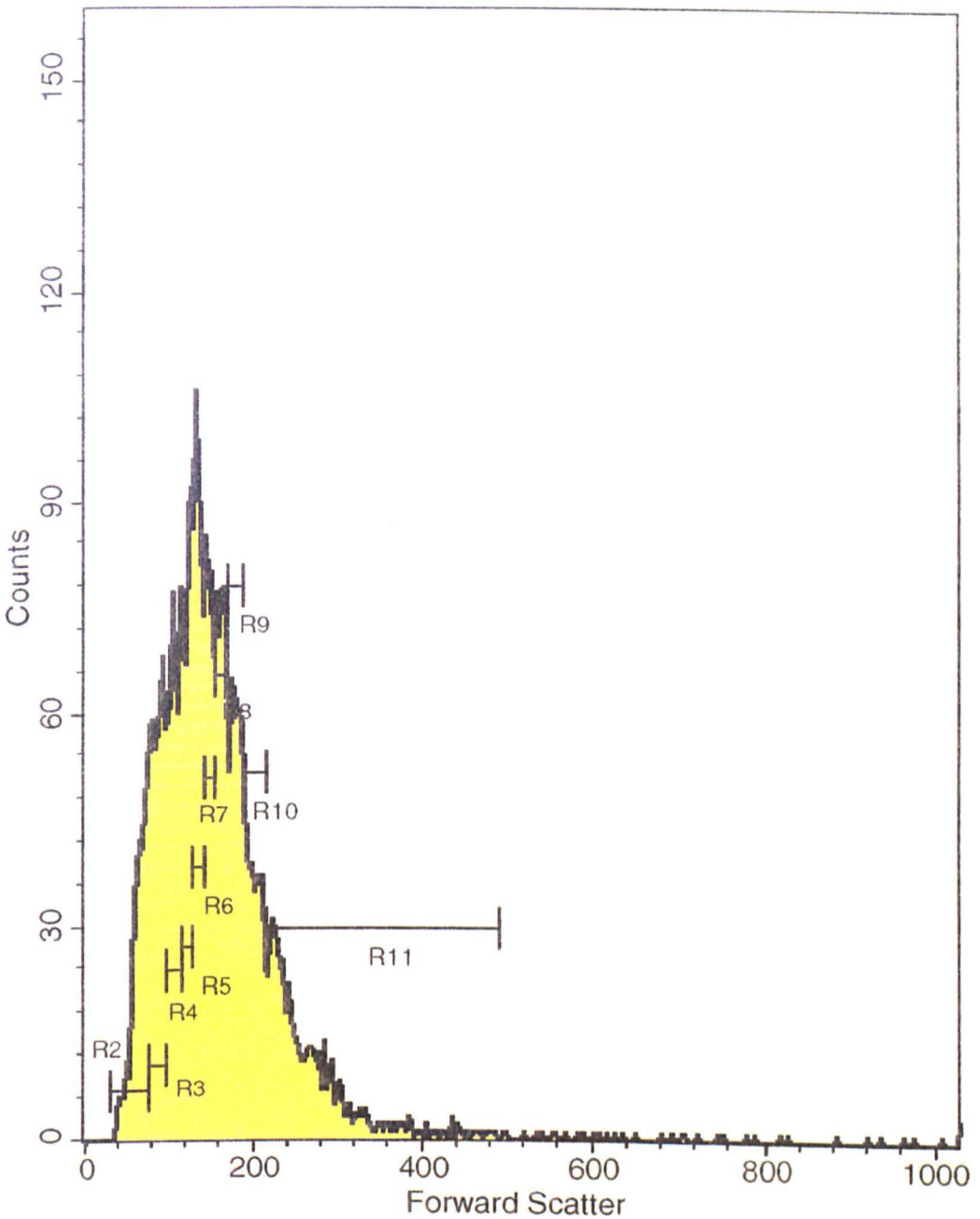
Counts
150
120
90
60
30
0
0
200
400
600
800
1000
Forward Scatter
R9
R7
R10
R6
R11
R5
R4
R2
R3

correspond to cells comprising 1C and 2C DNA contents. The number of cells consisting of 1C (G_1 phase) and 2C (G_2/M phase) DNA were approximately equal (Fig. 4.2b). The cellular DNA contents of regions R2 through R11, from Figure 4.1 are shown in Figures 4.2c-l. Cells in the 0-10% maximum cell volume fraction (R2) consist exclusively of 1C DNA, and thus correspond to cells in G_1 phase (Fig. 4.2c). Cells at 10-20% of maximum cell volume (R3) consist largely of 1C DNA, however a small 2C DNA peak, corresponding to 1% of the total number of cells, was observed. It can be inferred that cells approaching 20% maximum cell volume have reached the critical threshold size necessary to traverse START and enter S phase (S phase cells have a cellular DNA content between 1 and 2C) (Lew *et al.*, 1997). Figures 4.2e, f and g depict progression through S phase and emergence of the 2C DNA peak. Cells at 40-50% of maximum cell volume (R6) have a larger 2C DNA peak, corresponding to 53% of the total number of cells, and thus consist predominantly of G_2/M phase cells (Fig. 4.2g). Cells 90-100% maximum cell volume consist almost exclusively of 2C DNA and thus most likely correspond to cells approaching the M/G_1 phase boundary (Fig. 4.2l). The results clearly demonstrate the relationship between cell volume and cellular DNA content, and thus validate the use of FSC measurements (cell volume) for cell cycle analysis.

4.3.2. **Relationship between cell volume (cell cycle stage) and susceptibility to copper toxicity.** Here we sought to determine if sensitivity to copper toxicity was influenced by cell cycle stage. Cells previously grown in unsupplemented medium were exposed to 100 μM Cu^{2+} for 15 min. Samples were stained with FDA and PI and analysed by flow

Fig. 4.2. Relationship between % maximum cell volume and cellular DNA content (cell cycle stage) in *S. cerevisiae* NCYC 1383. Figure 4.2a represents a forward-angle light scatter (FSC) versus side-angle light scatter (SSC) dot plot of the exponential phase population. A region gate (R1) was applied to separate cells from cell debris. Figure 4.2b represents the propidium iodide fluorescence (FL2) histogram of the total population (R1). Figure 4.2c-l represent FL2 histograms for regions 2 to 11, derived from the FSC histogram (Fig. 4.1). Each histogram contains data collected from approximately 10,000 cells.

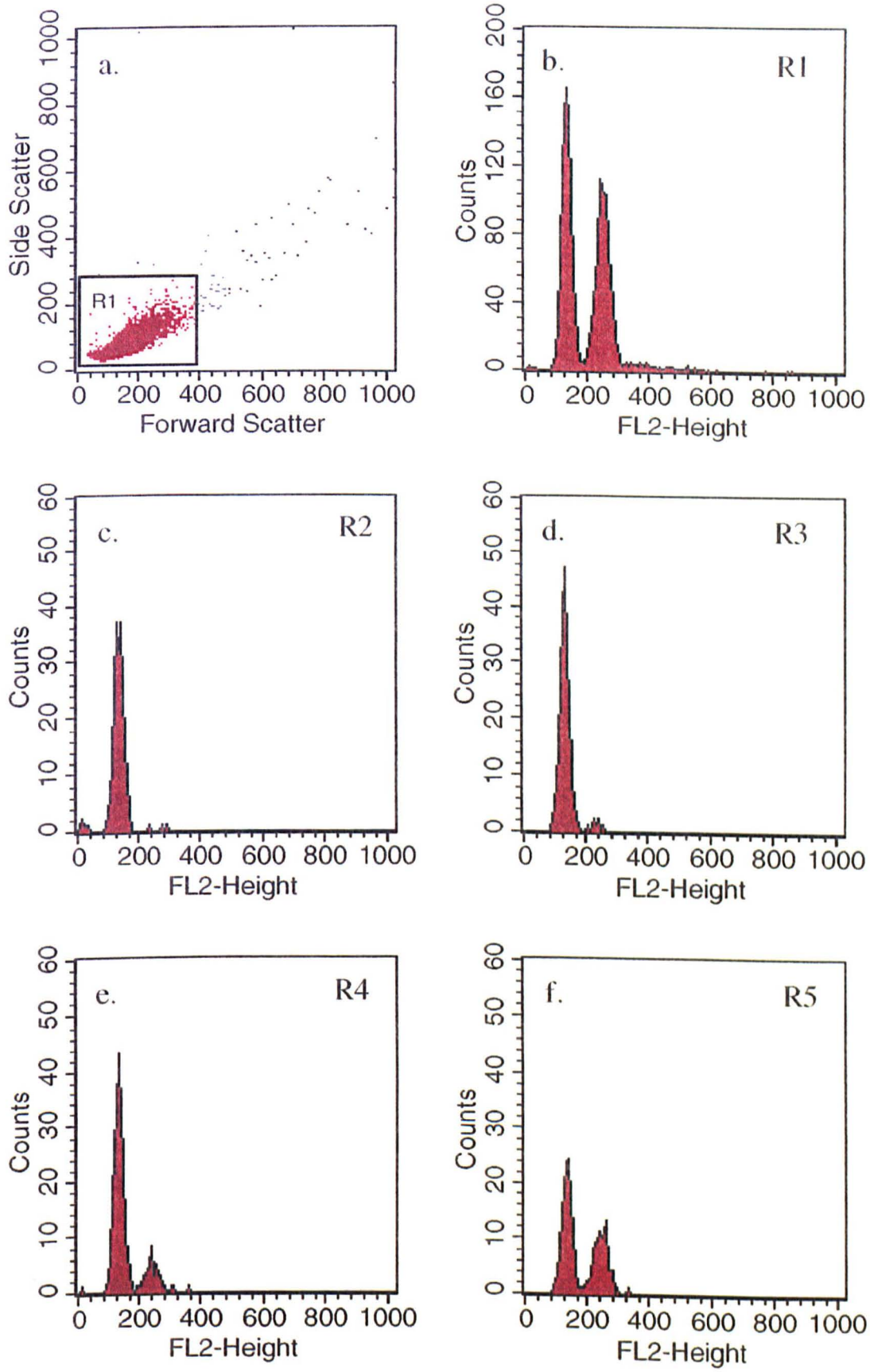
a.
Side Scatter
Forward Scatter
R1
0
200
400
600
800
1000
b.
R1
Counts
FL2-Height
0
40
80
120
160
200
c.
R2
Counts
FL2-Height
0
10
20
30
40
50
60
d.
R3
Counts
FL2-Height
e.
R4
Counts
FL2-Height
f.
R5
Counts
FL2-Height

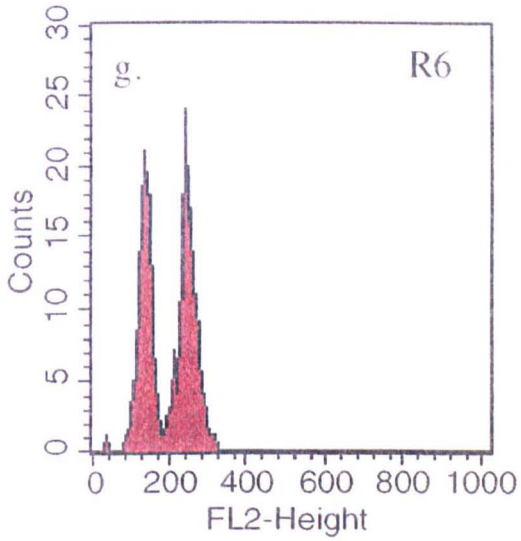
g.
R6
Counts
0 5 10 15 20 25 30
0 200 400 600 800 1000
FL2-Height

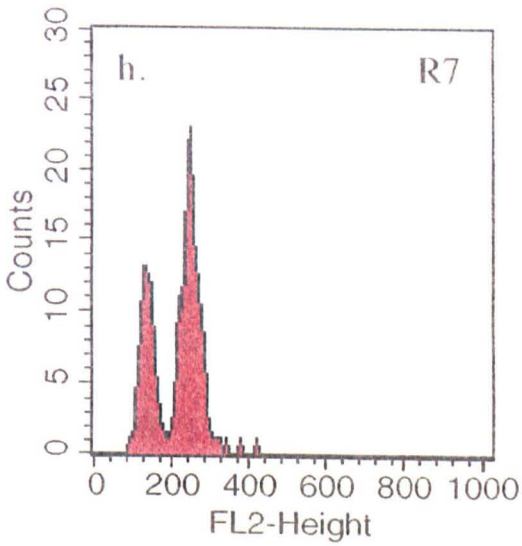
h.
R7
Counts
0 5 10 15 20 25 30
0 200 400 600 800 1000
FL2-Height

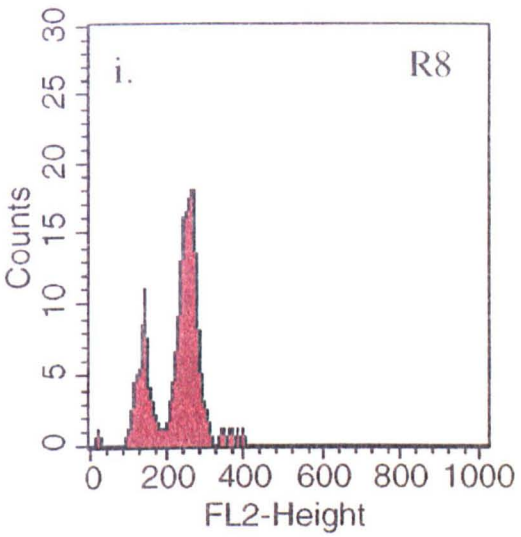
i.
R8
Counts
0 5 10 15 20 25 30
0 200 400 600 800 1000
FL2-Height

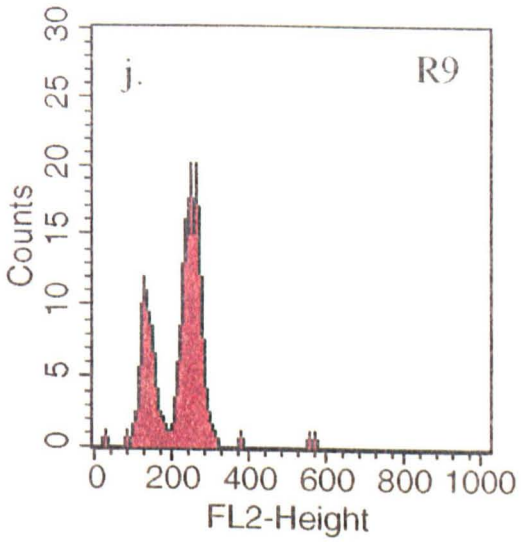
j.
R9
Counts
0 5 10 15 20 25 30
0 200 400 600 800 1000
FL2-Height

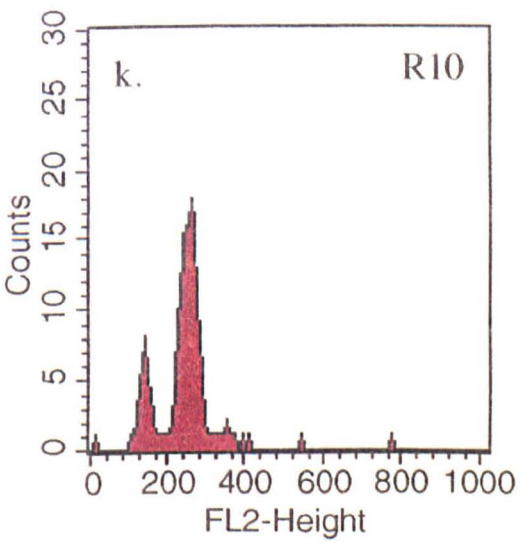
k.
R10
Counts
0 5 10 15 20 25 30
0 200 400 600 800 1000
FL2-Height

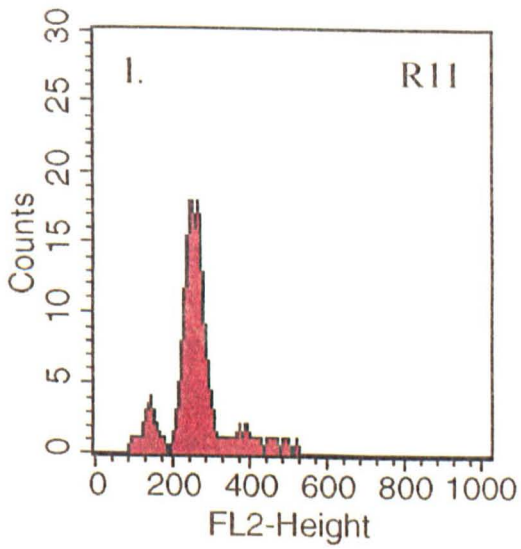
l.
R11
Counts
0 5 10 15 20 25 30
0 200 400 600 800 1000
FL2-Height

cytometry. At least 100,000 cells were analysed per sample. An FSC histogram was plotted and divided into fifty 2% regions (defined as gates) (see Fig. 4.1). An FL1 versus FL2 dot plot was subsequently prepared for each of the fifty 2% regions to determine the number of viable cells within each region (see Fig. 4.4a). FL1 versus FL2 region statistics were then used to construct a plot of % viability against % maximum cell volume (Fig. 4.3). The largest cells (98-100% of maximum cell volume) were the most resistant to copper, whereby after 15 min exposure to 100 μM Cu^{2+}, approximately 69% of these cells remained viable. Interestingly, the smallest cells (0-2% of maximum cell volume) were also relatively resistant to copper, whereby after 15 min exposure to 100 μM Cu^{2+}, approximately 57% of these cells remained viable. However, as % of maximum cell volume increased beyond 0-2%, Cu^{2+}-sensitivity increased and was maximal at 38-40% of maximum cell volume, whereby only 32% of cells remained viable after Cu^{2+}-exposure (Fig. 4.3). With increased cell volume beyond this point, % viability increased to a maximum with the largest cells. These results indicate differing susceptibilities of cells at different stages of the cell cycle towards copper toxicity.

4.3.3. **Cellular DNA content of *S. cerevisiae* NCYC 1383 exposed to a toxic concentration of copper.** To further characterise the relationship between cell cycle stage and sensitivity towards copper toxicity, *S. cerevisiae* was exposed to a toxic concentration of copper, and the cellular DNA content of sensitive and resistant sub-populations was compared. Cells previously grown in unsupplemented YEPD medium were exposed to 100 μM Cu^{2+} for 15 min. Samples were stained with FDA and PI and analysed by flow cytometry. An FL1 versus FL2 dot plot was created to distinguish between live and dead

Fig. 4.3. Relationship between cell volume (cell cycle stage) and susceptibility to copper toxicity in *S. cerevisiae* NCYC 1383. Cells were exposed to 100 μM $Cu(NO_3)_2$ for 15 min, and viability was determined by staining with FDA (FL1) and PI (FL2). An FSC histogram of the total population was gated into 50 x 2% regions. The number of viable cells of each region was determined from gate statistics attained from an FL1 versus FL2 dot plot. Data was collected from at least 100,000 cells, and each region represents approximately 2,000 cells.

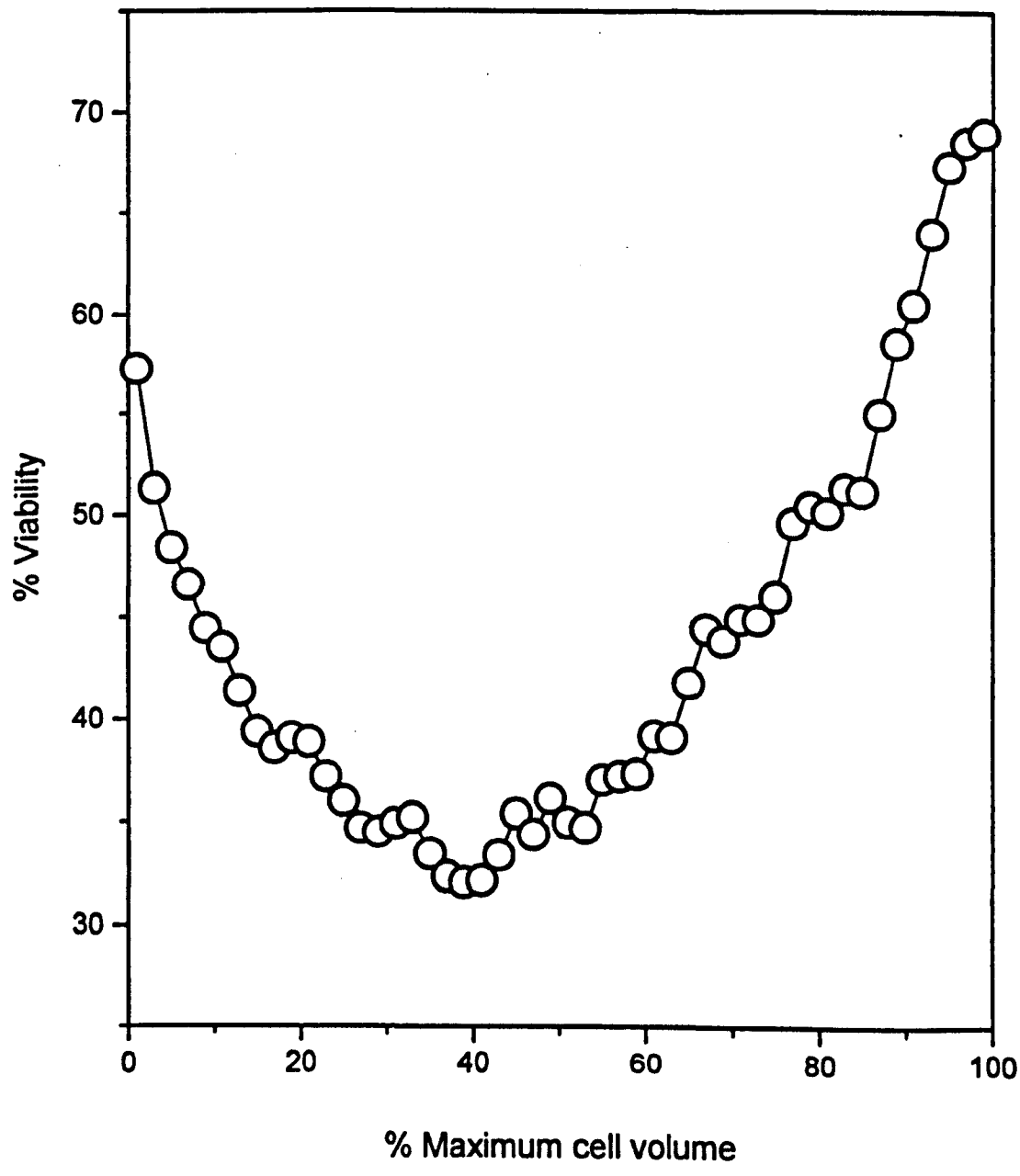
70
60
50
40
30
% Viability
0
20
40
60
80
100
% Maximum cell volume

sub-populations (Fig. 4.4a). Dead and live populations were gated R1 and R2, respectively. Both regions were sorted (physically separated into different Falcon tubes), fixed, and cellular DNA was stained with PI. The cellular DNA content of the copper-sensitive sub-population (R1) is shown in Figure 4.4b. Of the copper-sensitive sub-population, approximately 53% of cells comprised 2C DNA, as indicated by the slightly greater 2C DNA peak (Fig. 4.4b). The cellular DNA content of copper-resistant cells (R2) is shown in Figure 4.4c. The copper-resistant sub-population consisted predominantly of G_1 phase cells, whereby approximately 72% of cells comprised 1C DNA. These results indicate that cells at the cell cycle stage corresponding to a 1C DNA content (G_1 phase) are considerably less sensitive to the toxic effects of copper. It was also evident that the copper-resistant sub-population also consisted of a small proportion of 2C DNA cells (approximately 28% of the total number of cells) (Fig. 4.4c). It could be inferred from Figure 4.3 that this 2C DNA peak corresponds to cells of maximum cell volume. These results further demonstrate the differing sensitivities of cells of different cell cycle stage to the toxic effects of copper.

4.3.4. **Fatty acid composition of cells at different cell cycle stage.** The increased susceptibility of cells displaying higher degrees of membrane fatty acid unsaturation to heavy metal toxicity had previously been demonstrated (Avery *et al.*, 1996; Chapters 2 and 3). Here we sought to ascertain whether the above differences in the sensitivities of cells at different stages of the cell cycle towards copper toxicity could be attributed to cell cycle-induced changes in fatty acid composition. *Saccharomyces cerevisiae* NCYC 1383

Fig. 4.4. Cellular DNA content of live and dead *S. cerevisiae* NCYC 1383 after exposure to copper. Cells were exposed to 100 μM $Cu(NO_3)_2$ for 15 min, and viability was determined by staining with FDA (FL1) and PI (FL2). Figure 4.4a represents an FL1 versus FL2 dot plot indicating dead (R1) and live (R2) sub-populations. R1 and R2 were sorted, the cellular DNA of each sub-population was stained with PI, and FL2 histograms were plotted (Fig. 4.4b,c). Data was collected from at least 10,000 cells.

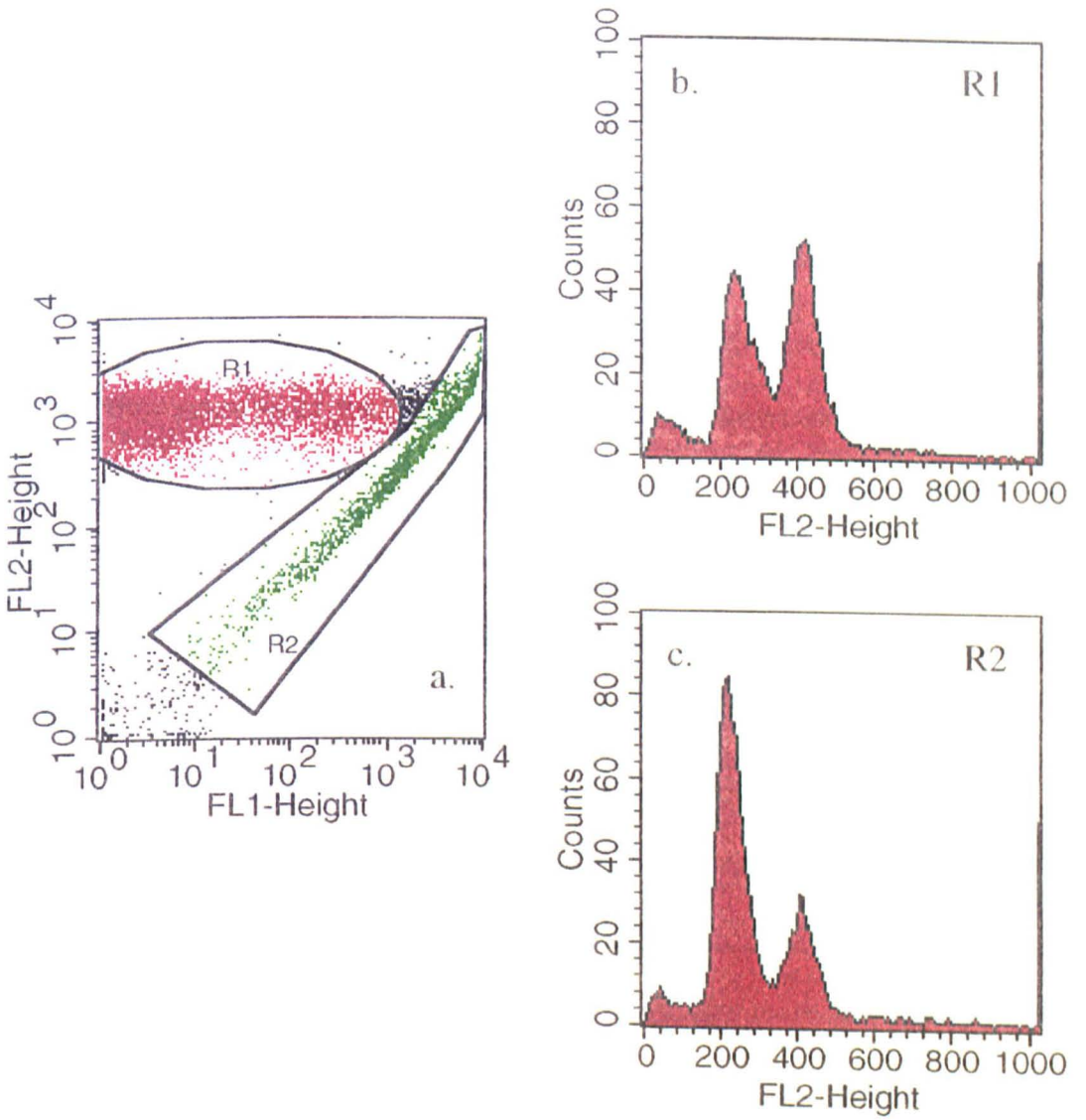
R1
R2
a.
FL2-Height
FL1-Height
b.
R1
Counts
FL2-Height
c.
R2
Counts
FL2-Height

previously grown in unsupplemented YEPD medium was analysed by flow cytometry. An FSC histogram was plotted and divided into four 25% regions (R1-R4), representing cells at different stages of the cell cycle (see Fig. 4.1). Each region was physically sorted, cells were resuspended in PBS, fatty acids were extracted, and FAMEs were analysed by gas-liquid chromatography as described previously (see Section 4.2.3). The cellular fatty acid compositions of regions 1, 2, 3 and 4 are displayed in Table 4.1. Levels of the monounsaturated fatty acids, 16:1 and 18:1 were similar for each region, only varying between approximately 21 and 26%, and 22 and 26% of total cellular fatty acids, respectively (Table 4.1). Thus, the unsaturation indices (average number of double bonds per fatty acid) were found to be similar, ranging between 0.44 and 0.49, for each of the sorted regions. The results indicate that the cellular fatty acid composition of *S. cerevisiae* remains relatively constant throughout the cell cycle, and the small differences that are evident appear too small to significantly influence Cu^{2+}-sensitivity (Chapter 3).

4.3.5. **Cellular DNA content of *S. cerevisiae* NCYC 1383 previously stained with the oxidative stress probe 2',7'-dichlorodihydrofluorescein diacetate (H_2DCFDA).** The oxidant status of cells at different stages of the cell cycle was next examined, to determine if repartition in the various cell cycle stages was associated with differences in endogenous levels of oxy-radicals. *Saccharomyces cerevisiae* NCYC 1383 was stained with the oxidant-sensitive probe H_2DCFDA and examined by flow cytometry. An FL1 histogram was plotted and on the basis of FL1 intensity, three sub-populations of low (R1), medium (R2) and high (R3) cellular oxidant status were gated and sorted for

Table 4.1. Cellular fatty acid composition of *S. cerevisiae* NCYC 1383 at different stages of the cell cycle

Fatty acid	Region			
	R1	R2	R3	R4
16:0	32.4±0.6	29.4±0.3	31.2±0.5	32.8±0.6
16:1	23.0±0.5	21.3±0.9	22.3±0.3	26.1±0.5
18:0	19.9±0.4	23.2±0.7	24.7±0.1	18.3±1.2
18:1	24.7±0.8	26.1±0.6	21.8±0.9	22.8±0.4
18:2	tr	tr	tr	tr
U.I.	*0.48*	*0.47*	*0.44*	*0.49*

Fatty acids are abbreviated with the first figure representing the number of carbon atoms in the fatty acyl chain and the second representing the number of double bonds. U.I. refers to the unsaturation index (average number of double bonds per fatty acid). Values for percentage fatty acid composition are means from two replicate determinations ± SD. (tr. < 0.1).

Fig. 4.5. Cellular DNA content of *S. cerevisiae* NCYC 1383 previously stained with the oxidant-sensitive probe 2',7'-dichlorodihydrofluorescein diacetate (H_2DCFDA) (FL1). Figure 4.5a represents an FL1 histogram gated on regions R1, R2 and R3 of low, medium and high FL1 intensity, respectively. R1, R2 and R3 were sorted, the cellular DNA of each sub-population was stained with PI, and FL2 histograms were plotted (Fig. 4.5b,c,d). Data was collected from at least 10,000 cells.

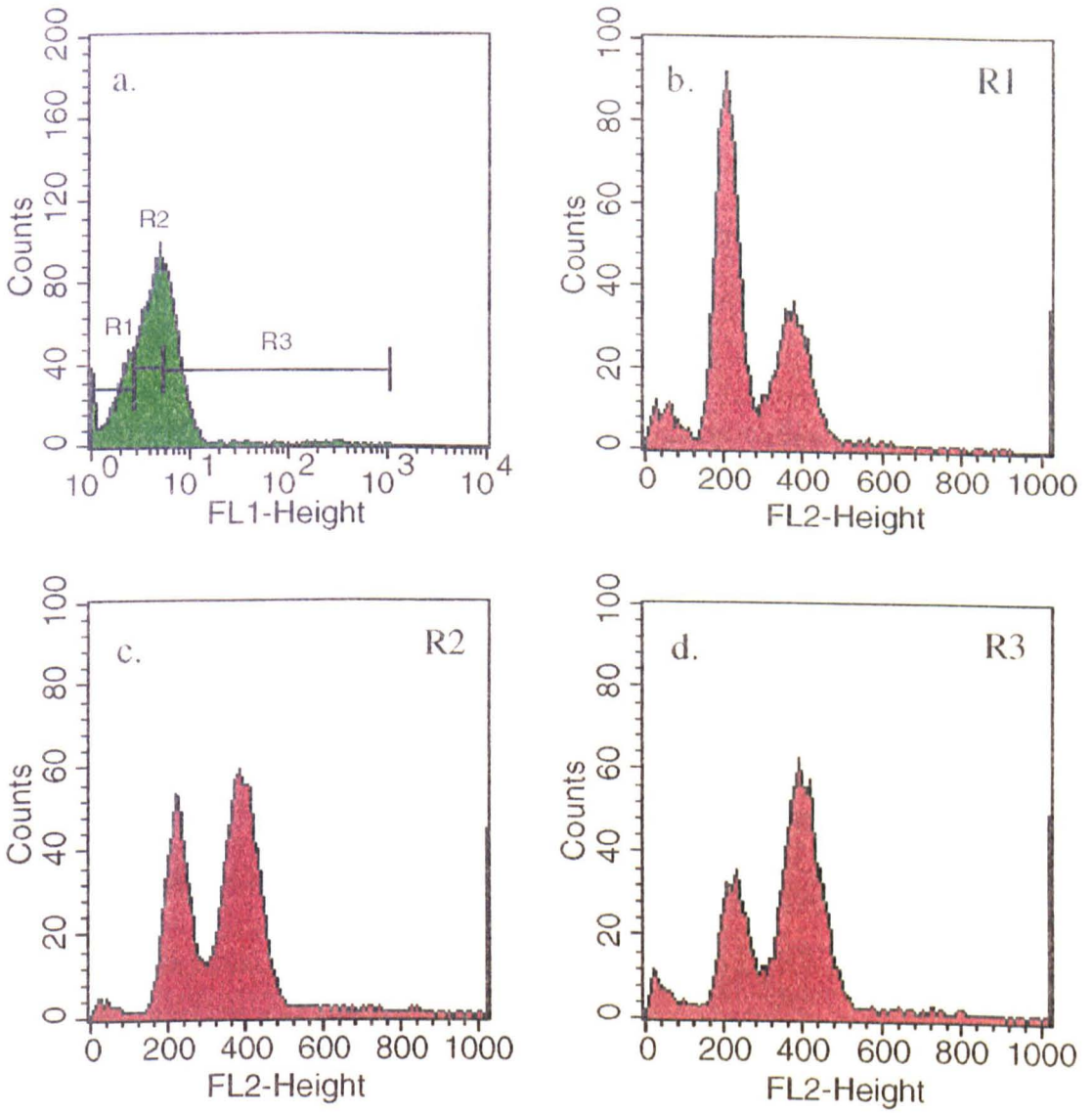
a.
R1
R2
R3
Counts
FL1-Height
b.
R1
Counts
FL2-Height
c.
R2
Counts
FL2-Height
d.
R3
Counts
FL2-Height

subsequent determination of the cells' DNA content (Fig. 4.5a). R1 (low oxidant status) comprised predominantly of 1C DNA cells (64% of the total number of cells), with a small proportion of 2C DNA cells (Fig. 4.5b). R2 (medium oxidant status) consisted of a greater proportion of 2C DNA cells (61% of the total number of cells) (Fig. 4.5c). Finally, R3 (high oxidant status) consisted predominantly of 2C DNA cells (69% of total number of cells), with a small proportion of 1C DNA cells (Fig. 4.5d). These results suggest that within a heterogeneous yeast population the generation of oxy-radicals, by normal metabolic processes, occurs to a greater extent at later cell cycle stages.

4.3.6. **Influence of initial oxidant status on the susceptibility of *S. cerevisiae* NCYC 1383 towards copper toxicity.** Here we sought to determine if differences in the levels of endogenously generated oxy-radicals of different cell cycle stage sub-populations could be correlated with differential susceptibility towards copper toxicity. Cells were stained with H_2DCFDA, and three different sub-populations were sorted as described above (see Fig. 4.5a). Cells were harvested and resuspended to a density of approximately 2×10^5 cells ml^{-1} in PBS, and exposed to 10 μM Cu^{2+} for 10 min. Samples were subsequently stained with PI and re-examined by flow cytometry to determine the number of viable cells of each sub-population. The % viability of regions 1, 2 and 3 of unsupplemented, 18:2- and 18:3-supplemented cultures after 10 min exposure to copper is shown in Figure 4.6. It is evident from the graph that cells of region 3 (high initial oxidant status) are the most susceptible to copper toxicity. Hence, with cells previously grown in unsupplemented medium, after 10 min exposure to 10 μM Cu^{2+} 72% of cells of region 3

Fig. 4.6. Influence of initial oxidant status on the susceptibility of *S. cerevisiae* NCYC 1383 to copper toxicity. Cells were stained with the oxidant-sensitive probe H_2DCFDA (FL1) and on the basis of initial oxidant status three different sub-populations of low (R1), medium (R2) and high (R3) FL1 intensity were sorted (see Fig. 4.5a). Each sub-population was subsequently exposed to 10 μM $Cu(NO_3)_2$ for 10 min and the number of viable cells of each sub-population was determined by staining with FDA and PI. Figure 4.6 shows the % viability of regions 1, 2 and 3 of unsupplemented (○), linoleate- (●) and linolenate- (□) supplemented cells after 10 min exposure to 10 μM $Cu(NO_3)_2$.

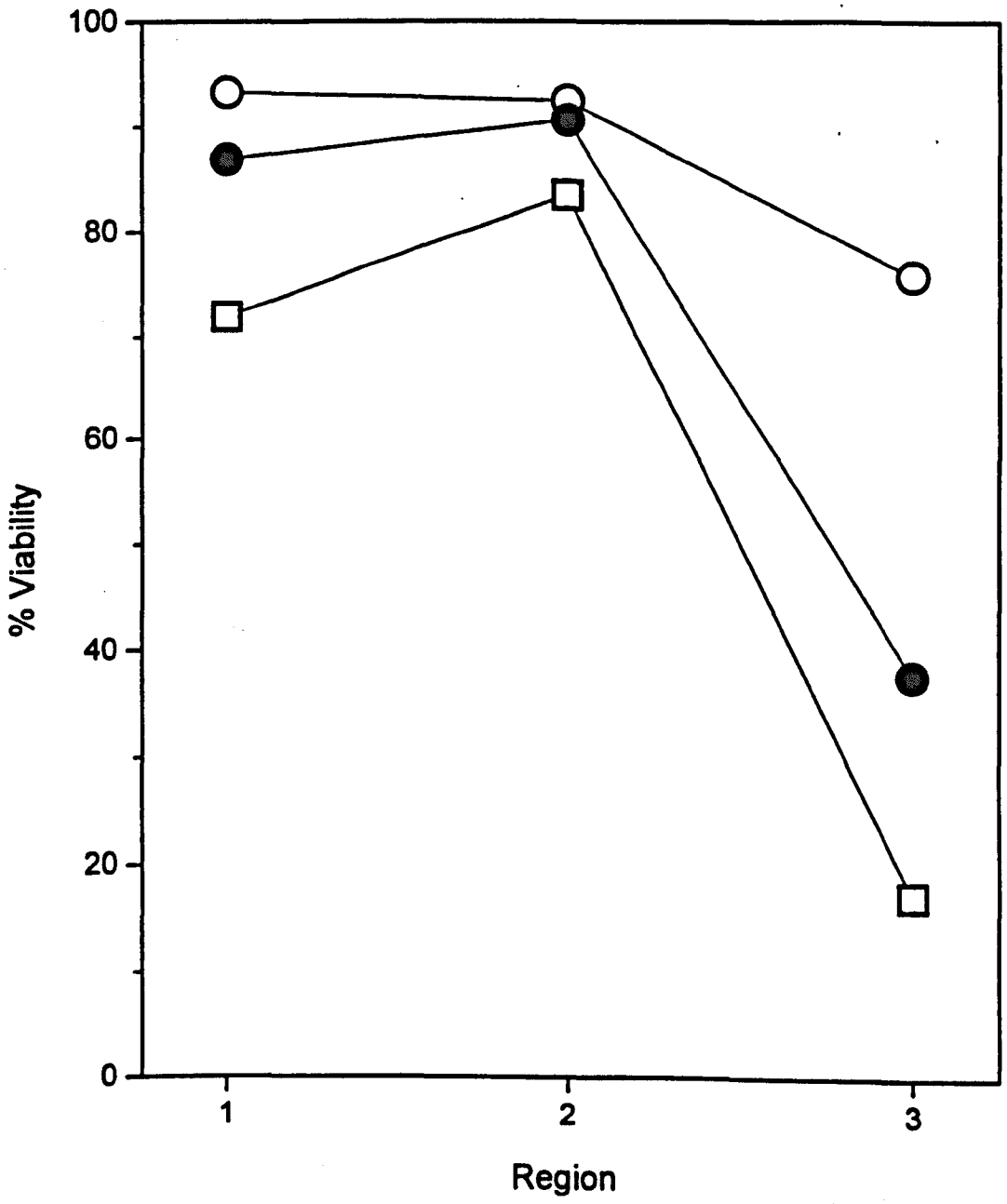
100
80
60
40
20
0
% Viability
1
2
3
Region

remained viable compared with 93% of cells of region 1. However, this effect was greatly accentuated with cells previously grown in 18:3-supplemented medium. Here only 17% of cells of region 3 remained viable after 10 min exposure to 10 μM Cu^{2+}, compared with 76% of cells of region 1. The results clearly demonstrate that cells with high initial oxidant status are predisposed to killing in the presence of toxic concentrations of copper.

4.3.7. ***CUP1*-expression in *S. cerevisiae* DY150 exposed to copper.** The differential sensitivity of different cell cycle stage fractions towards copper toxicity had previously been demonstrated. Here we sought to determine whether the cell cycle stage-dependency of susceptibility towards copper toxicity could be attributed to heterogeneous basal levels of *CUP1* metallothionein expression. While ideally promoter fusion experiments would also have been performed with *S. cerevisiae* NCYC 1383, this strain was particularly difficult to transform with plasmid DNA. Thus, the yeast strain *S. cerevisiae* DY150 (Clontech, CA) was selected for molecular biological experimentation because of its ease of transformation relative to NCYC 1383. DY150 was transformed with pYEX-GFP_{CUP1} (Fig. 4.7a), an episomal plasmid containing the *GFP* coding sequence under the control of the *CUP1* promoter. Thus, *CUP1* promoter activity could be monitored by GFP fluorescence (FL1) using flow cytometry. Transformed DY150 was exposed to 10 μM $Cu(NO_3)_2$ for 10 min to preclude *CUP1* induction, cells were stained with PI (FL2) and analysed by flow cytometry. Exposure to 10 μM $Cu(NO_3)_2$ for 10 min resulted in approximately 64% toxicity as demonstrated by the large proportion of

Fig. 4.7. The plasmid pYEX-GFP$_{CUP1}$ (a) was constructed by ligation of the 0.72 kb green fluorescent protein (GFP) coding sequence of *Aequorea victoria* to the large *Eco*RI-*Xho*I fragment of pYEX 4T-1 (Clontech, CA). The plasmid pYEX-GFP$_{SOD1}$ (b) was constructed by ligating a 0.6 kb *SOD1* promoter sequence, from –600 to +5 (relative to the ATG start codon), to the large *Xba*I-*Eco*RI fragment of pYEX-GFP$_{CUP1}$.

a.

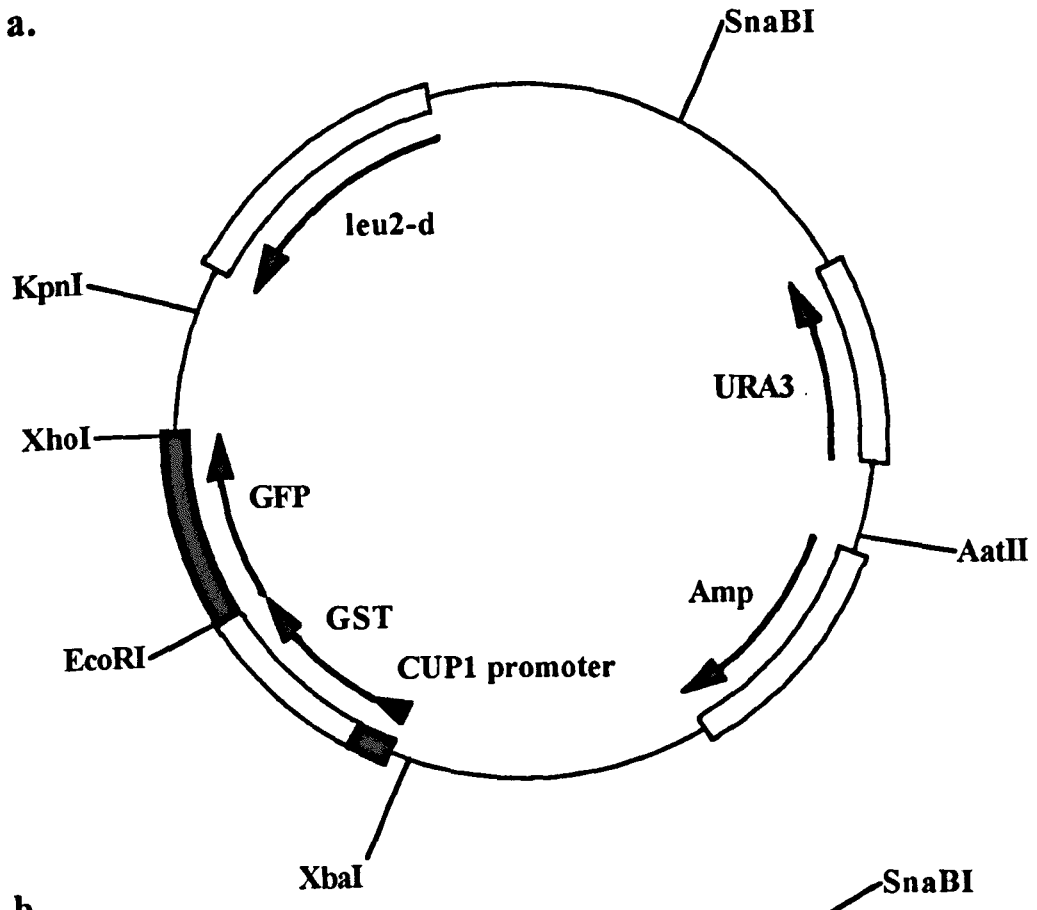
SnaBI
leu2-d
KpnI
URA3
XhoI
GFP
AatII
Amp
GST
EcoRI
CUP1 promoter
XbaI

b.

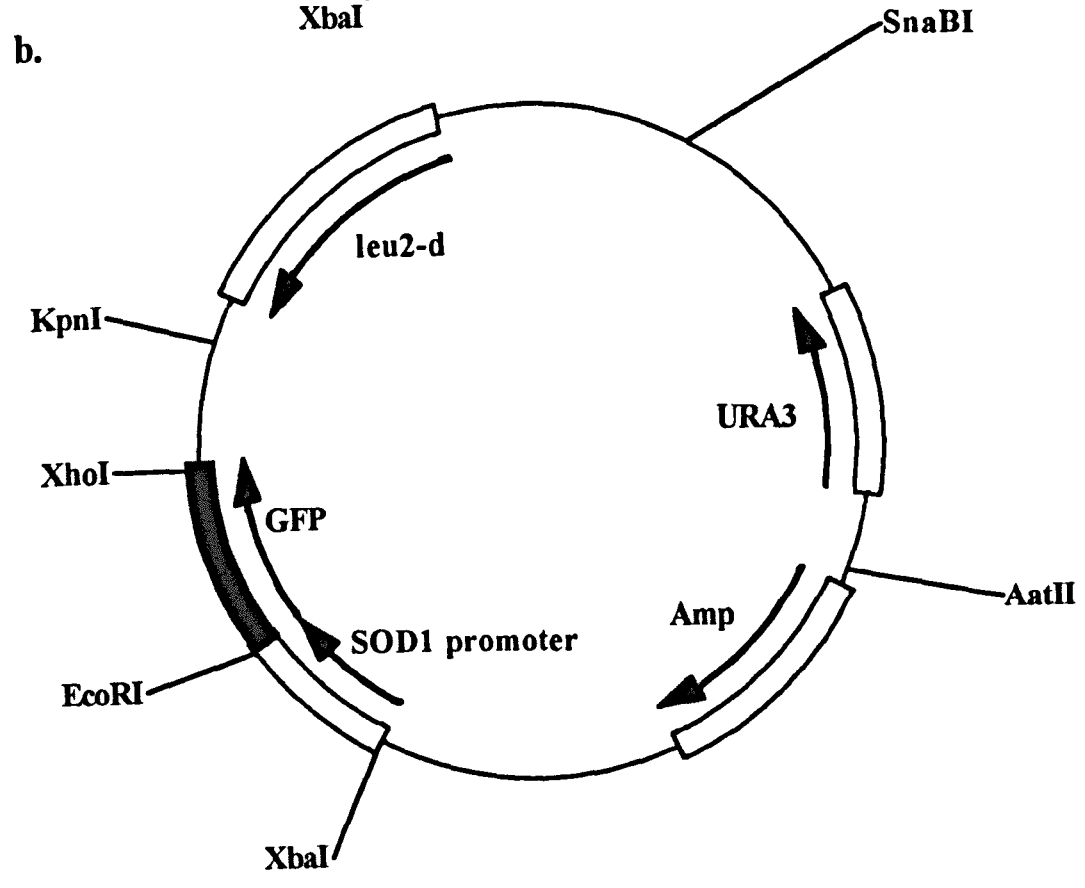
SnaBI
leu2-d
KpnI
URA3
XhoI
GFP
AatII
Amp
SOD1 promoter
EcoRI
XbaI

Fig. 4.8. *CUP1* expression in *S. cerevisiae* DY150 exposed to copper. Cells were exposed to 10 μM $Cu(NO_3)_2$ for 10 min and stained with PI (FL2). Figure 4.8a represents an FL1 (GFP) versus FL2 dot plot indicating dead (R1) and live (R2) sub-populations. Figure 4.8b shows the FL1 histogram of dead cells (R1) while figure 4.8c shows the FL1 histogram of live cells (R2). Data was collected from at least 10,000 cells.

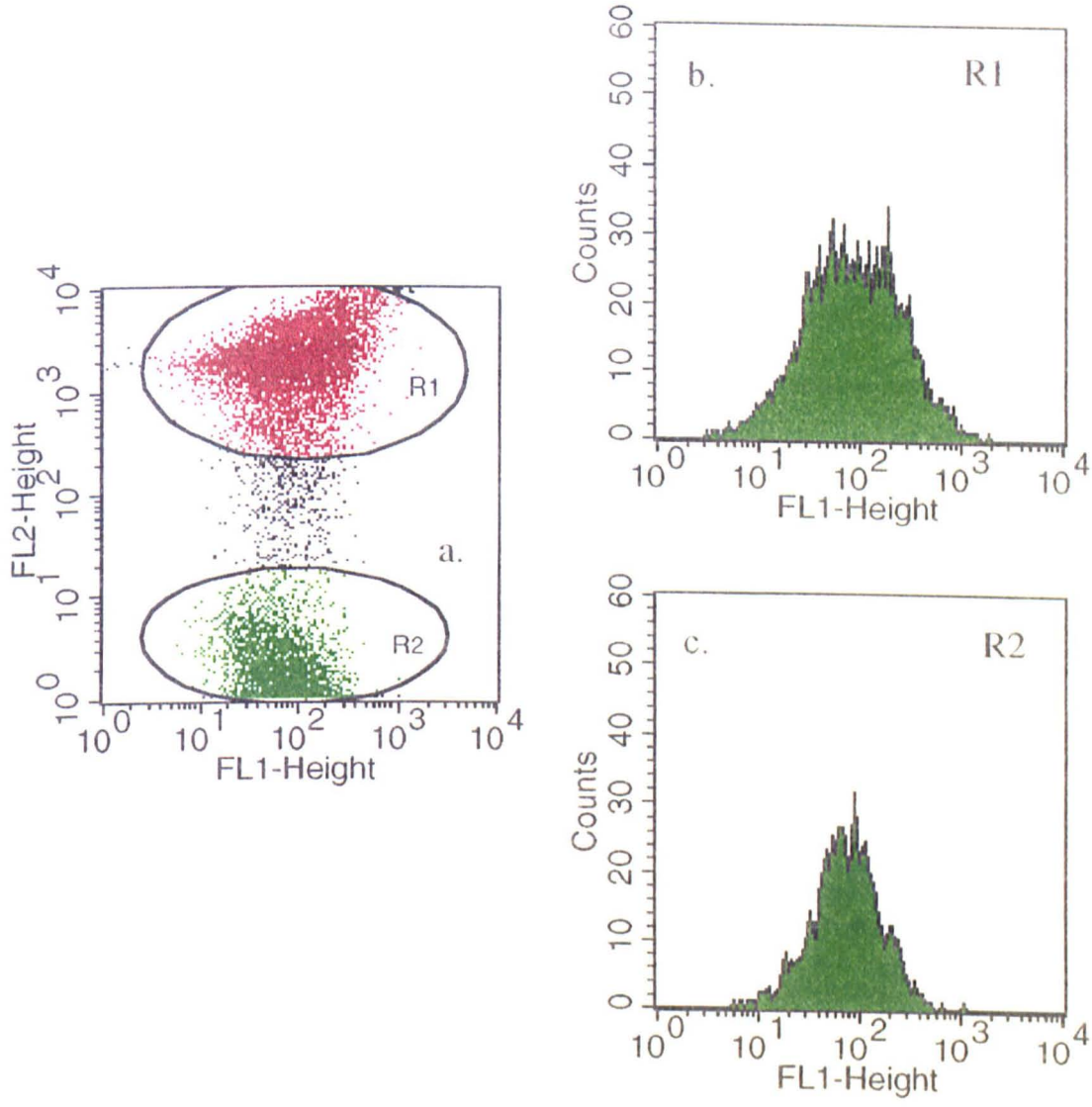
a.
R1
R2
FL2-Height
FL1-Height
b.
R1
Counts
FL1-Height
c.
R2
Counts
FL1-Height

PI-stained cells (Fig. 4.8a). The GFP fluorescence signal of dead cells (R1) is shown in Figure 4.8b, while that of live cells (R2) is shown in Figure 4.8c. The GFP fluorescence signal for both sub-populations demonstrated considerable heterogeneity, indicative of fluctuations in episomal plasmid copy number during the cell cycle (Mason, 1991). However, there were no significant differences in basal levels of *CUP1* promoter activity, as determined by GFP fluorescence, between live and dead sub-populations. Therefore, the results indicate that differences in basal levels of *CUP1* expression do not account for differential sensitivity towards copper toxicity. One would expect to observe increased live cell-GFP fluorescence for a gene whose differential expression was associated with increased Cu^{2+}-resistance.

Several reports have indicated that *CUP1* is an inducible component of the *S. cerevisiae* oxidative stress response system (Jensen *et al.*, 1996; Liu and Thiele, 1996). Here we also sought to confirm Cu^{2+}-induced *CUP1* transcription. DY150 transformed with pYEX-GFP_{CUP1} was exposed to 10 μM $Cu(NO_3)_2$ for up to 1 h, cells were stained with PI and analysed by flow cytometry. Exposure to 10 μM $Cu(NO_3)_2$ for 1 h resulted in approximately 70% killing, as demonstrated by the high proportion of PI-stained cells (R1) (Fig. 4.9a). GFP fluorescence in the absence of Cu^{2+} (t = 0) and after 1 h exposure to 10 μM Cu^{2+} (t = 1 h) is displayed in Figure 4.9b. Thus, exposure to 10 μM $Cu(NO_3)_2$ for 1 h results in both an increase and decrease in GFP fluorescence intensity as demonstrated by the lengthening of the GFP peak (Fig. 4.9b). GFP fluorescence after 1 h exposure to Cu^{2+}, gated on R1 and R2 is shown in Figure 4.9c. As can be seen from the histogram, live cells (R2) account for the high GFP fluorescence signal, while dead cells (R1) predominantly account for the reduction in GFP fluorescence signal. The results

Fig. 4.9. *CUP1* induction in *S. cerevisiae* DY150 exposed to copper. Cells were exposed to 10 μM $Cu(NO_3)_2$ for 1 h and stained with PI (FL2). Figure 4.9a represents an FL1 (GFP) versus FL2 dot plot indicating dead (R1) and live (R2) sub-populations. Figure 4.9b shows the FL1 histogram of cells prior to Cu^{2+} addition (t = 0), and after 1 h exposure to Cu^{2+} (t = 1 h). Figure 4.9c shows the FL1 histogram of both dead (R1) and live (R2) cells, after 1 h exposure to Cu^{2+}. Data was collected from at least 10,000 cells.

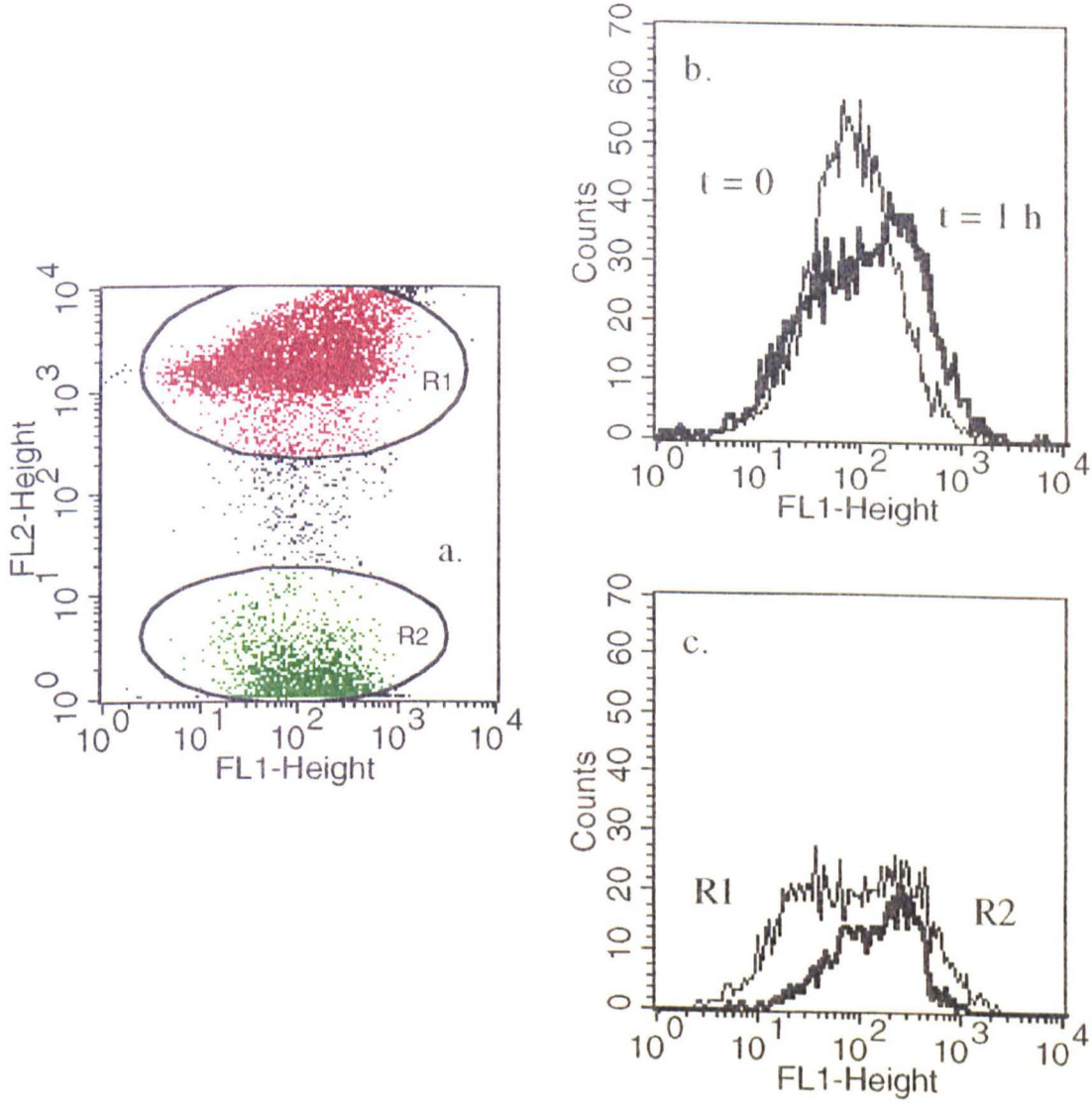
a.
R1
R2
FL2-Height
FL1-Height
b.
t = 0
t = 1 h
Counts
FL1-Height
c.
R1
R2
Counts
FL1-Height

demonstrate induction of the *CUP1* promoter in *S. cerevisiae* in the presence of 10 μM Cu^{2+}. Furthermore, the results demonstrate that live cells have higher levels of *CUP1* activity, as evidenced by their higher GFP signal. It is most likely that the decrease in GFP fluorescence observed for the dead cells is a consequence of membrane permeabilisation. GFP is normally found in the cytoplasm and leaks upon prolonged incubation with membrane permeabilising-agents, such as copper (Kalejta *et al.*, 1997).

4.3.8. ***SOD1*-expression in *S. cerevisiae* DY150 exposed to copper.** The yeast strain DY150 was also transformed with pYEX-GFP_{SOD1} (Fig. 4.7b), containing the GFP coding sequence under the control of the *SOD1* promoter, in order to determine whether differences in basal levels of *SOD1* expression could account for the differential susceptibility of different cell cycle stage fractions to copper toxicity. Transformed DY150 was exposed to an approximately 50% cytotoxic dose of $Cu(NO_3)_2$ for 10 min to preclude *SOD1* induction. Cells were stained with PI and analysed by flow cytometry (Fig. 4.10a). Thus, within a heterogeneous population *SOD1* appears to be constitutively expressed to varying degrees (Fig. 4.10a). The GFP fluorescence signal of dead cells (R1) is shown in Figure 4.10b, while that of live cells (R2) is shown in Figure 4.10c. Two distinct GFP peaks were evident for the live cells; a sub-population with high levels of GFP fluorescence (39% of the total number of cells), and a smaller sub-population with no appreciable levels of GFP fluorescence (10% of the total number of cells). It is most likely that the smaller sub-population corresponds to plasmid-free cells, as yeast episomal plasmids are highly unstable during growth on non-selective medium (Mason, 1991). Indeed, also using flow cytometry, Hjortsu *et al.* (1985) reported approximately

12% plasmid-free yeast cells during exponential batch growth. In addition, yeast cells not expressing GFP have a low level of autofluorescence when irradiated with the 488 nm argon ion laser (Niedenthal *et al.*, 1996). While a statistically significant difference between the GFP fluorescence signal of live and dead sub-populations could not be established, the results are not as outright as those of the *CUP1* experiments (Fig. 4.10b,c). The results are complicated by the fact that the emission spectra of PI and GFP overlap (an inherent disadvantage of the simultaneous use of red and green fluorophores for flow cytometric analysis), and thus PI-fluorescence is also detected by the FL1 detector (Haugland, 1996). Therefore, it remains to be elucidated whether heterogeneous basal levels of *SOD1* activity play a significant role in the cell cycle stage-dependency of susceptibility towards copper toxicity.

We also sought to determine if *SOD1* promoter expression could be induced upon prolonged exposure to either Cu^{2+} or the specific superoxide anion generating compound menadione. Transformed DY150 was exposed to 10 μM Cu^{2+} or 2 mM menadione for 1 h, cells were stained with PI and analysed by flow cytometry (Fig. 4.11). An FL1 versus FL2 dot plot of transformed DY150 prior to toxin exposure is shown in Figure 4.11a. Again two populations are evident; a smaller sub-population with no appreciable levels of GFP fluorescence (R1) (11% of the total number of cells) and a larger sub-population displaying appreciable levels of GFP fluorescence (R2). Again, it is most likely that the smaller sub-population corresponds to plasmid-free cells (see above). Figure 4.11b and c represent FL1 versus FL2 dot plots of transformed DY150 after 1 h exposure to 10 μM Cu^{2+} and 2 mM menadione, respectively. Exposure to 10 μM Cu^{2+} and 2 mM menadione for 1 h resulted in approximately 65% (R3) and 56% (R4) killing, respectively (Fig.

4.10b,c). However, exposure to either toxin did not appear to result in *SOD1* induction (Fig. 4.11b,c).

Fig. 4.10. *SOD1* expression in *S. cerevisiae* DY150 exposed to copper. Cells were exposed to 10 μM $Cu(NO_3)_2$ for 10 min and stained with PI (FL2). Figure 4.10a represents an FL1 versus FL2 dot plot indicating dead (R1) and live (R2) sub-populations. Figure 4.10b shows the FL1 histogram of dead cells (R1) while figure 4.10c shows the FL1 histogram of live cells (R2). Data was collected from at least 10,000 cells.

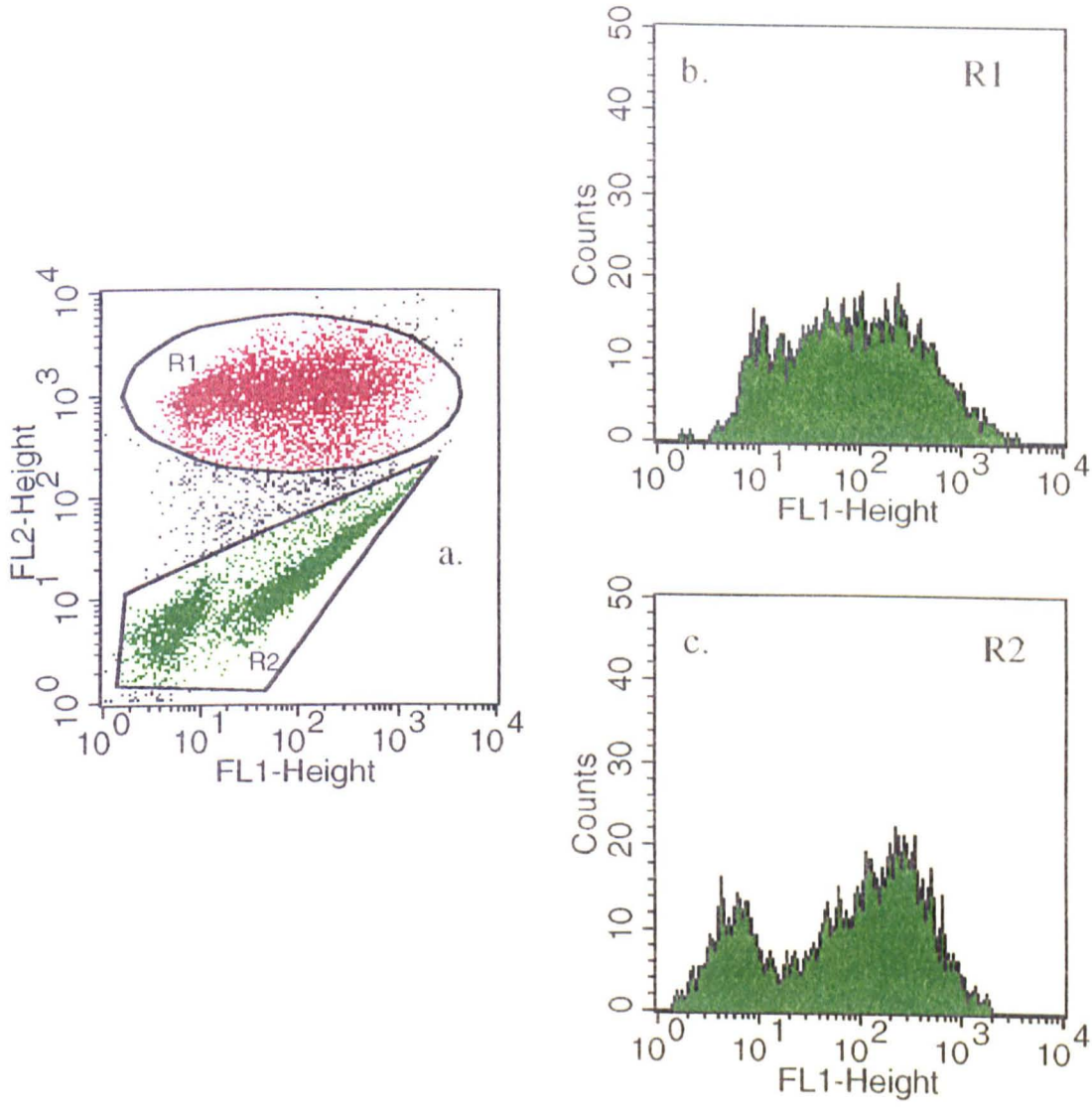
a.
R1
R2
FL2-Height
FL1-Height
b.
R1
Counts
FL1-Height
c.
R2
Counts
FL1-Height

Fig. 4.11. Exposure of *S. cerevisiae* DY150, transformed with pYEX-GFP$_{SOD1}$, to copper and menadione. Cells were exposed to 10 μM $Cu(NO_3)_2$ and 2 mM menadione for 1 h, and stained with PI (FL2). Figure 4.11a represents the FL1 (GFP) versus FL2 dot plot of DY150 prior to toxin exposure. Figure 4.11b represents an FL1 versus FL2 dot plot after 1 h exposure to copper while figure 4.11c depicts 1 h exposure to menadione.

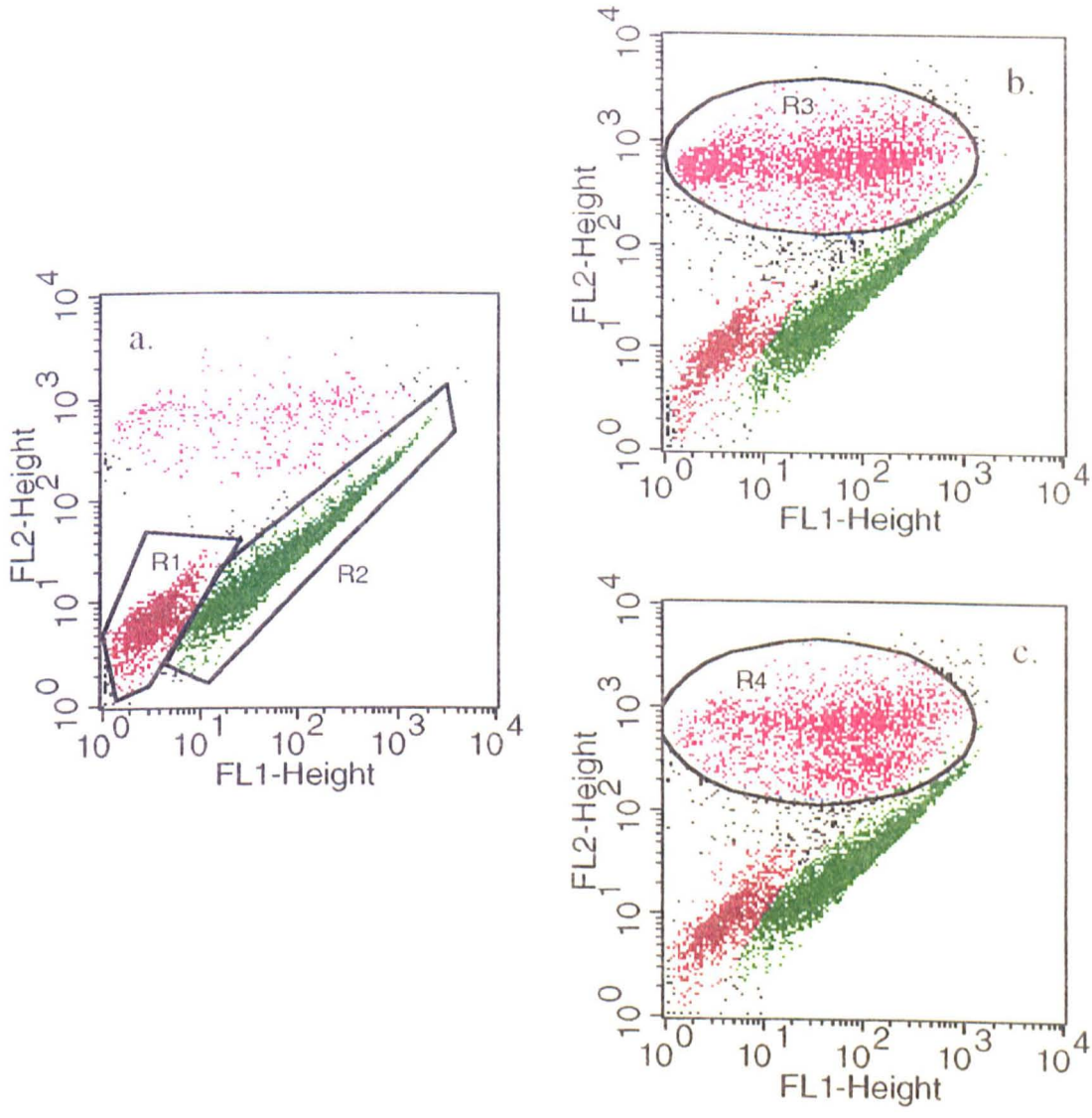
a.
R1
R2
FL2-Height
FL1-Height
b.
R3
FL2-Height
FL1-Height
c.
R4
FL2-Height
FL1-Height

4.4. Discussion

In this study we describe the use of flow cytometry for the analysis of specific cell cycle stage populations within heterogeneous populations of *S. cerevisiae*. More specifically we have examined the cell cycle stage-dependency of susceptibility towards copper toxicity in *S. cerevisiae*. Studies on specific cell cycle stage populations are normally carried out following cell synchronisation procedures (Porro *et al.*, 1995; Lloyd, 1987). However, conventional methods employed to induce synchronous populations often perturb cell population dynamics (Avery *et al.*, 1995*b*; Porro *et al.*, 1995; Lloyd, 1987). Thus, results obtained using conventional cell synchronisation methods often may not accurately reflect the normal physiological state of cells. Using flow cytometry, we have simultaneously monitored forward-angle light scatter (FSC), which is proportional to cell volume, and propidium iodide fluorescence, which is proportional to cellular DNA content. When cells reach a critical threshold size, and if environmental conditions are favourable, cells traverse START, DNA replication is initiated and cellular DNA content increases from 1C DNA during G_1 phase, to between 1C and 2C DNA during S phase, to 2C DNA during G_2/M phase, whereby cells undergo mitosis to produce haploid progeny (Lew *et al.*, 1997). By simultaneously monitoring both parameters we thus validated the use of FSC measurements for the analysis of specific cell cycle stage populations. Furthermore, by appropriate 'gate' setting on FSC histograms it was possible to physically separate and analyse cells differentiated by volume, i.e. cell populations at different stages of the cell cycle. A novel flow cytometric method for monitoring the

promoter activity of key oxidative stress response proteins of specific sub-populations, using the green fluorescent protein of *Aequorea victoria* was also described. Cell cycle-analysis using flow cytometry is relatively non-perturbing and facilitates rapid analysis of distinct cell cycle stage populations, and thus circumvents many of the problems encountered with conventional cell synchronisation methods.

Using the above methodology, we initially sought to examine the differential susceptibility to copper toxicity observed within a heterogeneous population exposed to a semi-lethal Cu^{2+} concentration. A distinct relationship between cell cycle stage and susceptibility to copper toxicity was observed, whereby cell populations consisting predominantly of G_2/M phase cells, excluding those approaching maximum cell volume, were the most susceptible to the toxic effects of copper. In chapters 2 and 3 we demonstrated that the sensitivity of *S. cerevisiae* towards both the redox-active metal copper and the nonredox-active metal cadmium is greatly influenced by cellular fatty acid composition. However, the elevated copper-sensitivity of cell fractions consisting predominantly of G_2/M phase cells could not be attributed to changes in cellular fatty acid composition, as cellular fatty acid composition did not vary significantly throughout the cell cycle.

The largest volume cell fraction, consisting exclusively of 2C DNA cells, i.e. budded cells about to undergo mitosis (M/G_1 phase boundary), were found to be the most resistant to copper. The smallest volume cell fractions, consisting almost exclusively of 1C DNA cells (G_1 phase cells) were also found to be relatively resistant towards copper toxicity. However, as cells traversed START and progressed through S phase, sensitivity towards copper toxicity increased to a maximum at a point corresponding to equal

proportions of G_1 and G_2/M phase cells. Cellular DNA staining of live and dead cells following exposure to an approximately 50% cytotoxic dose of copper revealed a predominance of G_1 phase cells in the live sub-population, with a small proportion of 2C DNA cells. Live 2C DNA cells corresponded to cells at the M/G_1 phase boundary.

Staining with the oxidant-sensitive probe 2',7'-dichlorodihydrofluorescein diacetate (H_2DCFDA), followed by cellular DNA staining revealed greater intracellular basal levels of reactive oxygen species in cell fractions consisting predominantly of G_2/M phase cells. ROS are generated endogenously in *S. cerevisiae* through mitochondrial respiration, steroidogenesis, and the β-oxidation of high-molecular weight fatty acids (Rapoport *et al.*, 1998; Davidge *et al.*, 1995). Copper toxicity experiments confirmed that the high oxidant status of cell fractions consisting predominantly of G_2/M cells correlated with their increased susceptibility towards copper toxicity. Numerous studies have examined the relationship between metal ion homeostasis and toxicity, and oxy-radical metabolism in yeast (Lapinskas *et al.*, 1995; Liu and Culotta, 1994; Greco *et al.*, 1990). Furthermore, in chapter 3 we demonstrated oxy-radical-mediated lipid peroxidation as a major means of heavy metal toxicity in *S. cerevisiae*. Thus, the results presented here are again suggestive of a major role of oxy-radical-mediated cellular damage during heavy metal exposure in yeast.

While elevated endogenous levels of ROS correlated with the increased sensitivity of cell fractions consisting predominantly of G_2/M phase cells towards copper toxicity, this relationship did not hold true for cells approaching maximum cell volume. The late-exponential phase asynchronous yeast cultures used during this study consisted of a small proportion of older stationary phase cells (initial stationary phase inoculum).

Entry to stationary phase is known to be associated with increased resistance towards oxidative stress (Jamieson *et al.*, 1994; Jamieson, 1992). The oxidative stress response genes *CTT1*, *CTA1*, *CCP1*, *SOD1*, and *SOD2* are all repressed by glucose (Krems *et al.*, 1995). Following glucose exhaustion and respiratory adaptation during yeast batch growth, de-repression of antioxidant genes occurs, thus contributing to the increased oxidative stress-resistance of stationary phase yeast (Steels *et al.*, 1994). De-repression of antioxidant genes facilitates tolerance to the greater levels of ROS that are generated during respiratory growth. Thus, despite the greatest endogenous levels of ROS being evident in cells approaching maximum cell volume (oldest cells), greater resistance towards the toxic effects of copper could be attributed partly to the presence of elevated levels of oxidative stress response proteins, prior to copper exposure.

Oxy-radical induced DNA damage has been implicated as a major means of copper toxicity (Flowers *et al.*, 1997; Lloyd *et al.*, 1997). The hydroxyl radical is a key culprit in DNA damage, generating several base lesions in double-stranded DNA including thymine glycol, 8-oxoguanine and formamido-pyrimidine as well as other base oxidation products (Brennan *et al.*, 1994; Hutchinson, 1985). As stated previously, G_1 phase cells (1C DNA), were also found to be relatively resistant towards the toxic effects of copper. Early G_1 phase cells have not yet reached the critical threshold cell size necessary to traverse START and enter S phase (Lew *et al.*, 1997). Maintenance of genome integrity during early G_1 phase, and during periods of quiescence is facilitated by chromatin condensation and basal transcription repression (Kadonaga, 1998). Previous studies have demonstrated that the physical distance between the compact-aggregates of 'condensed' or 'native' chromatin is greater than the effective damaging range of $HO^{\cdot}$

radicals (Nygren *et al.*, 1995). Furthermore, the water concentration of condensed chromatin aggregates has been shown to be too low to facilitate HO· radical-mediated DNA damage (Nygren *et al.*, 1995). Therefore, the elevated resistance of cell fractions consisting predominantly of G_1 phase cells could possibly be attributed in part to condensed chromatin assembly (Kadonaga, 1998; Demple and Harrison, 1994; Ljungman and Hanawalt, 1992). Furthermore, chromatin condensation occurs during late G_2 phase prior to M phase, to facilitate packaging of newly synthesised DNA into chromatin, thus affording greater protection of cells approaching maximum cell volume towards oxy-radical-mediated DNA damage (Kadonaga, 1998).

To further characterise the nature of the differential susceptibility of cells towards copper toxicity, we also investigated whether cell cycle-dependent transcription of critical heavy metal resistance genes could be correlated with differential Cu^{2+}-sensitivity. Thus, we specifically examined levels of *CUP1* and *SOD1* (key Cu^{2+}-resistance genes) promoter activity in live and dead cells, following exposure to a toxic concentration of copper, using GFP-promoter fusion plasmids. Despite the heterogeneity in the GFP fluorescence signal of live and dead sub-populations (most likely a function of variation in plasmid copy number during the cell cycle), it was apparent that basal levels of *CUP1* promoter activity did not differ significantly between live and dead sub-populations. Thus, differences in susceptibility towards copper toxicity could not be attributed to differences in *CUP1* activity at the time of Cu^{2+} addition (it was confirmed that *CUP1* promoter activity did not change during the short time of Cu^{2+} exposure). Increases in *CUP1* promoter activity were only evident after approximately 1 h exposure to Cu^{2+}, conducive with several reports indicating that *CUP1* is an inducible component

of the *S. cerevisiae* oxidative stress response system (Jensen *et al.*, 1996; Liu and Thiele, 1996). While results from the *SOD1::GFP* promoter fusion plasmid experiments also failed to reveal significant differences in basal levels of *SOD1* promoter activity between live and dead sub-populations, our findings were inconclusive. The increased heterogeneity in the GFP fluorescence signal of pYEX-GFP$_{SOD1}$-transformed DY150 (compared to pYEX-GFP$_{CUP1}$-transformed cells) appears to indicate that *SOD1* is constitutively expressed to varying degrees in different cell fractions. Indeed, changes in *SOD1* activity during the cell cycle have been demonstrated in both vascular endothelial and smooth muscle cells (Kong *et al.*, 1993). Furthermore, the likelihood that the FL1 signal of the dead sub-population includes contributions from PI fluoresence could possibly explain the lack of detectable differences between the GFP fluorescence of live and dead sub-populations (John Daly, Dana Farber Cancer Institute Core Cytometry facility, personal communication). Thus, it remains to be clearly elucidated whether differences in basal levels of *SOD1* activity play a role in the differential sensitivity of cells to copper toxicity.

Consistent with the findings of Jamieson *et al.* (1994), exposure to the specific superoxide anion-generating compound menadione for prolonged periods failed to induce *SOD1* gene promoter expression, indicating that *SOD1* is not an inducible part of the superoxide adaptive stress response. In addition, *SOD1* was not induced in the presence of copper. The promoter region of *SOD1* has previously been demonstrated to contain a single *ACE1* metalloregulatory trans-acting factor, which mediates transcriptional activation of *SOD1* in the presence of copper (Pena *et al.*, 1998; Culotta *et al.*, 1995; Gralla *et al.*, 1991). However, there are several possible explanations for the lack of

inducibility of our *SOD1*::*GFP* construct. The *SOD1* promoter fragment used in our construct may not contain all the regulatory factors necessary for induction. Also, it is possible that the late exponential/early stationary phase, aerobic cultures used for toxicity experiments already have maximally induced levels of *SOD1*. Furthermore, *ACE1*-dependent stimulation of the *CUP1* promoter has been demonstrated to be up to 50-fold greater than that of *SOD1* (*CUP1* contains four *ACE1* binding sites) (Culotta *et al.*, 1995; Gralla *et al.*, 1991). Thus, our flow cytometric method for analysis of *SOD1* promoter-stimulated GFP fluorescence may not be of sufficient sensitivity to detect such low levels of Cu^{2+}-induced, *ACE1*-dependent *SOD1* stimulation.

The use of episomal plasmids in this study prevented the direct comparison of *CUP1* and *SOD1* promoter activity of different cell cycle stage fractions, as plasmid copy number increases proportionately with cell volume, and cell volume increases as cells progress through the cell cycle (Mason, 1991; Lord and Wheals, 1980). The problems associated with the use of episomal plasmids encountered during this study, i.e. variations in plasmid copy number throughout the cell cycle, and inherent genetic instability, can be overcome through the use of integration plasmids (Wach *et al.*, 1997; Niedenthal *et al.*, 1996). Indeed, the specific targeted integration of the mutant GFP, GFPS65T (exhibiting elevated FACS-activated fluorescence), reporter module to the 3'-end of several yeast genes has recently been described (Wach *et al.*, 1997).

Thus, we have examined the differential susceptibility to copper toxicity in heterogeneous *S. cerevisiae* cultures. Sensitivity towards copper toxicity was demonstrated to be cell cycle-stage dependent, whereby G_2/M phase cells were the most susceptible to the toxic effects of copper. The increased sensitivity of G_2/M phase cells

was correlated with increased endogenous levels of ROS in these cells. While differences in basal levels of *CUP1* activity between Cu^{2+}-resistant and Cu^{2+}-sensitive sub-populations were not evident, further experimentation is necessary to determine whether constitutive differences in *SOD1* expression, in association with many other factors, plays an important role in the cell cycle stage-dependency of susceptibility to copper toxicity.

CHAPTER 5

The effects of heavy metals on DNA replication and the cellular DNA content of *Saccharomyces cerevisiae*

5.1. Introduction

Heavy metals such as nickel, chromium, cadmium, and possibly cobalt, are carcinogenic to humans (Kasprzak, 1995; Snow, 1994). It is postulated that the mechanisms of their carcinogenic activity include metal-mediated pro-mutagenic oxidative damage to DNA and nuclear proteins, and decreasing the fidelity of DNA replication and repair processes (Kasprzak, 1995). For example, human DNA ligase I, the major form of the enzyme in replicative cells, is inhibited by Zn^{2+} and Cd^{2+} ions (Yang *et al.*, 1996), while Cr^{3+}-induced DNA-DNA cross-links cause DNA polymerase I and T7 DNA polymerase arrest (Xu *et al.*, 1996; Bridgewater *et al.*, 1994). Furthermore, as stated previously, redox-active metals are capable of generating reactive oxygen species (ROS), such as the superoxide anion ($O_2^{\cdot-}$) and the hydroxyl radical ($OH^{\cdot}$), through redox cycling activity, while nonredox-active metals indirectly promote oxidative stress by depletion of free radical scavengers such as glutathione and protein-bound sulhydryl groups, e.g. Cd^{2+} coordination by glutathione (Figueiredo-Pereira *et al.*, 1998; Li *et al.*, 1997; Hassoun and Stohs, 1996; Stohs and Bagchi, 1995). The interaction of ROS with DNA may result in the generation of a wide variety of lesions including apurinic/apyrimidinic (AP) sites and both single- and double-strand breaks with 3'-deoxyribose fragments (Demple and Harrison, 1994; Ramotar *et al.*, 1991). Double-strand breaks in particular have been implicated as the causative lesions of genome rearrangements such as deletions, duplications, and translocations, which have been associated with the onset of carcinogenesis (Brennan and Schiestl, 1998; Manivasakam and Schiestl, 1998; Brennan

et al., 1994). The hydroxyl radical has been implicated as the key causative agent of DNA damage, generating several base lesions in double-stranded DNA including thymine glycol, hypoxanthine, 8-oxoguanine and formamido-pyrimidine (Hutchinson, 1985). A role of the hydroxyl radical in gross chromosomal rearrangements has also been implicated during hydrogen peroxide-induced intracellular and intercellular recombination events in *S. cerevisiae* (Brennan *et al.*, 1994). The class II AP endonucleases/3' esterase, encoded by the *APN1* gene, is the major cellular enzyme of *S. cerevisiae* responsible for initiating the direct repair of ROS-induced DNA lesions, such as AP sites and 3'-fragmented strands (Ramotar *et al*, 1991). In addition, genes belonging to the *RAD52* epistasis group repair double-strand breaks by homologous recombination (Guzder *et al.*, 1994; Klein, 1988). While numerous reports have examined the nature of the direct deleterious effects of ROS on DNA, and the physiological effects of mutations in key DNA damage repair genes, e.g. *apn1* and *rad52* mutants (Xiao and Chow, 1998; Kramer *et al.*, 1994), no studies have sought to examine the effects of PUFA-enrichment and heavy metals on cellular DNA and DNA replication *in vivo*.

In order to ensure the production of two viable progeny after mitosis, cell cycle events such as DNA replication and mitosis must be both temporally and spatially coordinated (Paulovich *et al.*, 1997; Weinert *et al.*, 1994). The prevailing theory of cell cycle control in *S. cerevisiae* involves two central coordinating mechanisms; the cell-cycle clock based on the serine/threonine cyclin-dependent kinases, particularly Cdc28p, and the checkpoint controls. Checkpoint controls ensure that cells maintain genome integrity (e.g. remain euploid) despite the low but continuous levels of DNA damage that

occur during normal cell growth, or during exposure to exogenous agents such as heavy metals (Weinert *et al.*, 1994). For example, the S-M phase checkpoint which inhibits mitosis in response to DNA damage is dependent on the *RAD53* and *MEC1* genes; *mec1-1* and *rad53* mutants replicate rapidly in the presence of DNA damage (Paulovich *et al.*, 1997; Weinert and Hartwell, 1988). Therefore, cells can be actively prevented from continuing in the cell cycle due to checkpoints that sense ongoing or aberrant DNA replication (Heichman and Roberts, 1996; Weinert *et al*, 1994).

Chromosomal DNA replication in *S. cerevisiae* is initiated at bidirectional sequence-specific origins (Oris) during S phase (Dalton and Whitbread, 1995). Oris are bound by the pre-replicative (pre-RC) protein complex from late M to early S phase, and by the post-replicative complex (post-RC) from late S to early M phase (Cocker *et al.*, 1996; Lei *et al.*, 1996; Tye, 1994). The initiation of DNA replication requires the minichromosome maintenance (MCM) family of polypeptides, which include Mcm2p, Mcm3p, Cdc54p/Mcm4p, Cdc46p/Mcm5p, Mcm6p and Cdc47p/Mcm7p (Dalton and Hopwood, 1997; Young and Tye, 1997; Lei *et al.*, 1996). The six MCM proteins carry a highly conserved motif (the MCM box), which resembles a conserved domain associated with transcription and replication factors with known or assumed DNA-dependent ATPase activity (Lei *et al.*, 1996). The role of MCM proteins as direct regulators of the initiation of DNA replication has been suggested by a number of lines of evidence; they are necessary for the maintenance of autonomously replicating sequence (ARS)-containing plasmids, mutants defective in *MCM* gene products have diminished usage of Oris (Young *et al.*, 1997), and members of the *MCM* gene family interact with components of the origin recognition complex (ORC) (Dalton and Hopwood, 1997).

Therefore, the MCM proteins may play an important role in controlling origin activity through direct recruitment into pre-RCs. The cyclin-dependent kinase (CDK) Cdc6p is necessary for origin firing and maintenance of pre-RCs in *S. cerevisiae* (Cocker *et al.*, 1996). Without Cdc6p, genomic footprints of pre-RCs closely resemble those of post-RCs suggesting that the ORC is also a component of the pre-RC (Cocker *et al.*, 1996). Cdc6p-dependent pre-RCs assemble at Oris at the end of M phase. Assembly of pre-RCs at Oris during late M phase is consistent with the cell cycle-regulated nuclear localisation of several of the MCM proteins, e.g. Cdc46p and Cdc47p (Dalton and Whitbread, 1995; Tye, 1994). The activation of the pre-RC results in origin firing and initiation of DNA replication. This activation step is known to require the activity of the CDKs Cdc7p and Cdc28p in association with any one of the B-type cyclins, Clb1p-Clb6p (Cocker *et al.*, 1996). Thus, it has been proposed that a key replication initiation protein of the pre-RC is phosphorylated by the Cdc7p- or Cdc28p-Clb1p-6p kinases, signalling its usage and targeting it for subsequent Cdc16p-Cdc23p-Cdc27p-dependent proteolysis (Heichman and Roberts, 1996). Temperature-sensitive *cdc16* and *cdc27* mutants over-replicate their DNA despite having continuously elevated mitotic Cdc28p-Clb2p and Cdc28p-Clp5p activity (Heichman and Roberts, 1996). DNA over-replication in these mutants involved all chromosomes and did not require passage through M phase or START. Cdc6p, Mcm2p and Mcm3p have been implicated as potential key phosphorylation target proteins of the pre-RC complex. Both Mcm2p and Mcm3p are chromatin-associated from late M phase through G_1 phase and dissociate from chromatin as cells progress through S phase (Young and Tye, 1997). Furthermore, a key role of Cdc6p has been suggested by recent studies with *S. pombe* whereby 10- to 20-fold overexpression of the

Cdc6p homolog, Cdc18p, induced over-replication of cellular DNA; *de novo* protein synthesis was not required for this effect (Stern and Nurse, 1996). Overexpression of the CDK inhibitor rum1p of *S. pombe* also leads to sequential, uninterrupted S phases (Moreno and Nurse, 1994; Correa-Bordes and Nurse, 1995). Stern and Nurse (1996) have proposed that a very low CDK activity towards the end of M phase enables dephosphorylated initiator protein-associated pre-RCs to assemble at Oris in *S. pombe*. A subsequent increase in CDK activity to a moderate level leads to phosphorylation of the initiator protein, origin firing and initiation of DNA replication. Phosphorylation of the initiator protein(s) simultaneously prevents the assembly of further pre-RCs, as phosphorylated initiator protein(s) cannot bind to Oris. Thus, according to the proposed model, DNA replication is limited to once per cell cycle, with each round of DNA replication requiring a change in CDK activity.

The purpose of this study was to examine the effects of heavy metal-exposure on DNA replication and the cellular DNA content in unsupplemented and PUFA-supplemented *S. cerevisiae*. Heavy metal-induced DNA over-replication in PUFA-enriched *S. cerevisiae* is demonstrated for the first time, whereby exposure of PUFA-enriched cells, particularly 18:3-enriched cells to redox-active metals caused repeated rounds of DNA replication, accumulation of up to 8C DNA, and the uncoupling of DNA synthesis from cell cycle progression.

5.2. Materials and Methods

5.2.1. **Organisms and culture conditions.** Yeast strains used for DNA replication experiments were *S. cerevisiae* NCYC 1383 (*MATα, his3-Δ1, leu2-3, leu2-112, ura3-52, trp1-289*) and RJD621 (*MAT***a**, *can1-100, leu2-3, -112, his3-11, -15, trp1-1, ura3-1, ade2-1, cdc28*::*CDC28*-HA::*TRP1*) (a gift from Ray DeShaies, Caltech, CA). RJD621 contains an HA-tagged *CDC28* gene in a W303 strain background. Maintenance of yeast strains, and preparation of strains for experimental purposes was as previously described (see Section 2.2.1.).

5.2.2. **Preparation of cell suspensions for toxicity experiments.** The preparation of cell suspensions for toxicity experiments was as described previously (see Section 4.2.4.). For the hydroxyurea experiments, cultures were incubated with 0.2 M hydroxyurea (Sigma, MO) for two hours prior to the addition of toxin. Hydroxyurea prevents DNA replication by inhibiting ribonucleotide reductase, thereby depleting cells of dNTP precursors (Weinert *et al.*, 1994).

5.2.3. **Cellular DNA staining.** Cellular nucleic acids were stained with PI and examined using flow cytometry as described previously (see Sections 4.2.7. and 4.2.8.).

5.2.4. **Diphenylamine determination of DNA concentration.** To confirm results from flow cytometry experiments, cellular DNA concentrations were determined using the

diphenylamine (DPA) assay (Burton, 1968), as modified by Sasaki (1992), with the following additional modifications. At specified time points after the addition of toxin, 20 ml samples (~1 x 10^9 cells) from control and toxin-treated cells were harvested by centrifugation at 1,500 *g* for 5 min, and washed twice with cold distilled deionised water. Cells were washed with 4 ml of 75% (v/v) ethanol and allowed to dry overnight at room temperature. Pellets were resuspended in 1.25 ml of 1.5 N perchloric acid and heated at 70°C for 30 min. Samples were allowed to cool, 0.75 ml of DPA solution (4% (w/v) diphenylamine, 1.5% (v/v) sulphuric acid, 0.01% (v/v) paraldehyde) was added, and the mixture was incubated at 30°C for 18 h. Samples were allowed to cool and 1.1 ml amyl acetate was added. Absorbances of samples were measured at 595 nm, using a Pharmacia Biotech Ultraspec 2000 UV/Visible spectrophotometer, against a reference solution comprising 1.1 ml amyl acetate, 0.75 ml DPA solution, and 1.25 ml 0.2 N perchloric acid. The concentrations of DNA in samples were calculated by reference to a standard curve prepared using bovine DNA (Promega, WI).

5.2.5. **Yeast subcellular fractionation.** Nuclear membrane-enriched fractions were isolated according to Ausubel *et al.* (1998) and Young and Tye (1997), with the following modifications. After 6 h incubation in the presence of $Cu(NO_3)_2$, cells were harvested by centrifugation at 1,500 *g* for 5 min and washed twice with 10 mM Mes buffer (pH 5.5), 1% (w/v) glucose. The approximate wet weight (in grams) of cells was measured, cells were resuspended in approximately 3 vol ice-cold distilled deionised water, and immediately centrifuged at 1,500 *g* for 5 min. Cells were resuspended in 1 vol spheroplasting buffer (50 mM Tris.Cl (pH 7.5), 10 mM $MgCl_2$, 1 M sorbitol, 30 mM

DTT) and incubated at room temperature for 15 min. Cells were harvested by centrifugation at 1,500 *g* for 5 min and resuspended in 1 vol spheroplasting buffer containing 1 mM DTT, protease inhibitors (0.1 μg ml^{-1} chymostatin, 2 μg ml^{-1} aprotinin, 1 μg ml^{-1} pepstatin A, 1.1 μg ml^{-1} phosphoramidon, 5 μg ml^{-1} E-64, 0.5 μg ml^{-1} leupeptin, 2.5 μg ml^{-1} antipain, 0.1 mM benzamidine, 0.1 mM sodium metabisulphite), and phosphatase inhibitors (5 mM sodium pyrophosphate, 0.1 mM sodium metavanadate, 50 mM sodium fluoride). Cell walls were digested with 20 U ml^{-1} recombinant lytic enzyme (ICN Biochemicals, CA) and 20 U ml^{-1} lytic enzyme 100T (ICN Biochemicals, CA) at 30 °C for 2 h with rotary shaking at 50 rev. min^{-1} (approximately 1 ml of cell suspension in sterile 15 ml centrifuge tubes). Spheroplast formation was followed by examining water-induced spheroplast lysis by light microscopy. Approximately 80-90% spheroplast yield was usually observed after 2 h incubation. Spheroplasts were centrifuged at 1,500 *g* for 10 min, washed twice in 2 vol ice-cold spheroplast buffer, and resuspended in 0.5 vol nuclei buffer (1 M sorbitol, 20 mM PIPES (pH 6.3), 0.5 mM $CaCl_2$, 1 mM DTT, 0.1 mM EDTA, 1 mM PMSF, with protease and phosphatase inhibitors). Spheroplasts were lysed by pipetting drop by drop into approximately 20 vol ice-cold Ficoll buffer (18% (w/v) Ficoll 400 (Pharmacia Biotech, NJ), 20 mM PIPES (pH 6.3), 0.5 mM $CaCl_2$, 1 mM DTT, 0.1 mM EDTA, 1 mM PMSF, with protease and phosphatase inhibitors) at 4 °C. Ficoll lyses spheroplasts but does not lyse nuclei (Lohr, 1988). Cell debris was removed by centrifugation at 3,000 *g* for 20 min at 4 °C, using a Sorvall RC-5B refrigerated superspeed centrifuge and SS-34 rotor. The resulting supernatant was centrifuged at 20,000 *g* for 30 min, yielding a total nuclear pellet. The supernatant was collected and stored at 4 °C (cytosolic fraction, C). The nuclear pellet was resuspended in 100 μl of

low salt extraction buffer (10 mM HEPES (pH 7.5), 1 mM EDTA, 0.5 M NaCl), transferred to a microcentrifuge tube and microcentrifuged at 14,500 rev. min^{-1} for 20 min. The low salt nucleosolic fraction (NSL) supernatant was collected and stored at 4 °C. The pellet was resuspended in 100 µl of high salt extraction buffer (10 mM HEPES (pH 7.5), 1 mM EDTA, 2.0 M NaCl) and microcentrifuged at 14,500 rev. min^{-1} for 20 min. The high-salt nucleosolic fraction (NSH) supernatant was collected and stored at 4 °C. The nuclear pellet was resuspended in 100 µl of low salt extraction buffer and incubated with four hundred units of deoxyribonuclease I (DNase I) (Boehringer Mannheim, IN) at 37 °C for 2 h. The debris was pelleted at 14,500 rev. min^{-1} for 20 min and the nuclear pellet fraction (NP) removed and stored at 4 °C.

5.2.6. **Lipid extraction and fatty acid analysis.** Lipids were extracted from nuclear membrane fractions as described previously (see Section 2.2.5). Fatty acid methyl ester separations and analysis were performed as described in Section 4.2.3.

5.2.7. **DAPI staining of yeast nuclei.** The purity of isolated yeast nuclei was assessed by staining with the DNA-binding fluorochrome 4',6-diamidine-2'-phenylindole dihydrochloride (DAPI) (Molecular Probes Inc., OR), using a modified method of M°Millan and Tatchell (1994). At specified intervals after the addition of toxin to cell suspensions, one and a half ml aliquots were removed, washed with 1 ml of 10 mM Mes buffer (pH 5.5), 1% (w/v) glucose, and immediately fixed in 70% (v/v) ethanol for 30 min at 4 °C. Samples were washed twice with distilled deionised water and resuspended in 1 ml of PBS containing 1 µg ml^{-1} DAPI for 20 min. DAPI has an absorption

maximum of 358 nm and emission maximum of 461 nm (Haugland, 1996). Samples were washed twice with distilled deionised water, resuspended in 1 ml of 50% (v/v) glycerol, and stored at 4 °C until analysis. DAPI-stained nuclei were visualised by video fluorescence microscopy, using an Olympus BH-2 fluorescence microscope and Javelin video camera.

5.2.8. **Protein determination.** Protein concentrations of yeast subcellular fractions were determined using the Micro-Lowry assay, with the following modifications. Samples (100 µl) were added to microcentrifuge tubes and made up to 1 ml with sterile, distilled deionised water. Protein was precipitated by adding 100 µl of 0.15% (w/v) sodium desoxycholate and 100 µl of 72% (w/v) trichloroacetic acid (TCA). Samples were microcentrifuged at high speed for 15 min, washed twice with 100% (v/v) ethanol, and the final pellet was dried under vacuum. The pellet was resuspended in 800 µl of CTC reagent (0.1% (w/v) $CuSO_4$, 0.2% (w/v) $C_4H_4Na_2O_6.2H_2O$, 10% (w/v) Na_2CO_3) and 200 µl of 17% (v/v) Folin-Ciocalteau reagent (Sigma, MO), and incubated at room temperature for 30 min. Absorbances of samples were measured at 750 nm using a Pharmacia Biotech Ultraspec 2000 UV/Visible spectrophotometer. Protein concentrations were calculated by reference to a standard curve prepared using bovine serum albumin (BSA) (Sigma, MO).

5.2.9. **SDS-PAGE and immunoblotting.** SDS-PAGE was performed according to standard protocol (Ausubel *et al.*, 1998). In preparation for SDS-PAGE, proteins were precipitated by mixing with an equal volume of 20% (w/v) TCA, and microcentrifuged at

full speed for 10 min. Protein pellets were washed twice with ice-cold 100% (v/v) ethanol, resuspended in sample loading buffer (50 mM Tris.Cl (pH 6.8), 100 mM DTT, 2% (w/v) SDS, 10% (v/v) glycerol, 0.1% (w/v) bromophenol blue), and denatured by boiling for 1-2 min. Protein samples were stored at 4 °C until analysis. Proteins were separated using the standard Laemmli system with homogenous 7.5% SDS-PAGE gels as follows. Separating gels (12 ml) comprised 2.4 ml of 1.875 M Tris (pH 8.8), 1.8 ml of 50% (w/v) acrylamide solution (24:1 (w/w) acrylamide:bis-acrylamide) (Bio-Rad Laboratories, CA), 120 µl of 10% (w/v) SDS, and 7.68 ml of sterile, distilled deionised water. Immediately before pouring, 12 mg of ammonium persulphate, and 6 µl N,N,N',N'-tetra-methyl-ethylenediamine (TEMED) (Bio-Rad Laboratories, CA) were added to facilitate polymerisation. The separating gel was layered with saturated n-butanol, to prevent the formation of internal air bubbles. Upon polymerisation, the overlay was decanted and the stacking gel was applied. The stacking gel (3 ml) comprised 0.3 ml of 1.25 M Tris (pH 6.8), 240 µl of 50% (w/v) acrylamide solution, 30 µl of 10% (w/v) SDS, and 2.43 ml of sterile, distilled deionised water. Immediately before pouring, 3 mg of ammonium persulphate and 3.5 µl TEMED were added. Proteins were separated at 20 mA for 1.5-2 h, in Laemmli buffer (0.025 M Tris, 0.192 M glycine, 0.1% (w/v) SDS), using the Bio-Rad Mini-PROTEAN II electrophoresis cell. Gels were stained for 1 h with gentle rotation in 0.25% (w/v) Coomassie blue (Bio-Rad Laboratories, CA), 50% (v/v) methanol, 10% (v/v) glacial acetic acid. Gels were destained by incubating in primary destaining solution (30% (v/v) methanol, 10% (v/v) glacial acetic acid) for 1 h, and in secondary destaining solution (16.5% (v/v) methanol, 5% (v/v) glacial acetic acid) (with frequent changes) overnight. Immunoblotting was

performed using standard techniques (Ausubel *et al.*, 1998). Separated proteins were transferred to 0.45 μm nitrocellulose membranes (Bio-Rad Laboratories, CA) at 150 mA overnight in transfer buffer (39 mM glycine, 48 mM Tris, 20% (v/v) methanol, pH 8.3) at 4 °C, again using the Bio-Rad Mini-PROTEAN II electrophoresis cell. Nitrocellulose membranes were washed in 5 x Tris-buffered saline (TBS) (0.25 M Tris (pH 7.4), 1 M NaCl), and incubated in 15 ml blocking buffer, comprising 1.5 ml of 10 x TBS, 750 μl of 10% (w/v) gelatin (EIA grade, 60 bloom) (Bio-Rad Laboratories, CA), 12.75 ml of sterile, distilled deionised water for 1 h. Nitrocellulose membranes were again washed with 5 x TBS, and incubated in antibody-binding buffer, of the same composition as blocking buffer, with antibody. The primary antibodies used for immunoblotting were 1:500 dilutions of affinity purified rabbit anti-Mcm3 (a gift from Rolf Knippers, Universite Konstanz; Hu *et al.*, 1993), and 5 μg ml^{-1} mouse anti-HA (12CA5) (Boehringer Mannheim, IN). Nitrocellulose membranes were then incubated in secondary antibody-binding buffer for 1 h. The secondary antibodies used were 1:5000 dilutions of alkaline phosphatase-conjugated anti-rabbit IgG (Fc) (Promega, WI) and alkaline phosphatase-conjugated anti-mouse IgG (H + L) (Promega, WI). Alkaline phosphatase was detected using the BCIP/NBT colour system (Promega, WI), as follows. Nitrocellulose membranes were incubated in 15 ml substrate buffer, comprising 1.5 ml of 1 M Tris.Cl (pH 9.5), 500 μl of 3 M NaCl, 75 μl of 1 M $MgCl_2$, 99 μl of 5-bromo-4-chloro-3-indolyl phosphate (BCIP), 49.5 μl of nitro blue tetrazolium (NBT), and 12.8 ml of sterile, distilled deionised water, and incubated with gentle rotation until the appearance of bands.

5.3. Results

5.3.1. **Effect of $Cu(NO_3)_2$ on the cellular DNA content of unsupplemented and PUFA-supplemented *S. cerevisiae* NCYC 1383.** The increased susceptibility of PUFA-enriched *S. cerevisiae* to both cadmium- and copper- induced membrane permeabilisation and whole-cell toxicity had previously been demonstrated (Chapters 2 and 3). The increased susceptibility of PUFA-enriched cells towards metal toxicity was attributed to greater levels of ROS-mediated lipid peroxidation in these cells. We therefore sought to investigate the effects of PUFA-enrichment on heavy metal-induced ROS-mediated DNA damage. Thus, we investigated the effects of $Cu(NO_3)_2$ on the cellular DNA content of *S. cerevisiae* previously grown in unsupplemented, 18:2- and 18:3-supplemented media, using flow cytometry. Late-exponential phase cells were exposed to $Cu(NO_3)_2$ in buffer for up to 20 h. Samples were taken at regular time intervals, fixed, and cellular DNA was stained with PI. Linear-scale histograms of FL2 against counts were plotted. The cellular DNA content of cells grown previously in unsupplemented medium, was examined at specified intervals during 20 h exposure to 100 μM $Cu(NO_3)_2$ (Fig. 5.1). Exposure of unsupplemented cells to 100 μM $Cu(NO_3)_2$ for up to 20 h had no marked effects on cellular DNA content, as evidenced by the presence of clear and resolved 1C and 2C DNA peaks (1C corresponds to an arbitrary FL2 intensity unit of ~ 120, 2C ~ 240) (Fig. 5.1f). In addition, exposure of unsupplemented cells to copper did not appear to result in checkpoint control-induced cell cycle arrest, as numbers of 1C and 2C DNA cells remained relatively constant throughout the 20 h exposure to copper. The cellular

Fig. 5.1. Effect of 100 μM $Cu(NO_3)_2$ on the cellular DNA content of *S. cerevisiae* NCYC 1383 previously grown in unsupplemented medium. The FL2 histograms depict the cellular DNA content of cells before copper addition (a), and after 15 min (b), 30 min (c), 4.5 h (d), 6 h (e) and 20 h (f) exposure to 100 μM $Cu(NO_3)_2$. Each histogram contains data collected from at least 10,000 cells.

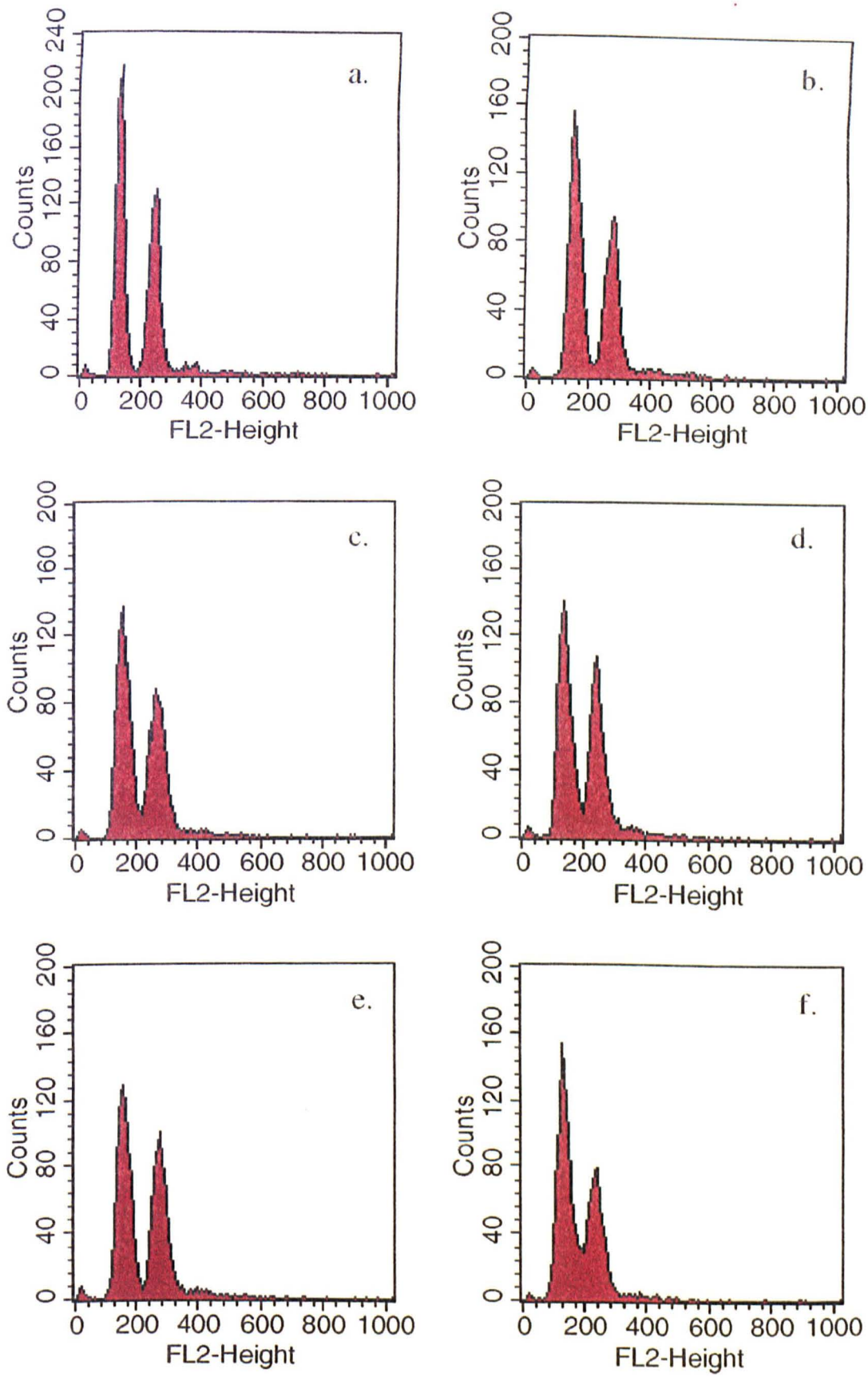
a.
b.
c.
d.
e.
f.
Counts
FL2-Height
0
40
80
120
160
200
240
200
400
600
800
1000

Fig. 5.2. Effect of 100 μM $Cu(NO_3)_2$ on the cellular DNA content of *S. cerevisiae* NCYC 1383 previously grown in linoleate-supplemented medium. The FL2 histograms depict the cellular DNA content of cells before copper addition (a), and after 15 min (b), 30 min (c), 4.5 h (d), 6 h (e) and 20 h (f) exposure to 100 μM $Cu(NO_3)_2$. Each histogram contains data collected from at least 10,000 cells.

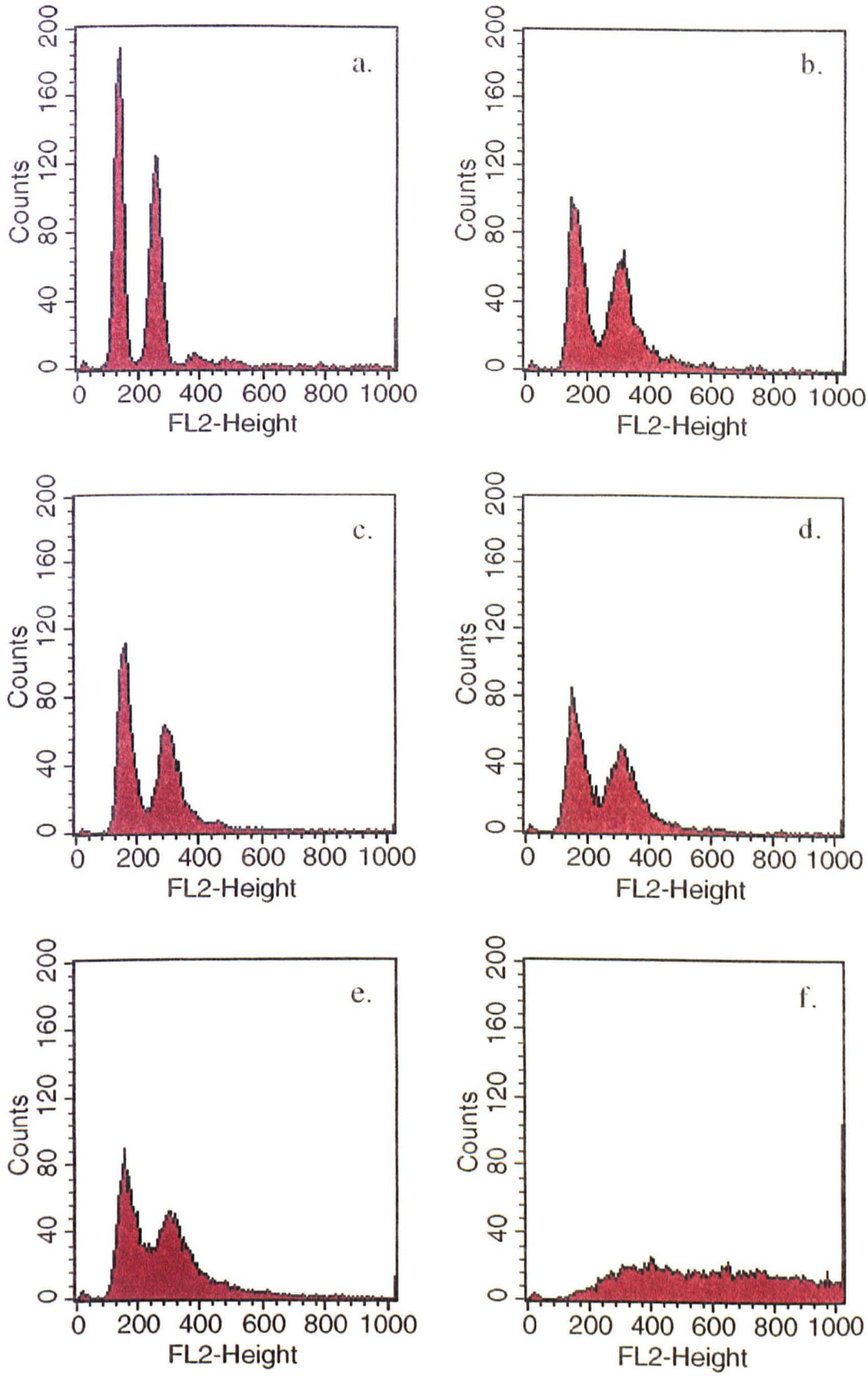
a.
b.
c.
d.
e.
f.
Counts
0
40
80
120
160
200
0
200
400
600
800
1000
FL2-Height

Fig. 5.3. Effect of 100 μM $Cu(NO_3)_2$ on the cellular DNA content of *S. cerevisiae* NCYC 1383 previously grown in linolenate-supplemented medium. The FL2 histograms depict the cellular DNA content of cells before copper addition (a), and after 15 min (b), 30 min (c), 4.5 h (d), 6 h (e) and 20 h (f) exposure to 100 μM $Cu(NO_3)_2$. Each histogram contains data collected from at least 10,000 cells.

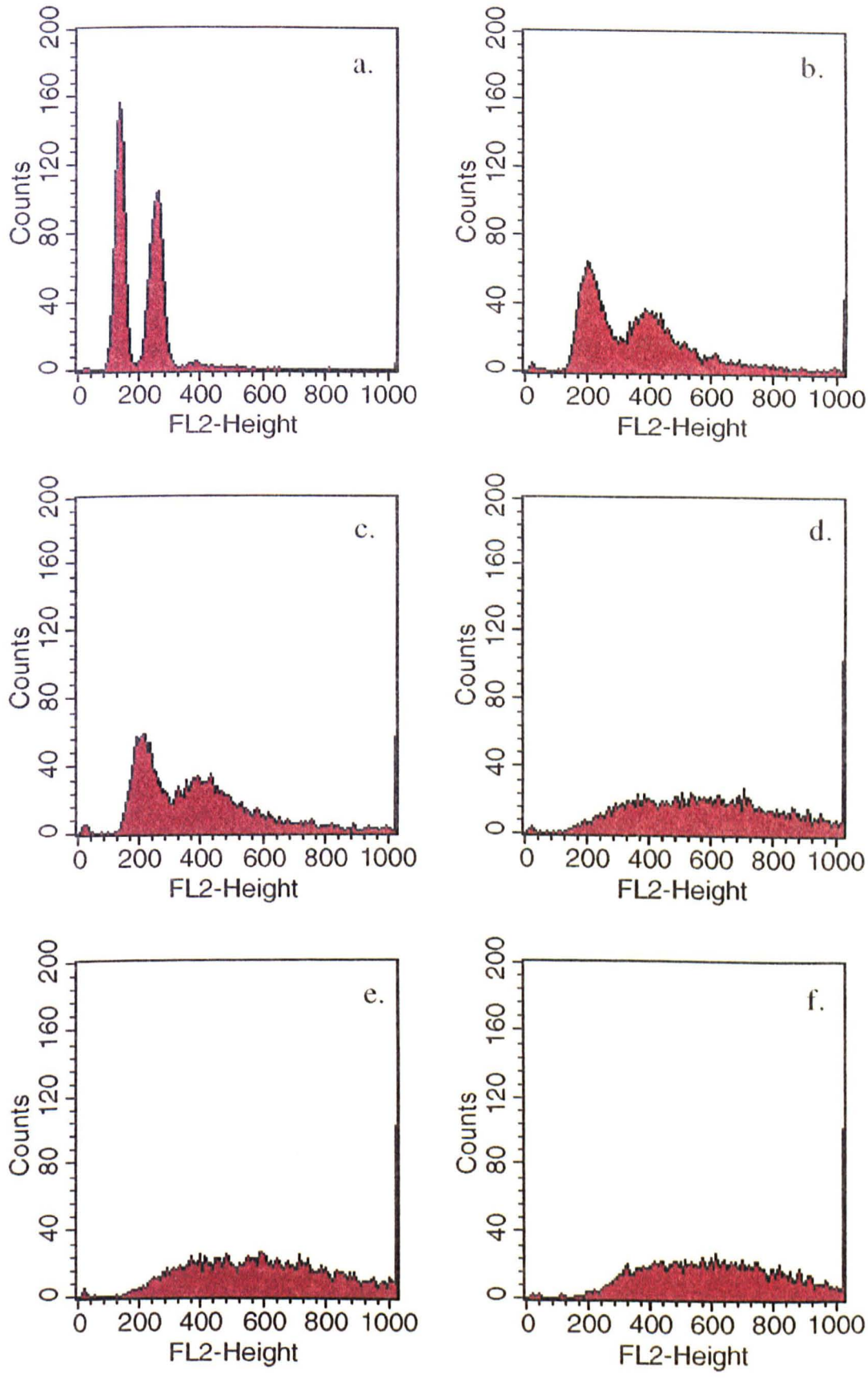
a.
b.
c.
d.
e.
f.
Counts
0
40
80
120
160
200
0
200
400
600
800
1000
FL2-Height

DNA content of cells previously grown in 18:2-supplemented medium, was also examined during 20 h exposure to 100 μM $Cu(NO_3)_2$ (Fig. 5.2). During the initial period of copper exposure 1C and 2C peak intensities were reduced, and peak broadening was evident (Fig. 5.2c,d,e). Furthermore, after 20 h exposure over-replication of cellular DNA was evident, whereby both 1C and 2C DNA peaks were severely diminished, and DNA levels upwards of 4C (FL2 > 480) were evident (Fig. 5.2f). The cellular DNA content of cells previously grown in 18:3-supplemented medium was also examined during 20 h exposure to 100 μM $Cu(NO_3)_2$ (Fig. 5.3). Here the effect of Cu^{2+} on DNA content was considerably more dramatic than in 18:2-supplemented cells; 1C and 2C peak intensities were significantly diminished after only 15 min exposure (Fig. 5.3b). Furthermore, after only 4.5 h cellular DNA levels greater than 4C and up to 8C (FL2 ~ 960) were evident (Fig. 5.3d). The results demonstrate continued DNA synthesis in PUFA-enriched *S. cerevisiae* exposed to toxic concentrations of $Cu(NO_3)_2$.

5.3.2. **Influence of hydroxyurea on $Cu(NO_3)_2$-induced over-replication in 18:3-enriched *S. cerevisiae* NCYC 1383.** In order to confirm that the flow cytometric DNA profiles of Cu^{2+}-exposed PUFA-enriched *S. cerevisiae* genuinely represented continued DNA synthesis, cells were incubated in the presence of hydroxyurea for two hours prior to the addition of $Cu(NO_3)_2$, and cellular DNA content was again examined by flow cytometry. Hydroxyurea prevents DNA replication by inhibiting ribonucleotide reductase, thereby depleting cells of dNTP precursors (Weinert *et al.*, 1994). The cellular DNA content of 18:3-enriched cells exposed to 100 μM $Cu(NO_3)_2$ for up to 20 h, after pre-incubation in the presence of 0.2 M hydroxyurea, is shown (Fig. 5.4). Exposure to $Cu(NO_3)_2$, after

Fig. 5.4. Influence of hydroxyurea on $Cu(NO_3)_2$-induced over-replication in linolenate-enriched *S. cerevisiae* NCYC 1383. Cells were incubated in the presence of 0.2 M hydroxyurea for 2 h prior to the addition of $Cu(NO_3)_2$. The FL2 histograms depict the cellular DNA content of linolenate-enriched cells before copper addition (a), and after 15 min (b), 30 min (c), 4.5 h (d), 6 h (e) and 20 h (f) exposure to 100 μM $Cu(NO_3)_2$. Each histogram contains data collected from at least 10,000 cells.

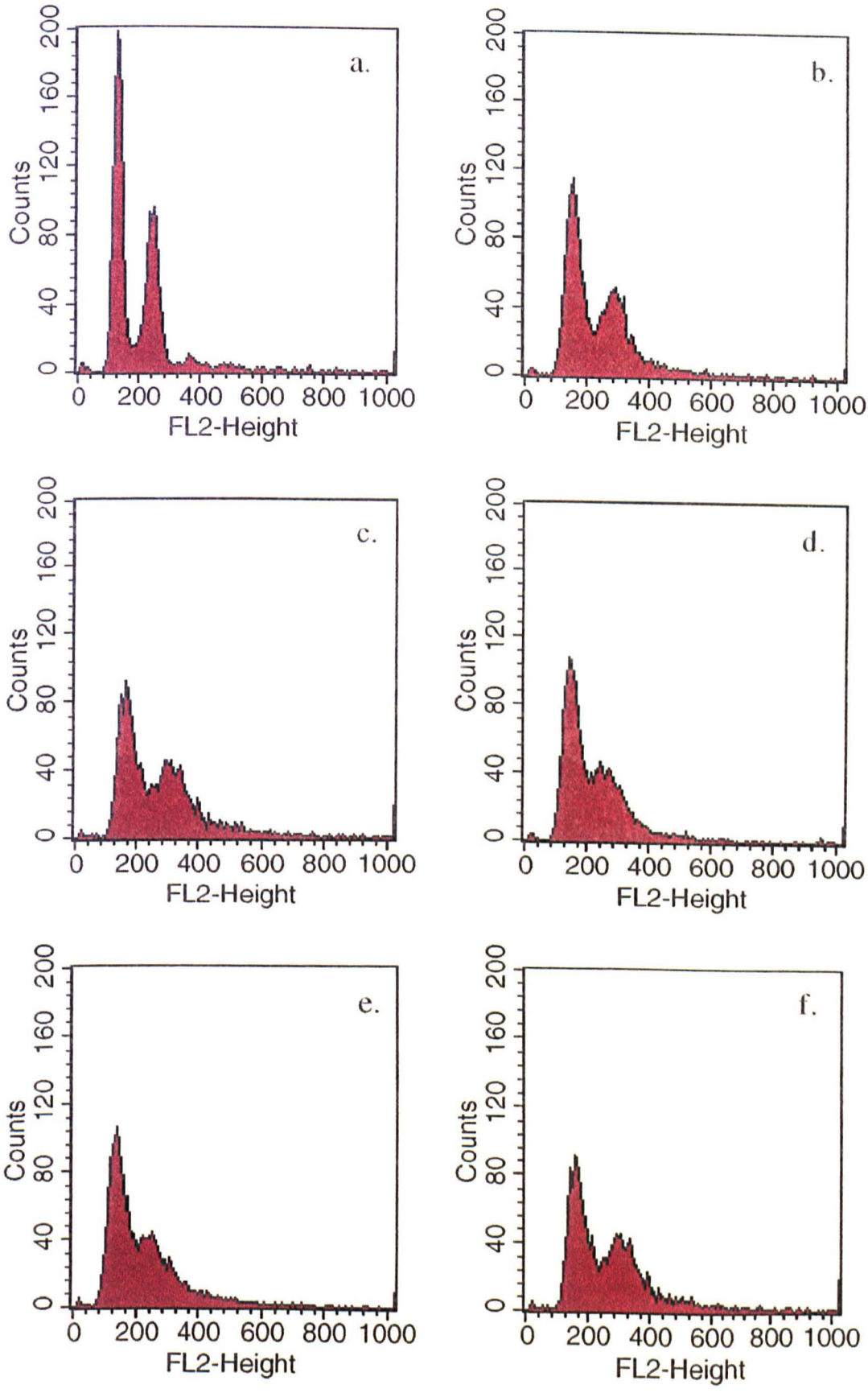
a.
b.
c.
d.
e.
f.
Counts
0
40
80
120
160
200
0
200
400
600
800
1000
FL2-Height

incubation with hydroxyurea, resulted in a reduction in both 1C and 2C DNA peak intensities, and peak broadening (Fig 5.4b-f). However, there is little evidence of continued DNA synthesis, even after 20 h exposure. The results demonstrate that pre-incubation of 18:3-enriched *S. cerevisiae* with the DNA synthesis inhibitor hydroxyurea prevents $Cu(NO_3)_2$-induced over-replication of cellular DNA. Thus, the results confirm continued DNA replication in 18:3-enriched *S. cerevisiae* upon prolonged exposure to toxic concentrations of $Cu(NO_3)_2$.

5.3.3. **Determination of cellular DNA concentrations.** Here we sought to further confirm DNA over-replication in PUFA-enriched *S. cerevisiae* upon exposure to $Cu(NO_3)_2$, using an alternative assay for cellular DNA content. Therefore, we measured the DNA content of unsupplemented and PUFA-supplemented *S. cerevisiae* incubated in the presence and absence of $Cu(NO_3)_2$ for 6 h, using the diphenylamine assay (Burton, 1968) (Table 5.1). Exposure to 100 μM $Cu(NO_3)_2$ for 6 h had only a small effect on the average amount of DNA per unsupplemented cell, resulting in a reduction of approximately 16.3%. However, marked increases in the average amount of DNA per cell were observed for PUFA-enriched cells. Here, the average amount of DNA per PUFA-enriched cell increased by approximately 38.5% and 76.9%, in 18:2- and 18:3-enriched cells, respectively, after 6 h exposure to 100 μM $Cu(NO_3)_2$ (Table 5.1). It was also evident that the average amount of DNA per PUFA-enriched cell was approximately 40% lower than that of unsupplemented cells, previously incubated in the absence of $Cu(NO_3)_2$. These results are most likely a consequence of variations in DNA extraction efficiencies, due to inherent differences in physical membrane properties, between unsupplemented and

Table 5.1. Cellular DNA concentrations of unsupplemented and PUFA-supplemented *S. cerevisiae* NCYC 1383 incubated in buffer, in the presence and absence of 100 μM $Cu(NO_3)_2$ for 6 h

Medium	[DNA] (fg $cell^{-1}$)	
	no metal	metal
unsupplemented	20.8 ± 2.6	17.4 ± 0.8
18:2-supplemented	13.0 ± 0.3	18.0 ± 0.1
18:3-supplemented	12.1 ± 1.2	21.4 ± 2.8

Values for [DNA] are means from two replicate determinations ± SEM.

PUFA-supplemented cells (Alterthum and Rose, 1973). Nevertheless, the results strongly support flow cytometric data indicating DNA over-replication in PUFA-supplemented *S. cerevisiae* exposed to $Cu(NO_3)_2$.

5.3.4. **Effects of non-toxic concentrations of $Cu(NO_3)_2$ on the cellular DNA content of unsupplemented and PUFA-supplemented *S. cerevisiae* NCYC 1383.** Here we investigated whether $Cu(NO_3)_2$-induced DNA over-replication in PUFA-enriched cells would also occur at lower, non-toxic concentrations of $Cu(NO_3)_2$. Cells grown previously in unsupplemented and PUFA-supplemented medium were exposed to 1 and 10 μM $Cu(NO_3)_2$ for up to 9 h. Exposure of 18:3-supplemented cells to 1 and 10 μM $Cu(NO_3)_2$ for 1 h resulted in approximately 7% and 28% lethality, respectively (results not shown). The cellular DNA content of cells previously grown in 18:3-supplemented medium, exposed to 10 μM $Cu(NO_3)_2$ is shown (Fig. 5.5). After 2 h exposure, both 1C and 2C DNA peak intensities were much reduced (similar detrimental effects were observed after only 15 min exposure of 18:3-enriched cells to 100 μM $Cu(NO_3)_2$ (see Fig. 5.3b)) (Fig. 5.5a). Furthermore, after 9 h exposure both 1C and 2C DNA peaks were severely diminished and DNA levels greater than 4C were evident (Fig. 5.5d). Over-replication of cellular DNA was not evident for unsupplemented or PUFA-supplemented cells exposed to 1 μM $Cu(NO_3)_2$, or unsupplemented and 18:2-supplemented cells exposed to 10 μM $Cu(NO_3)_2$ (results not shown). The results indeed demonstrate DNA over-replication in 18:3-enriched *S. cerevisiae* exposed to non-toxic concentrations of $Cu(NO_3)_2$. Furthermore, the results indicate a threshold concentration of $Cu(NO_3)_2$ below which over-replication of cellular DNA does not occur.

Fig. 5.5. Effect of 10 μM $Cu(NO_3)_2$ on the cellular DNA content of linolenate-enriched *S. cerevisiae* NCYC 1383. The FL2 histograms depict the cellular DNA content of cells after 2 h (a), 4.5 h (b), 6 h (c), and 9 h (d) exposure to 10 μM $Cu(NO_3)_2$. Each histogram contains data collected from at least 10,000 cells.

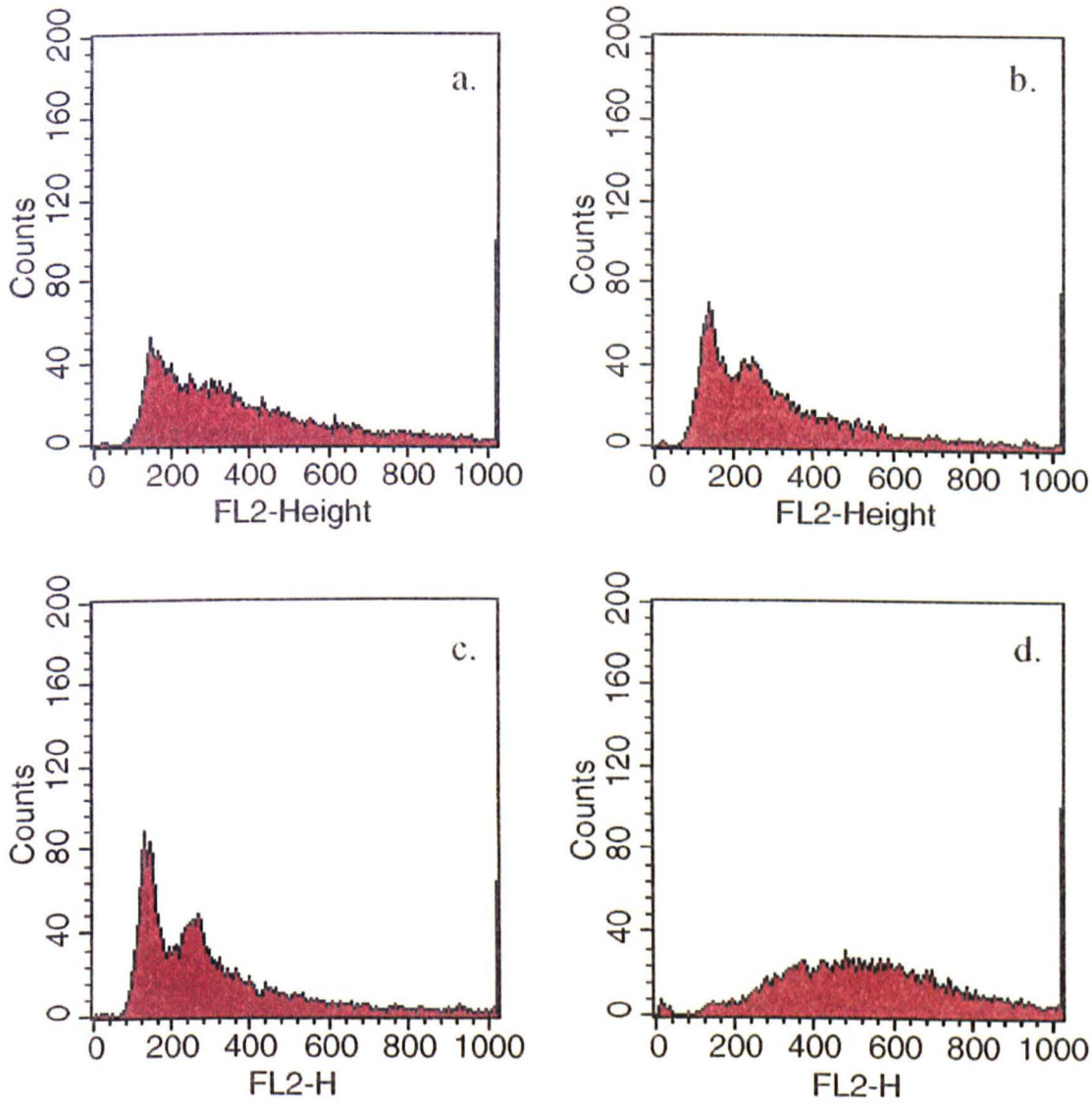
a.
b.
c.
d.
Counts
0
40
80
120
160
200
0
200
400
600
800
1000
FL2-Height
FL2-H

5.3.5. **Effects of the free radical scavengers mannitol and DMSO on $Cu(NO_3)_2$-induced over-replication in PUFA-supplemented *S. cerevisiae* NCYC 1383.** Redox-active metals such as copper directly promote oxidative stress through the generation of reactive oxygen species such as the hydroxyl radical ($OH^{\cdot}$) (Flowers *et al.*, 1997; Lloyd *et al.*, 1997). As the hydroxyl radical has been implicated as a key causative agent of DNA damage in *S. cerevisiae*, we examined whether Cu^{2+}-induced DNA over-replication in 18:3-enriched cells could be inhibited by the hydroxyl radical scavengers dimethyl sulfoxide (DMSO) and mannitol. Cells previously grown in unsupplemented, 18:2- and 18:3-supplemented medium were exposed to 20 μM $Cu(NO_3)_2$ for up to 22 h, in the presence of 0.2 M mannitol and 0.4 M DMSO. Incubation with DMSO and mannitol during Cu^{2+}-exposure had little protective effect against over-replication of cellular DNA in PUFA-enriched cells (results not shown). Repeated rounds of DNA replication, and accumulation of cellular DNA levels of up to 8C DNA were again evident, despite the presence of both DMSO and mannitol (see Fig. 5.3). The results suggest that the hydroxyl radical is most likely not directly involved in Cu^{2+}-induced DNA over-replication in PUFA-enriched cells.

5.3.6. **Effects of $Cd(NO_3)_2$, $CrK(SO_4)_2$, H_2O_2, and menadione on the cellular DNA content of unsupplemented and PUFA-supplemented *S. cerevisiae* NCYC 1383.** We sought to determine whether toxic concentrations of the nonredox-active metal ions Cd^{2+} and Cr^{3+}, the oxidative toxin H_2O_2, or the superoxide anion-generating compound menadione could also induce DNA over-replication in PUFA-supplemented *S. cerevisiae*. Cells previously grown in unsupplemented, 18:2- and 18:3-supplemented medium were

exposed to either 200 μM $Cd(NO_3)_2$, 5 mM $CrK(SO_4)_2$, 5 mM H_2O_2 or 2 mM menadione for up to 20 h. Prolonged exposure to all four toxins had no evident adverse effects on the cellular DNA content of both supplemented or PUFA-supplemented cells, whereby both 1C and 2C DNA peaks were still evident and clearly resolved (results not shown).

5.3.7. **Effects of reduced-glutathione on Cu^{2+}-induced DNA damage and over-replication in linolenate-enriched *S. cerevisiae* NCYC 1383.** The dithiol glutathione is one of the most important cellular antioxidants of *S. cerevisiae* (Stephen and Jamieson, 1996). Glutathione possesses a redox-active sulphydryl group which reacts with oxidants to produce oxidised glutathione (GSSG). Here we sought to determine if redox-cycling was essential for Cu^{2+}-induced DNA over-replication in linolenate-enriched cells, by inhibiting redox-cycling in the presence of excess reduced-glutathione. Cells previously grown in 18:3-supplemented medium were exposed to 20 μM $Cu(NO_3)_2$ for up to 6 h, in the presence and absence of 0.1 M reduced-glutathione (Fig. 5.6). Again, after only 1 h exposure to 20 μM $Cu(NO_3)_2$, 1C and 2C DNA peaks intensities were diminished (Fig. 5.6a). Furthermore, after 6 h exposure to 20 μM $Cu(NO_3)_2$ DNA levels greater than 4C were evident (Fig. 5.6e). However, DNA over-replication was not evident after 6 h exposure of 18:3-enriched cells to 20 μM $Cu(NO_3)_2$ in the presence of 0.1 M reduced-glutathione, whereby both 1C and 2C DNA peaks remained distinctly resolved (Fig. 5.6f). The results indicate that Cu^{2+} redox-cycling activity is essential for DNA over-replication in 18:3-enriched cells.

Fig. 5.6. Influence of reduced-glutathione on $Cu(NO_3)_2$-induced DNA over-replication in linolenate-enriched *S. cerevisiae* NCYC 1383. Cells were exposed to 20 μM $Cu(NO_3)_2$ in the presence and absence of 0.1 M reduced-glutathione for up to 6 h. The FL2 histograms depict the cellular DNA content of cells after 1 h (a), 4.5 h (c) and 6 h (e) exposure to $Cu(NO_3)_2$, in the absence of reduced-glutathione, and 1 h (b), 4.5 h (d) and 6 h (f) exposure in the presence of reduced glutathione. Each histogram contains data from at least 10,000 cells.

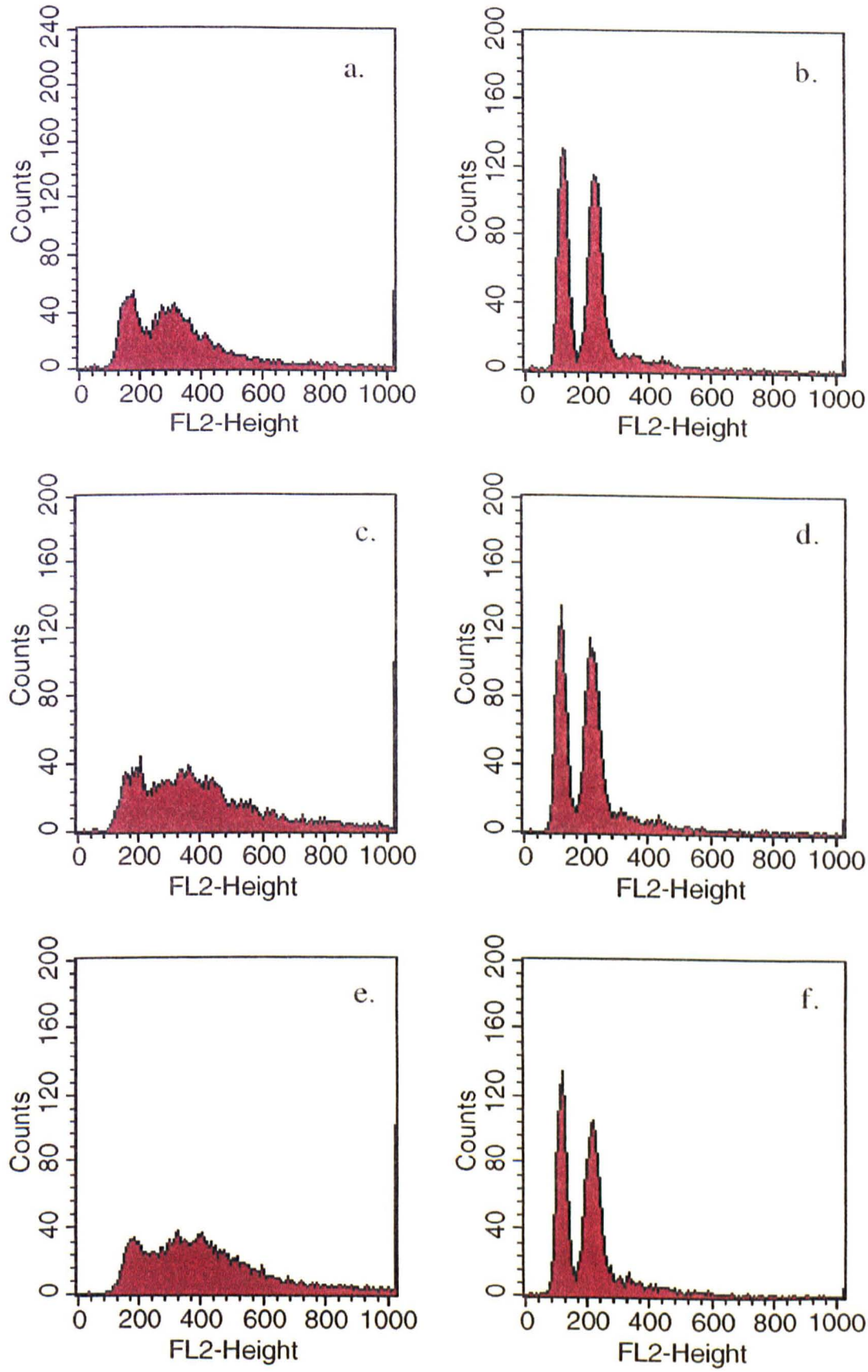
a.
b.
c.
d.
e.
f.
Counts
FL2-Height
0
40
80
120
160
200
240
200
400
600
800
1000

5.3.8. **Effect of CrO_3 on the cellular DNA content of unsupplemented and PUFA-supplemented *S. cerevisiae* NCYC 1383.** Cr^{6+} is a highly redox-active metal ion, exemplified by the limited number of chromium (VI) compounds, which include CrO_3 and peroxy compounds, that exist (Mackay and Mackay, 1989). Hence, we investigated whether metal-induced over-replication of cellular DNA in PUFA-enriched cells could also be induced by Cr^{6+}. Cells previously grown in 18:3-supplemented medium were exposed to 5 mM CrO_3 for up to 6 h. The cellular DNA content of 18:3-enriched *S. cerevisiae* exposed to CrO_3 is shown (Fig. 5.7). After only 15 min exposure to CrO_3 1C and 2C DNA peak intensities were reduced (similar to that observed for 18:3-enriched cells exposed to 100 μM $Cu(NO_3)_2$ (see Fig. 5.3)) (Fig. 5.7b). After 2 h exposure to 5 mM CrO_3 the cellular DNA content of 18:3-enriched cells increased to greater than 4C (Fig. 5.7d). Thus, the onset of DNA over-replication appeared to occur more rapidly in the presence of 5 mM Cr^{6+}, compared with 100 μM Cu^{2+} (see Fig. 5.3). Furthermore, upon continued exposure to CrO_3 DNA levels greater than 6C were evident (Figs. 5.7e,f). These results were very similar to those attained upon exposure of 18:3-enriched cells to 100 μM $Cu(NO_3)_2$ (see Fig. 5.3). These results confirm that exposure of 18:3-enriched *S. cerevisiae* to the redox-active metal Cr^{6+} also results in continued rounds of DNA synthesis.

5.3.9. **Fatty acid composition of nuclear membrane-enriched fractions.** We had previously demonstrated the incorporation of exogenous linoleate and linolenate into whole-cell and plasma membrane lipids (see Tables 2.1 and 2.4). As this particular study was primarily

Fig. 5.7. Effect of 5 mM CrO_3 on the cellular DNA content of linolenate-enriched *S. cerevisiae* NCYC 1383. The FL2 histograms depict the cellular DNA content of cells before chromium addition (a), and after 15 min (b), 30 min (c), 2 h (d), 4.5 h (e) and 6 h (f) exposure to 5 mM CrO_3. Each histogram contains data collected from at least 10,000 cells.

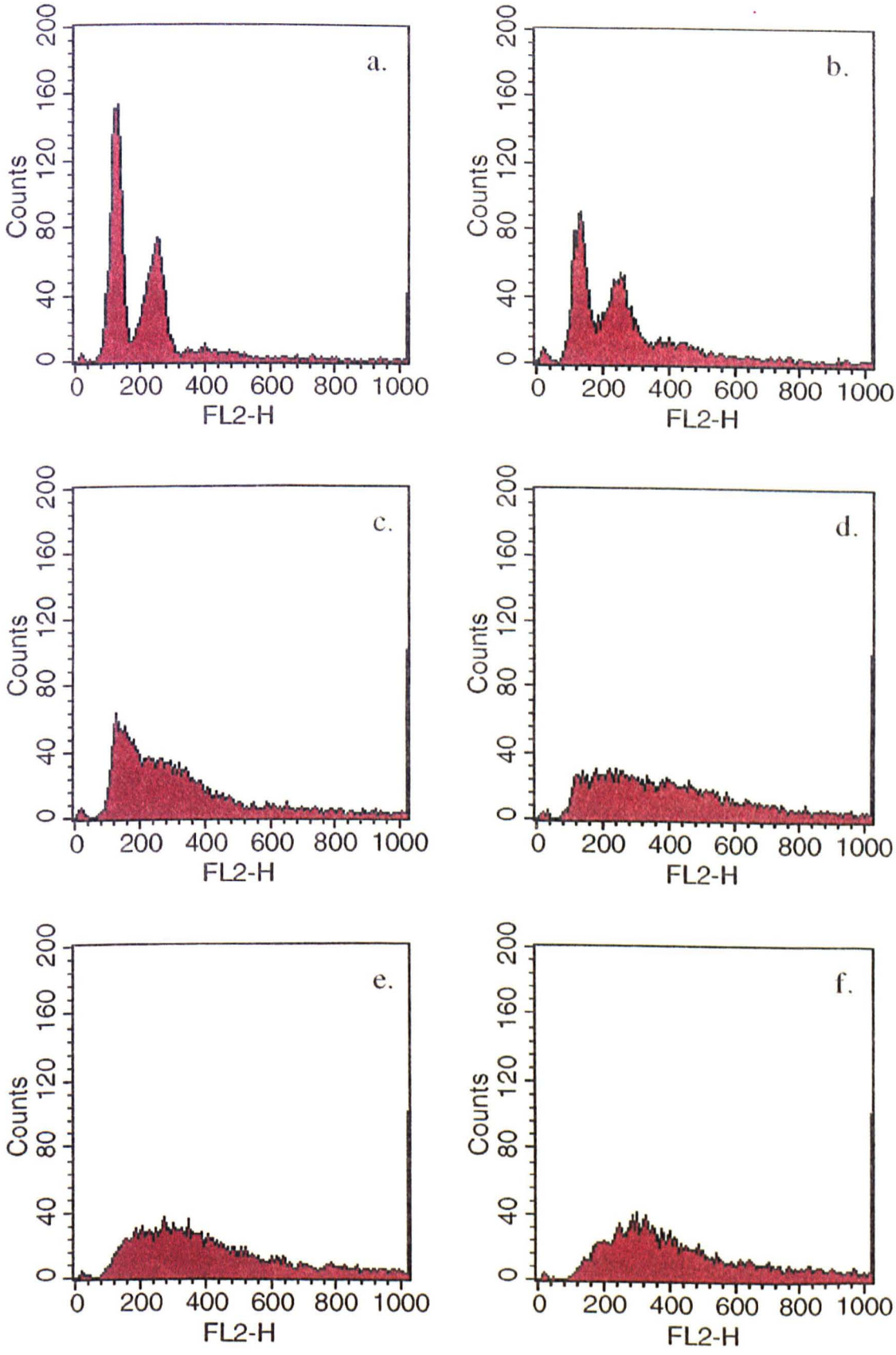
a.
b.
c.
d.
e.
f.
Counts
FL2-H
0
40
80
120
160
200
0
200
400
600
800
1000

concerned with the effects of toxins on cellular DNA content and DNA replication, we sought to confirm incorporation of exogenous 18:2 and 18:3 into nuclear membrane lipids, and examine the fatty acid composition of nuclear membranes after exposure to $Cu(NO_3)_2$. In order to assess the purity of isolated nuclear membrane fractions, nuclei were stained with the DNA-binding fluorochrome DAPI (M^{c}Millan and Tatchell, 1994). The purity of nuclear membrane-enriched fractions from cells grown in unsupplemented, 18:2- and 18:3-supplemented media was confirmed using both light and fluorescence microscopy, and by observing characteristic nuclear electrophoretic profiles using SDS-PAGE, e.g. the presence of the 38 kDa nucleolar protein fibrillarin (Aris and Blobel, 1991) (results not shown). Isolated nuclear membrane fractions were thus considered of sufficient purity for lipid analysis.

The fatty acid compositions of nuclear membrane-enriched fractions from cells grown for 16 h in unsupplemented, 18:2- and 18:3-supplemented media (Table 5.2) were generally similar to those of their corresponding whole-cell homogenates (Table 2.1), and plasma membrane-enriched fractions determined previously (Table 2.4). However, incorporation of the exogenous PUFAs 18:2 and 18:3 in to nuclear membrane lipids was approximately 48% lower and 33% lower, respectively, than those of the corresponding plasma membrane-enriched fractions (Table 5.2). Nevertheless, fatty acid unsaturation indices calculated for nuclear membrane-enriched fractions again decreased in the order 18:3-supplemented > 18:2-supplemented > unsupplemented (Table 5.2). While the results confirm incorporation of exogenous PUFAs into nuclear membrane lipids, genuine differences between levels of incorporation of PUFAs in to nuclear membrane and plasma membrane lipids were apparent. However, several factors, such as

Table 5.2. Fatty acid composition of nuclear membrane-enriched fractions from *S. cerevisiae* NCYC 1383 previously grown in unsupplemented, linoleate- and linolenate-supplemented media

Fatty acid	Medium		
	Unsupplemented	18:2-supplemented	18:3-supplemented
16:0	24.5±1.9	20.2±1.7	18.8±2.2
16:1	44.2±4.4	11.8±0.2	4.6±0.3
18:0	7.2±0.1	14.9±0.9	24.7±7.6
18:1	24.1±2.4	16.2±0.3	8.4±2.3
18:2	tr.	36.9±0.6	tr.
18:3	n.d.	n.d.	43.6±2.0
U.I.	0.68	1.02	1.44

Values for percentage fatty acid composition are means from two replicate determinations ± standard deviation (SD). (n.d. = not detectable; tr. < 0.1). U.I. refers to the unsaturation index (average number of double bonds per fatty acid).

differences in subcellular fractionation techniques, FAME separation and analysis procedures, and experimental conditions, e.g. ambient temperature, and presence or absence of buffer, during nuclear membrane and plasma membrane isolation (see Sections 4.2 and 5.2), may have contributed to the discrepancies observed.

The fatty acid composition of nuclear membrane-enriched fractions from *S. cerevisiae* incubated in buffer, in the presence of 100 μM $Cu(NO_3)_2$ for 6 h showed significant differences to that of nuclear membrane-enriched fractions of cells incubated in the absence of $Cu(NO_3)_2$ (Table 5.3). Nuclear membrane enriched-fractions from cells incubated in the presence of $Cu(NO_3)_2$ generally displayed a lower content of unsaturated fatty acids, as a proportion of total fatty acids, than those from cells incubated in the absence of $Cu(NO_3)_2$. This was most evident as lower proportions of 18:2 and 18:3. Hence, after 6 h exposure of PUFA-enriched cells to $Cu(NO_3)_2$, the unsaturation indices of 18:2- and 18:3-supplemented nuclear membrane-enriched fractions were approximately 37% and 17% lower, respectively, than nuclear membrane-enriched fractions from cells incubated in the absence of $Cu(NO_3)_2$.

5.3.10. **Determination of Mcm3p in nuclear fractions of *S. cerevisiae* NCYC 1383.** Mcm3p is present in high abundance and at relatively constant levels throughout the cell cycle in actively proliferating cells (Young and Tye, 1997). Furthermore, while Mcm3p is present in both the cytoplasm and nucleus throughout the cell cycle, it becomes tightly associated with chromatin only from late M phase to early S phase (Young and Tye, 1997). Mcm3p is thus thought to be involved in the assembly of the pre-replication

Table 5.3. Fatty acid composition of nuclear membrane-enriched fractions from *S. cerevisiae* NCYC 1383 previously grown in unsupplemented, linoleate- and linolenate-supplemented media, exposed to 100 μM $Cu(NO_3)_2$ for 6 h

Fatty acid	Medium		
	Unsupplemented	18:2-supplemented	18:3-supplemented
16:0	25.1±4.4	36.1±0.6	28.3±0.2
16:1	38.4±1.9	7.1±1.3	4.2±1.0
18:0	10.5±1.5	22.2±0.4	21.4±0.6
18:1	26.0±4.0	12.2±0.1	11.9±0.8
18:2	tr.	22.4±1.2	tr.
18:3	n.d.	n.d.	34.5±2.2
U.I.	0.64	0.64	1.20

Footnote as for Table 5.2.

initiation complex that precedes DNA replication initiation in *S. cerevisiae* (Aparicio *et al.*, 1997).

Therefore, Mcm3p in nuclear membrane-enriched fractions from unsupplemented and PUFA-supplemented cells, incubated in the absence and presence of 100 μM $Cu(NO_3)_2$, was examined to determine differences, if any, in the nuclear localisation, i.e. chromatin-bound or nucleosolic, of Mcm3p in over-replicating cells. After 6 h incubation, cells were sequentially fractionated in to nucleosolic (NS) and nuclear pellet (NP) fractions. Equal volumes of the NS and NP fractions (containing variable amounts of protein) were separated using 7.5% SDS-PAGE and analysed on nitrocellulose Western blots (Fig. 5.8). Mcm3p was detected with anti-Mcm3 antibodies (Hu *et al.*, 1993). The Mcm3p antibody cross-reacted with numerous proteins (Fig 5.8). Several studies with Mcm antibodies have revealed similar results (Merchant *et al.*, 1997; Lei *et al.*, 1996; Chong *et al.*, 1995), suggestive of cross-reactivity with the remaining members of the MCM family (all proteins carry a highly conserved motif (the MCM box)), and possibly protein degradation (Lei *et al.*, 1996). Mcm3p (107 kDa) was detected in the nucleosolic fractions of unsupplemented (lane 1), 18:2- (lane 2) and 18:3- (lane 3) supplemented cells, and in the nuclear pellet fractions of unsupplemented (lane 7) and 18:2-supplemented (lane 8) cells, incubated without $Cu(NO_3)_2$ (Fig. 5.8b). Significantly, of the Cu^{2+}-exposed cells, Mcm3p was only detected in the nucleosolic fraction of unsupplemented cells (lane 4).

5.3.11. **Determination of Cdc28p in nuclear fractions of *S. cerevisiae* RJD621.** Levels of the cyclin-dependent kinase Cdc28p do not fluctuate throughout the cell cycle. However,

Fig. 5.8. Detection of Mcm3p in nuclear fractions of *S. cerevisiae* NCYC 1383 incubated in the presence and absence of 100 μM $Cu(NO_3)_2$. After 6 h incubation nuclear fractions were purified, proteins were electrophoresed on 7.5% SDS-PAGE gels, western blotted onto nitrocellulose membranes, and probed with monoclonal anti-Mcm3p. Samples are abbreviated with the first letters, Y, L, and E, representing cells previously grown in unsupplemented, linoleate- and linolenate-supplemented medium, respectively. The letter M following Y, L, or E, corresponds to cells incubated in the presence of $Cu(NO_3)_2$. NS and NP represent nucleosolic and nuclear pellet fractions, respectively.

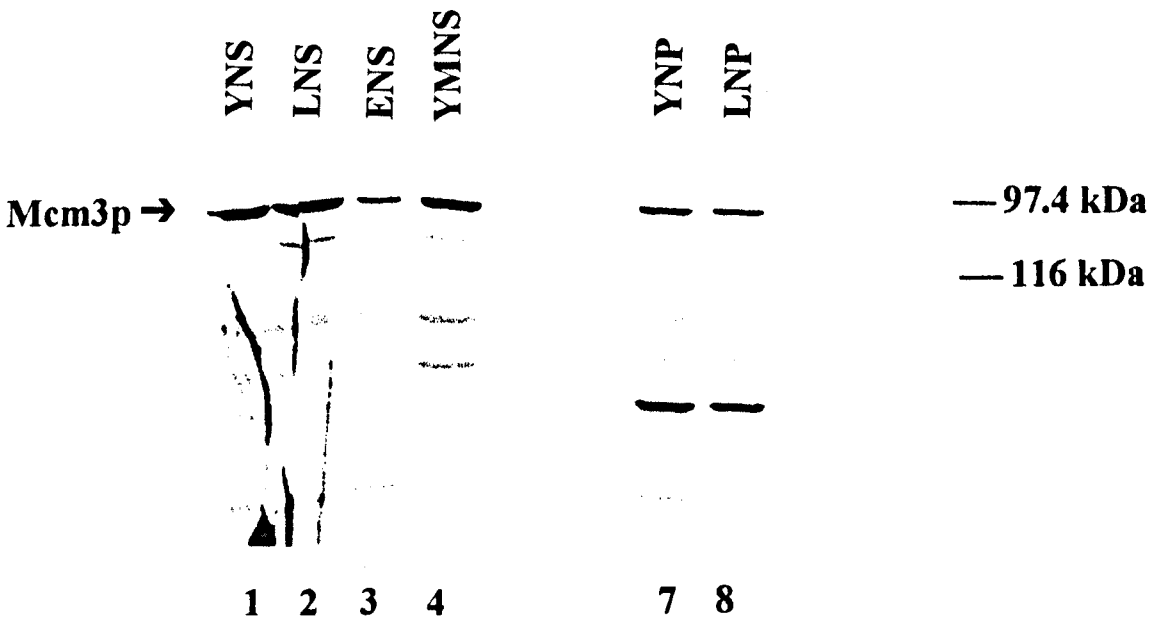
YNS
LNS
ENS
YMNS
YNP
LNP
Mcm3p →
— 97.4 kDa
— 116 kDa
1 2 3 4 7 8

through association with CLN- and B-type cyclins Cdc28p kinase activity rises from undetectable levels in early G_1 to maximal levels during nuclear division (Lew *et al.*, 1997). Cdc28p, in association with any of the six B-type cyclins, is required for the activation of pre-replication initiation complexes, resulting in the firing of origins of replication (Lew *et al.*, 1997). Cdc28p is thus central to the interdependence of DNA replication and mitosis under normal conditions. As these processes are evidently uncoupled in Cu^{2+}-exposed PUFA-enriched cells, we investigated whether differences, if any, in levels or localisation of Cdc28p in DNA over-replicating cells could be detected. The yeast strain *S. cerevisiae* RJD621 (*cdc28*::*CDC28*-HA) was used for this particular study as the epitope-tagged Cdc28p can be conveniently detected using anti-HA antibodies. Toxicity experiments confirmed even more accentuated DNA over-replication in 18:3-enriched RJD621 exposed to $Cu(NO_3)_2$ (Fig. 5.9). After only 2 h exposure to 100 μM $Cu(NO_3)_2$, DNA levels of up to 8C were detected (Fig. 5.9b). Thus, after 6 h incubation, cells were sequentially fractionated in to cytosolic (C), high-salt nucleosolic (NSH), low-salt nucleosolic (NSL) and nuclear pellet (NP) fractions. Equal volumes of all fractions (containing equal amounts of protein, verified using the Micro-Lowry assay) were separated using 7.5% SDS-PAGE, and analysed on nitrocellulose Western blots (Fig. 5.10). Cdc28p-HA was detected using anti-HA antibodies. Cdc28p was not detected in any fractions from cells previously incubated in the presence of $Cu(NO_3)_2$. Significantly, an approximately 90 kDa band, most likely representing Cdc28p (34 kDa) in association with Clb2p (56 kDa) (Surana *et al.*, 1991), was detected in the high-salt nucleosolic fractions of unsupplemented (lane 7), 18:2- (lane 8) and 18:3- (lane 9) supplemented cells, incubated without $Cu(NO_3)_2$ (Fig. 5.10). Elevated levels of

Cdc28p-Clb2p kinase activity are observed in *S. cerevisiae* during late G_2 phase prior to mitosis (Surana *et al.*, 1993).

Fig. 5.9. Effect of 100 μM $Cu(NO_3)_2$ on the cellular DNA content of linolenate-enriched *S. cerevisiae* RJD621. The FL2 histograms depict the cellular DNA content of cells before copper addition (a) and after 2 h (b), 4 h (c) and 6 h (d) exposure to 100 μM $Cu(NO_3)_2$. Each histogram contains data collected from at least 10,000 cells.

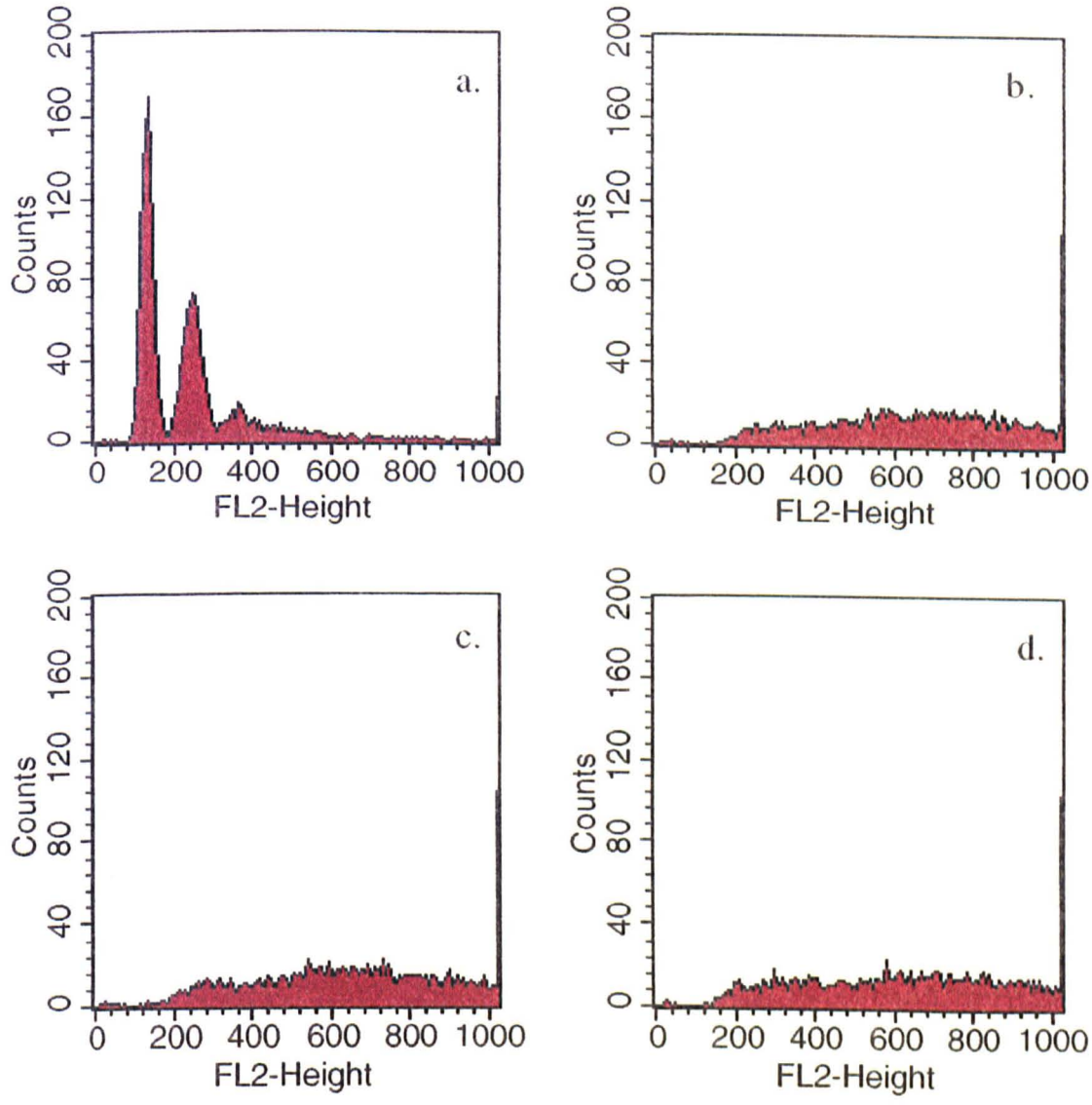
a.
b.
c.
d.
Counts
FL2-Height
0
40
80
120
160
200
400
600
800
1000

Fig. 5.10. Detection of Cdc28p in nuclear fractions of *S. cerevisiae* RJD621 incubated in the presence and absence of 100 μM $Cu(NO_3)_2$. After 6 h incubation nuclear fractions were purified, proteins were electrophoresed on 7.5% SDS-PAGE gels, western blotted onto nitrocellulose membranes, and probed with anti-HA. Samples are abbreviated with the first letters, Y, L, and E, representing cells previously grown in unsupplemented, linoleate- and linolenate-supplemented medium, respectively. NSH, NSL and NP represent high-salt nucleosolic, low-salt nucleosolic and nuclear pellet fractions, respectively.

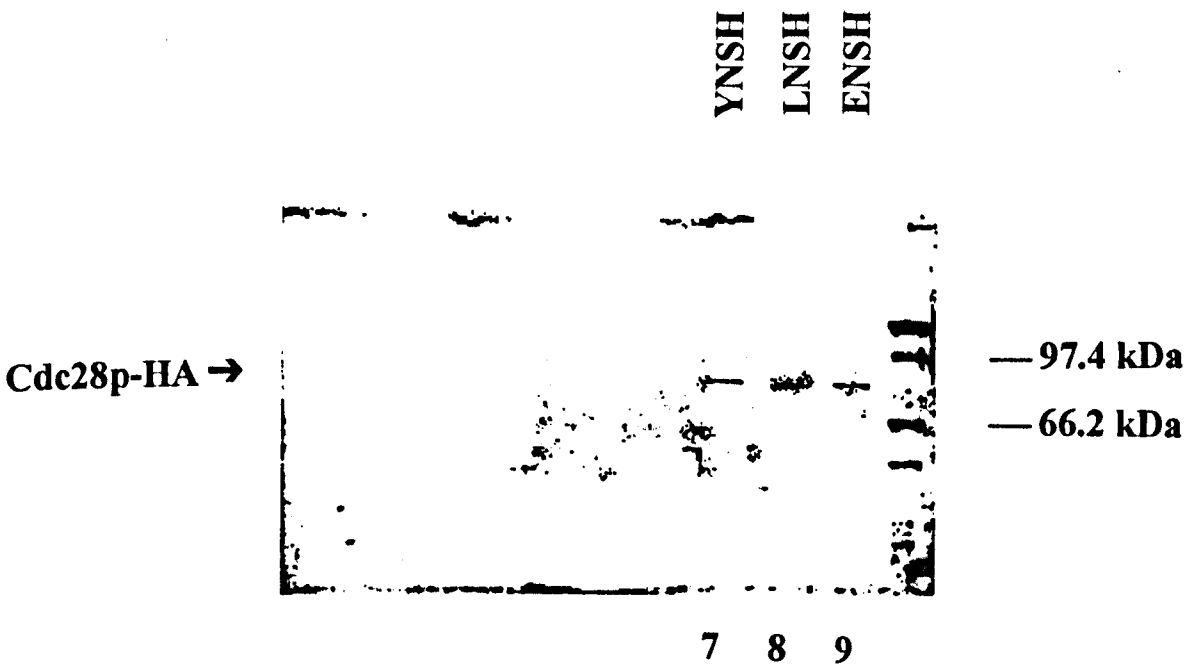
YNSH
LNSH
ENSH
Cdc28p-HA →
— 97.4 kDa
— 66.2 kDa
7
8
9

5.4. Discussion

In this particular study we have investigated the effects of heavy metals and oxidative toxins on the cellular DNA content of *S. cerevisiae* NCYC 1383. Lipid peroxidation as a major means of heavy metal toxicity in *S. cerevisiae* had previously been demonstrated in Chapter 3. Levels of the lipid peroxidation byproducts, thiobarbituric acid-reactive substances (TBARS) and conjugated dienes were found to be markedly elevated in cells exogenously-enriched with the polyunsaturated fatty acids (PUFAs) linoleate and linolenate, upon exposure to Cu^{2+} and Cd^{2+}. Lipid peroxidation is initiated in the presence of heavy metals through the generation of reactive oxygen species (ROS), such as the hydroxyl radical ($HO^{\cdot}$), superoxide anion ($O_2^{\cdot-}$), singlet oxygen (O), and the carbon-centered radical ($L^{\cdot}$), through Fenton and Haber-Weiss reactions (Dix and Aikens, 1993). These ROS have also been implicated as the causative agents of a broad spectrum of DNA damage, including double-strand breaks, which are thought to induce genome rearrangements such as deletions, duplications, and translocations (Brennan and Schiestl, 1998; Manivasakam and Schiestl, 1998). Therefore, we sought to investigate whether enrichment of *S. cerevisiae* with the PUFAs linoleate and linolenate would also predispose cells to greater levels of heavy metal-induced, ROS-mediated DNA damage

Significantly, DNA over-replication was demonstrated in PUFA-enriched cells upon exposure to the redox-active metal species Cr^{6+} and Cu^{2+}. Exposure of PUFA-enriched *S. cerevisiae*, particularly linolenate-enriched cells, to both Cu^{2+} and Cr^{6+} resulted in continued DNA synthesis and accumulation of DNA levels of up to 8C, in

certain cases. Metal-induced continued DNA synthesis in linolenate-enriched cells was confirmed by complete inhibition of DNA over-replication in the presence of the ribonucleotide reductase inhibitor hydroxyurea, and by the diphenylamine assay (Weinert *et al.*, 1994).

In addition, flow cytometric cellular DNA profiles, in the early stages of Cr^{6+} and Cu^{2+} exposure, were suggestive of minor levels of DNA fragmentation. DNA fragmentation was manifested as decreased 1C and 2C DNA peak intensities and resolution, and a decrease in FL2 positive signal to noise ratio. The induction of hypoploidy and loss of G_1 peak resolution have been used as markers of DNA fragmentation, characteristic of apoptosis in tumorigenic cells (increased noise signal is also a characteristic of apoptotic-cell DNA histograms) (Takasu *et al.*, 1998; Vernole *et al.*, 1998). Also, while there was little evidence of DNA over-replication in cells pre-incubated with hydroxyurea, decreased 1C and 2C DNA peak intensities and resolution were still evident. The progression of DNA over-replication in the temperature-sensitive *cdc16* and *cdc27* mutants of *S. cerevisiae*, and *cdc13* mutant of *S. pombe*, i.e. the absence of 1C and 2C DNA peak broadening and no decrease in the FL2 positive signal to noise ratio, lends further support for Cu^{2+}- and Cr^{6+}-induced DNA fragmentation, prior to DNA over-replication, observed in this study (Heichmann and Roberts, 1996; Hayles *et al.*, 1994). It is plausible that DNA fragmentation might be a consequence of degradation of single strands from exposed 5' ends of Cu^{2+}- and Cr^{6+}-induced double-strand breaks during 'single-strand annealing' or 'one sided invasion' intrachromosomal recombination processes (Galli and Schiestl, 1998). However, further experimentation in the form of

TdT-mediated dUTP-biotin nick end-labelling (TUNEL) and pulsed-field electrophoresis are required to conclusively confirm DNA fragmentation.

Cu^{2+}-induced DNA over-replication was found to occur at a range of concentrations between 10 and 100 μM, indicating a threshold level of Cu^{2+} ions below which induction does not occur. In addition, neither DNA over-replication or loss of peak resolution were evident in unsupplemented *S. cerevisiae* exposed to toxic concentrations of Cu^{2+}. This finding is consistent with earlier reports of hydroquinone (HQ) or benzoyl peroxide (BzPO) and Cu^{2+}-induced DNA-protein crosslinks (DPC) and DNA strand breaks, while Cu^{2+} alone elicited no significant DNA damage (Altman *et al.*, 1995; Akman *et al.*, 1993; Li and Trush, 1993). Thus, it appears that Cu^{2+} genotoxicity requires the presence of reducing agents such as HQ, BzPO or PUFAs.

DNA over-replication was also not observed after prolonged exposure of either unsupplemented or PUFA-supplemented *S. cerevisiae* to a highly toxic concentration of the nonredox-active metal Cd^{2+}. Exposure to the nonredox-active metals Cd^{2+}, Mn^{2+} and Zn^{2+}, in the presence of HQ, has previously been shown to result in negligible deleterious effects to cellular DNA (Li and Trush, 1993). However, exposure to redox-active Cu^{2+}/HQ has been associated with the generation of extensive DNA lesions (Li and Trush, 1993). Thus, it is proposed that redox-cycling activity is essential for DNA over-replication and damage in metal-exposed linolenate-enriched cells. Significantly, in agreement with other reports (Chiu *et al.*, 1995; Li and Trush, 1993; Rodriguez-Montelongo *et al.*, 1993), Cu^{2+}-induced over-replication in linolenate-enriched cells was completely inhibited in the presence of the antioxidant reduced-glutathione. Reduced-

glutathione maintains a strong cellular reducing environment thereby preventing the redox-cycling cycling activity of Cu^{2+} (Stephen and Jamieson, 1996; Li and Trush, 1993).

Hydrogen peroxide (H_2O_2), the hydroxyl radical ($HO^{\cdot}$), and the superoxide anion/perhydroxyl radical ($O_2^{\cdot-}$\$HO_2^{\cdot}$), have been implicated as the major ROS responsible for eliciting deleterious effects to DNA (Keyer and Imlay, 1996; Brennan *et al.*, 1994). The perhydroxyl radical exists in dynamic equilibrium with the superoxide anion in biological systems (Rego and Oliveira, 1995; Dix and Aikens, 1993). However, Cu^{2+}-induced DNA over-replication was also evident in the presence of elevated levels of the hydroxyl radical scavengers mannitol and DMSO. In addition, neither menadione or H_2O_2 alone induced deleterious effects to DNA in any of the cell types examined. Thus, a direct role of the ROS, $HO^{\cdot}$, $O_2^{\cdot-}$ or H_2O_2 in eliciting DNA over-replication in PUFA-enriched cells exposed to Cu^{2+} or Cr^{6+} could not be established. Conducive with our findings, the induction of DNA lesions in isolated nuclear chromatin by the Cu^{2+}- and Fe^{2+}-EDTA/H_2O_2 systems has also been shown to occur in the presence of both mannitol and DMSO (Chiu *et al.*, 1995).

The reduction of Cu^{2+} and Cr^{6+} by endogenous intracellular reductants, such as NADH or ascorbate, results in the generation of the ROS, $O_2^{\cdot-}$, H_2O_2, and the reduced forms of both metals, Cu^{+} and Cr^{3+} (Xu *et al.*, 1996; Bridgewater *et al.*, 1994; Rodriguez-Montelongo *et al.*, 1993). UV-visible spectroscopy and ESR have also indicated the facilitation of reduction of Cu^{2+} by NADH with the subsequent production of the highly reactive carbon-centered radical ($L^{\cdot}$) (Oikawa and Kawanishi, 1996). Furthermore, ROS-mediated propagation of the lipid peroxidative chain in PUFA-enriched cells results in the generation of the lipid hydroperoxides (LOOH) linoleate hydroperoxide and

linolenate hydroperoxide (Evans *et al.*, 1998; Dix and Aikens, 1993). LOOHs are known to form delocalised lipid radicals which self-react to form dienoic dimers, or react with other LOOHs resulting in the generation of highly reactive lipid peroxyl radicals (LOO·) (Evans *et al.*, 1998). We therefore propose that DNA over-replication in PUFA-enriched cells, particularly linolenate-enriched cells, is mediated through Fenton-type interactions of LOOHs with Cu^{+} or Cr^{3+}, resulting in the generation of Cu^{+}- and Cr^{3+}-peroxyl complexes (Chiu *et al.*, 1995). Copper is also known to bind to non-histone proteins at the nuclear matrix attachment sites of DNA loops (Chiu *et al.*, 1995). Thus, in addition to possible direct effects on nucleic acids, Cu^{2+}- and Cr^{6+}-induced DNA over-replication in linolenate enriched cells may be a consequence of Cu^{+}- and Cr^{3+}-peroxyl complex interactions with key DNA replication proteins.

Mcm3p and Cdc28p have been implicated as key DNA replication proteins in *S. cerevisiae* (Lew *et al.*, 1997; Young *et al.*, 1997). Mcm3p is constitutively present in the cytoplasm and nucleus throughout the cell cycle (Young *et al.*, 1997; Young and Tye, 1997). Mcm3p remains chromatin-associated throughout G_1 phase and dissociates from chromatin, most likely as a result of Cdc28p-Clb2p or Cdc7p-Dbf4p phosphorylation, as cells enter S phase (Lew *et al.*, 1997; Young *et al.*, 1997; Young and Tye, 1997; Lei *et al.*, 1996). Thus, Mcm3p is thought to form part of the pre-RCs that assemble at Oris from late M phase to early S phase, and thereby plays a significant role in restricting Ori activity to once per S phase (Dalton and Hopwood 1997; Young and Tye, 1997). Our results with unsupplemented and PUFA-supplemented cells, incubated in the absence of $Cu(NO_3)_2$, confirmed recent observations that two forms of Mcm3p exist in the nucleus of *S. cerevisiae*; a readily extractable form and a tightly chromatin-associated form, that

is released only upon treatment with DNase (Young and Tye, 1997). However, chromatin-associated Mcm3p was not detected in 18:3-enriched cells, previously incubated in the absence of $Cu(NO_3)_2$. This result may be a consequence of unequal protein loading; inherent differences in membrane physical properties of 18:3-enriched cells were associated with lower DNA and protein yields following nuclear fractionation. Of cells incubated in the presence of Cu^{2+}, Mcm3p was only detected in the nucleosolic fraction of unsupplemented cells (DNA over-replication not evident). Thus, our preliminary results indicate that Mcm3p is not present in the nucleosolic or nuclear pellet fractions of over-replicating cells. Therefore, it could be postulated that interactions of Cu^{+}-peroxyl complexes with Mcm3p prevent assembly of Mcm3p in to pre-RCs, resulting in continued firing of Oris for DNA replication.

Furthermore, Clb2p-associated Cdc28p (Surana *et al.*, 1991), was only detected in the high salt nucleosolic fractions of unsupplemented and PUFA-supplemented *S. cerevisiae*, incubated in the absence of $Cu(NO_3)_2$. *CLB2* transcription is activated during G_2 and M phases, and repressed during G_1 phase (Lew *et al.*, 1997). In addition, *S. cerevisiae* has a requirement for Cdc28p-Clb2p kinase activity to enter M phase (Surana *et al.*, 1993). Cdc28p was not detected in the nucleosolic or nuclear pellet fractions of unsupplemented or PUFA-supplemented cells previously incubated in the presence of $Cu(NO_3)_2$. *Schizosaccharomyces pombe* deleted for *cdc13*$^{+}$, encoding a B-type cyclin, or overexpressing rum1p, a specific CDK inhibitor, undergoes continued DNA replication and sequential S phases in the absence of mitosis (Correa-Bordes and Nurse, 1995; Moreno and Nurse, 1994). Thus, it has been proposed that moderate levels of Cdc2p-Cdc13p kinase activity are required in G_2 phase to prevent additional rounds of DNA

replication in *S. pombe* (Stern and Nurse, 1996). Therefore, Cu^{+}- or Cr^{3+}-peroxyl complex interactions with Cdc28p-Clb2p in PUFA-enriched cells may result in diminished CDK activity, which is manifested as DNA over-replication. Furthermore, unlike the *cdc2*$^{+}$ gene of *S. pombe*, which is down-regulated in response to inhibition of DNA replication, mitotic CDK activity (Cdc28p-Clb2p) in *S. cerevisiae* remains elevated in cells arrested in S and G_2/M phases by replication inhibition (Li and Cai, 1997). Our proposition is however complicated by the fact that elevated levels of Cdc28p-Clb2p kinase activity have previously been demonstrated during over-replication in the *S. cerevisiae cdc16* and *cdc27* temperature-sensitive mutants (Heichmann and Roberts, 1996).

We have also previously demonstrated Cu^{2+}-induced plasma membrane lipid peroxidation in PUFA-enriched cells (Chapter 3). Plasma membrane-lipid peroxidation was associated with a deterioration of membrane integrity and loss of membrane impermeability (Chapter 2; Van Ginkel and Sevanian, 1994). Nuclear membrane fatty acid compositional data of Cu^{2+}-exposed PUFA-enriched cells obtained in this study was also suggestive of lipid peroxidative membrane damage. Oxidative degradation of PUFAs was supported by the lower unsaturation indices of nuclear membranes of Cu^{2+}-exposed cells (De Vos *et al.*, 1993). Thus, in addition to possible direct interactions with Cu^{+}-peroxyl complexes, loss of membrane impermeability may also account for the absence of Mcm3p and Cdc28p from nuclear membrane fractions of PUFA-enriched cell exposed to Cu^{2+}.

As stated previously, repeated rounds of DNA replication have been observed for the *cdc16* and *cdc27 S. cerevisiae* mutants (Heichmann and Roberts, 1996), the *cdc2* and

cdc13 S. pombe mutants, and upon overexpression of *rum1*$^+$ and *cdc18*$^+$ (homolog of *S. cerevisiae* cdc6p) in *S. pombe* (Stern and Nurse, 1996; Correa-Bordes and Nurse, 1995; Moreno and Nurse, 1994), indicating the critical function of these proteins in limiting DNA replication to once per cell cycle. Here we have demonstrated redox-active metal-induced DNA polyploidy in PUFA-enriched *S. cerevisiae* for the first time. We propose that DNA over-replication could be mediated through direct interactions of Cu^+- and Cr^{3+}-peroxyl complexes with key pre-RC proteins (Cdc6p, Mcm3p or Mcm2p), critical cylin-dependent kinases (Cdc28p-Clb2p or Cdc7p-Dbf4p), or by Cu^{2+}- and Cr^{6+}-induced gross lipid peroxidation-mediated nuclear membrane structural alterations, leading to loss of nuclear membrane impermeability. While further extensive experimental work is required to elucidate the exact mechanism of redox-active metal-induced DNA over-replication in PUFA-enriched *S. cerevisiae*, a major role of membrane fatty acid composition on heavy metal-induced genomic instability has been demonstrated.

CHAPTER 6

Conclusions

The effects of altered membrane fatty acid composition on the toxic interactions of heavy metals with the model organism *S. cerevisiae* were investigated. While other studies have investigated the effects of altered plasma membrane phospholipid unsaturation on the kinetics of solute accumulation in *S. cerevisiae* (Hoptroff *et al.*, 1997; Keenan *et al.*, 1982), this was the first study to examine the effects of such alterations on toxic interactions with heavy metals. *Saccharomyces cerevisiae* was selected for this study for several reasons; many aspects of the cellular organisation, function and structure of *S. cerevisiae* are common to those found in higher eukaryotes. Also, many regulatory mechanisms found in yeast, e.g. cell cycle-control, are conserved among larger, more complex eukaryotes. With the advent of the *Saccharomyces cerevisiae* genome database (Cherry *et al.*, 1997), the development of powerful yeast genetic techniques, combined with its low DNA content and ease of culture, *S. cerevisiae* has been established as an excellent model eukaryotic system. Numerous studies have also proven *S. cerevisiae* highly amenable as a model organism for the specific examination of metal-microbe interactions (Aβmann *et al.*, 1996; Ohsumi *et al.*, 1988). In addition, studies of membrane biology in lower eukaryotes are most advanced for *S. cerevisiae* (Van der Rest *et al.*, 1995; Van der Westhuisen *et al.*, 1994). In agreement with several reports, we have demonstrated that *S. cerevisiae* is highly amenable to cultural manipulation of membrane composition, without adverse effects on growth rate (Avery *et al.*, 1996; Parks *et al.*, 1995; M^{c}Donough *et al.*, 1992; Bossie and Martin, 1989). The consequent advantages of this system of membrane compositional manipulation, over conventional methods have been highlighted throughout this thesis. While the enrichment of *S. cerevisiae* with PUFAs elicited no discernible adverse phenotypic variations under non-

stressed conditions, susceptibility towards the toxic effects of heavy metals was greatly accentuated. Thus, cells that were previously enriched with the PUFAs linoleate or linolenate displayed elevated sensitivity towards both copper- and cadmium-induced plasma membrane permeabilisation and whole-cell toxicity. The implications of these findings for metal-microbe interactions in the environment are potentially very significant. The possibility that the large variability in microbial fatty acid composition, which can result from adaptive responses to changes in external physico-chemical parameters (Hazel and Williams, 1990; Suutari *et al.*, 1990) as well as genetically-determined intrinsic differences, may partly dictate differing heavy metal sensitivities among microorganisms is potentially very important. Indeed, recent studies examining changes in microbial fatty acid profiles following metal addition to soil have suggested a greater impact on microorganisms rich in PUFAs (Pennanen *et al.*, 1996). Thus, a passive role of modification of membrane fatty acid composition as an additional (in association with constitutive and inducible elements) determinant of heavy metal resistance is plausible.

Initial results implied a role of oxy-radical mediated effects in the toxicity of cadmium towards *S. cerevisiae*. Prolonged incubation of both unsupplemented and PUFA-supplemented *S. cerevisiae* in the presence of cadmium was associated with reduced cellular fatty acid unsaturation indices during the exponential growth phase. The depletion of unsaturated fatty acids has been used as a marker for lipid peroxidation (De Vos *et al.*, 1993). As PUFAs are well known to be markedly susceptible to oxy-radical mediated lipid peroxidative degradation (Porter *et al.*, 1995; Dix and Aikens, 1993), the increased susceptibility of PUFA-enriched cells to plasma membrane permeabilisation

and whole-cell toxicity was postulated to be a direct consequence of increased lipid peroxidation in these cells. Elevated levels of TBARS and conjugated dienes (lipid peroxidation decomposition products) confirmed accentuated oxidative degradation of cellular unsaturated fatty acids in metal-exposed PUFA-enriched cells. Thus, lipid peroxidation as a major means of heavy metal toxicity in microorganisms was demonstrated for the first time. The present results may prove useful in modelling lipid peroxidative processes associated with a multitude of pathological conditions in higher organisms. For example, the accumulation of fibrous plaques within the endothelial lining of blood vessels (culminating in atherosclerosis) is a direct consequence of low density lipoprotein (LDL) oxidation (Steinbrecher *et al.*, 1990). More significantly, transition metal-induced (e.g. aluminium, iron, and mercury) lipid peroxidation has been implicated in the aetiology of the neurodegenerative diseases Parkinsons disease and Alzheimers dimentia (Bondy *et al.*, 1998; Hock *et al.*, 1998; Rajan *et al.*, 1997).

The influence of cellular fatty acid composition on the interactions of heavy metals with cellular nucleic acids was also investigated. PUFA-enrichment was clearly associated with enhanced heavy metal-induced genotoxic effects. Gross genomic instability, manifested as continued DNA synthesis in the absence of cell division, was evident following exposure of PUFA-enriched cells, particularly linolenate-enriched cells, to the redox active metals Cu^{2+} and Cr^{6+}. While ROS-induced DNA adducts and double-strand breaks have been associated with gross genome rearrangements, e.g. deletions, duplications, and translocations (Manivasakam and Schiestl, 1998; Brennan *et al.*, 1994), this is the first report of heavy metal-induced polyploidy. It is postulated that interactions of Cu^{+}- or Cr^{3+}-peroxyl complexes with key DNA replication proteins or

cyclin-CDK complexes could be one reason for the loss of cell cycle checkpoint control, leading to DNA over-replication. Elucidation of the precise molecular mechanism underlying heavy metal-induced DNA over-replication in PUFA-enriched cells may serve highly useful for carcinogenesis studies, as greatly accelerated endogenous gene amplification is a feature of tumorigenic cells. The expression of viral oncoproteins in human fibroblasts results in the inactivation of the p53 and Rb tumor suppressor genes, leading to subunit alterations of cyclin-CDK complexes (Xiong *et al.*, 1996; Schaefer *et al.*, 1993). The consequences of such alterations include loss of cell cycle checkpoint control and cytogenetic aberrations (Xiong *et al.*, 1996). Also, individuals with Li-Fraumeni Syndrome (LFS) carry congenital mutations in one of their p53 alleles, leading to accelerated gene amplification (polyploidy) and loss of cell cycle checkpoint control (Thea D. Tlsty, unpublished results).

We also examined the heterogeneity in copper sensitivity of genetically-homogeneous *S. cerevisiae* using flow cytometry. Flow cytometry is a powerful technique which enables the simultaneous, multiparametric analysis of single cells within heterogeneous populations (Jayat and Ratinaud, 1993; Lloyd, 1993). The use of flow cytometry for the analysis of specific cell cycle stage populations was validated. Using this methodology, a distinct relationship between cell cycle stage and sensitivity to copper toxicity was demonstrated, whereby cell populations consisting predominantly of 2C DNA cells (G_2/M phase) were the most susceptible to copper toxicity. The fatty acid compositions of different cell cycle stage sub-populations remained relatively constant, thus eliminating a role of fatty acid compositional variations in the cell cycle stage-dependency of sensitivity to copper toxicity. However, using the oxidant-sensitive probe

H_2DCFDA, the increased sensitivity of G_2/M phase cells was correlated with elevated levels of endogenous reactive oxygen species in these cells. Our findings are consistent with several reports demonstrating the elevated toxin-sensitivity of S and G_2 phase cells (Nitiss and Wang, 1996; Galli and Schiestl, 1995). We also describe a novel flow cytometric technique for the analysis of the promoter activity of genes of interest in distinct sub-populations, using the green fluorescent protein of *Aequorea victoria*. While differences in basal levels of *CUP1* activity between live and dead sub-populations were not evident, our results with *SOD1* were inconclusive and further experimentation is required to determine if the large heterogeneity in *SOD1* activity can be correlated with the cell cycle stage-dependency of susceptibility to copper toxicity. Indeed, several studies with higher organisms have demonstrated changes in *SOD1* activity during the cell cycle (Oberley *et al.*, 1995; Kong *et al.*, 1993). The major biological importance of the SOD oxidative stress response proteins has been highlighted by their role in familial amyotrophic lateral sclerosis (FALS), a motor neuron degenerative disease (Wiedau-Pazos *et al.*, 1996).

Thus, the effects of altered membrane fatty acid composition on the toxic interactions of heavy metals with *Saccharomyces cerevisiae* have been examined. The impact of increased membrane fatty acid composition on susceptibility to heavy metal-induced reactive oxygen species-mediated cellular damage was marked. As well as being of relevance to the stress biochemistry of yeast, the findings may have significant implications for metal-microbe interactions in the natural environment, and for deciphering the mechanisms of loss of cell cycle control under stress conditions.

References

1. **Akaike, T., Noguchi, Y., Ijiri, S., Setoguchi, K., Suga, M., Zheng, Y. M., Dietzschold, B., and Maeda, H. (1996).** Pathogenesis of influenza virus-induced pneumonia: involvement of both nitric oxide and oxygen radicals. *Proc. Natl. Acad. Sci. USA* **93**, 2448-2453.

2. **Akman, S. A., Kensler, T. W., Doroshow, J. H., and Dizdaroglu, M. (1993).** Copper ion-mediated modification of bases in DNA *in vitro* by benzoyl peroxide. *Carcinogenesis* **14**, 1971-1974.

3. **Alexandre, H., Rousseaux, I., and Charpentier, C. (1994).** Relationship between ethanol tolerance, lipid composition and plasma membrane fluidity in *Saccharomyces cerevisiae* and *Kloeckera apiculata*. *FEMS Microbiol. Lett.* **124**, 17-22.

4. **Alterthum, F. and Rose, A. H. (1973).** Osmotic lysis of sphaeroplasts from *Saccharomyces cerevisiae* grown anaerobically in media containing different unsaturated fatty acids. *J. Gen. Microbiol.* **77**, 371-382.

5. **Altman, S. A., Zastawny, T. H., Randerseichhorn, L., Cacciuttolo, M. A., Akman, S. A., Dizdaroglu, M., and Rao, G. (1995).** Formation of DNA-protein cross-links in cultured mammalian cells upon treatment with iron ions. *Free Radic. Biol. Med.* **19**, 897-902.

6. **Aβmann, S., Sigler, K., and Hofer, M. (1996).** Cd^{2+}-induced damage to yeast plasma membrane and its alleviation by Zn^{2+}: studies on *Schizosaccharomyces pombe* cells and reconstituted plasma membrane vesicles. *Arch. Microbiol.* **165**, 279-284.

7. **Anderson, M. T., Tjioe, I. M., Lorincz, M. C., Parks, D. R., Herzenberg, L. A., and Nolan, G. P. (1996).** Simultaneous fluorescence-activated cell sorter analysis of two distinct transcriptional elements within a single cell using engineered green fluorescent proteins. *Proc. Natl. Acad. Sci. USA* **93**, 8508-8511.

8. **Aparicio, O. M., Weinstein, D. M., and Bell, S. P. (1997).** Components and dynamics of DNA replication complexes in *S. cerevisiae*: redistribution of MCM proteins and Cdc45p during S phase. *Cell* **91**, 59-69.

9. **Aris, J. P. and Blobel, G. (1991).** Isolation of yeast nuclei. *Methods Enzymol.* **194**, 735-749.

10. **Aust, S. D. (1994).** Thiobarbituric acid assay reactants. *Methods Toxicol.* **1B**, 367-374.

11. **Ausubel, F. M., Brent, R., Kingston, R. E., Moore, D. D., Seidman, J. G., Smith, J. A., and Struhl, K. (1998).** *Current Protocols in Molecular Biology, vol. I, II* and *III.* John Wiley & Sons, New York.

12. **Avery, S. V. (1995*a*).** Caesium accumulation by microorganisms: uptake mechanisms, cation competition, compartmentalization and toxicity. *J. Indust. Microbiol.* **14**, 76-84.

13. **Avery, S. V. (1995*b*).** Microbial interactions with caesium-implications for biotechnology. *J. Chem. Tech. Biotechnol.* **62**, 3-16.

14. **Avery, S. V., Harwood, J. L., and Lloyd, D. (1995*b*).** Quantification and characterization of phagocytosis in the soil amoeba *Acanthamoeba castellanii* by flow cytometry. *Appl. Environ. Microbiol.* **61**, 1124-1132.

15. **Avery, S. V., Howlett, N. G., and Radice, S. (1996).** Copper toxicity towards *Saccharomyces cerevisiae*: Dependence on plasma membrane fatty acid composition. *Appl. Environ. Microbiol.* **62**, 3960-3966.

16. **Avery, S. V., Lloyd, D., and Harwood, J. L. (1995*a*).** Temperature-dependent changes in plasma-membrane lipid order and the phagocytotic activity of the amoeba *Acanthamoeba castellanii* are closely correlated. *Biochem. J.* **312**, 811-816.

17. **Awaya, J., Ohno, T., Ohno, H., and Omura, S. (1975).** Substitution of cellular fatty acids in yeast cells by the antibiotic cerulenin and exogenous fatty acids. *Biochim. Biophys. Acta* **409**, 267-273.

18. **Belde, P. J. M., Kessels, B. G. F., Moelans, I., and Borst-Pauwels, G. W. F. H. (1988).** Cd^{2+} uptake, Cd^{2+} binding and loss of K^+ by a Cd-sensitive and a Cd-resistant strain of *Saccharomyces cerevisiae*. *FEMS Microbiol. Lett.* **49**, 493-498.

19. **Bender, J., Rodriguez-Eaton, S., Ekanemesang, U. M., and Phillips, P. (1994).** Characterization of metal-binding bioflocculants produced by the cyanobacterial component of mixed microbial mats. *Appl. Environ. Microbiol.* **60**, 2311-2315.

20. **Bligh, E. G. and Dyer, W. J. (1959).** A rapid method of total lipid extraction and purification. *Can. J. Biochem. Physiol.* **37**, 911-917.

21. **Block, E. R. (1991).** Hydrogen peroxide alters the physical state and function of the plasma membrane of pulmonary artery endothelial cells. *J. Cell Physiol.* **146**, 362-369.

22. **Bondy, S. C., Guo-Ross, S. X., and Pien, J. (1998).** Mechanisms underlying the aluminum-induced potentiation of the pro-oxidant properties of transition metals. *Neurotoxicol.* **19**, 65-71.

23. **Bossie, M.A. and Martin, C.E. (1989).** Nutritional regulation of yeast Δ-9 fatty acid desaturase activity. *J. Bacteriol.* **171**, 6409-6413.

24. **Bradford, M. M. (1976).** A rapid and sensitive method for quantification of protein utilising the principles of protein-dye binding. *Anal. Biochem.* **72**, 248-254.

25. **Breeuwer, P. (1995).** Characterization of uptake and hydrolysis of fluorescein diacetate and carboxyfluorescein diacetate by intracellular esterases in *Saccharomyces cerevisiae,* which result in accumulation of fluorescent product. *Appl. Environ. Microbiol.* **61**, 1614-1619.

26. **Brennan, R. J. and Schiestl, R. H. (1996).** Cadmium is an inducer of oxidative stress in yeast. *Mutat. Res.* **356**, 171-178.

27. **Brennan, R. J. and Schiestl, R. H. (1998).** Free radicals generated in yeast by the *Salmonella* test-negative carcinogens benzene, urethane, thiourea and auramine O. *Mutat. Res.* **403**, 65-73.

28. **Brennan, R. J., Swoboda, B. E. P., and Schiestl, R. H. (1994).** Oxidative mutagens induce intrachromosomal recombination in yeast. *Mutat. Res.* **308**, 159-167.

29. **Bridgewater, L. C., Manning, F. C., Woo, E. S., and Patierno, S. R. (1994).** DNA-polymerase arrest by adducted trivalent chromium. *Molec. Carcinogenesis* **9**, 122-133.

30. **Burton, K. (1968).** Determination of DNA concentration with diphenylamine. *Methods Enzymol.* **12B**, 163-166.

31. **Butler, A. R., White, J. H., and Stark, M. J. R. (1991).** Analysis of the response of *Saccharomyces cerevisiae* cells to *Kluyveromyces lactis* toxin. *J. Gen. Microbiol.* **137**, 1749-1757.

32. **Butler, I. S. and Harrod J. F. (1989).** *Inorganic Chemistry: Principles and Applications,* 1st edition. Benjamin/Cummings, Redwood City, California.

33. **Carratu, L., Franceschelli, S., Pardini, C. L., Kobayashi, G. S., Horvath, I., Vigh, L., and Maresca, B. (1996).** Membrane lipid perturbation modifies the set point of the temperature of heat shock response in yeast. *Proc. Natl. Acad. Sci. USA* **93**, 3870-3875.

34. **Cervantes, C. and Gutierrez-Corona, F. (1994).** Copper resistance mechanisms in bacteria and fungi. *FEMS Microbiol. Rev.* **14**, 121-137.

35. **Chae, H. Z., Kim, I. H., Kim, K., and Rhee, S. G. (1993).** Cloning, sequencing, and mutation of thiol-specific antioxidant gene of *Saccharomyces cerevisiae*. *J. Biol. Chem.* **268**, 16815-16812.

36. **Chang, E. C., Crawford, B. F., Hong, Z., Bilinski, T., and Kosman, D. J. (1991).** Genetic and biochemical characterization of Cu,Zn superoxide dismutase mutants in *Saccharomyces cerevisiae*. *J. Biol. Chem.* **266**, 4417-4424.

37. **Cherry, J. M., Ball, C., Weng, S., Juvik, G., Schmidt, R., Adler, C., Dunn, B., Dwight, S., Riles, L., Mortimer, R. K., and Botstein, D. (1997).** Genetic and physical maps of *Saccharomyces cerevisiae*. *Nature* **387** (Suppl. 6632) 67-73.

38. **Chiu, S. M., Xue, L. Y., Friedman, L. R., and Oleinick, N. L. (1995).** Differential dependence on chromatin structure for copper and iron-ion induction of DNA double-strand breaks. *Biochemistry* **34**, 2653-2661.

39. **Chong, J. P. L., Mahbubani, H. M., Khoo, C., and Blow, J. J. (1995).** Purification of an MCM-containing complex as a component of the DNA replication licensing system. *Nature* **375**, 418-421.

40. **Cocker, J. H., Piatti, S., Santocanale, C., Nasmyth, K., and Diffley, J. F. X. (1996).** An essential role for the Cdc6 protein in forming the pre-replicative complexes of budding yeast. *Nature* **379**, 180-182.

41. **Cohen, G., Fessl, F., Traczyk, A., Rytka, J., and Ruis, H. (1985).** Isolation of the catalase A gene of *Saccharomyces cerevisiae* by complementation of the *cta1* mutation. *Mol. Gen. Genet.* **200**, 74-79.

42. **Cormack, B. P., Valdivia, R. H, and Falkow, S. (1996).** FACS-optimized mutants of the green fluorescent protein (GFP). *Gene* **173**, 33-38.

43. **Corongiu, F. P., Banni, S., and Lombardi, B. (1994).** Quantitation of conjugated dienes by second-derivative UV spectroscopy. *Methods Toxicol.* **1B**, 415-420.

44. **Correa-Bordes, J. and Nurse, P. (1995).** $p25^{rum1}$ orders S phase and mitosis by acting as an inhibitor of the $p34^{cdc2}$ mitotic kinase. *Cell* **83**, 1001-1009.

45. **Coudray, C., Richard, M. J., and Favier, F. P. (1995).** Determination of primary and secondary lipid peroxidation products: plasma lipid hydroperoxides and thiobarbituric acid reactive substances, p. 185-200. *In* A. E. Favier (ed.),

Analysis of Free Radicals in Biological Systems. Birkhauser-Verlag, Basel, Switzerland.

46. **Culotta, V. C., Joh, H. D., Lin, S. J., Slekar, K. H., and Strain, J. (1995).** A physiological role for *Saccharomyces cerevisiae* copper/zinc superoxide dismutase in copper buffering. *J. Biol. Chem.* **270**, 29991-29997.

47. **Dally, H. and Hartwig, A. (1997).** Induction and repair inhibition of oxidative DNA damage by nickel(II) and cadmium(II) in mammalian cells. *Carcinogenesis* **18**, 1021-1026.

48. **Dalton, S. and Hopwood, B. (1997).** Characterization of Cdc47p-minichromosome maintenance complexes in *Saccharomyces cerevisiae*: identification of Cdc45p as a subunit. *Molec. Cell. Biol.* **17**, 5867-5875.

49. **Dalton, S. and Whitbread, L. (1995).** Cell cycle-regulated nuclear import and export of Cdc47, a protein essential for initiation of DNA replication in budding yeast. *Proc. Natl. Acad. Sci. USA* **92**, 2514-2518.

50. **Dancis, A., Haile, D., Yuan, D. S., and Klausner, R. D. (1994).** The *Saccharomyces cerevisiae* copper transport protein (Ctr1p). Biochemical characterization, regulation by copper, and physiologic role in copper uptake. *J. Biol. Chem.* **269**, 25660-25667.

51. **Davidge, S. T., Baker, P. N., Laughlin, M. K., and Roberts, J. M. (1995).** Nitric oxide produced by endothelial cells increases production of eicosanoids through activation of prostaglandin H synthase. *Circ. Res.* **77**, 274-283.

52. **Davidson, J. F., White, B., Bissinger, P. H., and Schiestl, R. H. (1996).** Oxidative stress is involved in heat-induced cell death in *Saccharomyces cerevisiae*. *Proc. Natl. Acad. Sci. USA* **93**, 5116-5121.

53. **Davies, K. J. A. (1995).** Oxidative stress: the paradox of life. *Biochem. Soc. Symp.* **61**, 1-31.

54. **De Rome, L. and Gadd, G. M. (1987).** Measurement of copper uptake in *Saccharomyces cerevisiae* using a Cu^{2+}-selective electrode. *FEMS Microbiol. Lett.* **43**, 283-287.

55. **De Vos, C. H. R, Bookum, W. M. T, Vooijs, R., Schat, H., and De Kok, L. J. (1993).** Effects of copper on fatty acid composition and peroxidation of lipids in the roots of copper tolerant and sensitive *Silene cucubalas*. *Plant Physiol. Biochem.* **31**, 151-158.

56. **Demple, B. and Harrison, L. (1994).** Repair of oxidative damage to DNA: enzymology and biology. *Ann. Rev. Biochem.* **63**, 915-948.

57. **Dix, T. A., Hess, K. M., Medina, M. A., Sullivan, R. W., Tilly, S. L., and Webb, T. L. (1996).** Mechanism of site-selective DNA nicking by the hydrodioxyl (perhydroxyl) radical. *Biochemistry* **35**, 4578-4583.

58. **Dix, T. A. and Aikens, J. (1993).** Mechanisms and biological relevance of lipid peroxidation initiation. *Chem. Res. Toxicol.* **6**, 2-18.

59. **Elinder, C. G. (1992).** Cadmium as an environmental hazard. *IARC Sci. Publ.* **118**, 123-132.

60. **Evans, M. V., Turton, H. E., Grant, C. M., and Dawes, I. W. (1998).** Toxicity of linoleic acid hydroperoxide to *Saccharomyces cerevisiae*: involvement of a

respiration-related process for maximal sensitivity and adaptive response. *J. Bacteriol.* **180**, 483-490.

61. **Figueiredo-Pereira, M. E., Yakushin, S., and Cohen, G. (1998).** Disruption of the intracellular sulfhydryl homeostasis by cadmium-induced oxidative stress leads to protein thiolation and ubiquitination in neuronal cells. *J. Biol. Chem.* **273**, 12703-12709.

62. **Flattery O'Brien, J. A. and Dawes, I. W. (1998).** Hydrogen peroxide causes *RAD9*-dependent cell cycle arrest in G(2) in *Saccharomyces cerevisiae* whereas menadione causes G(1) arrest independent of *RAD* function. *J. Biol. Chem.* **273**, 8564-8571.

63. **Flowers, L., Ohnishi, S. T., and Penning, T. M. (1997).** DNA strand scission by polycyclic aromatic hydrocarbon o-quinones: role of reactive oxygen species, Cu(II)/Cu(I) redox cycling, and o-semiquinone anion radicals. *Biochemistry* **36**, 8640-8648.

64. **Fodor, E., Szabo-Nagy, A., and Erdei, L. (1995).** The effects of cadmium on the fluidity and H^+-ATPase activity of plasma membrane from sunflower and wheat roots. *J. Plant Physiol.* **147**, 87-92.

65. **Fude, L., Harris, B., Urrutia, M. M., and Beveridge, T. J. (1994).** Reduction of Cr(VI) by a consortium of sulfate-reducing bacteria (SRB III). *Appl. Environ. Microbiol.* **60**, 1525-1531.

66. **Gadd, G. M. (1993).** Interactions of fungi with toxic metals. *New Phytol.* **124**, 25-60.

67. **Gadd, G. M. and Mowll, J. L. (1983).** The relationship between cadmium uptake, potassium release and viability in *Saccharomyces cerevisiae*. *FEMS Microbiol. Lett.* **16**, 45-48.

68. **Galiazzo, F. and Labbe-Rois, R. (1993).** Regulation of Cu,Zn- and Mn-superoxide dismutase transcription in *Saccharomyces cerevisiae*. *FEBS Lett.* **315**, 197-200.

69. **Galli, A. and Schiestl, R. H. (1995).** *Salmonella* test positive and negative carcinogens show different effects on intrachromosomal recombination in G2 arrested cells. *Carcinogenesis* **16**, 659-663.

70. **Galli, A. and Schiestl, R. H. (1998).** Effects of DNA double-strand and single-strand breaks on intrachromosomal recombination events in cell cycle-arrested yeast cells. *Genetics* **149**, 1235-1250.

71. **Gan, Z.-R. (1991).** Yeast thioredoxin genes. *J. Biol. Chem.* **266**, 1692-1696.

72. **Gille, G., Sigler, K., and Hofer, M. (1993).** Response of catalase activity and membrane fluidity of aerobically grown *Schizosaccharomyces pombe* and *Saccharomyces cerevisiae* to aeration and the presence of substrates. *J. Gen. Microbiol.* **139**, 1627-1634.

73. **Glende, E. A. and Recknagel, R. O. (1994).** Spectrophotometric detection of lipid-conjugated dienes. *Methods Toxicol.* **1B**, 400-406.

74. **Gralla, E. B. and Valentine, J. S. (1991).** Null mutants of *Saccharomyces cerevisiae* Cu,Zn superoxide dismutase: Characterization and spontaneous mutation rates. *J. Bacteriol.* **173**, 5918-5920.

75. **Gralla, E. B., Thiele, D. J., Silar, P., and Valentine, J. S. (1991).** *ACE1*, a copper-dependent transcription factor, activates expression of the yeast copper, zinc superoxide dismutase gene. *Proc. Natl. Acad. Sci. USA* **88**, 8558-8562.

76. **Greco, M. A., Hrab, D. I., Magner, W., and Kosman, D. J. (1990).** Cu,Zn superoxide dismutase and copper deprivation and toxicity in *Saccharomyces cerevisiae*. *J. Bacteriol.* **172**, 317-325.

77. **Griffiths, G. and Harwood, J. L. (1991).** The regulation of triacylglycerol biosynthesis in cocoa (*Theobroma cacao* L.). *Planta* **184**, 279-284.

78. **Guerzoni, M. E., Sinigaglia, M., and Gardini, F. (1993).** Interaction between isolation source, cellular fatty acid composition and stress tolerance in *Saccharomyces cerevisiae* and its subspecies. *J. Appl. Bacteriol.* **75**, 588-594.

79. **Guzder, S., Qiu, H., Sommers, C., Sung, P., Prakash, L., and Prakash, S. (1994).** DNA repair gene *RAD3* is essential for transcription by RNA polymerase II. *Nature* **367**, 91-94.

80. **Halliwell, B. and Gutteridge, J. M. C. (1989).** *Free radicals in biology and medicine*, 2nd edition. Clarendon Press, Oxford.

81. **Hama-Inaba, H., Shimazu, Y., Takusagawa, M., Sato, K., and Morimyo, M. (1994).** CHO.K1 cell mutants sensitive to active oxygen-generating agents. I. Isolation and genetic studies. *Mutat. Res.* **311**, 95-102.

82. **Harjula, R. and Lehto, J. (1986).** Effect of sodium and potassium ions on caesium absorption from nuclear power plant waste solutions on synthetic zeolites. *Nucl. Chem. Waste Manage.* **6**, 133-139.

83. **Hassoun, E. A. and Stohs, S. J. (1996).** Cadmium-induced production of superoxide anion and nitric oxide, DNA single strand breaks and lactate dehydrogenase leakage in J774A.1 cell cultures. *Toxicology* **112**, 219-226.

84. **Haugland, R. P. (1996).** *Handbook of Fluorescent Probes and Research Chemicals,* 6th edition. Molecular Probes Inc., Eugene, OR.

85. **Hayles, J., Fisher, D., Woollard, A., and Nurse, P. (1994).** Temporal order of S phase and mitosis in fission yeast is determined by the state of the $p34^{cdc2}$-mitotic B cyclin complex. *Cell* **78**, 813-822.

86. **Hazel, J. R. and Williams, E. E. (1990).** The role of alterations in membrane lipid composition in enabling physiological adaptation of organisms to their physical environment. *Prog. Lipid Res.* **29**, 167-227.

87. **Heichman, K. A. and Roberts, J. M. (1996).** The yeast *CDC16* and *CDC27* genes restrict DNA replication to once per cell cycle. *Cell* **85**, 39-48.

88. **Hjortsu, M. A., Dennis, K. E., and Bailey, J. E. (1985).** Quantitative characterization of plasmid instability in *Saccharomyces cerevisiae* using flow cytometry cell sorting. *Biotechnol. Lett.* **7**, 21-24.

89. **Hock, C., Drasch, G., Golombowski, S., Muller-Spahn, F., Willershausen-Zonnchen, B., Schwarz, P., Hock, U., Growdon, J. H., and Nitsch, R. M. (1998).** Increased blood mercury levels in patients with Alzheimers disease. *J. Neural Transmission* **105**, 59-68.

90. **Hoptroff, M. J., Thomas, S. and Avery, S. V. (1997).** Influence of altered plasma membrane fatty acid composition on cesium transport characteristics and toxicity in *Saccharomyces cerevisiae. Can. J. Microbiol.* **43**, 954-962.

91. **Hortner, H., Ammerer, G., Hartter, E., Hamilton, B., Rytka, J., Bilinski, T., and Ruis, H. (1982).** Regulation of synthesis of catalases and iso-1-cytochrome c in *Saccharomyces cerevisiae* by glucose, oxygen and heme. *Eur. J. Biochem.* **128**, 179-184.

92. **Hosono, K. (1992).** Effect of salt stress on lipid composition and membrane fluidity of the salt-tolerant yeast *Zygosaccharomyces rouxii*. *J. Gen. Microbiol.* **138**, 91-96.

93. **Hu, B., Burkhart, R., Schulte, D., Musahl, C., and Knipper, R. (1993).** The P1 family: a new class of nuclear mammalian proteins related to the yeast Mcm replication proteins. *Nucl. Acids. Res.* **21**, 5289-5293.

94. **Hughes, M. N. and Poole, R. K. (1989).** *Metals and Micro-organisms*. Chapman and Hall, London.

95. **Hussain, M. and Lenard, J. (1991).** Characterisation of *PDR4*, a *Saccharomyces cerevisiae* gene that confers pleiotropic drug resistance in high-copy number. *Gene* **101**, 149-152.

96. **Hutchinson, F. (1985).** Chemical changes induced in DNA by ionizing radiation. *Prog. Nucl. Acid Res. Molec. Biol.* **32**, 115-154.

97. **Iwai, K., Drake, S. K., Wehr, N. B., Weissman, A. M., LaVaute, T., Minato, N., Klausner, R. D., Levine, R. L., and Rouault, T. A. (1998).** Iron-dependent oxidation, ubiquitination, and degradation of iron regulatory protein 2: implications for degradation of oxidized proteins. *Proc. Natl. Acad. Sci. USA* **95**, 4924-4928.

98. **Izawa, S., Inoue, Y., and Kimura, A. (1996).** Importance of catalase in the adaptive response to hydrogen peroxide-analysis of acatalasaemic *Saccharomyces cerevisiae*. *Biochem. J.* **320**, 61-67.

99. **James, P. E., Grinberg, O. Y., and Swartz, H. M. (1998).** Superoxide production by phagocytosing macrophages in relation to the intracellular distribution of oxygen. *J. Leukoc. Biol.* **64**, 78-84.

100. **Jamieson, D. J. (1992).** *Saccharomyces cerevisiae* has distinct adaptive responses to both hydrogen peroxide and menadione. *J. Bacteriol.* **174**, 6678-6681.

101. **Jamieson, D. J. (1995).** The effect of oxidative stress on *Saccharomyces cerevisiae*. *Redox Rep.* **1**, 89-95.

102. **Jamieson, D. J., Rivers, S. L., and Stephen, D. W. S. (1994).** Analysis of *Saccharomyces cerevisiae* proteins induced by peroxide and superoxide stress. *Microbiol.* **140**, 3277-3283.

103. **Jayat, C. and Ratinaud, M. (1993).** Cell-cycle analysis by flow cytometry-principals and applications. *Biol. Cell* **78**, 15-25.

104. **Jensen, L. T., Howard, W. R., Strain, J. J., Winge, D. R., and Culotta, V. C. (1996).** Enhanced effectiveness of copper ion buffering by *CUP1* metallothionein compared with *CRS5* metallothionein in *Saccharomyces cerevisiae*. *J. Biol. Chem.* **271**,18514-18519.

105. **Jungmann, J., Reins, H. A., Schobert, C., and Jentsch, S. (1993*a*).** Resistance to cadmium mediated by ubiquitin-dependent proteolysis. *Nature* **361**, 369-371.

106. **Jungmann, J., Reins, H. A., Lee, J., Romeo, A., Hassett, R., Kosman, D., and Jentsch, S. (1993*b*).** MAC1, a nuclear regulatory protein related to Cu-dependent transcription factors is involved in Cu/Fe utilization and stress resistance in yeast. *EMBO J.* **12**, 5051-5056.

107. **Kadonaga, J .T. (1998).** Eukaryotic transcription: An interlaced network of transcription factors and chromatin-modifying machines. *Cell* **92**, 307-313.

108. **Kalejta, R. F., Shenk, T., and Beavis, A. J. (1997).** Use of membrane-localized green fluorescent protein allows simultaneous indentification of transfected cells and cell cycle analysis by flow cytometry. *Cytometry* **29**, 286-291.

109. **Kalyanaraman, B., Darley-Usmar, V. M., Wood, J., Joseph, J., and Parthasarathy, S. (1992).** Synergistic interaction between the probucol phenoxyl radical and ascorbic acid in inhibiting the oxidation of low density lipoprotein. *J. Biol. Chem.* **267**, 6789-6795.

110. **Kasprzak, K. S. (1995).** Possible role of oxidative damage in metal-induced carcinogenesis. *Cancer Invest.* **13**, 411-430.

111. **Keenan, M. H. J., Rose, A. H., and Silverman, B. W. (1982).** Effect of plasma-membrane phospholipid unsaturation on solute transport into *Saccharomyces cerevisiae* NCYC 366. *J. Gen. Microbiol.* **128**, 2547-2556.

112. **Kessels, B. G. F., Belde, P. J. M., and Borst-Pauwels, G. W. F. H. (1985).** Protection of *Saccharomyces cerevisiae* against Cd^{2+} toxicity by Ca^{2+}. *J. Gen. Microbiol.* **131**, 2533-2537.

113. **Keyer, K. and Imlay, J. A. (1996).** Superoxide accelerates DNA damage by elevating free iron levels. *Proc. Natl. Acad. Sci. USA* **93**, 13635-13640.

114. **Kim, K., Kim, I. H., Lee, K. Y., Rhee, S. G. and Stadtman, E. R. (1988).** The isolation and purification of a specific "protector" protein which inhibits enzyme inactivation by a thiol/Fe(III)/O_2 mixed-function oxidation system. *J. Biol. Chem.* **263**, 4704-4711.

115. **Kitada, K., Johnston, L., Sugino, T., and Sugino, A. (1992).** Temperature-sensitive *cdc7* mutations of *Saccharomyces cerevisiae* are suppressed by the *DBF4* gene, which is required for the G_1/S cell cycle transition. *Genetics* **131**, 21-29.

116. **Klein, H. (1988).** Different types of recombination events are controlled by the *RAD1* and *RAD52* genes of *Saccharomyces cerevisiae*. *Genetics* **120**, 367-377.

117. **Knight, S. A. B., Labbe, S., Kwon, L. F., Kosman, D. J., and Thiele, D. J. (1996).** A widespread transposable element masks expression of a yeast copper transport gene. *Genes Dev.* **10**, 1917-1929.

118. **Kong, X. J., Lee, S. L., Lanzillo, J. J., and Fanburg, B. L. (1993).** Cu, Zn superoxide-dismutase in vascular cells changes during cell cycling and exposure to hyperoxia. *Am. J. Physiol.* **264**, 365-373.

119. **Kramer, K. M., Brock, J. A., Bloom, K., Moore, J. K., and Haber, J. E. (1994).** Two different types of double-strand breaks in *Saccharomyces cerevisiae* are repaired by similar *RAD52*-independent, nonhomologous recombination events. *Mol. Cell Biol.* **14**, 1293-1301.

120. **Krems, B., Charizanis, C., and Entian, K. D. (1995).** Mutants of *Saccharomyces cerevisiae* sensitive to oxidative and osmotic stress. *Curr. Genetics* **27**, 427-434.

121. **Kuge, S. and Jones, N. (1994).** YAP1 dependent activation of *TRX2* is essential for the response of *Saccharomyces cerevisiae* to oxidative stress by hydroperoxides. *EMBO J.* **13**, 655-664.

122. **Kuypers, G. A. J. and Roomans, G. M. (1979).** Mercury-induced loss of K^+ from yeast cells investigated by electron probe X-ray microanalysis. *J. Gen. Microbiol.* **115**, 13-18.

123. **Lapinskas, P. J., Cunningham, K. W., Liu, X. F., Fink, G. R., Culotta, V. C. (1995).** Mutations in *PMR1* suppress oxidative damage in yeast cells lacking superoxide dismutase. *Mol. Cell Biol.* **15**, 1382-1388.

124. **Lapinskas, P., Ruis, H., and Culotta, V. (1993).** Regulation of *Saccharomyces cerevisiae* catalase expression by copper. *Curr. Genet.* **24**, 388-393.

125. **LeBel, C. P., Ischiropoulos, H., and Bondy, S. C. (1992).** Evaluation of the probe 2',7'-dichlorofluorescin as an indicator of reactive oxygen species formation and oxidative stress. *Chem. Res. Toxicol.* **5**, 227-231.

126. **Lei, M., Kawasaki, Y., and Tye, B. K. (1996).** Physical interactions among Mcm proteins and effects of Mcm dosage on DNA replication in *Saccharomyces cerevisiae*. *Molec. Cell. Biol.* **16**, 5081-5090.

127. **Lesuisse, E. and Labbe, P. (1995).** Effects of cadmium and of *YAP1* and *CAD1/YAP2* genes on iron metabolism in the yeast *Saccharomyces cerevisiae*. *Microbiol.* **141**, 2937-2943.

128. **Lew, D. J., Weinert, T., and Pringle, J. R. (1997).** Cell cycle control in *Saccharomyces cerevisiae*, p. 607-695. *In* J. R. Pringle, J. R. Broach and E. W.

Jones (ed.), The Molecular and Cellular Biology of the Yeast *Saccharomyces*. Cold Spring Harbor Laboratory Press, New York.

129. **Li, X. and Cai, M. (1997).** Inactivation of the cyclin-dependent kinase Cdc28 abrogates cell cycle arrest induced by DNA damage and disassembly of mitotic spindles in *Saccharomyces cerevisiae*. *Molec. Cell. Biol.* **17**, 2723-2734.

130. **Li, Y. B. and Trush, M. A. (1993).** DNA-damage resulting from the oxidation of hydroquinone by copper-role for a Cu(II)/Cu(I) redox cycle and reactive oxygen generation. *Carcinogenesis* **14**, 1303-1311.

131. **Li, Z. S., Lu, Y. P., Zhen, R. G., Szczypka, M., Thiele, D. J., and Rea, P. A. (1997).** A new pathway for vacuolar cadmium sequestration in *Saccharomyces cerevisiae*: YCF1-catalyzed transport of bis(glutathionato)cadmium. *Proc. Natl. Acad. Sci. USA* **94**, 42-47.

132. **Liu, X. D. and Thiele, D. J. (1996).** Oxidative stress induces heat shock factor phosphorylation and HSF-dependent activation of yeast metallothionein gene transcription. *Genes Dev.* **10**, 592-603.

133. **Liu, X. F. and Culotta, V. C. (1994).** The requirement for yeast superoxide dismutase is bypassed through mutations in *BSD2*, a novel metal homeostasis gene. *Mol. Cell Biol.* **14**, 7037-7045.

134. **Ljungman, M. and Hanawalt, P. C. (1992).** Efficient protection against oxidative DNA damage in chromatin. *Molec. Carcinogenesis* **5**, 264-269.

135. **Lloyd, D. (1987).** Biochemistry of the cell cycle. *Biochem. J.* **242**, 313-321.

136. **Lloyd, D. (1992).** Intracellular timekeeping: epigenetic oscillations reveal the functions of an ultradian clock, p. 5-22. *In* D. Lloyd and E. L. Rossi (ed.), Ultradian Rhythms in Life Processes. Springer-Verlag, London.

137. **Lloyd, D. (1993).** *Flow cytometry in microbiology.* Springer-Verlag, Berlin.

138. **Lloyd, D. R., Phillips, D. H., and Carmichael, P. L. (1997).** Generation of putative intrastrand cross-links and strand breaks in DNA by transition metal ion-mediated oxygen radical attack. *Chem. Res. Toxicol.* **10**, 393-400.

139. **Lohr, D. (1988).** Isolation of yeast nuclei and chromatin for studies of transcription-related processes, p. 125-145. *In* I. Campbell and J. H. Duffus (ed.), Yeast: a Practical Approach. IRL Press, Oxford.

140. **Lopezamoros, R., Comas, J., and Vivesrego, J. (1995).** Flow cytometric assessment of *Escherichia coli* and *Salmonella typhimurium* starvation-survival in seawater using rhodamine-123, propidium iodide, and oxonol. *Appl. Environ. Microbiol.* **61**, 2521-2526.

141. **Lord, P. G. and Wheals, A. E. (1980).** Asymmetrical division of *Saccharomyces cerevisiae. J. Bacteriol.* **142**, 808-818.

142. **Luikenhuis, S., Perrone, G., Dawes, I. W., and Grant, C. M. (1998).** The yeast *Saccharomyces cerevisiae* contains two glutaredoxin genes that are required for protection against reactive oxygen species. *Mol. Cell Biol.* **9**, 1081-1091.

143. **Macaskie, L. E. (1991).** The application of biotechnology to the treatment of wastes produced from the nuclear fuel cycle: biodegradation and bioaccumulation as a means of treating radionuclide-containing streams. *Crit. Rev. Biotechnol.* **11**, 41-112.

144. **Mackay, K. M. and Mackay, R. A. (1991).** *Introduction to Modern Inorganic Chemistry*, 4th edition. Blackie, Glasgow.

145. **Manivasakam, P. and Schiestl, R. H. (1998).** Nonhomologous end joining during restriction enzyme-mediated DNA integration in *Saccharomyces cerevisiae*. *Molec. Cell Biol.* **18**, 1736-1745.

146. **Maresca, B. and Cossins, A. R. (1993).** Fatty feedback and fluidity. *Nature* **365**, 606-607.

147. **Mason, C. A. (1991).** Physiological aspects of growth and recombinant DNA stability in *Saccharomyces cerevisiae*. *Antonie Von Leeuwenhoek* **59**, 269-283.

148. **M^{c}Donough, V. M., Stukey, J. E., and Martin, C. E. (1992).** Specificity of unsaturated fatty acid-regulated expression of the *Saccharomyces cerevisiae* *OLE1* gene. *J. Biol. Chem.* **267**, 5931-5936.

149. **M^{c}Millan, J. N. and Tatchell, K. (1994).** The *JNM1* gene in the yeast *Saccharomyces cerevisiae* is required for nuclear migration and spindle orientation during the mitotic cell cycle. *J. Cell Biol.* **125**, 143-158.

150. **Mehlhorn, R. J. (1986).** The Interaction of Inorganic Species with Biomembranes, p. 85-97. *In* M. Bernhard, F. E. Brinckman and P. J. Sadler (ed.), The Importance of Chemical 'Speciation' in Environmental Processes. Springer-Verlag, Berlin.

151. **Menendez, A., Larsson, C., and Ugalde, U. (1995).** Purification of functionally sealed side-out plasma membrane vesicles from *Saccharomyces cerevisiae*. *Anal. Biochem.* **230**, 308-314.

152. **Merchant, A. M., Kawasaki, Y., Chen, Y., Lei, M., and Tye, B. K. (1997).** A lesion in the DNA replication initiation factor Mcm10 induces pausing of elongation forks through chromosomal replication origins in *Saccharomyces cerevisiae*. *Molec. Cell. Biol.* **17**, 3261-3271.

153. **Mihaljevic, B., Katusin-Razem, B., and Razem, D. (1996).** The reevaluation of the ferric thiocyanate assay for lipid hydroperoxides with special considerations of the mechanistic aspects of the response. *Free Radic. Biol. Med.* **21**, 53-63.

154. **Minasi, L. A. and Willsky, G. R. (1991).** Characterization of vanadate-dependent NADH oxidation stimulated by *Saccharomyces cerevisiae* plasma membranes. *J. Bacteriol.* **173**, 834-841.

155. **Moradas-Ferreira, P., Costa, V., Piper, P., and Mager, W. (1996).** The molecular defences against reactive oxygen species in yeast. *Molec. Microbiol.* **19**, 651-658.

156. **Moreno, S. and Nurse, P. (1994).** Regulation of progression through the G1 phase of the cell cycle by the *rum1*$^+$ gene. *Nature* **367**, 236-242.

157. **Moskovitz, J., Berlett, B. S., Poston, J. M., and Stadtman, E. R. (1997).** The yeast peptide methionine sulfoxide reductase functions as an antioxidant *in vivo*. *Proc. Natl. Acad. Sci. USA* **94**, 9585-9589.

158. **Muller, E. G. D. (1991).** Thioredoxin deficiency in yeast prolongs S phase and shortens the G_1 interval of the cell cycle. *J. Biol. Chem.* **266**, 9164-9202.

159. **Muller, E. G. D. (1996).** A glutathione reductase mutant of yeast accumulates high levels of oxidized glutathione and requires thioredoxin for growth. *Mol. Biol. Cell* **7**, 1805-1813.

160. **Murata, N. (1989).** Low-temperature effects on cyanobacterial membranes. *J. Bioenerg. Biomemb.* **21**, 61-75.

161. **Niedenthal, R. K., Riles, L., Johnston, M., and Hegemann, J. H. (1996).** Green fluorescent protein as a marker for gene expression and subcellular localization in budding yeast. *Yeast* **12**, 773-786.

162. **Nisbet, E.G. and Fowler, C.M.R. (1995).** Is metal disposal toxic to deep oceans? *Nature* **375**, 715.

163. **Nitiss, J. L. and Wang, J. C. (1996).** Mechanisms of cell killing by drugs that trap covalent complexes between DNA topoisomerases and DNA. *Mol. Pharmacol.* **50**, 1095-1102.

164. **Norris, P. R. and Kelly, P. D. (1977).** Accumulation of cadmium and cobalt by *Saccharomyces cerevisiae. J. Gen. Microbiol.* **99**, 317-324.

165. **Novotny, V. (1995).** Diffuse sources of pollution by toxic metals and impact on receiving waters, p. 33-53. *In* W. Salomons, U. Förstner, and P. Mader (ed.), Heavy Metals; Problems and Solutions. Springer-Verlag, Berlin.

166. **Nriagu, J. O. (1991).** Human influence on the global cycling of trace metals, p. 1-5. *In* J. G. Farmer (ed.), Heavy Metals in the Environment. CEP Consultants, Edinburgh.

167. **Nygren, J., Ljungman, M., and Ahnstrom, G. (1995).** Chromatin structure and radiation-induced DNA strand breaks in human cells-soluble scavengers and DNA-bound proteins offer a better protection against single-strand than double-strand breaks. *Inter. J. Radiat. Biol.* **68**, 11-18.

168. **Oberley, T. D., Schultz, J. L., Li, N., and Oberley, L. W. (1995).** Antioxidant enzyme levels as a function of growth state in cell culture. *Free Radic. Biol. Med.* **19**, 53-65.

169. **Ohsumi, Y., Kitamoto, K., and Anraku, Y. (1988).** Changes induced in the permeability barrier of the yeast plasma membrane by cupric ion. *J. Gen. Physiol.* **43**, 621-633.

170. **Oikawa, S. and Kawanishi, S. (1996).** Site-specific DNA damage induced by NADH in the presence of copper(II)-role of active oxygen species. *Biochemistry* **35**, 4584-4590.

171. **Paltauf, F., Kohlwein, S., and Henry, S.A. (1992).** Regulation and compartmentalization of lipid synthesis in yeast. *In* J. Broach, E. Jones and J. Pringle (ed.), Molecular Biology of the Yeast *Saccharomyces cerevisiae.* Cold Spring Harbor Laboratory Press, New York.

172. **Park, J. L., Grant, C. M., Davies, M. J., and Dawes, I. W. (1998).** The cytoplasmic Cu,Zn superoxide dismutase of *Saccharomyces cerevisiae* is required for resistance to freeze-thaw stress. Generation of free radicals during freezing and thawing. *J. Biol. Chem.* **273**, 22921-22928.

173. **Parks, L. W., Smith, S. J., and Crowley, J. H. (1995).** Biochemical and physiological effects of sterol alterations in yeast. *Lipids* **30**, 227-230.

174. **Paulovich, A. G., Margulies, R. U., Garvik, B. M., and Hartwell, L. H. (1997).** *RAD9, RAD17,* and *RAD24* are required for S phase regulation in *Saccharomyces cerevisiae* in response to DNA damage. *Genetics* **145**, 45-62.

175. **Pena, M. M., Koch, K. A., and Thiele, D. J. (1998).** Dynamic regulation of copper uptake and detoxification genes in *Saccharomyces cerevisiae*. *Mol. Cell. Biol.* **18**, 2514-2523.

176. **Pennanen, T., Frostegard, A., Fritze, H., and Baath, E. (1996).** Phospholipid fatty acid composition and heavy metal tolerance of soil microbial communities along two heavy metal-polluted gradients in coniferous forests. *Appl. Environ. Microbiol.* **62**, 420-428.

177. **Polla, B. S., Richard, M.-J., Robinson, D. R., and Maresca, B. (1997).** Effects of membrane fatty acids on thermal and oxidative injury in the human premonocytic line U937. *Biochem. Pharmacol.* **54**, 773-780.

178. **Pongracz, J. and Lord, J. M. (1998).** Superoxide production in human neutrophils: evidence for signal redundancy and the involvement of more than one PKC isoenzyme class. *Biochem. Biophys. Res. Commun.* **247**, 624-629.

179. **Porro, D., Ranzi, B. M., Smeraldi, C., Martegani, E., and Alberghina, L. (1995).** A double flow cytometric tag allows tracking of the dynamics of cell cycle progression of newborn *Saccharomyces cerevisiae* cells during balanced exponential growth. *Yeast* **11**, 1157-1169.

180. **Porter, N. A., Caldwell S. E., and Mills, K. A. (1995).** Mechanisms of free radical oxidation of unsaturated lipids. *Lipids* **30**, 277-290.

181. **Prasad, M. R., Engelman, R. M., Jones, R. M., and Das, D. K. (1989).** Effects of oxyradicals on oxymyoglobin. Deoxygenation, haem removal and iron release. *Biochem. J.* **263**, 731-736.

182. **Price, N. M. and Morel, F. M. M. (1990).** Cadmium and cobalt substitution for zinc in a marine diatom. *Nature* **344**, 658-660.

183. **Rajan, M. T., Rao, K. S., Mamatha, B. M., Rao, R. V., Shanmugavelu, P., Menon, R. B., and Pavithran, M. V. (1997).** Quantification of trace elements in normal brain by inductively-coupled plasma-atomic emission spectrometry. *J. Neurological Sciences* **146**, 153-166.

184. **Ramotar, D., Popoff, S. C., Gralla, E. B., and Demple, B. (1991).** Cellular role of yeast Apn1 apurinic endonuclease/3'-diesterase: repair of oxidative and alkylation DNA damage and control of spontaneous mutation. *Mol. Cell. Biol.* **11**, 4537-4544.

185. **Rapoport, R., Sklan, D., Wolfenson, D., Shaham-Albalancy, A., and Hanukoglu, I. (1998).** Antioxidant capacity is correlated with steroidogenic status of the corpus luteum during the bovine estrous cycle. *Biochim. Biophys. Acta* **1380**, 133-140.

186. **Rattray, J. B. M., Schibeci, A., and Kirby, D. K. (1975).** Lipids of yeasts. *Bacteriol. Rev.* **39**, 197-231.

187. **Rego, A. C. and Oliveira, C. R. (1995).** Dual effects of lipid peroxidation on the membrane order of retinal cells in culture. *Arch. Biochem. Biophys.* **321**, 127-136.

188. **Rodriguez-Montelongo, L., De la Cruz-Rodriguez, L. C., Farias, R. N., and Massa, E. M. (1993).** Membrane-associated redox cycling of copper mediates hydroperoxide toxicity in *Escherichia coli*. *Biochim. Biophys. Acta* **1144**, 77-84.

189. **Ropp, J. D., Donahue, C. J., Wolfgangkimball, D., Hooley, J. J., Chin, J. Y., Hoffman, R. A., Cuthbertson, R. A., and Bauer, K. D. (1995).** Aequorea green fluorescent protein-analysis by flow cytometry. *Cytometry* **21**, 309-317.

190. **Rose, A. H. and Veazey, F. J. (1992).** Membranes and lipids of yeasts, p. 255-275. *In* I. Campbell and J. H. Duffus (ed.), Yeast: a Practical Approach. IRL Press, Oxford.

191. **Rudolph, H. K., Antebi, A., Fink, G. R., Buckley, C. M., Dorman, T. E., LeVitre, J., Davidow, L. S., Mao, J. I., and Moir, D. T. (1989).** The yeast secretory pathway is perturbed by mutations in *PMR1*, a member of a Ca^{2+}-ATPase family. *Cell* **58**, 133-145.

192. **Ruis, H. and Hamilton, B. (1992).** Regulation of yeast catalase genes, p153-172. *In* J. G. Scandalios (ed.), Molecular Biology of Free Radical Scavenging Systems. Cold Spring Harbor Laboratory Press, New York.

193. **Santoro, N. and Thiele, D. J. (1997).** Oxidative stress responses in the yeast *Saccharomyces cerevisiae*, p171-211. *In* S. Hohmann and W. H. Mager (ed.), Yeast Stress Responses. Chapman and Hall, New York.

194. **Sasaki, T. (1992).** Induction of ploidy level increments in an asporogenous industrial strain of the yeast *Saccharomyces cerevisiae* by UV irradiation. *Appl. Environ. Microbiol.* **58**, 948-952.

195. **Schaefer, D. I., Livanos, E. M., White, A. E.,, and Tlsty, T. D. (1993).** Multiple mechanisms of N-(phosphonoacetyl)-L-aspartate drug resistance in SV40-infected precrisis human fibroblasts. *Cancer Res.* **53**, 4946-4951.

196. **Schmidt, R., Ackermann, R., Kratky, Z., Wasserman, B., and Jacobson, B. (1983).** Fast and efficient purification of yeast plasma membranes using cationic silica microbeads. *Biochim. Biophys. Acta* **732**, 421-427.

197. **Schüller, C., Brewster, J. L., Alexander, M. R., Gustin, M. C., and Ruis, H. (1994).** The HOG pathway controls osmotic regulation of transcription via the stress response element (STRE) of the *Saccharomyces cerevisiae CTT1* gene. *EMBO J.* **13**, 4382-4389.

198. **Schulthess, G. and Hauser, H. (1995).** A unique feature of lipid dynamics in small intestinal brush border membrane. *Molec. Memb. Biol.* **12**, 105-112.

199. **Seaman, W. E., Gindhart, T. D., Blackman, M. A., Dalal, B., Talal, N., and Werb, Z. (1982).** Suppression of natural killing *in vitro* by monocytes and polymorphonuclear leukocytes: requirement for reactive metabolites of oxygen. *J. Clin. Invest.* **69**, 876-888.

200. **Serrano, R. (1978).** Characterisation of the plasma membrane ATPase of *Saccharomyces cerevisiae*. *Mol. Cell. Biochem.* **22**, 51-62.

201. **Serrano, R. (1988).** H^+-ATPase from plasma membranes of *Saccharomyces cerevisiae* and *Avena sativa* roots: purification and reconstitution. *Methods Enzymol.* **157**, 533-544.

202. **Shinar, E., Rachmilewitz, E. A., Shifter, A., Rahamim, E., and Saltman, P. (1989).** Oxidative damage to human red cells induced by copper and iron complexes in the presence of ascorbate. *Biochim. Biophys. Acta* **1014**, 66-72.

203. **Shumate II, S. E. and Strandberg, G. W. (1985).** Accumulation of metals by microbial cells, p. 235-247. *In* M. Moo-Young, C. N. Robinson and J. A. Howell (ed.), Comprehensive Biotechnology, vol. 4. Pergamon Press, New York.

204. **Siede, W., Friedberg, A. S., Dianova, I., and Friedberg, E. C. (1994).** Characterization of G_1 checkpoint control in the yeast *Saccharomyces cerevisiae* following exposure to DNA-damaging agents. *Genetics* **138**, 271-281.

205. **Snow, E. (1994).** Effects of chromium on DNA-replication *in vitro*. *Environ. Health Perspect.* **102**, 41-44.

206. **Stearman, R., Yuan, D. S., Yamaguchi-Iwai, Y., Klausner, R. D., and Dancis, A. (1996).** A permease-oxidase complex involved in high-affinity iron uptake in yeast. *Science* **271**, 1552-1557.

207. **Steels, E. L., Learmonth, R. P., and Watson, K. (1994).** Stress tolerance and membrane lipid unsaturation in *Saccharomyces cerevisiae* grown aerobically or anaerobically. *Microbiol.* **140**, 569-576.

208. **Steinbrecher, U. P., Zhang, H., and Lougheed, M. (1990).** Role of oxidatively modified low density lipoprotein in atherosclerosis. *Free Radic. Biol. Med.* **9**, 155-168.

209. **Stephen, D. W. S. and Jamieson, D. J. (1996).** Glutathione is an important antioxidant molecule in the yeast *Saccharomyces cerevisiae*. *FEMS Microbiol. Lett.* **141**, 207-212.

210. **Stephen, D. W. S., Rivers, S. L., and Jamieson, D. J. (1995).** The role of *YAP1* and *YAP2* in the regulation of the adaptive oxidative stress responses of *Saccharomyces cerevisiae*. *Molec. Microbiol.* **16**, 415-423.

211. **Stern, B. and Nurse, P. (1996).** A quantitative model for the *cdc2* control of S phase and mitosis in fission yeast. *TIG* **12**, 345-350.

212. **Stohs, S. J. and Bagchi, D. (1995).** Oxidative mechanisms in the toxicity of metal ions. *Free Radic. Biol. Med.* **18**, 321-336.

213. **Stukey, J. E., McDonough, V. M., and Martin, C. E. (1989).** Isolation and characterisation of *OLE1*, a gene affecting fatty acid desaturation from *Saccharomyces cerevisiae*. *J. Biol. Chem.* **28**, 16537-16544.

214. **Surana, U., Amon, A., Dowzer, C., McGrew, J., Byers, B., and Nasmyth, K. (1993).** Destruction of the *CDC28*/CLB mitotic kinase is not required for the metaphase to anaphase transition in budding yeast. *EMBO J.* **12**, 1969-1978.

215. **Surana, U., Robitsch, H., Price, C., Schuster, T., Fitch, I., Futcher, A. B., and Nasmyth, K. (1991).** The role of *CDC28* and cyclins during mitosis in the budding yeast *Saccharomyces cerevisiae*. *Cell* **65**, 163-174.

216. **Suutari, M., Liukkonen, K., and Laakso, S. (1990).** Temperature adaptation in yeasts: the role of fatty acids. *J. Gen. Microbiol.* **136**, 1469-1474.

217. **Takasu, T., Lyons, J. C., Park, H. J., and Song, C. W. (1998).** Apoptosis and perturbation of cell cycle progression in an acidic environment after hyperthermia. *Cancer Res.* **58**, 2504-2508.

218. **Tamai, K. T., Gralla, E. B., Ellerby, L. M., Valentine, J. S., and Thiele, D. J. (1993).** Yeast and mammalian metallothioneins functionally substitute for yeast copper-zinc superoxide dismutase. *Proc. Natl. Acad. Sci. USA* **90**, 8013-8017.

219. **Teoule, R. (1986).** Radiation-induced DNA damage and its repair. *Int. J. Radiat. Biol.* **51**, 573-589.

220. **Thiele, D. J. (1992).** Metal-regulated transcription in eukaryotes. *Nucl. Acids Res.* **20**, 1183-1191.

221. **Tran, L. T., Inoue, Y., and Kimura, A. (1993).** Oxidative stress response in yeast: purification and some properties of a membrane-bound glutathione peroxidase from *Hansenula mrakii*. *Biochim. Biophys. Acta* **1164**, 166-172.

222. **Trevors, J. T., Stratton, G. W., and Gadd, G. M. (1986).** Cadmium transport, resistance, and toxicity in bacteria, algae, and fungi. *Can. J. Microbiol.* **32**, 447-464.

223. **Triveldi, A., Fantin, D. J., and Tustanoff, E. R. (1987).** Role of phosphatidylinositol on the activity of yeast plasma membrane ATPase, p. 207-215. *In* S. C. Goheen (ed.), Membrane Proteins. Bio-Rad Laboratories, Richmond, CA.

224. **Triveldi, A., Khare, S., Singhal, G. S., and Prasad, R. (1982).** Effect of phosphatidylcholine and phosphatidylethanolamine on the structure and function of yeast membranes. *Biochim. Biophys. Acta* **692**, 202-209.

225. **Tye, B. K. (1994).** The MCM2-3-5 proteins: Are they replication licensing factors ? *Trends Cell Biol.* **4**, 160-166.

226. **Tyson, C. A. and Frazier, J. M. (1994).** Methods in Toxicology, vol. 1, part B. In Vitro Toxicity Indicators. Academic Press, San Diego.

227. **Valentine, M. R., Rodriguez, H., and Termini, J. (1998).** Mutagenesis by peroxy radical is dominated by transversions at deoxyguanosine: evidence for the lack of involvement of 8-oxo-dG1 and/or abasic site formation. *Biochemistry* **37**, 7030-7038.

228. **Van der Leij, I., Van den Berg, Boot, R., Franse, M., Distel, B., and Tabak, H. F. (1992).** Isolation of peroxisome assembly mutants from *Saccharomyces cerevisiae* with different morphologies using a novel positive selection procedure. *J. Cell Biol.* **119**, 153-162.

229. **Van der Rest, M. E., Kamminga, A. H., Nakano, A., Anraku, Y., Poolman, B., and Konings, W. N. (1995).** The plasma membrane of *Saccharomyces cerevisiae*: structure, function and biogenesis. *Microbiol. Rev.* **59**, 304-322.

230. **Van der Westhuizen, J. P. J., Kock, F., Botha, A., and Botes, P. J. (1994).** The distribution of the ω3- and ω6-series of cellular long-chain fatty acids in fungi. *System. Appl. Microbiol.* **17**, 327-345.

231. **Van Ginkel, G. and Sevanian, A. (1994).** Lipid peroxidation-induced membrane structural alterations. *Methods Enzymol.* **233**, 273-288.

232. **Vernet, J.-P. (1992).** *Impact of heavy metals on the environment*, vol. 2. Elsevier, Amsterdam.

233. **Vernole, P., Tedeschi, B., Caporossi, D., Maccarrone, M., Melino, G., and Annicchiarico-Petruzzelli, M. (1998).** Induction of apoptosis by bleomycin in resting and cycling human lymphocytes. *Mutagenesis* **13**, 209-215.

234. **Verstraeten, S. V. and Oteiza, P. L. (1995).** Sc^{3+}, Ga^{3+}, In^{3+}, Y^{3+} and Be^{2+} promote changes in membrane physical properties and facilitate Fe^{2+}-initiated lipid peroxidation. *Arch. Biochem. Biophys.* **322**, 284-290.

235. **Vestal, J. R. and White, D. C. (1989).** Lipid analysis in microbial ecology. *Bioscience* **39**, 535-541.

236. **Vossen, R. C. R. M., van Dam-Mieras, M. C. E., Hornstra, G., and Zwaal, R. F. A. (1995).** Differential effects of endothelial cell fatty acid modification on the sensitivity of their membrane phospholipids to peroxidation. *Prostagland. Leukotr. Essent. Fatty Acids* **52**, 341-347.

237. **Wach, A., Brachat, A., Alberti-Segui, C., Rebischung, C., and Philippsen, P. (1997).** Heterologous *HIS3* marker and GFP reporter modules for PCR-targeting in *Saccharomyces cerevisiae*. *Yeast* **13**, 1065-1075.

238. **Wagner, S. and Paltauf, F. (1994).** Generation of glycerophospholipid molecular species in the yeast *Saccharomyces cerevisiae*. Fatty acid pattern of phospholipid classes and selective acyl turnover at *sn*-1 and *sn*-2 positions. *Yeast* **10**, 1429-1437.

239. **Watson, K. and Rose, A. H. (1980).** Fatty-acyl composition of the lipids of *Saccharomyces cerevisiae* grown aerobically or anaerobically in media containing different fatty acids. *J. Gen. Microbiol.* **117**, 225-233.

240. **Weckx, J. E. J. and Clijsters, H. M. M. (1996).** Oxidative damage and defence mechanisms in primary leaves of *Phaseolus vulgaris* as a result of root assimilation of toxic amounts of copper. *Physiol. Plant.* **96**, 506-512.

241. **Weinert, T. A. and Hartwell, L. H. (1988).** The *RAD9* gene controls the cell cycle response to DNA damage in *Saccharomyces cerevisiae*. *Science* **241**, 317-322.

242. **Weinert, T. A., Kiser, G. L., and Hartwell, L. H. (1994).** Mitotic checkpoint genes in budding yeast and the dependence of mitosis on DNA replication and repair. *Genes Dev.* **8**, 652-665.

243. **Wetterhahn, K. E. and Dudek, E. J. (1996).** Environmental metal carcinogens - genotoxicity and altered gene expression by metal-mediated and indirect oxidative pathways. *New J. Chem.* **20**, 199-203.

244. **White, D. C. (1993).** *In-situ* measurement of microbial biomass, community structure and nutritional status. *Philos. Trans. R. Soc. Lond. A Math. Phys. Sci.* **344**, 59-67.

245. **Widell, S. and Larsson, C. (1990).** A critical evaluation of markers used in plasma membrane purification, p. 16-43. *In* C. Larsson and I. M. Moller (ed.), The Plant Plasma Membrane: Structure, Function and Molecular Biology. Springer-Verlag, Berlin.

246. **Wiedau-Pazos, M., Goto, J. J., Rabizadeh, S., Gralla, E. B., Roe, J. A., Lee, M. K., Valentine, J. S., and Bredesen, D. E. (1996).** Altered reactivity of superoxide dismutase in familial amyotrophic lateral sclerosis. *Science* **271**, 515-518.

247. **Wu, A., Wemmie, J. A., Edgington, N. P., Goebl, M., Guevara, J. L., and Moye-Rowley, W. S. (1993).** Yeast bZip proteins mediate pleiotropic drug and metal resistance. *J. Biol. Chem.* **268**, 18850-18858.

248. **Xiao, W. and Chow, B. L. (1998).** Syngerism between yeast nucleotide and base excision repair pathways in the protection against DNA methylation damage. *Curr. Genetics* **33**, 92-99.

249. **Xiong, Y., Kuppuswamy, D., Li, Y., Livanos, E. M., Hixon, M., White, A., Beach, D., and Tlsty, T. D. (1996).** Alteration of cell cycle kinase complexes in

human papillomavirus E6- and E7-expressing fibroblasts precedes neoplastic transformation. *J. Virol.* **70**, 999-108.

250. **Xu, J., Bubley, G. J., Detrick, B., Blankenship, L. J., and Patierno, S. R. (1996).** Chromium (VI) treatment of normal human-lung cells results in guanine-specific DNA-polymerase arrest, DNA-DNA cross-links and S-phase blockage of cell-cycle. *Carcinogenesis* **17**, 1511-1517.

251. **Xu, J., Manning, F. C., and Patierno, S. R. (1994).** Preferential formation and repair of chromium-induced DNA-adducts and DNA-protein cross-links in nuclear matrix DNA. *Carcinogenesis* **15**, 1443-1450.

252. **Yang, S. W., Becker, F. F., and Chan, J. Y. (1996).** Inhibition of human DNA ligase I activity by zinc and cadmium and the fidelity of ligation. *Environ. Molec. Mutag.* **28**, 19-25.

253. **Yeagle, P.L. (1989).** Lipid regulation of cell membrane structure and function. *FASEB J.* **3**, 1833-1842.

254. **Yim, M. B., Chae, H. Z., Rhee, S. G., Chock, P. B., and Stadtman, E. R. (1994).** On the protective mechanism of the thiol-specific antioxidant enzyme against oxidative damage of bio-macromolecules. *J. Biol. Chem.* **269**, 1621-1626.

255. **Young, M. R. and Tye, B. K. (1997).** Mcm2 and Mcm3 are constitutive nuclear proteins that exhibit distinct isoforms and bind chromatin during specific cell cycle stages of *Saccharomyces cerevisiae*. *Molec. Biol. Cell* **8**, 1587-1601.

256. **Young, M. R., Suzuki, K., Yan, H., Gibson, S., and Tye, B. K. (1997).** Nuclear accumulation of *Saccharomyces cerevisiae* Mcm3 is dependent on its nuclear-localization sequence. *Genes Cells* **2**, 631-643.

257. **Zinser, E., Sperka-Gottlieb, C. D. M., Fasch, E. V., Kohlwein, S. D., Paltauf, F., and Daum, G. (1991).** Phospholipid synthesis and lipid composition of subcellular membranes in the unicellular eukaryote *Saccharomyces cerevisiae. J. Bacteriol.* **173**, 2026-2034.

Published Material

PUBLISHED MATERIAL AFTER PAGE 251 IS EXCLUDED FROM THE DIGITISED THESIS

PLEASE REFER TO THE ORIGINAL TEXT TO SEE THIS MATERIAL